The Mutant Components of Wnt/β-catenin Signaling in Liver Cancer

Pengyu Liu

The studies presented in this thesis were performed at the Laboratory of Gastroenterology and Hepatology, Erasmus MC-University Medical Center Rotterdam, the Netherlands.

The research was funded by:

- China Scholarship Council Scholarship

Financial support for printing of this thesis was provided by:
Erasmus Postgraduate School Molecular Medicine

Cover design and layout by the author of this thesis.

Printed by: Ridderprint BV, www.ridderprint.nl

ISBN: 978-94-6375-433-0

The Mutant Components of Wnt/β-catenin Signaling in Liver Cancer

De gemuteerde componenten van Wnt/β-catenine signalering in leverkanker

Thesis

to obtain the degree of Doctor from the
Erasmus University Rotterdam
by command of the
rector magnificus

Prof.dr. R.C.M.E. Engels

and in accordance with the decision of the Doctorate Board
The public defense shall be held on

Wednesday 5th June 2019 at 9:30 hrs

by

Pengyu Liu

born in JiLin, JiLin Province, China

Erasmus University Rotterdam

Doctoral Committee

Promoter:

Prof. dr. M.P. Peppelenbosch

Other Members:

Prof. dr. W.N.M. Dinjens

Prof. dr. M.J. Bruno

Dr. P. Hohenstein

Co-promoter:

Dr. M.J.M. Smits

CONTENTS

Chapter 1

General Introduction and Outline of This Thesis

1 Liver cancer

According to a recent report of the world health organization (WHO), primary liver cancer is the fifth most common cancer worldwide, which has become a serious global health issue [1]. The most common risk factor for hepatocellular carcinoma (HCC) was identified as cirrhosis of any etiology, as more than 90% of HCC patients showed a history of cirrhosis [2]. The underlying causes of cirrhosis are however heterogenous. Hepatitis B virus (HBV) and hepatitis C virus (HCV) as well as vinyl chloride [3], smoking [4], aflatoxin exposure [5], and nonalcoholic steatohepatitis (NASH) [6] are all regarded as critical risk factors, leading to HCC heterogeneity.

Due to the lack of sensitive and valid biomarkers for early diagnosis of HCC, the majority of HCC patients are diagnosed at a late stage, leaving a limited number of treatment options. At present, for patients detected at an early stage of tumor formation, tumor resection and liver transplantation are the main suitable treatment options, resulting in a 5-year overall survival rate of only 30%-40% [7]. For HCC patients with advanced disease, Sorafenib is the only treatment option, which can extend the median overall survival with a modest 2-3 months [8]. Therefore, it is necessary to explore the underlying molecular mechanisms contributing to HCC development, as they may provide novel treatment options.

HCC development is a long-term multi-step process, involving a complex interplay between the tumor microenvironment and (epi)genetic alterations within the tumor cells. Throughout this stepwise progression, liver fibrosis and cirrhosis are essential steps toward malignancy, which among others can be provoked by chronic hepatitis virus infections, leading to hepatocyte apoptosis, necrosis and compensatory regeneration. During this long period, somatic mutations accumulate that provide growth advantages to the emerging tumor cells. Most frequently mutations within the *TERT* promoter (59%) are observed [9], which is recognized as an early event in HCC and promotes upregulation of TERT protein expression, thereby maintaining telomere length. Other frequently mutated genes include *TP53* (10%-40%) related to HBV infection, *CTNNB1* (20%-25%) which encodes β-catenin and appears to be more commonly observed with alcohol addiction or HCV infection, and *AXIN1* (10%) [10, 11].

2 Wnt signaling pathway

The highly conserved Wnt signaling pathway is involved in a variety of biological processes including homeostasis, cell proliferation, differentiation, migration and apoptosis [12]. The human Wnt gene family is made up of 19 members that encode secreted signaling proteins with 22–24 conserved cysteine residues [13]. Generally, Wnt signaling is subdivided in three major embranchments, that is (1) the canonical Wnt/β-catenin pathway, (2) the noncanonical planar cell polarity pathway, and (3) the noncanonical Wnt/calcium pathway. In this thesis I will mainly deal with the role of the Wnt/β-catenin signaling pathway and its role in liver cancer [14].

In this latter pathway (see Figure 1), Wnt ligands trigger cellular signal transduction by binding with the transmembrane receptor Frizzled (FZD) and low-density lipoprotein receptor-related protein 5 or 6 (LRP5/6), leading to Dishevelled(Dsh/Dvl) phosphorylation. Next, phosphorylated Dvl protein binds with AXIN protein, which inhibits GSK-3β function that is required for phosphorylation of β-catenin. As a result, the destruction complex consisting of the adenomatous polyposis coli (APC) tumor suppressor, scaffold proteins AXIN1 and AXIN2, and the kinases GSK3 and CK1α will be temporarily inhibited. This results in the cytoplasmic accumulation of β-catenin and translocation into the nucleus for binding with one of the T-cell factor/lymphoid enhancer-binding factor (TCF/LEF) transcription factors, ultimately leading to activation of target gene transcription.

However, in the absence of Wnt ligands, within the destruction complex initially Ser45 of β-catenin is phosphorylated by CK1α, followed by sequential GSK-3β phosphorylation at T41, S37 and finally S33. Next, the phosphorylated 32DpSGXXpS37 motif promotes binding of the ubiquitin ligase β-TrCP which targets β-catenin for proteasomal degradation, maintaining the free cytoplasmic β-catenin at a low level [15].

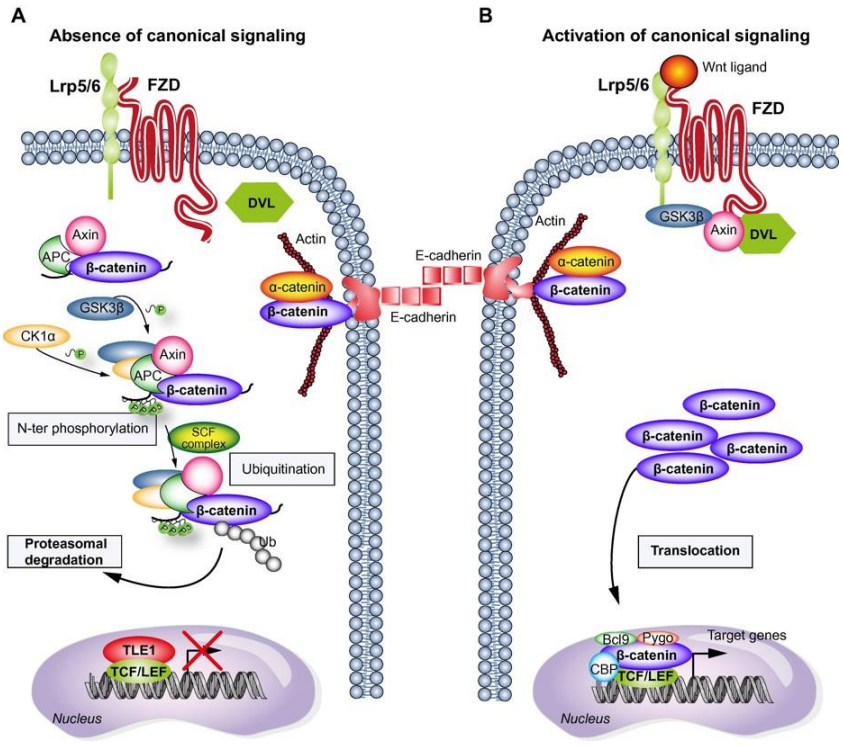

Figure.1 The canonical Wnt/β-catenin signaling pathway. (A) In the absence of Wnt ligands, β-catenin is phosphorylated by a degradation complex consisting of GSK3β, CK1α, APC and AXIN1/AXIN2. Phosphorylated β-catenin is targeted for proteasomal degradation after ubiquitination by the SCF protein complex. (B) Activation of canonical Wnt/β-catenin signaling leads to the dissociation of the degradation complex. As a result, β-catenin accumulates in the cytoplasm and translocates into the nucleus, where it promotes the expression of target genes via interaction with TCF/LEF transcription factors and other proteins such as CBP, Bcl9, and Pygo. Both figure and text adapted from reference Pez F, et al [16].

3 Aberrant activation of Wnt/β-catenin signaling by frequently observed mutations in HCC

1/β-catenin

β-catenin encoded by the *CTNNB1* gene, is the key component of Wnt/β-catenin signaling, and is mutated in 20-25% of HCC patients. One frequently observed mechanism is oncogenic β-catenin mutations containing the exon3 encoded S/T phosphorylation residues and β-TrCP binding motif (residues S33-S45), making the protein more resistant to proteolytic degradation and leading to enhanced nuclear signaling. However, amino-acid alterations lead to varying degrees of signaling activity. D32-S37 amino-acid substitutions were associated with strong activation of β-catenin signaling. T41 mutation resulted in a moderate activity, while S45 only weakly activated downstream genes.

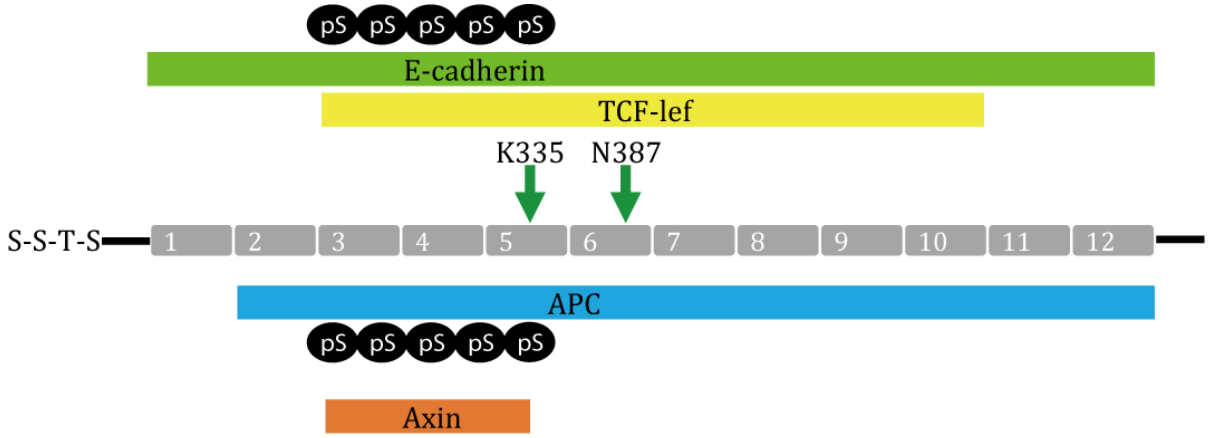

Figure 2. Schematic representation of the reported binding domains of APC, AXIN, TCF/LEF and E-cadherin to the armadillo repeat region of β-catenin. Position of K335I and N387K mutations are indicated by arrows. pS indicates Serine phosphorylation present at binding interface of APC or E-cadherin.

More recently, a new mutational hotspot region was identified in armadillo repeats 5 and 6 of β-catenin (encoded by exons 7 and 8). Especially K335 and N387 amino acid alterations are commonly observed in HCC and hepatomas, and were shown to lead to a weak to moderate activation of the pathway [17, 18]. These mutations are located in the core region of β-catenin which is composed of 12 armadillo repeats that mediate in the interaction with a number of proteins, such as E-cadherin, the TCF/LEF-family of transcription factors, APC, AXIN1/2, and multiple others (Figure 2) [19, 20]. Therefore, K335 and N387 mutations can potentially affect the binding affinity with several of these protein partners. At present, the mechanism leading to their increased signaling propensity remains however unknown.

2/AXIN

AXIN proteins were first identified in mouse. They play an important role in controlling embryonic development. For example, forced expression of AXIN1 in Xenopus oocytes inhibited dorsal-ventral axis formation. In addition, homozygous inactivation of *Axin1* in mouse embryos, gave rise to axial duplications [21]. These phenotypes were reminiscent of other developmental defects observed when interfering with proper β-catenin signaling, which was later confirmed when AXIN's role in the

β-catenin destruction complex was discovered. Nowadays AXIN proteins are regarded as negative regulators of Wnt signaling serving as a scaffold for the proteolytic degradation of β-catenin. As critical components of Wnt/β-catenin signaling, mutations in both *AXIN1* (10%) and *AXIN2* (3%) have been detected in HCC patients and cell lines [22]. Within *AXIN1* the alterations are randomly distributed throughout most of the domains, including the RGS domain, the middle region and C-terminal DIX domain, which respectively bind with APC, GSK-3β, β-catenin, DVL and AXIN itself [23, 24]. Although there are no hotspot mutations in *AXIN1*, most mutations cause premature translational termination, leading to truncated proteins with loss of original function. Besides potentially leading to enhanced β-catenin signaling, the AXIN proteins have also been linked to other proteins relevant for tumorigenesis such as cMYC [25], p53 [26], TGF-β [27], and Smad3 signaling pathways [28].

Originally, given its prominent role in the β-catenin destruction complex, mutational inactivation of AXIN1 was considered to support HCC development by aberrantly enhancing β-catenin signaling. This view has however been challenged in the last decade by several reports showing neither a clear nuclear β-catenin accumulation nor clearly enhanced expression of β-catenin target genes in AXIN1-mutant HCCs [29-31]. Hence, the extent of β-catenin signaling following AXIN1 mutation and its relevance for supporting HCC growth is still under debate.

4 Identifying genes whose altered expression in HCC may promote tumor progression and affect patient outcome

HCC is unusually resistant to all therapeutic interventions, and thus is associated with very high fatality. The reasons for the poor prognosis are mainly caused by the complex and variable pathogenesis and high rates of recurrence and metastasis [32, 33]. Generally, the 5-year overall survival rate (OS) for HCC patients with early stage disease is significantly higher than for patients at advanced stages [34]. Therefore, the best strategy for preventing liver cancer-related deaths is the early diagnosis.

Alpha-Fetoprotein (AFP) has long been the preferred biomarker to diagnose and assess the prognosis for HCC patients. AFP is however not entirely specific for HCC, and about half of the lesions do not clearly express this marker, meaning that a big proportion of liver cancers cannot be faithfully identified by AFP. For these and other

reasons assaying AFP levels is not recommended anymore as a biomarker for HCC by the American and European liver disease organizations [35].

Hence, it is necessary to explore other differentially expressed genes to greatly increase the accuracy and sensitivity of early diagnosis and prognosis prediction. For example, Hidenari et al found that FBP1 is specifically downregulated in HCC tissues, which facilitated tumor progression. Meanwhile, FBP1 can also serve as a prognosis marker and represents a potential therapeutic target [36]. Guo et al showed that miR-199a-5p promotes glycolysis and has potential as a prognosis marker for HCC patients [37].

In conclusion, exploring differentially expressed genes in liver cancers has important value for the early diagnosis, prediction of treatment responses and prognosis assessment. At the same time, if the proteins encoded by these differentially expressed genes play important roles in the disease process, they may even become potential therapeutic targets and contribute to personalized treatment.

5 The aim of this thesis

Hepatocellular carcinoma is a global public health issue all over the world. During the last few decades tremendous progress has been made in treating various tumor types by combinations of chemotherapy, immunotherapy, and targeted therapies. Nevertheless, for HCC patients who are in advanced stages of their disease, the 5-year survival rate is still very low (<10%). Therefore, it is necessary to better understand the complex mechanisms contributing to liver carcinogenesis. In view of this, we focused on two main issues in my thesis. Given the important role played by the Wnt/β-catenin signaling pathway in HCC development, the first aim is to study the function of the frequently mutated genes *CTNNB1* and *AXIN1*. In more detail we wish to understand how the novel identified mutations in the armadillo repeats 5 and 6 of β-catenin lead to enhanced signaling, to what extent AXIN1 mutations lead to enhanced β-catenin signaling, and to identify other mechanisms that may potentially affect β-catenin signaling in HCC.

As a second aim, we wished to identify genes whose altered expression in HCC may promote tumor progression and affect the prognosis of patients. To this aim, we screened the TCGA database for genes whose altered expression correlates with survival.

Next, candidate genes were evaluated by various in vitro assays. We identified *UCK2*, *MIR324*, and *CEBPD* as potential interesting targets of which the functional analysis of CEBPD is described in this thesis.

6 Outline of this thesis

In **Chapter 1,** I have reviewed how mutations within key components of the Wnt/β-catenin signaling pathway contribute to the progression and development of HCC, and described the general aim of the thesis.

In **Chapter 2,** we explore mechanisms that may potentially explain the increased signaling propensity of the hotspot mutations within armadillo repeats 5 and 6 of β-catenin. By doing so, we identify a novel mechanism of enhanced β-catenin signaling in cancer, as they lead to enhanced signaling through reduced binding to APC, while simultaneously retaining the interaction with their nuclear TCF/LEF transcriptional co-factors. Available structural and mutational data further support the observed change in relative binding affinities.

In **Chapter 3**, we show that AXIN1 inactivation leads to enhanced β-catenin signaling in a panel of HCC cell lines. These results question the strong statements that have been made in the literature, which suggest that *AXIN1* mutation in liver cancer does not lead to increased signaling. Secondly, we show that enhancing AXIN activity by tankyrase monotherapy does not significantly affect their growth.

In **Chapter 4**, we investigate to what extent nine HCC cell lines depend on extracellular Wnt secretion to support their growth. These cell lines are classified by mutations in either *CTNNB1*, *AXIN1* or no obvious mutation in a β-catenin signaling related component.

In **Chapter 5,** we found that the serine-threonine kinase receptor-associated protein (STRAP) protein is increased in expression in HCC tissues and regulates Wnt/β-catenin signaling activity in vitro.

In **Chapter 6** By analyzing the Cancer Genome Atlas (TCGA) and HCC tissue microarrays, we identify that *CEBPD* expression correlates with the prognosis of HCC patients. Next, we investigate its function and possible mechanism through which it contributes to HCC development.

The novel insights derived from this thesis will be summarized and discussed **in chapter 7.**

References:

1 Panel, A.I.H.G. (2015) Hepatitis C guidance: AASLD-IDSA recommendations for testing, managing, and treating adults infected with hepatitis C virus. *Hepatology* 62, 932-954

2 Flemming, J.A., *et al.* (2014) Risk prediction of hepatocellular carcinoma in patients with cirrhosis: the ADRESS-HCC risk model. *Cancer* 120, 3485-3493

3 Boffetta, P., *et al.* (2003) Meta-analysis of studies of occupational exposure to vinyl chloride in relation to cancer mortality. *Scandinavian journal of work, environment & health* 29, 220-229

4 Tsukuma, H., *et al.* (1990) A case-control study of hepatocellular carcinoma in Osaka, Japan. *International journal of cancer* 45, 231-236

5 Soini, Y., *et al.* (1996) An aflatoxin-associated mutational hotspot at codon 249 in the p53 tumor suppressor gene occurs in hepatocellular carcinomas from Mexico. *Carcinogenesis* 17, 1007-1012

6 Hashimoto, E., *et al.* (2004) Comparison of hepatocellular carcinoma patients with alcoholic liver disease and nonalcoholic steatohepatitis. *Alcoholism, clinical and experimental research* 28, 164S-168S

7 Blum, H.E. (2005) Hepatocellular carcinoma: therapy and prevention. *World journal of gastroenterology* 11, 7391-7400

8 Llovet, J.M., *et al.* (2008) Sorafenib in advanced hepatocellular carcinoma. *The New England journal of medicine* 359, 378-390

9 Nault, J.C., *et al.* (2013) High frequency of telomerase reverse-transcriptase promoter somatic mutations in hepatocellular carcinoma and preneoplastic lesions. *Nature communications* 4, 2218

10 Buendia, M.A. and Neuveut, C. (2015) Hepatocellular carcinoma. *Cold Spring Harbor perspectives in medicine* 5, a021444

11 Schulze, K., *et al.* (2015) Exome sequencing of hepatocellular carcinomas identifies new mutational signatures and potential therapeutic targets. *Nature genetics* 47, 505-511

12 Nelson, W.J. and Nusse, R. (2004) Convergence of Wnt, beta-catenin, and cadherin pathways. *Science* 303, 1483-1487

13 Katoh, M. (2002) WNT and FGF gene clusters (review). *International journal of oncology* 21, 1269-1273

14 Nusse, R. and Clevers, H. (2017) Wnt/beta-Catenin Signaling, Disease, and Emerging Therapeutic Modalities. *Cell* 169, 985-999

15 Liu, C., *et al.* (1999) beta-Trcp couples beta-catenin phosphorylation-degradation and regulates Xenopus axis formation. *Proceedings of the National Academy of Sciences of the United States of America* 96, 6273-6278

16 Pez, F., *et al.* (2013) Wnt signaling and hepatocarcinogenesis: molecular targets for the development of innovative anticancer drugs. *Journal of hepatology* 59, 1107-1117

17 Pilati, C., *et al.* (2014) Genomic Profiling of Hepatocellular Adenomas Reveals Recurrent FRK-Activating Mutations and the Mechanisms of Malignant Transformation. *Cancer Cell* 25, 428-441

18 Rebouissou, S., *et al.* (2016) Genotype-phenotype correlation of CTNNB1 mutations reveals different ss-catenin activity associated with liver tumor progression. *Hepatology* 64, 2047-2061

19 Rubinfeld, B., *et al.* (1993) Association of the APC gene product with beta-catenin. *Science* 262, 1731-1734

20 Valenta, T., et al. (2012) The many faces and functions of beta-catenin. The EMBO journal 31, 2714-2736

21 Zeng, L., *et al.* (1997) The mouse Fused locus encodes Axin, an inhibitor of the Wnt signaling pathway that regulates embryonic axis formation. *Cell* 90, 181-192

22 Taniguchi, K., *et al.* (2002) Mutational spectrum of beta-catenin, AXIN1, and AXIN2 in hepatocellular carcinomas and hepatoblastomas. *Oncogene* 21, 4863-4871

23 Behrens, J., *et al.* (1998) Functional interaction of an axin homolog, conductin, with beta-catenin, APC, and GSK3beta. *Science* 280, 596-599

24 Fagotto, F., *et al.* (1999) Domains of axin involved in protein-protein interactions, Wnt pathway inhibition, and intracellular localization. *The Journal of cell biology* 145, 741-756

25 Zhang, X., *et al.* (2012) Mechanistic insight into Myc stabilization in breast cancer involving aberrant Axin1 expression. *Proceedings of the National Academy of Sciences of the United States of America* 109, 2790-2795

26 Li, Q., *et al.* (2009) Axin determines cell fate by controlling the p53 activation threshold after DNA damage. *Nature cell biology* 11, 1128-1134

27 Liu, W., *et al.* (2006) Axin is a scaffold protein in TGF-beta signaling that promotes degradation of Smad7 by Arkadia. *The EMBO journal* 25, 1646-1658

28 Guo, X., *et al.* (2008) Axin and GSK3- control Smad3 protein stability and modulate TGF- signaling. *Genes & development* 22, 106-120

29 Bruix, J., *et al.* (2014) Hepatocellular carcinoma: clinical frontiers and perspectives. *Gut* 63, 844-855

30 Sherman, M. (2010) Hepatocellular carcinoma: epidemiology, surveillance, and diagnosis. *Seminars in liver disease* 30, 3-16

31 Zhang, T.T., *et al.* (2016) Factors affecting the recurrence and survival of hepatocellular carcinoma after hepatectomy: a retrospective study of 601 Chinese patients. *Clinical & translational oncology : official publication of the Federation of Spanish Oncology Societies and of the National Cancer Institute of Mexico* 18, 831-840

32 Chen, D.S., *et al.* (1984) Serum alpha-fetoprotein in the early stage of human hepatocellular carcinoma. *Gastroenterology* 86, 1404-1409

33 Hirata, H., *et al.* (2016) Decreased Expression of Fructose-1,6-bisphosphatase Associates with Glucose Metabolism and Tumor Progression in Hepatocellular Carcinoma. *Cancer research* 76, 3265-3276

34 Guo, W., *et al.* (2015) MiR-199a-5p is negatively associated with malignancies and regulates glycolysis and lactate production by targeting hexokinase 2 in liver cancer. *Hepatology* 62, 1132-1144

Chapter 2

A new mechanism for β-catenin stabilization in cancer through reduced APC binding

Pengyu Liu[1], Menggang Liu[1,2], Joyce H.G. Lebbink[3,4], Shan Li[1], Marla Lavrijsen[1], Maikel P. Peppelenbosch[1], Ron Smits[1*]

1. Department of Gastroenterology and Hepatology, Erasmus MC-University Medical Center, Rotterdam.

2. Department of Hepatobiliary Surgery, Daping Hospital, The Third Military Medical University, 10 Changjiangzhilu Daping, Chongqing 400042, China.

3. Department of Molecular Genetics, Cancer Genomics Netherlands, Erasmus MC, Rotterdam, The Netherlands

4. Department of Radiation Oncology, Erasmus MC, Rotterdam, the Netherlands

In revision for resubmission to Gastroenterology

Abstract:

Background and aims: The β-catenin signaling pathway is one of the most commonly deregulated pathways in cancer. Recently, amino-acid alterations within armadillo repeats 5/6 of β-catenin (residues K335, W383 and N387) are being recognized as novel hotspots for mutation, especially in liver cancers. The mechanism leading to their enhanced signaling activity is however completely unknown.

Methods: We analyzed a panel of β-catenin variants for differences in N-terminal phosphorylation, half-life and association with various partners relevant for signaling. Available protein structures were used to support our observations.

Results: The armadillo repeat mutants behave like wild-type protein in most assays. However, they associate weakly with APC, one of the core proteins of the destruction complex, while simultaneously retaining the interaction with their nuclear TCF/LEF co-factors, thereby permitting transcriptional activation of target genes. Available protein structures further support the observed change in relative binding affinities. In contrast to hepatocellular carcinomas where these armadillo repeat mutations appear to be the sole mutational activators of β-catenin signaling, in colorectal cancers co-occurrence with other "weak" mutations of the *APC* or *AXIN2* genes is often observed.

Conclusion: Our analyses uncover a novel mutational mechanism to increase β-catenin signaling in cancers. In contrast to the N-terminal mutations in β-catenin that directly impair its phosphorylation by GSK3 or binding to β-TrCP, the hotspot mutations within armadillo repeats 5 and 6 lead to enhanced signaling through reduced binding to APC, while simultaneously retaining the interaction with their nuclear TCF/LEF co-factors.

Keywords: Wnt/β-catenin signaling; hepatocellular carcinoma; APC; β-catenin; Armadillo repeat

Introduction

The β-catenin signaling pathway is one of the most commonly deregulated pathways among cancers.[1] In normal cells, β-catenin signaling is maintained at low levels by the so-called destruction complex consisting of the adenomatous polyposis coli (APC) tumor suppressor, scaffold proteins AXIN1, AXIN2, and the kinases GSK3 and CK1α. In this complex, CK1α initiates β-catenin phosphorylation at S45, followed by sequential GSK3 phosphorylation at T41, S37 and finally S33. Next, the phosphorylated 32DpSGXXpS37 motif promotes binding of the ubiquitin ligase β-TrCP, which targets β-catenin for proteasomal degradation. When cells are exposed to Wnt ligands, this β-catenin breakdown complex is temporarily inhibited, leading to the stabilization of β-catenin. As a result, it translocates into the nucleus and associates with members of the TCF/LEF family of transcription factors, thus regulating the expression of specific downstream Wnt/β-catenin target genes.[2, 3]

In several tumor types this pathway is constitutively activated through mutational (in)activation of one of the core elements of the destruction complex. In colorectal cancers predominantly 'loss-of-function' mutations are observed in the *APC* gene. For these mutations it has become well-accepted that they are selected on providing a "just-right" level of β-catenin signaling that is optimal for tumor initiation and progression.[4] Other tumor types, such as hepatocellular and endometrial carcinomas,[5-7] mainly acquire oncogenic β-catenin (*CTNNB1*) mutations at the N-terminal S/T phosphorylation residues, making the protein more resistant to proteolytic degradation. Recently, Rebouissou and co-workers showed that also for these *CTNNB1* mutations a clear genotype-phenotype correlation exists in liver cancer.[8] In-frame exon 3 deletions that remove the entire N-terminal phosphorylation domain and D32-S37 amino-acid alterations directly affecting the β-TrCP recognition motif, lead to highly active β-catenin variants. T41 mutations were associated with moderate activity, while S45 mutations showed a weak but clearly present activation of the pathway. The reduced activity of the latter two mutation types is most likely the result of residual phosphorylation of the β-TrCP interaction domain, leading to some breakdown of these mutants.[9] In this liver cancer study also two more recently recognized mutational *CTNNB1* hotspots were included, that is K335I and N387K, which are located in

armadillo repeat domains 5 and 6 of the β-catenin protein, respectively. Currently, according to the COSMIC website, [10] mutations at these residues have been observed in more than 100 individual tumors, especially in liver cancers (Figure 1). They lead to a weak but significant enhancement of β-catenin signaling. However, the mechanism leading to their increased activity is still unknown.[11] Here, by exploring potential mechanisms that may explain their increased signaling propensity, we identify a novel mechanism of enhanced β-catenin signaling.

Figure 1

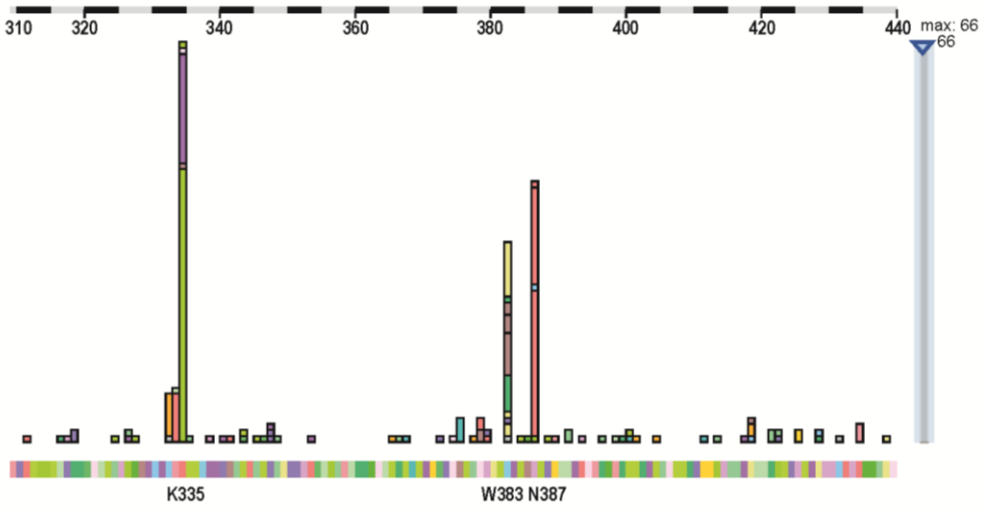

Figure 1. Oncogenic hotspot mutations observed in armadillo repeats 5 and 6 of β-catenin. Three amino acids are commonly mutated in cancers, that is K335, W383, and N387. Data were obtained from the COSMIC website (https://cancer.sanger.ac.uk/cosmic/gene/analysis?ln=CTNNB1), and filtered on amino acids 310-440; version of January 2019. The following alterations have been observed at least 4 times: Y333F 7x; E334K 8x; K335T 18x; K335I 46x; R376H 4x; W383C 12x; W383R 12x; W383G 7x; N387K 40x

Method

Database analyses

The TCGA LIHC illuminahiseq_rnaseqv2_RSEM_genes_normalized (MD5) data were obtained from the Broad Institute's Firehose GDAC website (http://firebrowse.org/?cohort=LIHC&download_dialog=true). In this dataset 373 hepatocellular carcinoma samples are available for which gene expression analysis was

performed. In addition, 50 paired adjacent tumor-free tissues are also available for gene expression analysis. The *CTNNB1* mutation status of these tumors was obtained from www.cbioportal.org using the Liver Hepatocellular Carcinoma (TCGA, PanCancer Atlas) study. Sample IDs were used to match the *CTNNB1* mutations with RNAseq levels of *AXIN2*, *GLUL*, and *LGR5*.

To obtain the cancer-related *CTNNB1* mutations depicted in Figure 1, we analyzed the COSMIC website (https://cancer.sanger.ac.uk/cosmic/gene/analysis?ln=CTNNB1) filtering it on amino acids 310-440. Data were updated until January 2019.

Plasmids and construction

N-terminal FLAG-tagged β-catenin variants were constructed by using the pcDNA-5′ UT-FLAG vector as previously described[12]. Briefly, the constructs of wild-type (WT), S33Y and exon3 deletion were generated by using the Gibson assembly method (NEB). Based on the WT backbone, all other variants which included G34V, S37F, T41A, S45P, Y333F, E334K, K335I, K335T, R376H, W383G, W383R, N387K and R582W mutations were constructed by using Q5 site-directed mutagenesis (NEB). β-catenin coding sequence of all variants was fully verified. The GFP-APC (1199-2167) plasmid was generated by cloning a 2.9 kb EcoRI fragment of mouse *Apc* into pEGFP-C1. It encodes all 20 amino acid β-catenin binding repeats and all AXIN-binding domains of APC. pcDNA3.1 myc-mβTrCP WD1-7 (241-569) was a gift from Michael Ruppert (Addgene # 62977)[13.] pCS2-MT mouse Axin (Axin MTFu1) was a gift from Frank Costantini (Addgene # 21287) and encodes an N-terminal 6xMyc-tagged mouse AXIN1 variant of 832 aa[14].

Cell culture

HEK293 cells (Mycoplasma-free) and HCT116 cells (Mycoplasma-free) were maintained in DMEM medium (Lonza, Breda, The Netherlands) supplemented with 10% fetal bovine serum (Sigma–Aldrich). Identity of cell lines was confirmed by STR genotyping.

Half-life determination

N-terminal FLAG-tagged β-catenin variant plasmids (200ng) were co-transfected into

HEK293 cells with pEGFP-C1 (50ng) using FuGENE® HD. The pEGFP-C1 plasmid generates a highly stable GFP protein serving as loading control. After 24 hours, the cells were treated with cycloheximide (50 µg/ml) for 0, 30, 60, 90, 120, and 150 minutes. Next, cells were washed with cold PBS for two times and lysed in 2x Laemmli sample buffer (120 mM Tris-Cl pH 6.8, 20% glycerol, 4% SDS) with 0.1 M DTT, and heated for 5 min at 95˚C.

Immunoprecipitation

For the immunoprecipitation (IP) assays, HEK293 cells were seeded in 6-well plates before transfection. When reaching 60-80% confluence, 1µg N-terminal FLAG-tagged β-catenin variant plasmids were co-transfected with either 1µg of APC-, AXIN- or βTrCP-expression plasmids by using FuGENE® HD. A similar approach was used for the HCT116 cells. After 24 hours, cells were washed by cold PBS two times and then cold 500 µl lysis buffer was added to each well for 15 minutes. Our main lysis buffer consisted of 30 mM Tris-Cl pH 7.4, 1% Triton X-100, 150 mM NaCl, 5 mM EDTA, 5mM NaF. For the β-TrCP and a subset of GFP-APC co-IP experiments we used the following lysis buffer: 10 mM Hepes pH 7.9, 100 mM NaCl, 1.5 mM MgCl2, 0.1% NP40. To the lysis steps Halt™ Protease Inhibitor Cocktail (Thermo Scientific™) was added according to the manufacturer's instructions. Cells were collected by scraping and lysate was cleared at 4°C by centrifugation at 11,000g for 15 minutes. From the cleared lysate, 10% was taken as input control to which directly the same volume of 2x Laemmli/DTT was added followed by heating for 5 min at 95˚C. To the remainder of the supernatant we added 10µl pre-washed ANTI-FLAG® M2 Affinity Gel (Sigma-Aldrich) followed by incubation at 4˚C for 2 hours. Next, FLAG-beads were centrifuged and washed with lysis buffer for three times. Finally, the pellet was lysed in 50 µl 2x Laemmli sample buffer with 0.1M DTT, and heated.

Western blotting, antibodies and quantification

Fluorescent western blotting and quantitative analysis were performed basically as previously described[15]. The following primary antibodies were used: anti-FLAG (clone M2) Mouse mAb (Sigma-Aldrich #F3165), anti-P-β-Catenin (Ser33/37) Rabbit pAb (CST #2009), anti-P-β-Catenin(Ser33/37/Thr41) Rabbit pAb (CST #9561), anti-P-β-Catenin (Thr41/Ser45) Rabbit pAb (CST #9565), anti-P-β-Catenin (Ser45) Rabbit pAb (CST

#9564), anti-TCF4 (clone 6H5-3) Mouse mAb (Merck #05-511), anti-E-Cadherin (clone 24E10) Rabbit mAb (CST #3195), anti-Myc tag Rabbit pAb (Abcam ab9106), anti-GFP Tag Rabbit pAb (Thermo Fisher Scientific # A-11122) . A 1:1000 dilution was used for all the primary antibodies. As secondary antibodies we used anti-rabbit or anti-mouse IRDyeconjugated antibodies (LI-COR Biosciences, Lincoln, USA). Protein intensity was detected with the Odyssey 3.0 Infrared Imaging System and analyzed by Image Studio Lite Ver5.2.

β-catenin reporter assays

HEK293 cells were seeded in 24-well plates to reach approximately 50% confluency on the day of transfection. Each well was transfected with 5 ng of the β-catenin expression vectors, 250 ng Topflash or Fopflash, and 10 ng CMV-Renilla using Fugene HD (Promega). After two days, luciferase activities were measured in a LumiStar Optima luminescence counter (BMG LabTech, Offenburg, Germany) and normalized for transfection efficiency by using the Dual Luciferase Reporter Assay system (Promega) according to the manufacturer's instruction. Transfections were performed in triplicate and the mean and standard error were calculated for each condition. The β-catenin reporter activities are shown as TOP/FOPflash ratios.

Structure analysis

Structures were analyzed and figures were created using the PyMOL Molecular Graphics System, Version 2.0 Schrödinger, LLC. Overlays were created by superimposing β-catenin (chain A) from the β-catenin-TCF complex (1G3J.pdb), β-catenin-E-cadherin complex (1I7W.pdb) or the β-catenin-AXIN (1Q27) onto chain A of the β-catenin-phosphorylated 20AA APC complex (1TH1.pdb).

Statistical method

Multiple group comparisons were performed by one way analysis of variance (ANOVA) followed by Tukey-Kramer tests. $P<0.05$ (indicated in the figures as single asterisk) was considered statistically significant. Meanwhile, $P<0.01$ (double asterisks) and $P<0.001$ (triple asterisks), and $P<0.0001$ (quadruple asterisks) were regarded as highly significant. All statistical analyses were performed using GraphPad Prism 6.

Results

Confirmation of the association of CTNNB1 mutation type with target gene expression

Previously, Rebouissou and coworkers have shown that specific correlations exist between β-catenin mutation type and target gene expression[8]. To confirm their results, we analyzed an independent dataset, that is the Cancer Genome Atlas (TCGA) liver cancer cohort, which includes 373 hepatocellular carcinoma (HCC) cases that were analyzed by whole-exome sequencing.7 In total 97 cases (26%) were identified carrying a CTNNB1 mutation, for which RNA expression profiles were available in 96 cases. We correlated the CTNNB1 mutation type to expression of the β-catenin target genes AXIN2, GLUL and LGR5 and compared them with 50 normal adjacent liver tissues (Supplemental Figure S1). Basically, the same trends were observed as previously reported. Mutations in the D32-S37 region lead to the highest induction of target gene expression, followed by T41 and S45 mutations. K335 and N387 mutations associated with the least activation of target genes, and especially the N387 mutant tumors showed no obvious induction of target genes exceeding those of normal liver tissue, although only 4 tumors were available with N387 mutation. The weak induction associated with those latter two mutations is in line with β-catenin reporter assays performed by others, showing that these mutants lead to a modest 1.5-3 fold increase in signaling compared with the wild-type protein[8, 16].

Half-life time of β-catenin mutants correlates with their activation potential

The signaling activity of β-catenin is strongly regulated by proteolytic degradation. Therefore, we analyzed the half-life times of various commonly observed β-catenin variants in comparison with wildtype protein. To this aim, we generated N-terminal FLAG-tagged β-catenin variant expression vectors. These were transiently co-transfected in HEK293 cells with EGFP-C1 generating a highly stable GFP protein serving as loading control. Next, cells were treated with cycloheximide to block new protein synthesis, followed by protein preparation at the indicated time points (Figure 2). Interestingly, K335I and N387K variants seem to have almost the same protein

stability as wild-type β-catenin, with half-life times between 65-100 minutes. The S45P mutation increases the half-life up to 110 minutes, while mutations affecting the D32-S37 β-TrCP binding motif extend it to more than 2 hours. Especially the EX3-del variant in which the N-terminal domain encoding all S/T phosphorylation residues is deleted, leads to a highly stable protein for which we cannot determine an exact half-life during our time of analysis. Thus, these analyses show that protein stability largely correlates with the reported signaling activities, that is, mutants with weak enhanced signaling capabilities show a turnover comparable to the wild-type protein, whereas more active signaling variants show a clearly increased half-life.

Figure 2

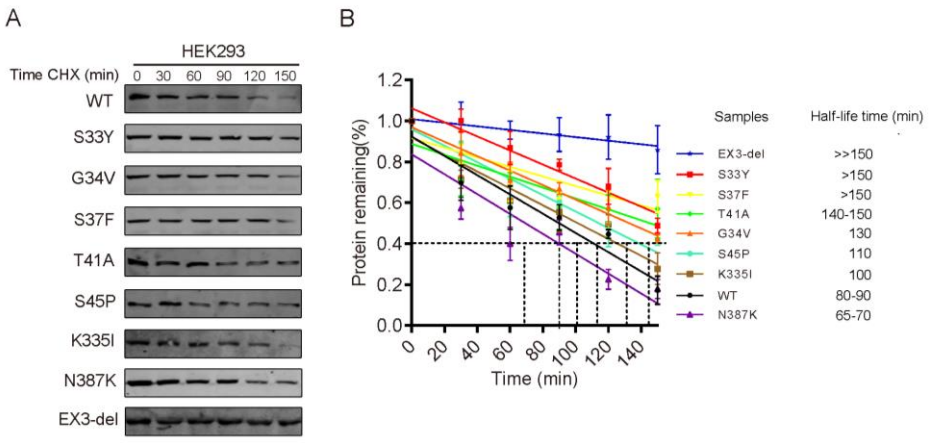

Figure 2. Half-life time determination of β-catenin mutants. (A) Indicated FLAG-tagged β-catenin variants were co-transfected with pEGFP-C1 into HEK293 cells, followed by cycloheximide (CHX) treatment to block new protein synthesis for the indicated times. Next, quantitative fluorescent western blotting was performed using the highly stable GFP protein for transfection normalization. (B) Values obtained for the 0 hr time point were arbitrarily set to 1. Normalized values for other time points were plotted. Linear regression was performed to estimate the half-life for each variant, which is depicted on the right. Experiment was performed at least 3 times for each variant producing similar trends in each experiment.

K335 and N387 variants are not affected in N-terminal phosphorylation and β-TrCP binding

β-catenin protein stability is largely regulated by the sequential N-terminal S/T phosphorylation. Hence, we determined the phosphorylation status of transfected β-catenin variants (Figure 3A). In line with expectation, the shortened mutant product generated by the EX3-del variant cannot be recognized by any of the phospho-antibodies.

All other variants are readily phosphorylated at S45 comparable to the wild-type protein, except for the S45P mutant. In contrast, the GSK3 mediated phosphorylation at residues T41, S37 and S33 is reduced in all S33 to S45 mutants. In accordance with previous reports, we still observed some residual S/T phosphorylation in all these variants[9]. Importantly, in this over-expression assay the K335 and N387 mutants showed no obvious deviation from the phosphorylation pattern observed for the wild-type protein.

Next, we determined the binding capacity of β-TrCP to each variant. To this aim, we co-transfected them with a Myc-tagged β-TrCP expression vector followed by FLAG-tagged β-catenin immunoprecipitation (IP). As the interaction between both proteins is short-lived because of the rapid turnover by the proteasome, we applied 2 hr proteasome inhibition using MG132 prior to precipitation. Our IP-protocol resulted in a weak unspecific binding of Myc-tagged β-TrCP in the negative control (lane 2 of Figure 3B). For the S33-S45 mutants similar or at most slightly increased levels of co-IPed β-TrCP were observed, whereas both K335 and N387 mutants showed equal binding capabilities comparable to the wild-type protein. Overall, these analyses show that K335I and N387K mutant proteins are not seriously affected in N-terminal phosphorylation and binding to β-TrCP.

Figure 3

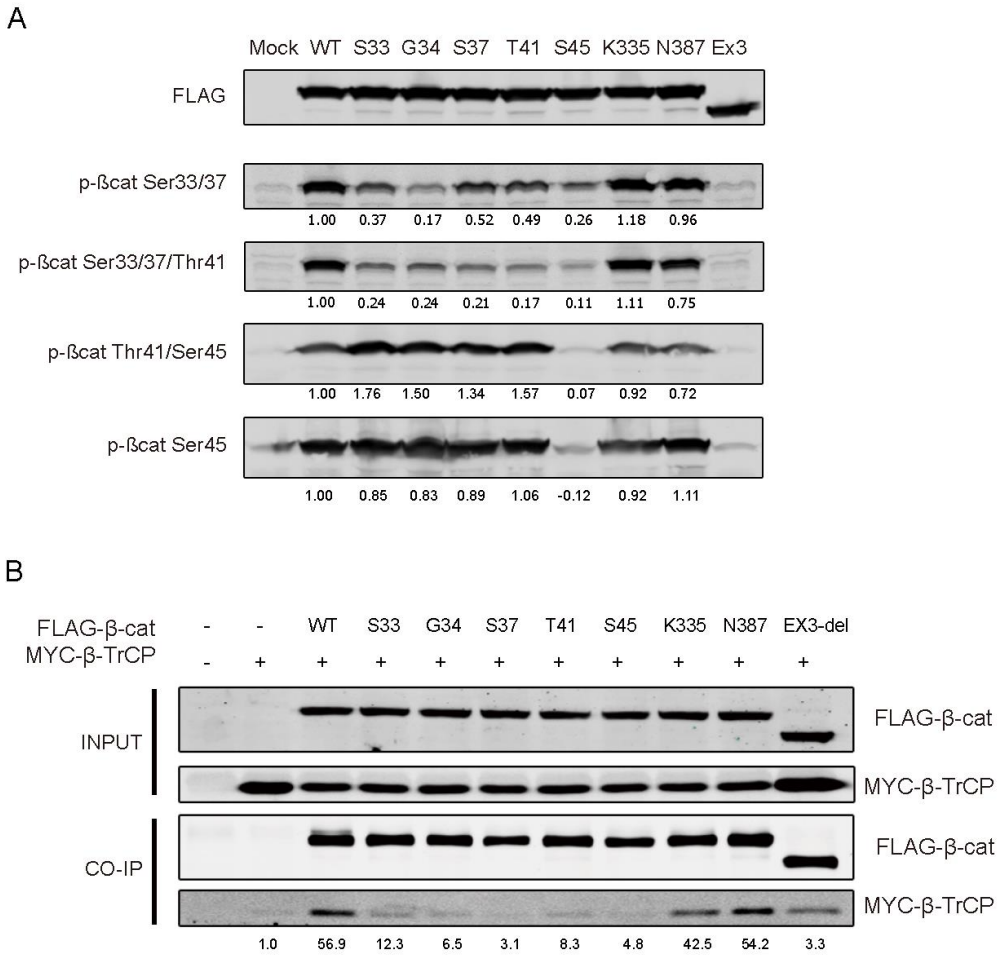

Figure 3. K335 and N387 variants are not affected in N-terminal phosphorylation and β-TrCP binding. (A) Indicated FLAG-tagged β-catenin variants were transfected in HEK293 and subjected to western blotting with phospho-specific β-catenin antibodies. Signals were quantified with Odyssey software. The weak full-length β-catenin band visible in the mock and Ex3-del transfected lanes is signal from the endogenous HEK293 β-catenin protein. This signal was subtracted from the values of the transfected variants before determining their signal intensity. Signal of the wild-type (WT) protein was arbitrarily set to 1. All other values are normalized relative to WT and depicted below the bands. The K335I and N387K variants are similarly phosphorylated as the wild-type protein. Antibody specificities as provided by Cell Signaling Technology are as follows: p-βcat Ser33/37 recognizes β-catenin when phosphorylated at Ser33 OR Ser37, or both; p-βcat Ser33/37/Thr41 recognizes any phosphorylation at Ser33/37/Thr41 except for pSer33 alone; p-βcat Thr41/Ser45 recognizes pThr41 OR pSer45, or both. FLAG-tagged β-catenin variants were co-transfected with Myc-tagged β-TrCP into HEK293 cells. (B)Two hours prior to IP with FLAG-beads, cells were treated with the proteasome inhibitor MG132. The amount of co-IPed β-TrCP was determined after normalization with β-TrCP input signal. Signal of IP obtained with Myc-tagged β-TrCP alone was arbitrarily set to 1. The K335I and N387K variants are not affected in their association with β-TrCP.

K335 and N387 variants show reduced binding to the APC protein

As protein half-life, N-terminal phosphorylation and β-TrCP binding are not clearly affected for the K335I and N387K variants, we sought for an alternative explanation explaining their slightly increased signaling behavior. Both residues are located in armadillo repeats 5 and 6 of β-catenin in the center of the protein. In total 12 armadillo repeats form a superhelix with a positively charged groove, which can associate with a large number of proteins.[2] We focused on well-established binding partners at the cell membrane, nucleus and within the destruction complex, that is E-cadherin, TCF7L2 (also known as TCF4), AXIN1, and APC. Except for AXIN1, these have all been shown to bind an extended area encompassing both K335 and N387 residues (Figure 4A). Within epithelial cells, most β-catenin is captured at the cell membrane through interactions with cadherins. Hence, a reduced binding affinity between β-catenin and E-cadherin is expected to increase the signaling pool of β-catenin, possibly leading to enhanced nuclear signaling. However, immunoprecipitation of wild-type, K335I and N387K variants from HCT116 cells showed no altered binding to E-cadherin (Figure 4B). Alterations in binding to TCF7L2 within the nucleus are also expected to affect activation of β-catenin target genes, but again we failed to show any difference between the tested variants (Figure 4B). Likewise, binding of a co-transfected MYC-tagged AXIN1 was not affected by both mutations (Figure 4C), which is to be expected given that AXIN1 associates most prominently with repeats 3 and 4.[17, 18] In contrast, binding of a co-transfected GFP-tagged APC fragment was strongly impaired for the K335I and N387K mutants (Figure 4D). Taken together, these IP experiments show that compared to wild type β-catenin, both mutants associate less strongly with APC, one of the core proteins of the destruction complex.

Figure 4

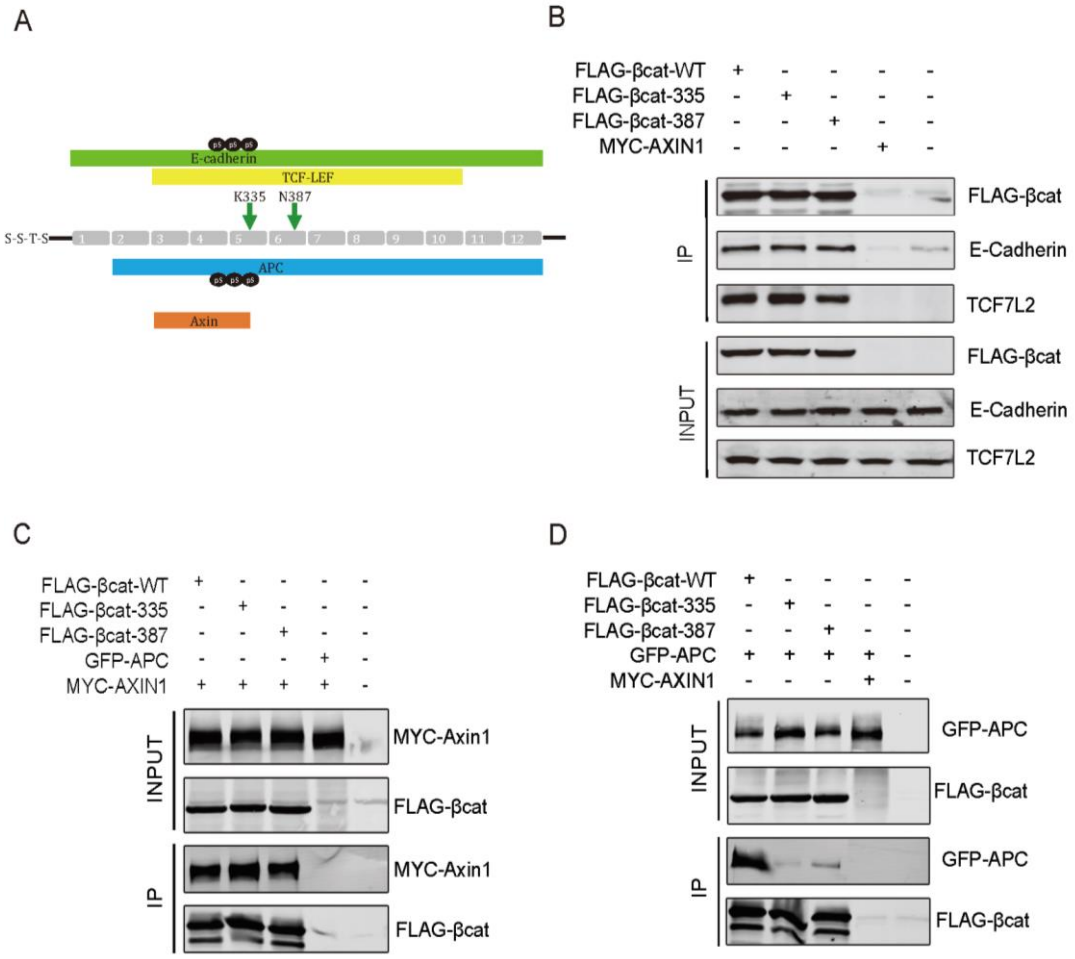

Figure 4. K335I and N387K variants selectively show reduced binding to APC. (A) Schematic representation of the reported binding domains of APC, AXIN, TCF/LEF and E-cadherin to the armadillo repeat region of β-catenin. Position of K335I and N387K mutations are indicated by arrows. pS indicates Serine phosphorylation present at binding interface of APC or E-cadherin. (B) FLAG- tagged WT, K335I and N387K β-catenin variants were transfected in HCT116 cells. Transfection with Myc-tagged AXIN1 and non-transfected cells were used as negative controls. Following FLAG-IP, endogenous E-cadherin and TCF7L2 were shown to bind equally to wild-type β-catenin and both variants. (C) The same β-catenin variants were co-transfected with Myc-tagged AXIN1 into HEK293 cells. All variants bind equally to AXIN1. (D) Co-transfection with GFP-APC in HEK293 cells. GFP- APC expresses a GFP-tagged murine APC fragment (aa 1199-2167) encoding all the 20 amino-acid repeats binding to β-catenin and all AXIN-binding domains. Both the K335I and N387K variants associate much weaker to GFP-APC. In the latter two experiments co-transfection of GFP-APC and Myc-AXIN1 was used as negative IP-control. All transfections experiments were performed at least 3 times with identical results

Protein structures of β-catenin complexes provide a rationale for reduced binding of mutant β-catenin selectively to the APC protein

To identify potential mechanisms underlying the differential binding of AXIN1, APC, TCF7L2 and ECadherin to both mutants, we analyzed available protein structures of β-catenin in complex with fragments of these proteins (Figure 5A).[18-21] In all complexes, K335 from β-catenin forms a hydrogen bond with a backbone carbonyl oxygen of the bound partner protein (Figure 5B-D). In addition, K335 forms specific interactions with sidechains from the bound proteins, which are different for each partner and depend on its phosphorylation status. APC contains four 15-amino acid repeats (AAR) and seven 20-AARs that directly associate with β-catenin. The latter contain a conserved SxxxSLSSL motif that is phosphorylated on multiple Serine sidechains by GSK3 and CK1 when APC is associated with AXIN, which strongly increases the binding to β-catenin.[21-23] Interestingly, in the β-catenin-APC complex the positively charged K335 sidechain forms ionic interactions and hydrogen bonds with two negatively charged phosphorylated Serines (pS1504 and pS1507) in the APC 20-AAR motif (Figure 5B), all of which are lost when the Lysine is mutated to Isoleucine. In the β-catenin-TCF complex, no Serines are available within this region for phosphorylation, instead K335 forms a single ionic interaction with the negatively charged sidechain of D40 (Figure 5C). E-cadherin carries a phosphorylated Serine (S692) at the corresponding position of APC-Ser1507 and forms an ionic bond with K335, however it carries an apolar A688 at the position corresponding to the phosphorylated S1504 in APC (Figure 5D). In AXIN only hydrophobic residues are present at this interface (not shown), which form weak van der Waals contacts with the polar amine of K335, but might form more favorable contacts when the Lysine is mutated to hydrophobic Isoleucine. Summarized, K335 forms more energetically favorable interactions with APC than with any of the other proteins, explaining the observed relatively large effect of mutation of K335 on APC binding specifically. The mutation of N387 to Lysine will influence hydrogen bond formation between β-catenin and the peptide backbone of APC, LEF/TCF and E-cadherin, and is expected to reduce the strength of the interaction in all complexes (Figure 5E, Supplemental Figure S2A/S2B). In this case the structural analysis provided no direct clues explaining the reduced binding of specifically APC to this variant.

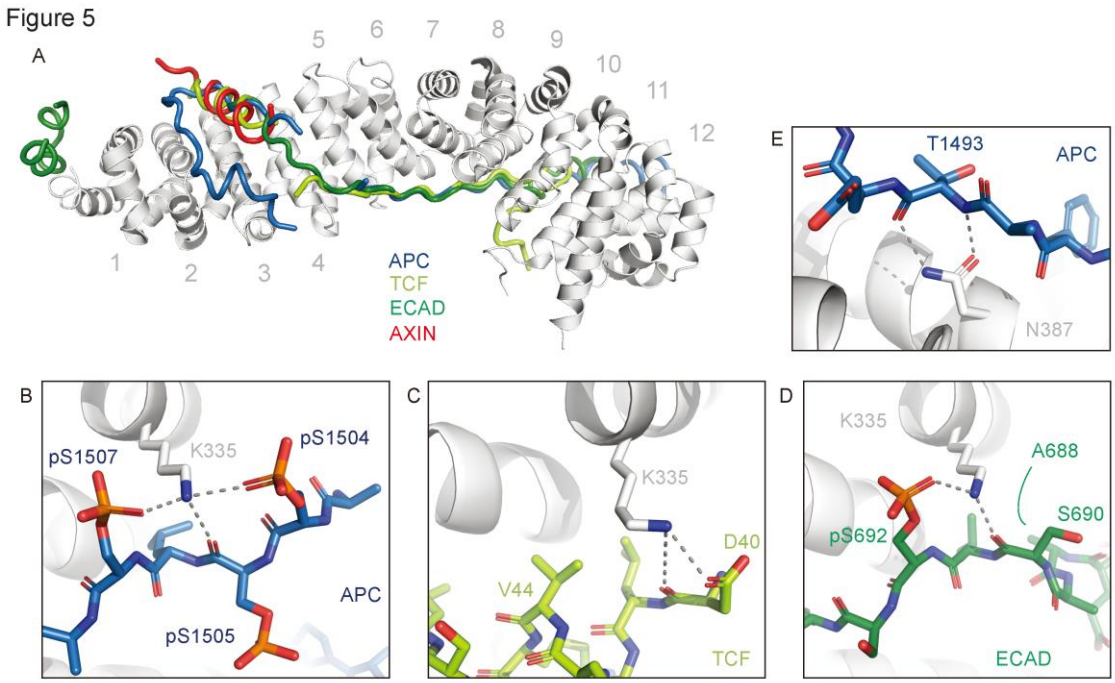

Figure 5. K335 and N387 directly interact with APC, TCF/LEF and E-cadherin. (A) Cartoon representation of β-catenin in grey with its 12 armadillo repeats numbered. Bound APC (blue;1TH1.pdb), TCF (yellow;1G3J.pdb), E-cadherin (green;1I7W.pdb) and AXIN (red;1QZ7.pdb) share binding sites in the β-catenin groove and are shown as tube representation. (B-E) Details of the complexes depicted with β-catenin as cartoon and bound ligands as stick representation with carbons in the same color code as panel A; oxygen atoms in red, nitrogen atoms in dark blue, phosphorus in orange. (B) K335 from β-catenin forms two ionic interactions and three hydrogen bonds (dashed lines) with phosphorylated Serine residues and backbone atoms of APC. (C) K335 from β-catenin forms one ionic bond and two hydrogen bonds (dashed lines) with the sidechain and backbone of D40 in TCF. (D) K335 from β-catenin forms one ionic bond with phosphorylated S692 and a hydrogen bond (dashed line) with the backbone of E-cadherin. (E) N387 from β-catenin forms two hydrogen bonds (dashed lines) with backbone atoms of T1493 in APC

Selective loss of APC binding is a common feature of armadillo repeat 5 and 6 mutations

Currently, more than 150 individual neoplasias have been identified carrying amino acid alterations in repeats 5 and 6 of β-catenin (Figure 1). Besides the K335 and N387 amino acid alterations, residues Y333, E334, R376 and especially W383 are also mutated in neoplasias regularly. Within the β-catenin structure these residues are organized in two clusters in close proximity of each other (Figure 7A). We generated

expression plasmids for these variants and tested them for binding to APC, TCF7L2 and Ecadherin. We also took along one commonly observed R582W variant (n=14) located towards the end of the armadillo repeats. As can be seen in Figure 6 most of these newly generated mutants show a loss of binding to APC, while all retain binding to TCF7L2 and E-cadherin. The only exceptions are the E334K and R582W variants that behave identical to wild-type protein with respect to APC binding.

Next, we performed β-catenin reporter assays for all the armadillo repeat 5 and 6 variants taking S33Y and wild-type β-catenin along as controls (Figure 6C). All variants showing a reduced binding to APC, yield a 1.5-3 fold higher induction of reporter activity compared with wild-type, while the E334K and R582W variants behave similar to wild-type. Importantly, analysis of the available protein structures shows that all additional mutated residues associated with increased signaling (Y333, R376, and W383), form direct interactions with APC (Figure 7B/7C). In fact, binding of cluster 1 residues of APC to β-catenin creates an extensive network in which oppositely charged groups alternate and form multiple ionic interactions and hydrogen bonds with neighboring residues. Any mutation in this network will affect several highly optimized interactions, explaining the relatively large effect on APC binding that we have observed. E334 does not form direct interactions with APC, possibly explaining its lack of increased signaling when mutated, although it may be involved in proper orienting the R376 residue (Figure 7B).

In TCF and E-cadherin, the highly cooperative cluster 1 network is much reduced in size due to replacement of crucial Serine side chains (that are phosphorylated in APC) with hydrophobic residues (V44 in TCF and A688 in E-cadherin; Supplemental Figure S2C/S2D). These apolar residues cannot favorably interact with the polar side chains in cluster 1, which means that the contribution of cluster 1 to the stability of TCF and cadherin complexes with β-catenin is weaker than for APC, explaining why cluster 1 mutations have a relatively smaller effect on binding of TCF and cadherin than on APC binding. In cluster 2, the sidechain of W383 forms van der Waals contacts with two Threonine residues on APC, forming a small hydrophobic core that contributes to the stability of the complex (Figure 7C). Mutation of W383 will disrupt this energetically favorable region, resulting in loss of APC binding. TCF residues are further away from and do not interact with the side chain of W383 in beta-catenin, and mutation of W383

will not affect stability of the TCF complex (Figure S2E). The situation is less clear in E-cadherin, in which favorable interactions between W383 from β-catenin and Y681 from E-cadherin are formed (Figure S2F).

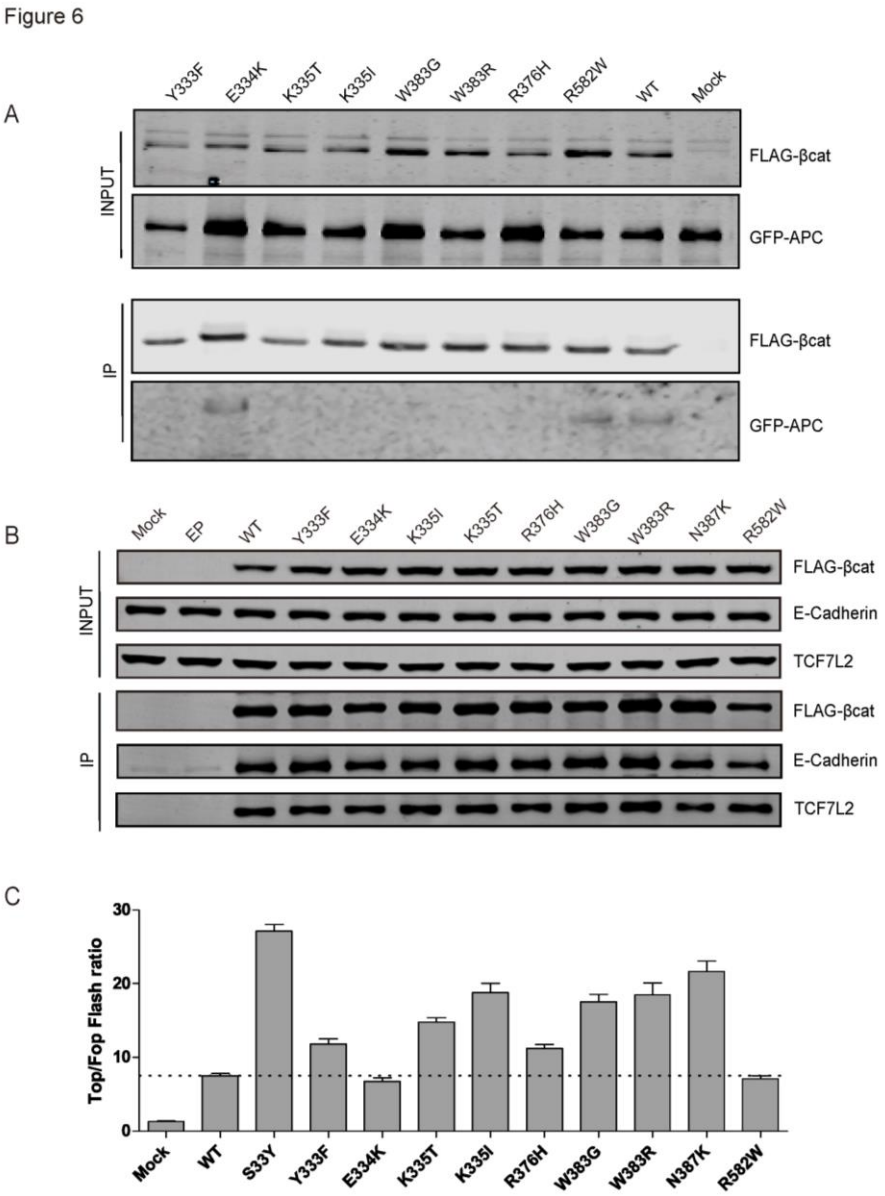

Figure 6. Increased signaling and selective reduction of APC binding for most armadillo repeat 5 and 6 variants. (A) Co-transfection of indicated FLAG-tagged β-catenin variants with GFP-APC in HEK293 cells. Following FLAG-IP, most of the commonly observed armadillo repeat 5 and 6 variants associate much weaker to GFP-APC. Exceptions are the E334K variant and the R582W located towards the end of the armadillo repeats. (B) FLAG-tagged β-catenin variants were transfected in HCT116 cells. Following FLAG-IP all variants are shown to bind equally to endogenous TCF7L2 and E-cadherin. (C) A Top-Fopflash β-catenin reporter assay in HEK293 cells shows that all armadillo repeat 5 and 6 variants that bind weaker to APC show a 1.5-3 fold increased signaling compared with wild-type β-catenin. Top-Fopflash ratios are shown. All experiments were performed in triplo and repeated twice

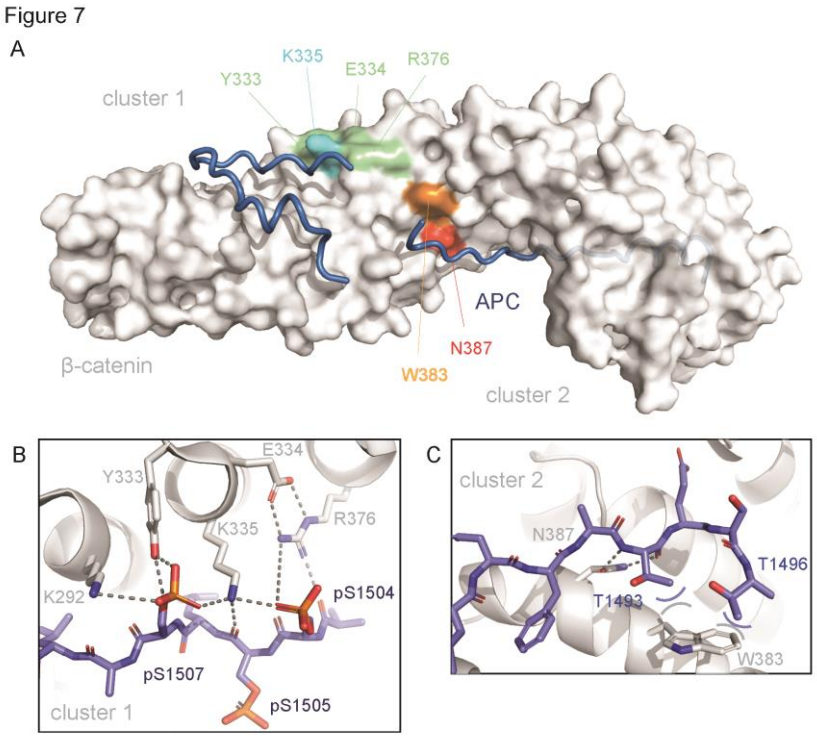

Figure 7. Armadillo repeat 5/6 residues on β-catenin involved in enhanced signaling are organized in two clusters. (A) Surface representation of β-catenin in grey with bound APC as tube representation in blue. K335 in cluster 1 is colored light blue, with surrounding residues Y333, E334 and R376 in light green. N387 in cluster 2 is colored red, while the other commonly mutated W383 is colored orange. B) Details of the complex at cluster 1, with β-catenin as grey cartoon and APC as blue stick representation. A six-residue ion-pair network is formed between E334-R376; R376-pS1504; pS1504-K335; K335-pS1507; pS1507-K292. In fact, the network is even bigger and extends beyond K292 (not shown here). Hydrogen bonds are indicated with dashed lines. C) Details of the complex at cluster 2. Hydrogen bonds are indicated with dashes. W383 packs against the hydrophobic methyl- groups (blue carbons) of the side chains of T1493 and T1496 and so forms favorable van der Waals interactions (indicated with curved lines)

Armadillo repeat 5 and 6 mutations co-occur with other β-catenin enhancing mutations in colorectal, but not in hepatocellular carcinomas

Mutations in the repeats 5 and 6 region of β-catenin have been mainly reported in liver cancers, Wilms tumors and those of the large intestine,[5, 8, 24-27] and anecdotally in several other tumor types. The stronger activating β-catenin mutations encompassing exon 3 have been shown to occur in a mutually exclusive fashion with disease-causing APC mutations,[28] showing that either the oncogenic β-catenin or inactivating APC

mutation is sufficient to drive tumorigenesis. When we analyzed the colorectal cancers carrying armadillo repeat 5 and 6 mutations for concomitant defects in other genes linked to β-catenin signaling, these were observed in 11 out of 13 cancers present in the cbioportal database (Supplemental Table S1). Seven out of 13 cancers carried APC mutations, but interestingly 3 out of 7 express a truncated APC protein that is expected to retain a significant level of β-catenin regulation, that is 3 or more of the 20 AARs.[4] Three other cancers carry truncating AXIN2 or RNF43 mutations that are generally also considered to be weak activators of signaling. A similar analysis of 21 hepatocellular carcinomas identified no accompanying mutations that are expected to affect β-catenin signaling, except for a single truncating ZNRF3 mutation in one lesion (Supplemental Table S2). Thus, in contrast to liver cancers, the armadillo hotspot mutations observed in colorectal cancers are often accompanied by other "weak" mutations that may synergistically enhance β-catenin signaling to levels supporting tumor growth.

Discussion

The β-catenin signaling pathway is one of the most commonly deregulated pathways among cancers.[1] In colorectal cancers this is predominantly accomplished by inactivating *APC* mutations, while e.g. in liver cancers aberrant activation has been mainly attributed to activating somatic mutations in the *CTNNB1* gene (20-25%).[4, 7, 29-31] The exon 3 related β-catenin mutations acquire enhanced signaling activities by interfering with proper N-terminal phosphorylation and subsequent proteolytic degradation. Instead, we uncover a novel mode of action for the armadillo repeat 5 and 6 mutations (exons 7 and 8), that is they reduce the binding to APC, while simultaneously retaining binding to TCF/LEF. The latter is important to allow sufficient enhancement of β-catenin target genes driving tumor formation. A weaker binding to APC is expected to increase the signaling pool of β-catenin, thereby enhancing the expression of β-catenin target genes driving tumor formation. If such a mutation would however simultaneously reduce binding to the essential nuclear TCF/LEF transcriptional co- factors, the overall activation of target genes would not increase or even be reduced compared to wild- type β-catenin. In accordance, mutation of K312 and K435 residues is rarely observed. These so-called "charged buttons" of β-catenin are essential for binding of most proteins to the armadillo superhelix by forming an

ionic bond to conserved glutamate residues.[19,32]

Mapping the mutated residues on the protein structure of β-catenin, two clusters emerge that appear critical binding domains with APC (Figure 7A). Cluster 1 is centered around K335 and further involves residues Y333 and R376. Previously, these have all been identified to directly interact with phosphorylated 20AA repeats of APC, but also to some extent with cadherins and TCF/LEF.[21] However, the IP experiments show that their mutation selectively results in loss of APC binding, while leaving binding to TCF and E-cadherin unaffected. For the K335 residue itself, the structural analyses provide a rationale as it forms more energetically favorable interactions with APC than with any of the other proteins. Likewise, the structural analyses reveal that Y333 is not critical for TCF binding, while R376 is not important for cadherin binding. It is interesting to consider that an extensive ion-pair network is formed upon β-catenin-APC complex formation, while much smaller, fragmented networks are present in the TCF and E-cadherin complexes. Ion-pair networks are cooperative entities from which removal of a single residue through mutation will have a relatively large effect on the stability of this region.[33-35] this may explain why the mutation of K335 has a much larger effect on complex formation with APC (in which it is a central residue forming multiple ionic bonds) than on complex formation with TCF and E-cadherin (in which the Lysine is a peripheral residue in the smaller network). Cluster 2 involves residues W383 and N387. Previously, the W383 residue was already identified as important for APC binding as a W383A mutant failed to bind APC, while retaining LEF/TCF7L2 association,[17] which is in accordance with the structural analyses because TCF does not interact with W383. For the commonly mutated N387 residue the structural analysis provided no direct clues explaining the reduced binding of specifically APC. Nevertheless, our IP and structural analyses provide clear evidence that both clusters are more relevant for APC binding than TCF and cadherins.

Despite two decades of research the exact mechanism through which APC functions in the destruction complex is still not fully understood. Several models not necessarily excluding each other have been proposed.[36, 37] One model proposes that APC is involved in sequestering β-catenin within the cytoplasm, thereby preventing it from entering the nucleus.[38, 39] Other models suggest that APC protects S/T phosphorylated

β-catenin from dephosphorylation by PP2A, that it may be required to interface β-catenin with the ubiquitin and proteasome machinery, or that it is required to displace AXIN from phosphorylated β-catenin to allow a new cycle of β-catenin breakdown.[18, 40, 41] Whichever model will turn out to be true, in all cases a weaker association of mutant β-catenin with APC will make the process less efficient and effectively lead to more signaling.

How to reconcile the weak APC/mutant β-catenin interaction with the rather modest increased signaling activity associated with these variants? Current models of APC's contribution to the destruction complex propose that direct binding of β-catenin to APC is not absolutely required for a proper level of β-catenin turnover, as long as APC is present within the destruction complex, for example through binding to AXIN.[36, 37, 39, 42] This (partial) functional redundancy between APC and AXIN is most likely also responsible for keeping the signaling activity of the armadillo repeats 5/6 mutants in check, although it will be less efficient when compared with wild-type β-catenin.

Mutations in this region of β-catenin have been mainly reported in liver cancers, Wilms tumors and those of the large intestine,[5, 8, 24-27] and anecdotally in several other tumor types, but their true frequency is probably underestimated as in the past *CTNNB1* mutation analysis was largely restricted to the exon 3 hotspot. Therefore, whole-exome or genome mutational analyses that are becoming more routine procedures for tumor investigations nowadays, are likely to uncover more frequently these specific mutations. Given their weak activation nature, these mutations are more likely going to be identified in tumor types that require a minimal to moderate activation of the pathway to support their growth.[4, 43, 44] In that respect, their presence in colorectal cancer was somewhat surprising as these cancers generally select for higher levels of β-catenin signaling.[4] Our analysis shows however that in colorectal cancer the armadillo hotspot mutations are often accompanied by other "weak" mutations that synergistically may enhance β-catenin signaling to levels supporting tumor growth. A similar scenario may be at work for Wilms tumors, in which the armadillo repeat 5 and 6 mutations often associate with those of *WTX* (official name *AMER1*), [27] which also leads to a modest signaling enhancement. In liver cancers however, the weak signaling associated with these mutated armadillo repeat variants

appears to be sufficient to support tumor growth as they are not clearly associated with defects in other Wnt/β-catenin signaling related components.

In conclusion, our molecular and structural analyses uncover a novel mutational mechanism of enhanced β-catenin signaling. In contrast to the N-terminal mutations in β-catenin that directly impair its phosphorylation by GSK3/CK1α or binding to β-TrCP, the hotspot mutations within armadillo repeats 5 and 6 lead to enhanced signaling through reduced binding to APC, while simultaneously retaining the interaction with their nuclear TCF/LEF transcriptional co-factors. The latter is important to allow sufficient enhancement of β-catenin target genes driving tumor formation. A second difference with the N-terminal mutants appears to be that they often co-occur with other mutations affecting β- catenin signaling, at least in colorectal and Wilms tumors

Supplemental Figure S1

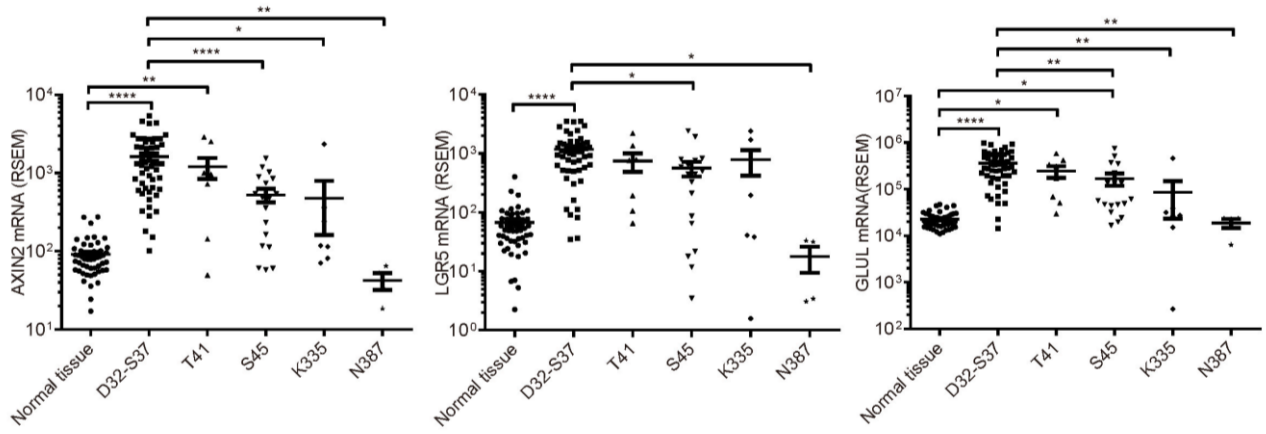

Supplemental Figure S1. Association of CTNNB1 mutation type with target gene expression confirmed. Expression levels of the β-catenin target genes AXIN2, GLUL, and LGR5 were obtained from 96 CTNNB1 mutant hepatocellular cancers investigated by the Cancer Genome Atlas (TCGA) consortium. The mutation types were grouped as follows: D32-S37 (n=52), T41 (n=8), S45 (n=18), K335 (n=7); N387 (n=4). Seven lesions were excluded from analysis as the specific mutation could not be linked to a specific group, e.g. small intra-exonic deletion, double mutation. Expression levels were compared with 50 normal adjacent liver tissues. Expression values are depicted as RNA-seq by expectation-maximization (RSEM) values. Only significant changes are shown. Significance is as follows: * $p<0.05$; ** $p<0.01$; **** $p<0.0001$.

Supplemental Figure S2

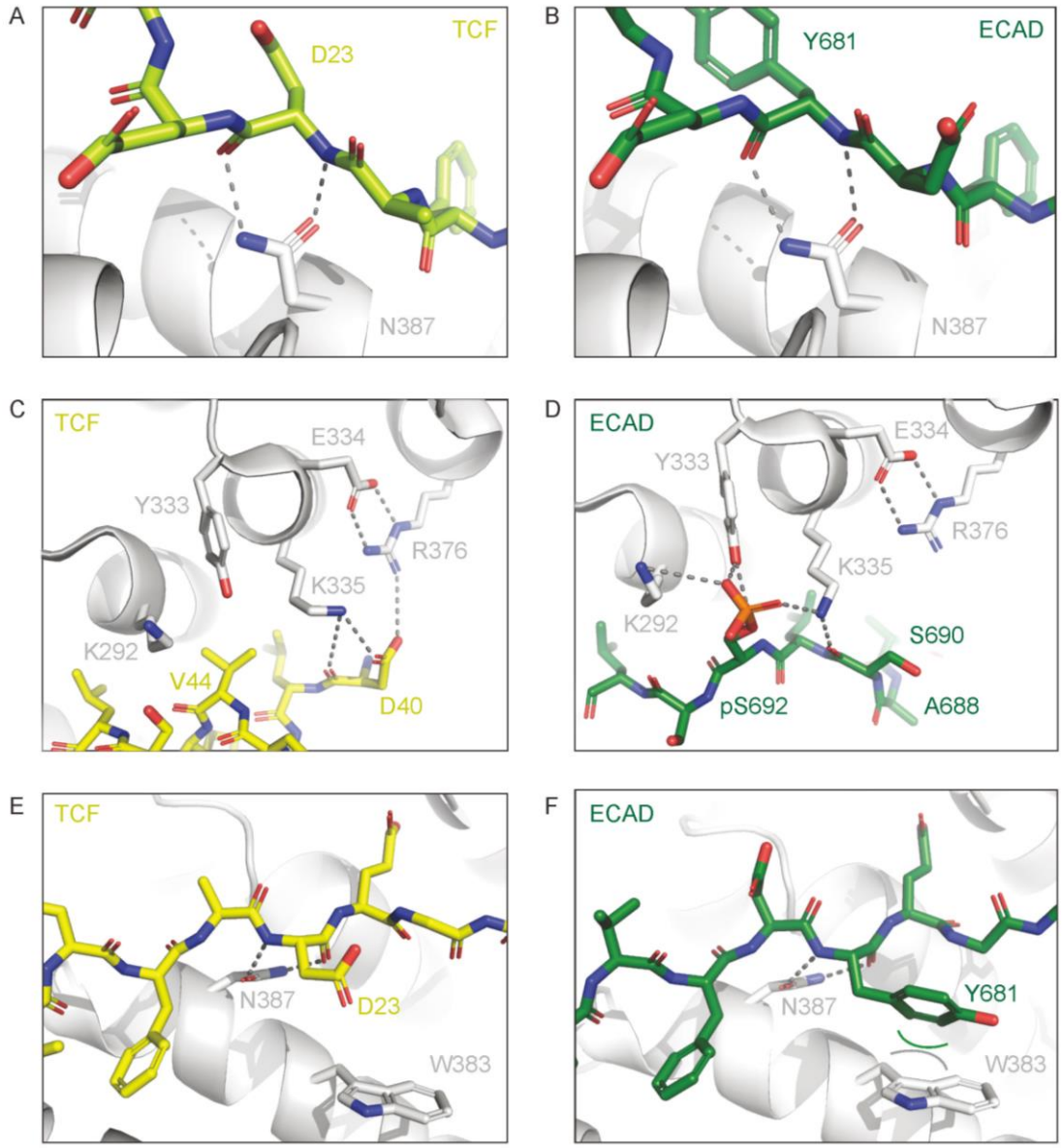

Supplemental Figure S2. Details of TCF and E-cadherin binding to β-catenin. A) N387 from β-catenin forms two hydrogen bonds with backbone groups of D23 in TCF. Hydrogen bonds are indicated with dashes. B) N387 from β-catenin forms two hydrogen bonds with backbone groups of Y681 in E-cadherin. C) TCF is bound to β-catenin via a four-residue ion-pair network (E334-R376-D40-K335). The presence of the hydrophobic V44 side chain in TCF prevents polar interactions with surrounding residues in β-catenin. D) E-cadherin is bound to β-catenin via a different four-residue ion-pair network (K292-Y333-pS692-K335). Formation of ionic interactions to connect the two isolated networks is impossible because of residue 688 in E-cadherin being an Alanine rather than a (phosphorylated) Serine. E) The sidechain of D23 in TCF is too short to form energetically favorable interactions with W383 in β-catenin. F) The aromatic sidechain of E-cadherin Y681 interacts with the double ring of W383 in β-catenin via van der Waals interactions (indicated with curved lines).

Supplemental Table S1. Within colorectal cancers, armadillo 5 and 6 repeat mutations often associate with other 'weak' activating mutations of β-catenin signaling. From the cbioportal website (http://www.cbioportal.org/) all bowel studies were selected and screened for *CTNNB1* mutations. The ones carrying armadillo repeat mutations discussed in our manuscript were further analyzed for mutations in *APC*, *AXIN1*, *AXIN2*, *RNF43*, *ZNRF3* and *AMER1*. For the depicted missense alterations of AXIN1, AXIN2 and RNF43 not always the functional consequences are known, and thus these were not considered as inactivating. Truncating APC mutations with 3 or more 20 amino acid repeats are shaded.

Patient ID	CTNNB1	APC	AXIN1	AXIN2	RNF43	AMER1
coadread_dfci_2016_280091	Y333F R386M C419Y			N666Afs*24 G63W	G659Vfs*41	
P-0000616	K335I				P660Sfs*87	
P-0006999	K335I	R554*				
P-0007361	K335I	T1556Nfs*3 S833Afs*9				
coadread_dfci_2016_291403	K335T	T1556Nfs*3				
coadread_dfci_2016_2271	R376H	V1472Efs*35				
P-0006960	R376H	R1114* S1400*	R533Q	R465H	L285I	E1115D
coadread_dfci_2016_2635	W383G					
TCGA-AG-A020	W383G	R1450* A1246Gfs*10				
coadread_dfci_2016_3321	W383R		E618K			
P-0008782	W383R	T1556Nfs*3 R876*				
TCGA-A6-5661	W383R		S654L	G665Afs*24	W200*	
TCGA-AA-3534	N387K T257I					

Supplemental Table S2. Within hepatocellular carcinomas, armadillo 5 and 6 repeat mutations do not associate with other activating mutations of β-catenin signaling. From the cbioportal website (http://www.cbioportal.org/) all hepatocellular carcinomas were selected and screened for *CTNNB1* mutations. The ones carrying armadillo repeat mutations discussed in our manuscript and associated with increased signaling, were further analyzed for mutations in *APC*, *AXIN1*, *AXIN2*, *RNF43*, *ZNRF3* and *AMER1*. For the depicted missense alterations of APC, AMER1 and AMER2 not always the functional consequences are known, and thus these were not considered as inactivating.

Patient ID	CTNNB1	APC	AMER1	AMER2	ZNRF3
CHC1603T	K335I			G126R	
CHC1763T	K335I				
CHC2029T	K335T				
CHC2200T	K335T				
CHC1626T	N387K				
CHC1736T	N388K				
TCGA-G3-A5SJ	Y333F				
TCGA-K7-A6G5	K335T				
TCGA-DD-A1EE	K335I		G820V		
TCGA-DD-A1EJ	K335I				
TCGA-DD-A3A4	K335I				
TCGA-DD-A4NL	K335I				
TCGA-MI-A75C	K335I				
TCGA-DD-AACK	K335I				
TCGA-BC-A5W4	L368H				
TCGA-CC-5262	W383C				
TCGA-BC-A69H	N387Y				
TCGA-FV-A2QQ	N387K				V568Gfs*5
TCGA-EP-A3JL	N387K				
TCGA-DD-AADM	N387K	D1297G			
TCGA-DD-A73A	N387I				

Reference

1. Zhan T, Rindtorff N, Boutros M. Wnt signaling in cancer. Oncogene 2017;36:1461-1473.

2. Valenta T, Hausmann G, Basler K. The many faces and functions of beta-catenin. EMBO J2012;31:2714-36.

3. Nusse R, Clevers H. Wnt/beta-Catenin Signaling, Disease, and Emerging Therapeutic Modalities. Cell 2017;169:985-999.

4. Albuquerque C, Bakker ER, van Veelen W, et al. Colorectal cancers choosing sides. Biochim Biophys Acta Rev Cancer 2011;1816:219-231.

5. Pilati C, Letouze E, Nault JC, et al. Genomic Profiling of Hepatocellular Adenomas Reveals Recurrent FRK-Activating Mutations and the Mechanisms of Malignant Transformation. Cancer Cell 2014;25:428-41.

6. Network CGAR, Kandoth C, Schultz N, et al. Integrated genomic characterization of endometrial carcinoma. Nature 2013;497:67-73.

7. Network CGAR. Comprehensive and Integrative Genomic Characterization of Hepatocellular Carcinoma. Cell 2017;169:1327-1341 e23.

8. Rebouissou S, Franconi A, Calderaro J, et al. Genotype-phenotype correlation of CTNNB1mutations reveals different β-catenin activity associated with liver tumor progression. Hepatology 2016;64:2047-2061.

9. Wang Z, Vogelstein B, Kinzler KW. Phosphorylation of beta-catenin at S33, S37, or T41 can occur in the absence of phosphorylation at T45 in colon cancer cells. Cancer Res 2003;63:5234-5.

10. Forbes SA, Beare D, Gunasekaran P, et al. COSMIC: exploring the world's knowledge of somatic mutations in human cancer. Nucleic Acids Res 2015;43:D805-11.

11. Colnot S. Focusing on beta-catenin activating mutations to refine liver tumor profiling. Hepatology 2016;64:1850-1852.

12. Dubbink HJ, Hollink I, Avenca Valente C, et al. A novel tissue-based β-catenin gene and immunohistochemical analysis to exclude familial adenomatous polyposis among children with hepatoblastoma tumors. Pediatr Blood Cancer 2018;65:e26991.

13. Deng W, Vanderbilt DB, Lin CC, et al. SOX9 inhibits beta-TrCP-mediated protein degradation to promote nuclear GLI1 expression and cancer stem cell properties. J Cell Sci 2015;128:1123-38.

14. Zeng L, Fagotto F, Zhang T, et al. The mouse Fused locus encodes Axin, an inhibitor of the Wnt signaling pathway that regulates embryonic axis formation. Cell 1997;90:181-92.

15. Wang W, Xu L, Liu P, et al. Blocking Wnt Secretion Reduces Growth of Hepatocellular Carcinoma Cell Lines Mostly Independent of beta-Catenin Signaling. Neoplasia 2016;18:711-723.

16. Li CM, Kim CE, Margolin AA, et al. CTNNB1 mutations and overexpression of Wnt/betacatenin target genes in WT1-mutant Wilms' tumors. Am J Pathol 2004;165:1943-53.

17. von Kries JP, Winbeck G, Asbrand C, et al. Hot spots in beta-catenin for interactions with LEF-1, conductin and APC. Nat Struct Biol 2000;7:800-7.

18. Xing Y, Clements WK, Kimelman D, et al. Crystal structure of a beta-catenin/axin complex suggests a mechanism for the beta-catenin destruction complex. Genes Dev 2003;17:2753-64.

19. Graham TA, Weaver C, Mao F, et al. Crystal structure of a beta-catenin/Tcf complex. Cell 2000;103:885-96.

20. Huber AH, Weis WI. The structure of the beta-catenin/E-cadherin complex and the molecular basis of diverse ligand recognition by beta-catenin. Cell 2001;105:391-402.

21. Xing Y, Clements WK, Le Trong I, et al. Crystal Structure of a beta-Catenin/APC Complex Reveals a Critical Role for APC Phosphorylation in APC Function. Mol Cell 2004;15:523-33.

22. Rubinfeld B, Albert I, Porfiri E, et al. Binding of GSK3beta to the APC-beta-catenin complex and regulation of complex assembly. Science 1996;272:1023-6.

23. Liu J, Xing Y, Hinds TR, et al. The third 20 amino acid repeat is the tightest binding site of APC for beta-catenin. J Mol Biol 2006;360:133-44.

24. Gadd S, Huff V, Walz AL, et al. A Children's Oncology Group and TARGET initiative exploring the genetic landscape of Wilms tumor. Nat Genet 2017;49:1487-1494.

25. Cancer Genome Atlas N. Comprehensive molecular characterization of human colon and rectal cancer. Nature 2012;487:330-7.

26. Yaeger R, Chatila WK, Lipsyc MD, et al. Clinical Sequencing Defines the Genomic Landscape of Metastatic Colorectal Cancer. Cancer Cell 2018;33:125-136 e3.

27. Perotti D, Hohenstein P, Bongarzone I, et al. Is Wilms tumor a candidate neoplasia for treatment with WNT/beta-catenin pathway modulators? Mol Cancer Ther 2013;12:2619-27.

28. Morin PJ, Kinzler KW, Sparks AB. beta-Catenin Mutations: Insights into the APC Pathway and the Power of Genetics. Cancer Res 2016;76:5587-5589.

29. Zucman-Rossi J, Villanueva A, Nault JC, et al. Genetic Landscape and Biomarkers of Hepatocellular Carcinoma. Gastroenterology 2015;149:1226-1239 e4.

30. Dahmani R, Just PA, Perret C. The Wnt/beta-catenin pathway as a therapeutic target in human hepatocellular carcinoma. Clin Res Hepatol Gastroenterol 2011;35:709-13.

31. Wang W, Pan Q, Fuhler GM, et al. Action and function of Wnt/beta-catenin signaling in the progression from chronic hepatitis C to hepatocellular carcinoma. J Gastroenterol 2017;52:419-431.

32. Xu W, Kimelman D. Mechanistic insights from structural studies of beta-catenin and its binding partners. J Cell Sci 2007;120:3337-44.

33. Lebbink JH, Knapp S, van der Oost J, et al. Engineering activity and stability of Thermotoga maritima glutamate dehydrogenase. II: construction of a 16-residue ion-pair network at the subunit interface. J Mol Biol 1999;289:357-69.

34. Lebbink JH, Consalvi V, Chiaraluce R, et al. Structural and thermodynamic studies on a saltbridge triad in the NADP-binding domain of glutamate dehydrogenase from Thermotoga maritima: cooperativity and electrostatic contribution to stability. Biochemistry 2002;41:15524-35.

35. Karshikoff A, Nilsson L, Ladenstein R. Rigidity versus flexibility: the dilemma of understanding protein thermal stability. FEBS J 2015;282:3899-917.

36. Stamos JL, Weis WI. The beta-catenin destruction complex. Cold Spring Harb Perspect Biol 2013;5:a007898.

37. van Kappel EC, Maurice MM. Molecular regulation and pharmacological targeting of the beta-catenin destruction complex. Br J Pharmacol 2017;174:4575-4588.

38. Ha NC, Tonozuka T, Stamos JL, et al. Mechanism of phosphorylation-dependent binding of APC to beta-catenin and its role in beta-catenin degradation. Mol Cell 2004;15:511-21.

39. Roberts DM, Pronobis MI, Poulton JS, et al. Deconstructing the β-catenin destruction complex: mechanistic roles for the tumor suppressor APC in regulating Wnt signaling. Mol Biol Cell 2011;22:1845-63.

40. Su Y, Fu C, Ishikawa S, et al. APC is essential for targeting phosphorylated beta-catenin to the SCFbeta-TrCP ubiquitin ligase. Mol Cell 2008;32:652-61.

41. Pronobis MI, Rusan NM, Peifer M. A novel GSK3-regulated APC:Axin interaction regulates Wnt signaling by driving a catalytic cycle of efficient betacatenin destruction. Elife 2015;4:e08022.

42. Pronobis MI, Deuitch N, Posham V, et al. Reconstituting regulation of the canonical Wnt pathway by engineering a minimal beta-catenin destruction machine. Mol Biol Cell 2017;28:41-53.

43. Buchert M, Athineos D, Abud HE, et al. Genetic dissection of differential signaling threshold requirements for the Wnt/beta-catenin pathway in vivo. PLoS Genet 2010;6:e1000816.

44. Bakker ER, Hoekstra E, Franken PF, et al. beta-Catenin signaling dosage dictates tissuespecific tumor predisposition in Apc-driven cancer. Oncogene 2013;32:4579-85.

Chapter 3

Evaluation of AXIN1 and AXIN2 as targets of tankyrase inhibition in hepatocellular carcinoma cells

Wenhui Wang[1,†], Pengyu Liu[1,†], Marla Lavrijsen[1], Shan Li[1], Wesley S. van de Geer[2,3], Harmen J. G. van de Werken[2,3], Maikel P. Peppelenbosch[1], Ron Smits[1,*]

1. Department of Gastroenterology and Hepatology, Erasmus MC-University Medical Center, Rotterdam, The Netherlands.
2. Department of Urology, Erasmus MC Cancer Institute, Erasmus MC-University Medical Center, Rotterdam, The Netherlands.
3. Cancer Computational Biology Center, Erasmus MC Cancer Institute, Erasmus MC-University Medical Center, Rotterdam, The Netherlands.

†These authors contributed equally to this paper

Submitted

Abstract

AXIN1 mutations are observed in 10% of hepatocellular carcinomas (HCCs) and originally were considered to support tumor growth by aberrantly enhancing β-catenin signaling. This view has however been challenged by reports showing neither a clear nuclear β-catenin accumulation nor clearly enhanced expression of β-catenin target genes. Here, using nine HCC lines, we show that AXIN1 mutation or siRNA mediated knockdown contributes to enhanced β-catenin signaling in all AXIN1-mutant and non-mutant lines, also confirmed by reduced signaling in AXIN1-repaired SNU449 cells using CRISPR-Cas9. Both AXIN1 and AXIN2 work synergistically to control β-catenin signaling. While in the AXIN1-mutant lines, AXIN2 is solely responsible for keeping signaling in check, in the non-mutant lines both AXIN proteins contribute to β-catenin regulation to varying levels. The AXIN proteins have gained substantial interest in cancer research for a second reason. Their activity in the β-catenin destruction complex can be increased by tankyrase inhibitors, which thus may serve as a therapeutic option to reduce the growth of β-catenin-dependent cancers. Application of the tankyrase inhibitor XAV939 does not clearly stabilize AXIN1 or AXIN2 protein in our HCC cell lines, with the exception of AXIN2 in the *CTNNB1*-mutant ones. Nevertheless, tankyrase inhibition diminished β-catenin signaling in most non-*CTNNB1*-mutant lines, which was however not sufficient to suppress their growth. Overall, our analyses show that AXIN1 inactivation leads to enhanced β-catenin signaling in HCC cell lines, questioning the strong statements that have been made in this regard. Enhancing AXIN activity by tankyrase monotherapy provides however no effective treatment to affect their growth.

Keywords: Hepatocellular carcinoma (HCC), Wnt/β-catenin signaling, AXIN1, AXIN2, Tankyrase inhibition

1 Introduction

Hepatocellular carcinoma (HCC) is the sixth most prevalent cancer and the third leading cause for cancer related deaths worldwide with around 500,000 new cases diagnosed each year (1,2). Hepatocarcinogenesis initiates with the accumulation of aberrant genetic and epigenetic modifications leading to the dysregulation of signaling pathways, which transform the normal hepatocytes towards malignant phenotypes (3).

Inappropriate activation of Wnt/β-catenin signaling has been reported frequently in HCC (4). As the central component of Wnt/β-catenin signaling, intracellular β-catenin levels are tightly regulated by a multiprotein complex composed of the adenomatous polyposis coli (APC) tumor suppressor, scaffold proteins AXIN1, AXIN2 and the kinases GSK3 and CK1α (4,5). In the absence of Wnt ligands, β-catenin is constitutively phosphorylated and degraded to maintain a minimal level in the cytoplasm. Upon Wnt stimulation, the multiprotein complex dissociates causing the accumulation of cytosolic and nuclear β-catenin, which in turn triggers the transcription of specific target genes. Aberrant activation of Wnt/β-catenin signaling in HCC has been mainly attributed to activating somatic mutations in the *CTNNB1* gene coding for β-catenin (20-25%) (4,6-8). These mutations result in single amino-acid alterations or small in-frame deletions at N-terminal phosphorylation residues that make the protein more resistant to proteolytic degradation. For these activating mutations it is well-accepted that they support tumor growth by enhancing β-catenin signaling in a dominant fashion.

Another component of the Wnt/β-catenin signaling pathway regularly inactivated in HCC is *AXIN1* (10%), while inactivating mutations of the *AXIN2* (3-4%) and *APC* (1-2%) genes are observed less frequently (4,6,7,9). Originally, given its prominent role in the β-catenin destruction complex, mutational inactivation of AXIN1 was considered to support HCC development by aberrantly enhancing β-catenin signaling. This view has however been challenged in the last decade by several reports showing neither a clear nuclear β-catenin accumulation nor clearly enhanced expression of β-catenin target genes in *AXIN1*-mutant HCCs (10-12). In support, AXIN1 has also been shown to potentially regulate the activity of other proteins relevant for tumorigenesis, such as MYC, TP53 and SMAD3 (13-16). Other reports, including our own work, have provided some evidence of increased β-catenin signaling in *AXIN1* mutant HCC cells, albeit modest

(11,17,18). Hence, the extent of β-catenin signaling following AXIN1 mutation and its relevance for supporting HCC growth is still under debate.

Besides their frequent mutational inactivation in liver cancer, the AXIN proteins have gained substantial interest in cancer research for a second reason. Their activity in the β-catenin destruction complex can be increased by so-called tankyrase inhibitors, which thus may serve as a therapeutic option to reduce the growth of β-catenin-dependent cancers. The AXIN proteins, like β-catenin itself, are under tight proteolytic control. Poly-ADP-ribosyltransferases tankyrase-1 and -2 (encoded by *TNKS* and *TNKS2*) associate with the N-terminus of AXIN proteins, resulting in their PARsylation and subsequent RNF146 mediated protein ubiquitylation and degradation (19-22), thereby limiting the activity of the destruction complex. Blocking the catalytic activity of the tankyrases, first results in accumulation of the tankyrases themselves by inhibition of their auto-PARsylation, followed by AXIN accumulation. Next, so-called degradasomes are assembled in which all components of the β-catenin destruction complex aggregate to form large multiprotein complexes leading to an efficient β-catenin turnover. The formation of these degradasomes can be visualized as discrete cytoplasmic puncta within tankyrase inhibitor treated cells. Application of these tankyrase inhibitors has been investigated for the treatment of breast (23), lung (24) and especially colorectal cancer (25-29), with some successful initial results for a subset of tumors. Investigating their potential to treat HCC has been limited to a single study in which high inhibitor levels blocked the growth of some liver cancer cell lines (30).

In this study, we employed *CTNNB1*-, *AXIN1*- and non-mutant HCC cell lines to investigate the impact of tankyrase inhibition on Wnt/β-catenin signaling as well as cell growth, and to further explore the function of AXIN1 and AXIN2 in regulating Wnt/β-catenin signaling in HCC cells.

2 Materials and methods

2.1. Cell lines

CTNNB1 mutant HepG2, Huh6, SNU398, *AXIN1* mutant Hep3B, PLC/PRF/5, SNU449 and non-mutant HepaRG, Huh7, SNU182 HCC as well as CRC (DLD1 and SW480) cell lines were cultured as reported previously (18). The term "non-mutant" is used throughout the paper to indicate that these lines do not contain mutations in genes known to be linked to β-catenin signaling. Identity of all cell lines and clones thereof, was confirmed by the Erasmus Molecular Diagnostics Department, using Promega Powerplex-16 STR genotyping in October 2018. All cell lines tested negative for mycoplasma. Mutation status depicted in supplemental Table S1 was confirmed in all the nine HCC cell lines by Sanger sequencing and was consistent with those reported at COSMIC, the Catalogue Of Somatic Mutations In Cancer (http://cancer.sanger.ac.uk) (31).

2.2. Reagents

XAV939 and IWR-1 were purchased from Sigma-Aldrich. Antibodies specific for β-catenin (610154, BD Transduction Laboratories™), phospho-β-catenin (Ser33/37) (#2009, Cell Signaling Technology), AXIN1 (#2087 and #3323 Cell Signaling Technology; AF3287 R&D systems), AXIN2 (#2151, Cell Signaling Technology), Tankyrase-1/2 (sc-365897, Santa Cruz), β-actin (sc-47778, Santa Cruz) and anti-rabbit or anti-mouse IRDye-conjugated secondary antibodies (LI-COR Biosciences, Lincoln, USA) were used for western blot analysis.

2.3. β-catenin reporter assays

The β-catenin reporter assays were performed as previously described (32). In short, we plated 5×10^4 cells per well on 24-well plates, which were transfected with 250 ng Wnt Responsive Element (WRE) or Mutant Responsive Element (MRE) vectors and 10 ng CMV-Renilla using FuGENE® HD Transfection Reagent. We measured luciferase activities and normalized the data for the transfection efficiency by using the Dual Luciferase Reporter Assay system. Following normalization, WRE/MRE ratios are obtained, which are depicted in all figures.

2.4. MTT assay

After incubation with XAV939 for 72 hours, cells were analyzed by MTT assay as previously reported (18). The mean and standard error were calculated for each condition.

2.5. Western blotting

Cells were lysed for western blotting analysis as previously reported (18). Results were visualized with Odyssey 3.0 software.

2.6. Immunocytochemistry

Cells were seeded on Nunc™ Lab-Tek™ II CC2™ Chamber Slides (Thermo-Fisher Scientific). After 16 hours treatment with 1 μM XAV939 or DMSO, cells were washed with PBS, fixed in PBS-buffered 4% paraformaldehyde for 10 mins, permeabilized with PBS-0.2% Triton X-100 solution for 5 min and blocked with PBS containing 3% BSA for 30 minutes. Samples were incubated with primary antibodies at room temperature for 1 hr, followed by PBS-Tween 20 0.05% washes and incubation with appropriate secondary antibodies for 1 hr. Primary antibodies were diluted as follows: AXIN1 (AF3287, 1:100); AXIN2 (#2151, 1:200); Tankyrase-1/2 (sc-365897, 1:200). The following secondary reagents were used: Donkey anti-Goat-Alexa 647 (#A-21447), Donkey anti-Rabbit-Alexa 488 (#A-21206), Donkey anti-Mouse-Alexa 594 (#A-21203); all from Invitrogen, at 1:500 dilution. Slides were mounted with Vectashield mounting medium with DAPI (H-1200, Vector Laboratories). Images were generated using a Zeiss LSM510META confocal electroscope.

2.7. Quantitative real-time polymerase chain reaction

RNA was isolated with a Machery-NucleoSpin RNA II kit (Bioke, Leiden, The Netherlands) and quantified using a Nanodrop ND-1000 (Wilmington, DE, USA). CDNA was prepared from total RNA using a cDNA Synthesis Kit (TAKARA BIO INC). Quantitative PCR was performed using Sensimix SYBRGreen (Applied Biosystems) or TaqMan (AXIN1; Hs00394718_m1, AXIN2; Hs00610344_m1, GAPDH; Hs02786624-g1) Gene Expression Assays (Applied Biosystems). Analyses were performed using the StepOne Real-Time PCR System and the StepOnev2.0 software (Applied Biosystems,

Darmstadt, Germany). All expression levels are depicted relative to the expression of *GAPDH*. Primer sequences are provided in supplemental Table S2.

2.8. Gene knockdown by small interfering RNA (siRNA)

Smartpool ON-TARGETplus siRNAs targeting *AXIN1*, *AXIN2* or *APC* were purchased from Dharmacon. The ON-TARGETplus Non-targeting siRNA #2 was used as negative control. Cells were reverse-transfected in a 24-well plate using a total of 0.8 µl DharmaFECT formulation 4 (Thermo-Fisher Scientific) and 25nM of each siRNA per well. Following 72h incubation, the effect of knock-down was tested by qRT-PCR. Alternatively, 48h after siRNA transfection, the cells were transfected with WRE or MRE vectors and CMV-Renilla for a β-catenin reporter assay.

2.9. Colony formation assay

After trypsinization, 1000 cells for each cell line were seeded in 6-well plates and were cultured in complete DMEM medium containing 1uM XAV939 or DMSO as control. Medium was changed every three days. Two weeks later, the cells were washed with PBS, fixed in 4% PBS-buffered paraformaldehyde for 10 min and stained with crystal violet solution. Tests were performed at least in triplicates.

2.10. CRISPR/Cas9 mediated repair of *AXIN1* mutation in SNU449 cells

A single guide RNA (sgRNA) encompassing the homozygous c.2134C>T *AXIN1* mutation present in SNU449 cells was designed and cloned into pSpCas9(BB)-2A-GFP (PX458), a gift from Feng Zhang (Addgene plasmid # 48138)(33) using standard procedures. To repair this mutation we designed a single-stranded oligodeoxynucleotide (ssODN), following the guidelines proposed by Richardson et al. (34). The ssODN was ordered as Ultramer from Integrated DNA Technologies. Both the sgRNA and ssODN are described in supplemental Table S3. Transfections were performed with the Amaxa Cell Line Nucleofector Kit V (Lonza) and Nucleofector IIb device according to the manufacturer's instructions. In brief, $5x10^6$ SNU449 cells were cotransfected with 2µg PX458 and 2µg ssODN. After nucleofection, complete DMEM medium with 7.5µM RAD51-stimulatory compound-1 (RS-1, Sigma-Aldrich)(35) was used for cell culture. After 48 hours, GFP positive cells were sorted by FACS and seeded as single cells in 96-well plates. DNA from clones grown successfully from single cells was isolated using

the QuickExtract™ DNA Extraction Solution (Epicentre). For each clone, a PCR product encompassing the mutation was subjected to sequencing.

2.11. RNA extraction, Ilumina library preparation and sequencing

Total RNA was isolated with the Machery-NucleoSpin RNA II kit (BIOKE, Leiden, The Netherlands) and quantified using a Nanodrop ND-1000 (Wilmington, DE, USA). RNA quality was checked using a RNA Pico chip on the Agilent Bioanalyzer. Library was constructed and sequenced with an Illumina HiSeqTM2000 (GATC Biotech, Konstanz, Germany). Briefly, the mRNA was enriched using oligo-dT magnetic beads, followed by fragmentation (about 200 bp). Then first strand cDNA was synthesized using random hexamer-primers and the second strand was further synthesized in a reaction buffer including dNTPs, RNase H and DNA polymerase I. Double stranded cDNA was purified with magnetic beads. Then, the 3'-end single nucleotide A (adenine) was added and adapters were ligated to the fragments which were enriched by PCR amplification.

2.12. RNA-sequencing analysis

RNA-seq data of control and *AXIN1*-repaired SNU449 samples (n=3 each) was analyzed using UCSC human genome build hg38 and GENCODE annotation release 26 (GRCh38). FASTQC (v0.11.5) (36) was applied on the single-end FASTQ files for quality control, both before and after running trimmomatic (v0.36) (37), which removed TrueSeq adapter sequences. STAR (v2.5.3a) was used as aligner, with 2-pass mapping for each sample separately (38). Mapping quality plot was generated and checked based on sambamba Flagstat (v0.6.7) statistics (39). Count files, with the number of reads for each gene were created with subread FeatureCounts (1.5.2) (40). Settings of different tools can be seen in supplemental Table S4. R (version 3.4.3) was used for further statistics calculation and data visualizations. Differential expression analysis were performed with condition 'Repaired' (n=3) versus 'Mutated' (n=3) using the DESeq2 package (v1.18.1) (41) and the Wald-test. A significance cut-off of 0.05 on the adjusted P-value was utilized, using the Benjamini-Hochberg procedure. The RNA-sequencing data from this study have been submitted to the Gene Expression Omnibus (GEO)-database under the accession number GSE119001.

2.13. Statistical analysis

All results were presented as mean ± SD. Comparisons between groups were performed with Mann Whitney test. Differences were considered significant at a *P* value less than 0.05 (**P*<0.05, ***P*<0.01, ****P*<0.001).

3. Results

3.1. Baseline levels of AXIN1 and AXIN2 in HCC cell lines

To explore the function of AXIN1 and AXIN2 in regulating Wnt/β-catenin signaling in HCC cells, we employed 9 HCC cell lines listed in supplemental Table S1, in which gene mutations related to Wnt/β-catenin signaling are depicted. By western blotting, AXIN1 was noticeably expressed in the β-catenin mutant lines and AXIN1-mutant PLC/PRF/5 (lacks exon4 encoded GSK3-binding domain) (Figure 1A). In all other lines some AXIN1 was discernible on over-exposure, with the exception of the mutant pR146* AXIN1 present in Hep3B. The truncated p.R712* AXIN1 protein present in SNU449 could only be detected using the N-terminal AXIN1 antibody. Also AXIN2 was clearly detectable in the β-catenin mutant lines, but was barely/not visible in the remaining lines.

Next, we compared *AXIN1* and *AXIN2* RNA expression levels by qRT-PCR using two independent methods (Figure 1B,C). Uniformly, *AXIN2* was expressed at higher levels than *AXIN1* in all HCC cell lines, independent of their β-catenin related mutation status. The low *AXIN1* RNA levels were independently confirmed with two additional primer sets (Supplemental Figure S1). In accordance with *AXIN2* being a β-catenin target gene, the expression differences were largest in the *CTNNB1* mutant lines.

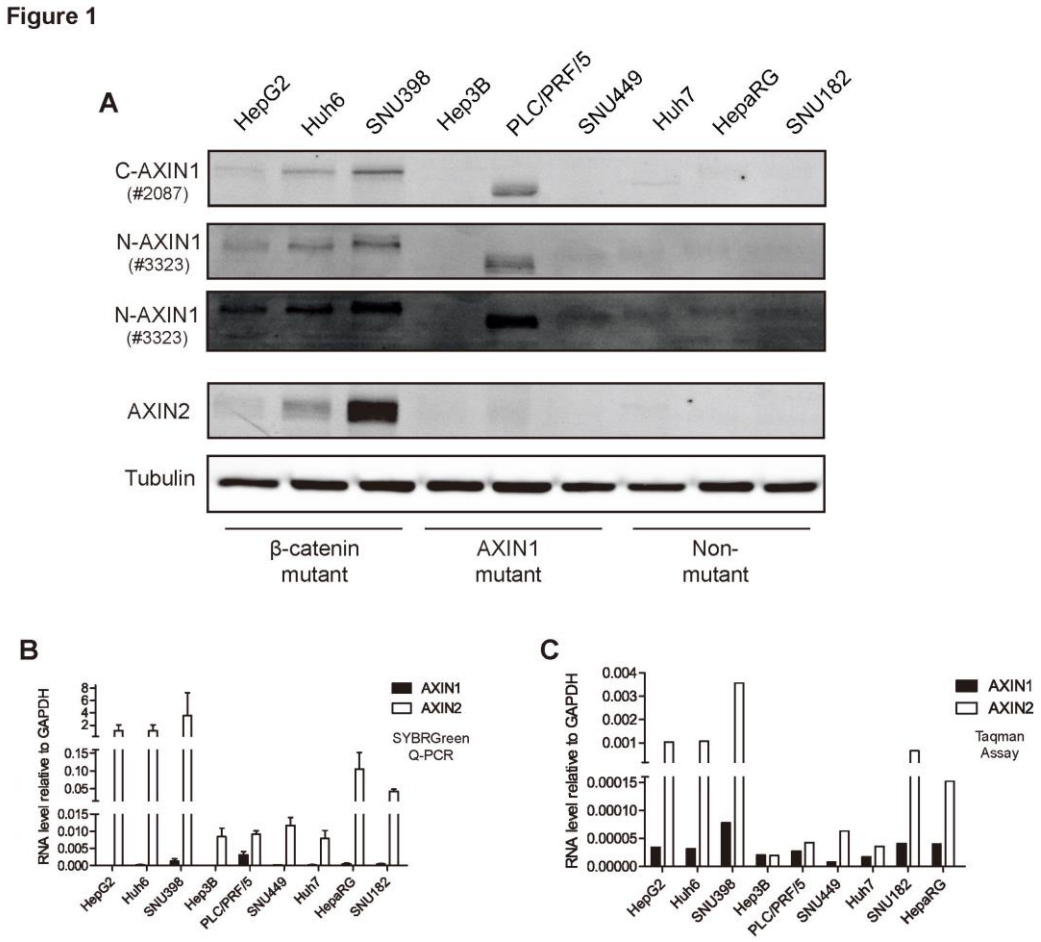

Figure 1. Baseline levels of AXIN1 and AXIN2 in HCC cell lines. (A) Western blotting assay showing the basal protein levels of AXIN1 and AXIN2. For the N-terminal AXIN1 antibody a stronger exposure is also shown. (B) RNA levels tested by qRT-PCR (mean ± SD, n=2, twice). (C) RNA levels tested by TaqMan Gene Expression Assay. All expression levels are depicted relative to the housekeeping gene *GAPDH*. Note the interrupted Y-axis scales.

3.2. Both AXIN1 and AXIN2 contribute to β-catenin signaling regulation in HCC cell lines

The above results indicate an apparent discrepancy, i.e. while *AXIN2* seems to be clearly higher expressed than *AXIN1* on RNA level, its protein levels are barely detectable in most HCC lines. This can have various reasons, both technical (antibody quality) as well as biological (protein stability). To more directly evaluate the functionality of either AXIN1 or AXIN2 to the regulation of β-catenin signaling in each cell line, we applied siRNA mediated knockdown. We focused our analysis on the *AXIN1*-mutant and non-mutant lines, using SNU398 as a *CTNNB1* mutant control. *APC* knockdown was used as a positive control for activation of β-catenin signaling. Analysis

by qRT-PCR confirmed the efficient knockdown of all targeted genes (Figure S2A). As expected, *APC* knockdown resulted in a strong increase of β-catenin reporter activity and *AXIN2* expression in all cell lines, with exception of the *CTNNB1* mutant SNU398 (Figure 2 and S2B). In all three *AXIN1*-mutant lines, a comparable increase in reporter activity was observed as a consequence of *AXIN2* knockdown, showing that AXIN2 is expressed at biologically functional levels and also confirming that the AXIN1 mutation impairs its role in β-catenin regulation. Among the non-mutant cell lines a variable response was noted. In SNU182 cells reporter activity was increased to levels approaching *APC* knockdown. In Huh7 cells a clear 5-fold increase was observed, but far less-prominent as by *APC* knockdown, while HepaRG cells were barely affected in their β-catenin signaling activity. QRT-PCR analyses for *AXIN2* were also performed in all AXIN2 knockdown samples (Figure S2C). However, a meaningful interpretation is complicated by the fact that total *AXIN2* RNA levels are simultaneously downregulated by siRNA as well as upregulated by the enhanced β-catenin signaling (a more detailed explanation is provided accompanying Figure S2). Hence, for the interpretation of the *AXIN2* knockdown experiments we restricted ourselves to the reporter assay.

The partial increase in reporter activity observed in the non-mutant lines following *AXIN2* knockdown suggests that AXIN1 still contributes to β-catenin turnover. Therefore, we knocked down its expression, using the *AXIN1*-mutant PLC/PRF/5 as negative control. We also evaluated simultaneous knockdown with *AXIN2*. As expected, β-catenin signaling in the PLC/PRF/5 line was not enhanced by *AXIN1* knockdown, confirming the defective status of the mutant protein (Figure 2B, S2D). HepaRG and SNU182 did not show clear changes in reporter activity, but showed 2-4 fold increases of *AXIN2* expression. Huh7 cells showed a clear increase of reporter activity and a 2-fold increase in *AXIN2* RNA levels. Simultaneous knockdown of *AXIN1* and *AXIN2* led to a robust induction of β-catenin reporter activity in all tested lines (Fi).

Taken together, these analyses show that (i) in HCC cell lines both AXIN1 and AXIN2 work synergistically to control β-catenin signaling. In the AXIN1-mutant lines, AXIN2 is solely responsible for keeping signaling in check, whereas in the non-mutant lines both AXIN proteins contribute to β-catenin regulation to varying levels depending on the cell line under investigation; (ii) both proteins are expressed at functionally relevant levels despite their low detectability by western blotting; (iii) in *CTNNB1*-mutant HCC lines

β-catenin signaling is dominantly regulated by the mutant β-catenin protein and cannot be effectively modulated by alterations in APC or AXIN1/2 levels.

Figure 2

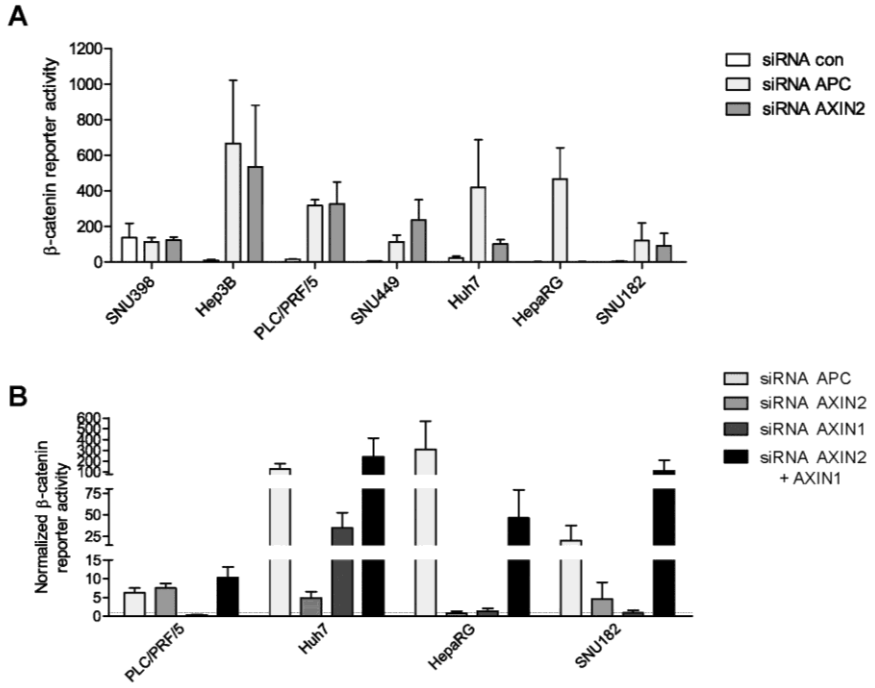

Figure 2. Both AXIN1 and AXIN2 contribute to β-catenin signaling regulation in HCC cell lines. (A) Indicated cell lines were subjected to a β-catenin reporter assay after siRNA-mediated knockdown of *APC* or *AXIN2*. Both *APC* and *AXIN2* knockdown are equally effective in enhancing signaling in *AXIN1* mutant cells (Hep3B, PLC and SNU449). *AXIN2* knockdown in the non-mutant lines (Huh7, HepaRG, SNU182) results in an incomplete increase in reporter activity when compared with *APC* knockdown. Absolute WRE/MRE β-catenin reporter ratios are shown following Renilla transfection normalization (mean ± SD, n=2, twice). (B) Indicated cell lines were subjected to a β-catenin reporter assay after siRNA-mediated knockdown of *AXIN1*, *AXIN2*, a combination thereof or *APC*. WRE/MRE ratios for the control siRNA were arbitrarily set to 1 for each cell line. All β-catenin reporter WRE/MRE ratios for the other siRNAs were normalized to this control (mean ± SD, n=2, twice). Note the interrupted Y-axis scale.

3.3. Tankyrase inhibition stabilizes AXIN2 exclusively in β-catenin mutant HCC cell lines

The tankyrase enzymes have been shown to antagonize the activity of the β-catenin destruction complex by PARsylation and subsequent breakdown of AXINs (19-22). Their inhibition can lead to an enhanced β-catenin turnover and growth suppression of a subset of β-catenin-dependent cancers (23-29). At baseline all HCC cell lines showed readily detectable RNA expression of both *TNKS* and *TNKS2* genes, while by western

blotting predominantly the larger tankyrase-1 protein was visible (Figure S3). We treated HCC cell lines with tankyrase inhibitors XAV939 or IWR-1, using the CRC cell line SW480 as positive control. In accordance with previous studies on SW480 cells, XAV939 stabilized tankyrase-1/2, AXIN1 and AXIN2, increased phospho-β-catenin (p-β-catenin) and diminished total β-catenin levels (Figure S4A). In all HCC cell lines, XAV939 treatment at two different concentrations led to a robust accumulation of both tankyrase proteins by blocking its auto-PARsylation (Figure 3). Strikingly, we did not observe a clear stabilization of either AXIN1 or AXIN2 protein in most HCC cell lines. Solely in the *CTNNB1* mutant lines HepG2, Huh6, and especially SNU398, the AXIN2 signal was noticeably enhanced. With respect to β-catenin, only in Huh6 an increase in pS33/37 phosphorylation was observed accompanied with a slight reduction in total β-catenin levels, but only clearly following treatment with 5μM XAV939. Basically identical results were obtained with a second tankyrase inhibitor (IWR-1) in the Huh6, PLC/PRF/5 and SW480 cell lines (Figure S4B).

In various cell lines tankyrase inhibition has been shown to lead to the formation of so-called β-catenin degradasomes, consisting of higher-order structures in which all components required for β-catenin degradation are present (42). These degradasomes can be visualized as AXIN- and tankyrase-positive cytoplasmic puncta (43), which were readily visible in XAV939 treated SW480 cells (Figure 4). This was also the case in Huh6 cells, expressing intermediate levels of both AXIN proteins, although not as prominent as in SW480. By western blotting PLC/PRF/5 cells express clear levels of a mutant AXIN1 protein retaining the DIX domain required for multimerization. Accordingly, accumulation of tankyrase- and AXIN1-positive puncta was detectable, but no obvious change in abundance and subcellular localization of AXIN2 was visible. Lastly, in Hep3B cells exclusively tankyrase-positive puncta were observed, in line with the low AXIN1/2 levels observed by western blot.

Thus, both the western blot and immunocytochemistry analysis suggest that tankyrase inhibition leads to an efficient stabilization of AXIN2 and the formation of β-catenin degradasomes exclusively in β-catenin mutant HCC cell lines, while AXIN1 remains largely unaltered. In all other lines no obvious change in AXIN1 or AXIN2 is observed.

Figure 3

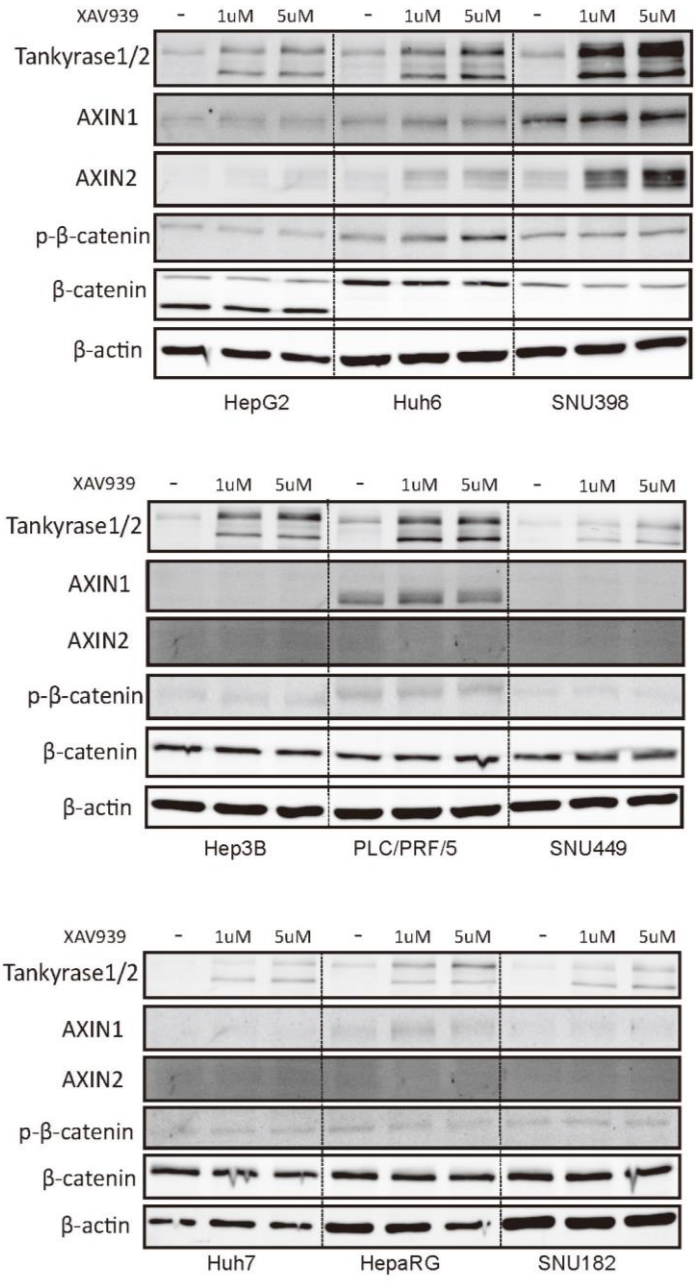

Figure 3. Tankyrase inhibition stabilizes AXIN2 exclusively in *CTNNB1* mutant HCC cell lines. (A) Western blotting assay showing levels of tankyrase-1/2, AXIN1/2, p-β-catenin (pS33/37) and total β-catenin after XAV939 treatment (1 or 5μM, 16 h).

Figure 4

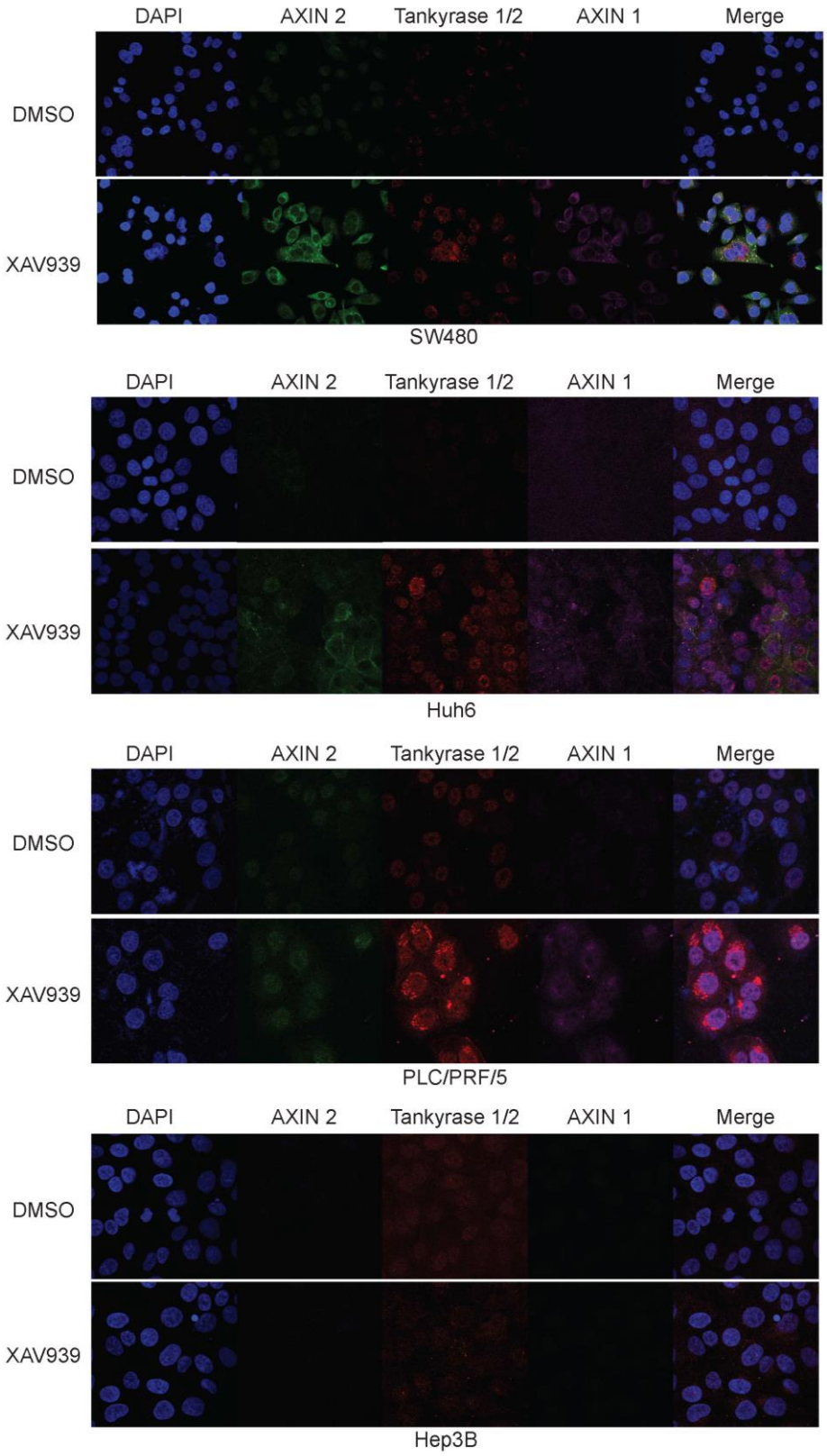

Figure 4. Immunofluorescence staining showing the abundance and subcellular localization of tankyrase-1/2 and both AXINs, following tankyrase inhibition. Original magnification is 63x. Cells were treated with 1μM XAV939 for 16h.

3.4. TNKS inhibition diminishes Wnt/β-catenin signaling activity in most non-*CTNNB1* mutant HCC cells

Despite that we observed no clear visual AXIN accumulation in most HCC cell lines, we set out to determine the impact of tankyrase inhibition on Wnt/β-catenin signaling activity. In line with our previous work, in untreated samples we observed a clear induction of β-catenin reporter activity in both the *CTNNB1*- and *AXIN1*-mutant lines (Figure 5A), supporting our observation that AXIN1-mutant lines show increased β-catenin signaling (18). Following XAV939 treatment, *CTNNB1* mutant cells still gave a high β-catenin reporter activity, comparable to the untreated cells (Figure 5), in accordance with the supposed dominant activity of mutant β-catenin. Except for HepaRG, reporter activity was however suppressed in both the *AXIN1* mutant as well as non-mutant lines, although it should be noted that β-catenin induced reporter activity is not completely blocked. The most prominent decreases were observed in PLC/PRF/5 and Huh7, which also displayed a minor but noticeable decrease of *AXIN2* at RNA level, a well-established β-catenin target gene (supplemental Figure S5). Thus, this analysis shows that tankyrase inhibition can reduce β-catenin signaling in most *AXIN1*-mutant and non-mutant lines, despite that no obvious AXIN accumulation is observed.

Figure 5

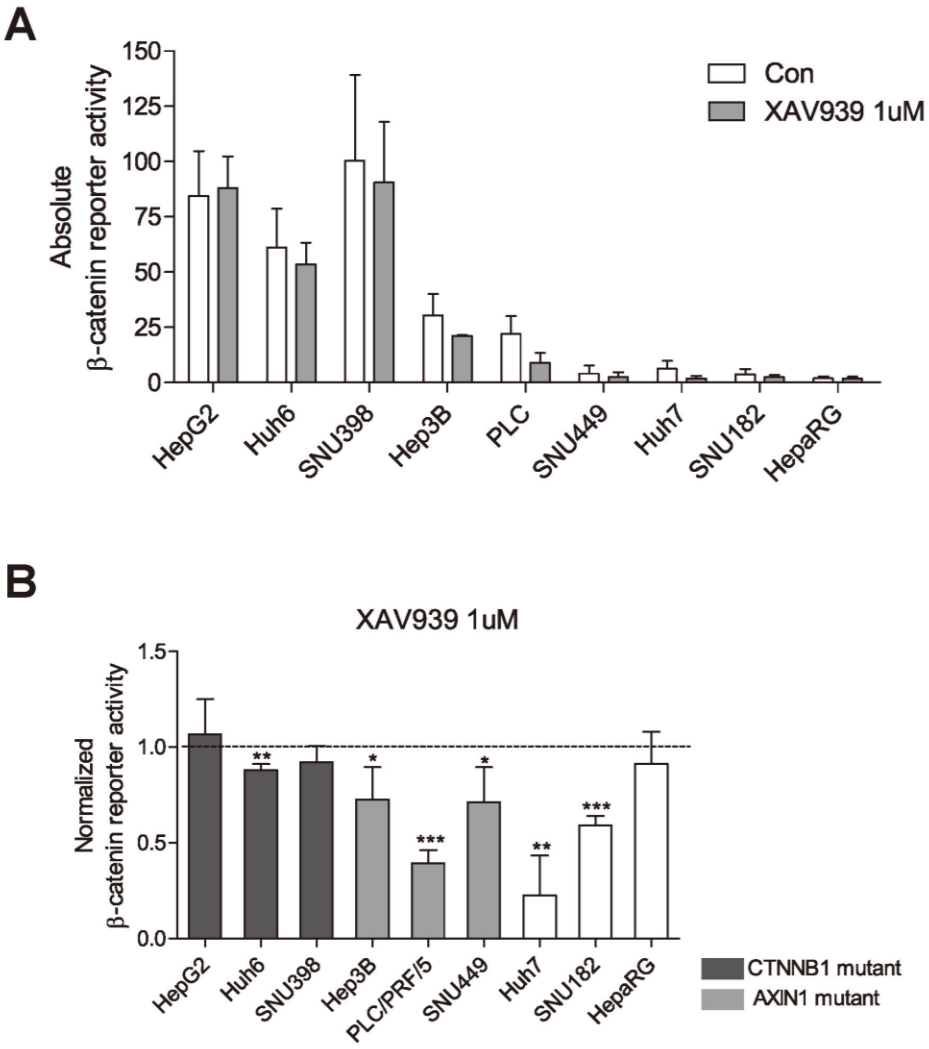

Figure 5. Tankyrase inhibitor diminishes Wnt/β-catenin signaling activity in most non-*CTNNB1* mutant HCC cells. HCC cell lines were incubated with 1μM XAV939 for 24 h followed by a β-catenin reporter assay (mean ± SD, n=2, twice). (A) Absolute WRE/MRE β-catenin reporter ratios observed for each cell line following Renilla transfection normalization. (B) Same reporter values normalized to the numbers obtained for the DMSO control-treated samples, which are arbitrarily set to 1 (*P<0.05, **P<0.01, ***P<0.001).

3.5. TNKS inhibitor XAV939 does not inhibit cell growth of HCC lines effectively

Tankyrase inhibitors have been shown to inhibit the proliferation of a subset of APC-mutant CRC cells (25-29). As a significant reduction in β-catenin signaling was observed in a subset of our HCC cell lines following XAV939 treatment, we examined whether this compound also exerts an inhibitory effect on HCC cells. Following three days of treatment, we noticed a reduced cell viability in a dose-dependent manner in the CRC DLD1 cell line, which was used as positive control (supplemental Figure S6). However, HCC cell growth was unaltered, even at higher 5μM concentration (Figure 6A). To test the effect of long-term treatment, we performed a colony formation assay treating HCC cells with 1μM XAV939 for two weeks. As indicated in Figure 6B, no obvious reduction in colony number and size was observed for most cell lines (HepG2 failed to form colonies) with the exception of SNU398 and HepaRG. As these two lines did not show any evidence of reduced β-catenin signaling by XAV939 (see Figure 5), this is most likely the consequence of other cellular processes regulated by tankyrases, such as telomere maintenance, mitosis or DNA strand break repair (44-46). Another explanation could be the potential repressive effect of XAV939 on poly(ADP-ribose) polymerases PARP1 and PARP2 (25), Collectively, these findings suggest that XAV939 cannot or at most modestly affect the growth of HCC cell lines at concentrations that block tankyrase activity.

Figure 6

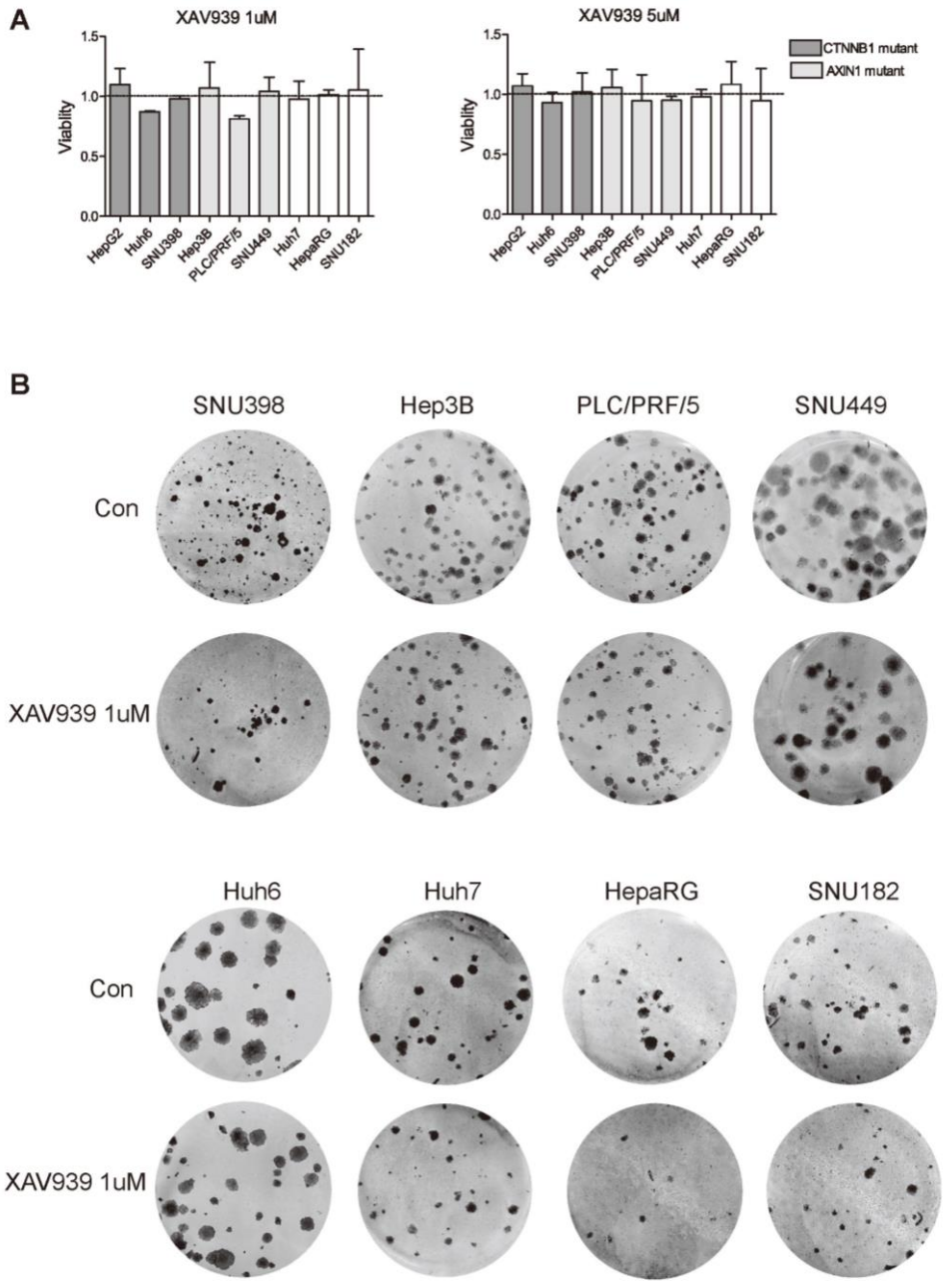

Figure 6. Tankyrase inhibitor XAV939 does not or at most modestly affect the viability and colony formation capacity of HCC lines. (A) HCC cell lines were treated with XAV939 at 1μM or 5μM for three days followed by a MTT-assay. (B) Colony formation with 1μM XAV939 for two weeks. Medium was changed every three days. Tests were performed at least in triplicates. HepG2 did not form colonies using this assay.

3.6. Restoring full-length AXIN1 expression in SNU449 cells reduces *AXIN2* expression, but has overall minimal effects on cell behavior

To more directly investigate the consequences of AXIN1 mutation for supporting β-catenin signaling and liver cancer growth, we used CRISPR-Cas9 technology to repair the homozygous p.R712* mutation present in SNU449 cells. This truncating mutation removes the C-terminal DIX domain that is essential for AXIN1 to form higher order structures through multimerization and fulfil its function in β-catenin regulation (47,48). We successfully obtained several independent clones with complete repair of AXIN1 (Figure 7A). Protein expression levels are 2-3 fold higher compared with the parental cells, which can be attributed to higher expression levels of *AXIN1* RNA (Figure 7B). The latter is most likely resulting from nonsense-mediated decay of the mutant transcript in the parental line. Importantly, all repaired clones show a significant reduction in *AXIN2* expression to almost undetectable levels by qRT-PCR (Figure 7C), indicating an improved β-catenin turnover. When these repaired cells are treated with XAV939, they show a clear accumulation of AXIN1, in contrast to unchanged levels of the mutant protein (Figure 7D). Accordingly, we observe the formation of AXIN1 and tankyrase-positive puncta exclusively in the repaired cells (supplemental Figure S7). AXIN2 is not detectable using IF, in line with its virtual absence observed by qRT-PCR and western blotting. Thus, we successfully resulted in restoring AXIN1 expression in SNU449 cells, which was accompanied by reduced expression of the β-catenin target gene *AXIN2*.

The fact that we successfully obtained SNU449 cells with normalized AXIN1 expression also highlights that its mutation is not essential to sustain growth in culture. AXIN1 has also been functionally linked to various other proteins relevant for tumorigenesis (13-16). To determine in an unbiased manner the consequences of restoring AXIN1 expression in SNU449 cells, we subjected 3 repaired clones and 3 controls to RNA sequencing. Surprisingly, only 5 genes were significantly altered in expression including *AXIN2* (supplemental Table S5).

In conclusion, the analyses of the AXIN1 repaired SNU449 cells show that in this cell line the *AXIN1* mutation has minimal effects on cell behavior and gene expression, with the exception of one well-established β-catenin target gene, i.e. *AXIN2.*

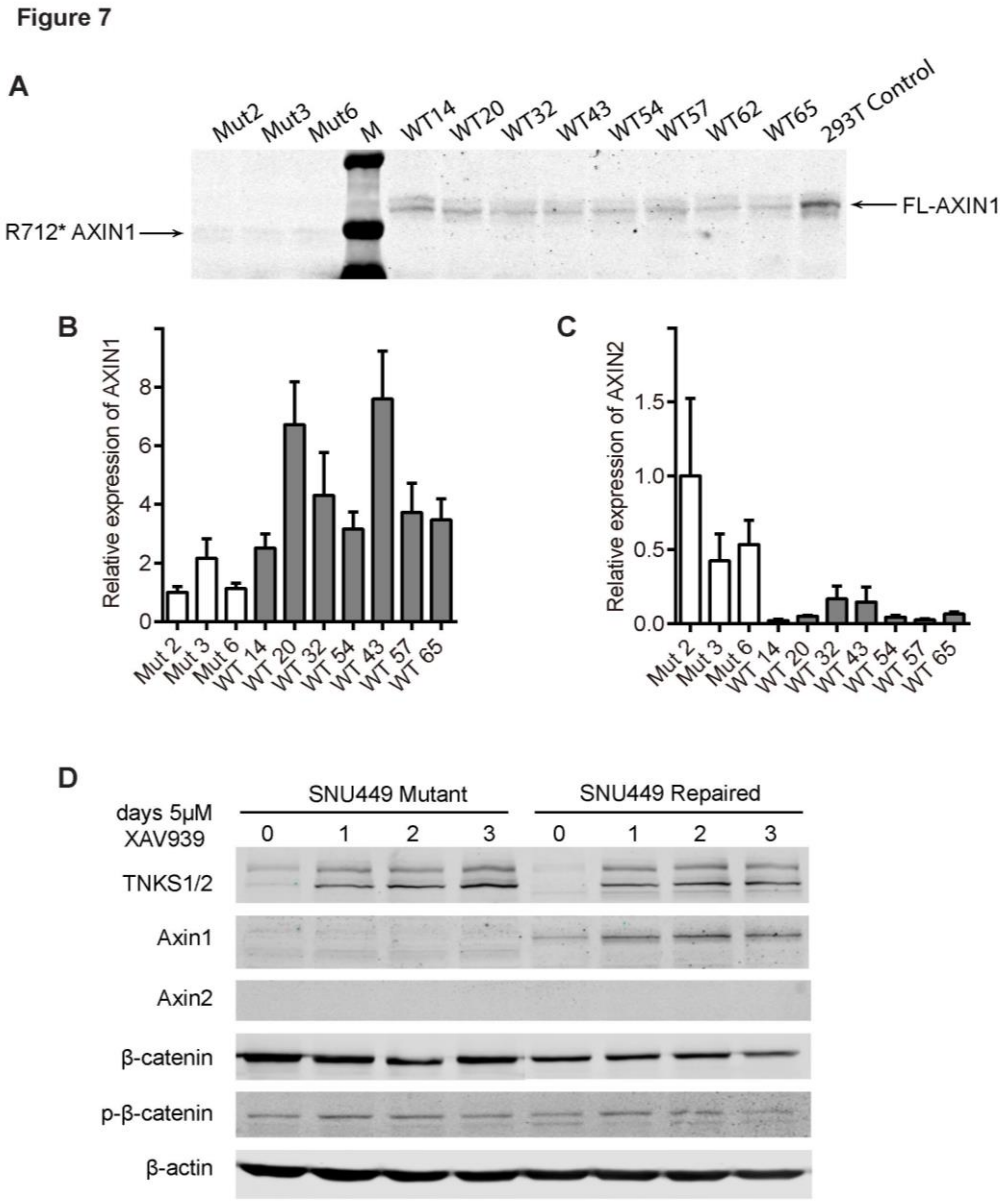

Figure 7. Successful repair of AXIN1 mutation in SNU449 cells. (A) Using Crispr-cas technology we successfully repaired the homozygous c.2134C>T mutation in *AXIN1* resulting in several independent clones with full-length (FL) AXIN1 expression. (B) QRT-PCR of *AXIN1* shows 2-3 fold increased expression in all repaired (WT) clones. (C) *AXIN2* RNA expression is consistently down-regulated in all repaired clones. AXIN1/2 qRT-PCRs were normalized to the value obtained for mutant clone 2 (Mut2), which was arbitrarily set to 1. (D) XAV939 treatment for 1-3 days shows the accumulation of AXIN1 exclusively in the AXIN1 repaired SNU449 cell line. Total β-catenin and p-β-catenin (pS33/37) levels are not significantly changed following XAV939 treatment.

4. Discussion

Inappropriate activation of Wnt/β-catenin signaling has been reported frequently in HCC. This has been mainly attributed to somatic mutations in the *CTNNB1* gene (20-25%) (4,6-9). A second common mechanism originally considered to lead to enhanced β-catenin signaling, is mutational inactivation of *AXIN1* observed in about 10% of HCCs, putting it among the ten most commonly mutated genes in HCC (4,6-9). Given its activity in the β-catenin destruction complex this was a logic assumption, however several more recent reports have suggested that AXIN1 mutation in liver cancer leads to no or at most a modest increase in β-catenin signaling (10,11,17). Hence, the exact mechanism through which AXIN1 mutation supports HCC growth is still under debate. In addition, the AXIN proteins have gained substantial interest in cancer research because their activity in the β-catenin destruction complex can be increased by tankyrase inhibitors, which thus may serve as a therapeutic option to reduce the growth of β-catenin-dependent cancers. Here, using a panel of 9 HCC cell lines with specific mutations in components of the β-catenin signaling pathway, we have investigated both aspects of AXIN biology.

The original assumption that AXIN1 mutation drives tumorigenesis by enhancing β-catenin signaling has been questioned for the following reasons: (i) AXIN1 and AXIN2 show high similarity to one another in most domains responsible for binding to other proteins (49). In accordance, AXIN2 can at least partially compensate for AXIN1-loss in the β-catenin destruction complex (50). (ii) AXIN1 has been suggested to regulate the activity of other proteins relevant for tumorigenesis, such as MYC, TP53 and SMAD3 (13-16). (iii) Immunohistochemical analysis for β-catenin fails to identify an efficient nuclear accumulation in AXIN1-mutant tumors (10). Although nuclear accumulation of β-catenin is a reliable predictor of active signaling, its absence does however not fully exclude that a low level of biologically relevant signaling is active (51). (iv) Deletion of *AXIN1* in the mouse liver led to enlarged livers, a feature that has also been associated with increased β-catenin signaling, and a weak induction of some β-catenin target genes (11). Only late-onset hepatocellular cancers with no or at most a few cells staining positive for nuclear β-catenin were observed in these mice (11,12). (v) Expression profile analysis using a gene signature representative of β-catenin target genes, clustered most AXIN1-mutated HCCs in a group with no evident β-catenin program

activation, and about 20% in groups with weak or strong activation (12). Overall, these reports make a strong point that β-catenin signaling is not prominent in AXIN1-mutant HCCs, but they also hint to some low level activation that might be biologically relevant. In this respect, several examples have been presented in the literature showing that minor alterations in the level of β-catenin signaling can have profound biological effects (5,32,52,53). In case of hepatocellular cancer, Buchert et al. have shown that late-onset hepatocellular tumors were present in all mice carrying a hypomorphic *APC* mutation associated with just a modest increase in β-catenin signaling, while tumor formation was absent or largely prevented with slightly increased or decreased signaling (52). This narrow window of signaling effective in liver cancer formation highlights the importance of low level signaling for some cancer types and shows that it is difficult to fully exclude a role for β-catenin signaling. Our analysis shows that all three AXIN1-mutant HCC cell lines have increased β-catenin reporter activity, also confirmed by reduced *AXIN2* levels following AXIN1 repair in SNU449 cells. Furthermore, *AXIN1* knockdown in three non-mutant lines leads to enhanced signaling, also supported by a recent investigation of *AXIN1* knockdown in Huh7 cells (12). Previously, we have also shown that all AXIN1-mutant lines are impaired in their growth following siRNA mediated knockdown of β-catenin, suggesting that sufficiently high β-catenin signaling levels are needed for an optimal growth (18). Taken together, this suggests that AXIN1 mutation leads to a modest increase of β-catenin signaling that may be relevant for hepatocellular tumorigenesis.

AXIN1-mutant tumors depend to a large extent on AXIN2 to counterbalance signals that induce β-catenin signaling, as shown by the strong increase in β-catenin reporter activity that we observe after *AXIN2* knockdown, comparable to levels seen with *APC* siRNA. Hence, they are expected to be more prone to signal in conditions that normally activate the β-catenin signaling pathway, such as commonly encountered local tissue injury or inflammation within the tumor micro-environment, or in instances of chronic hepatitis or liver cirrhosis. Under such circumstances, AXIN1-mutant cells may carry a selective advantage through β-catenin mediated induction of for example tumor stem cell features. Such local effects are likely missed when expression profiles are obtained from tumors as a whole. As such, we feel that a role for β-catenin signaling in AXIN1-mutant HCCs cannot be ruled out completely, and will require additional

experimentation such as combined *AXIN1* and *CTNNB1* inactivation in mouse livers, to determine if AXIN1-mutant tumors can arise without β-catenin signaling.

Nevertheless, it is clear that AXIN1 mutation by itself is not a strong driver of liver tumorigenesis. Deletion of *AXIN1* in the mouse liver only leads to few tumors with late onset (11,12), implying that other oncogenic hits are required to successfully initiate tumor formation. This notion is also supported by the minimal changes we observe in the AXIN1-repaired SNU449 cells. Apparently, this cell line does not depend anymore on the AXIN1 mutation to grow efficiently, at least using the culture conditions that we tested thus far. The RNA sequencing analysis also shows that no signaling routes previously linked to AXIN1 are clearly affected, except for the β-catenin target gene *AXIN2*. As reported by others, it is also clear that AXIN1-mutant HCCs follow a different route to tumorigenesis than the ones carrying oncogenic β-catenin mutations, and may more heavily depend on the activation of other signaling pathways such as the recently described involvement of YAP/TAZ and Notch signaling (12).

To our initial surprise, tankyrase inhibition did not lead to a clear visual accumulation of both AXIN1 and AXIN2 protein in most HCC cell lines, with the exception of AXIN2 in the *CTNNB1*-mutant ones. This is in apparent contrast with studies of breast (23), lung (24) and especially colorectal cancer, where its application leads to an efficient accumulation of either one or both AXIN proteins (25-29). As a potential explanation we identified low RNA expression levels of *AXIN1.* Recently, it was shown that sustained protein translation is required for AXIN accumulation to occur (21). Apparently, the low RNA levels are inadequate to generate sufficient new AXIN1 protein to visibly accumulate, whereas for AXIN2 this is only the case in the high *AXIN2* expressing *CTNNB1*-mutant cell lines; the quality of available antibodies most likely plays an additional role, as the siRNA experiments demonstrate that both proteins are expressed at functionally relevant levels. In contrast, most colorectal cancers are characterized by APC mutations leading to a strongly enhanced β-catenin signaling, which in turn leads to hyper-activation of *AXIN2*, explaining the efficient AXIN2 accumulation observed in this cancer type following tankyrase inhibition (25-27). Thus, our investigation suggests that *AXIN1* and *AXIN2* RNA levels could be a good predictor for the level of their tankyrase-inhibitor induced accumulation.

Despite that we observed no clear visual AXIN accumulation in the non-*CTNNB1*-mutant HCC cell lines, we notice the suppressing effect of XAV939 on β-catenin signaling activity in most of them. In addition to their enzymatic activity, the tankyrase enzymes are increasingly being recognized as scaffolding proteins that catalyze the formation of the β-catenin destruction complex (22). Most likely the XAV939 induced tankyrase stabilization allows a more efficient formation of these AXIN-containing destruction complexes leading to more β-catenin breakdown, even though thus far we fail to show the AXIN-puncta microscopically. In accordance with previous reports investigating β-catenin mutant CRC lines, the HCC cell lines expressing constitutively active mutant β-catenin variants are not affected in their signaling activity (25-27).

The reduction in β-catenin signaling accomplished with tankyrase inhibition in a subset of our lines, is however not sufficient to significantly affect their growth. This seems to contradict our previous study where all HCC cell lines were inhibited in their growth after siRNA-mediated β-catenin knockdown (18). In this latter study we reached more than 80% reduction in total β-catenin protein levels, which is in strong contrast to basically unaltered levels in our current study. XAV939 has also been evaluated in another study involving three HCC cell lines (HepG2, Huh7 and Hep40) (30). In this report growth inhibitory effects were observed only at drug concentrations (IC50s of 25-80μM) far-exceeding the levels required for selective tankyrase inhibition, which most likely will also have inhibited the activity of other PARP enzymes (54). Taken together, these studies suggest that tankyrase inhibition at physiologically relevant concentrations is unlikely to contribute to HCC treatment as monotherapy. A potential exception could be the rare subset of HCCs carrying APC mutations leading to high level signaling of wild-type β-catenin (9,55,56).

In conclusion, using a panel of nine HCC cell lines we observe that all three AXIN1-mutant lines display a clearly increased activity in a β-catenin reporter assay. Repair of the AXIN1 mutation in SNU449 confirms this observation as it results in reduced activation of the β-catenin target gene *AXIN2*. In the three non-mutant lines reducing *AXIN1* levels also in all cases leads to enhanced signaling. Overall, these analyses show that AXIN1 mutation or inactivation leads to enhanced β-catenin signaling in HCC, questioning the strong statements that have been made in this regard.

We also show that AXIN1 and AXIN2 work synergistically to control β-catenin signaling. While in the AXIN1-mutant lines, AXIN2 is solely responsible for keeping signaling in check, in the non-mutant lines both AXIN proteins contribute to β-catenin regulation to varying levels. Lastly, enhancing AXIN activity by tankyrase monotherapy does result in a modest to intermediate reduction in β-catenin signaling in most AXIN1-mutant and non-mutant lines, but this is not sufficient to seriously affect their growth.

Data accessibility: All data generated or analyzed during this study are included in this published article and its supplementary information files. The RNA-sequencing data from this study have been submitted to the Gene Expression Omnibus (GEO)-database under the accession number GSE119001.

Authors' contributions: WW and PL performed the majority of experimental work as well as data analysis and authored the manuscript. ML and SL assisted with the experiments. WSvdG and HJvdW analyzed the raw data generated by RNA sequencing. MPP supervised the project and improved the manuscript. RS coordinated the project and participated in authoring of the manuscript. All authors reviewed the results and approved the final version of the manuscript.

Acknowledgements: This research was financially supported by a China Scholarship Council PhD fellowship to Wenhui Wang (File NO. 201306190123), Pengyu Liu (File NO. 201408220029), and Shan Li (File NO. 201408060053).

Conflict of interest: The authors declare that they have no conflicts of interest.

Figure S1

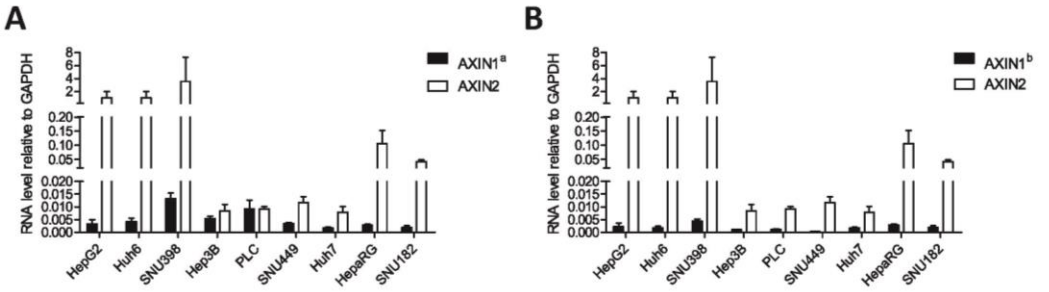

Figure S1. **(A,B)** Baseline RNA level of AXIN2 is higher than AXIN1 in HCC cell lines as validated by two additional sets of AXIN1 oligos (a and b) tested by qRT-PCR (mean ± SD, n=2, twice). All expression levels are depicted relative to the housekeeping gene GAPDH.

Figure S2

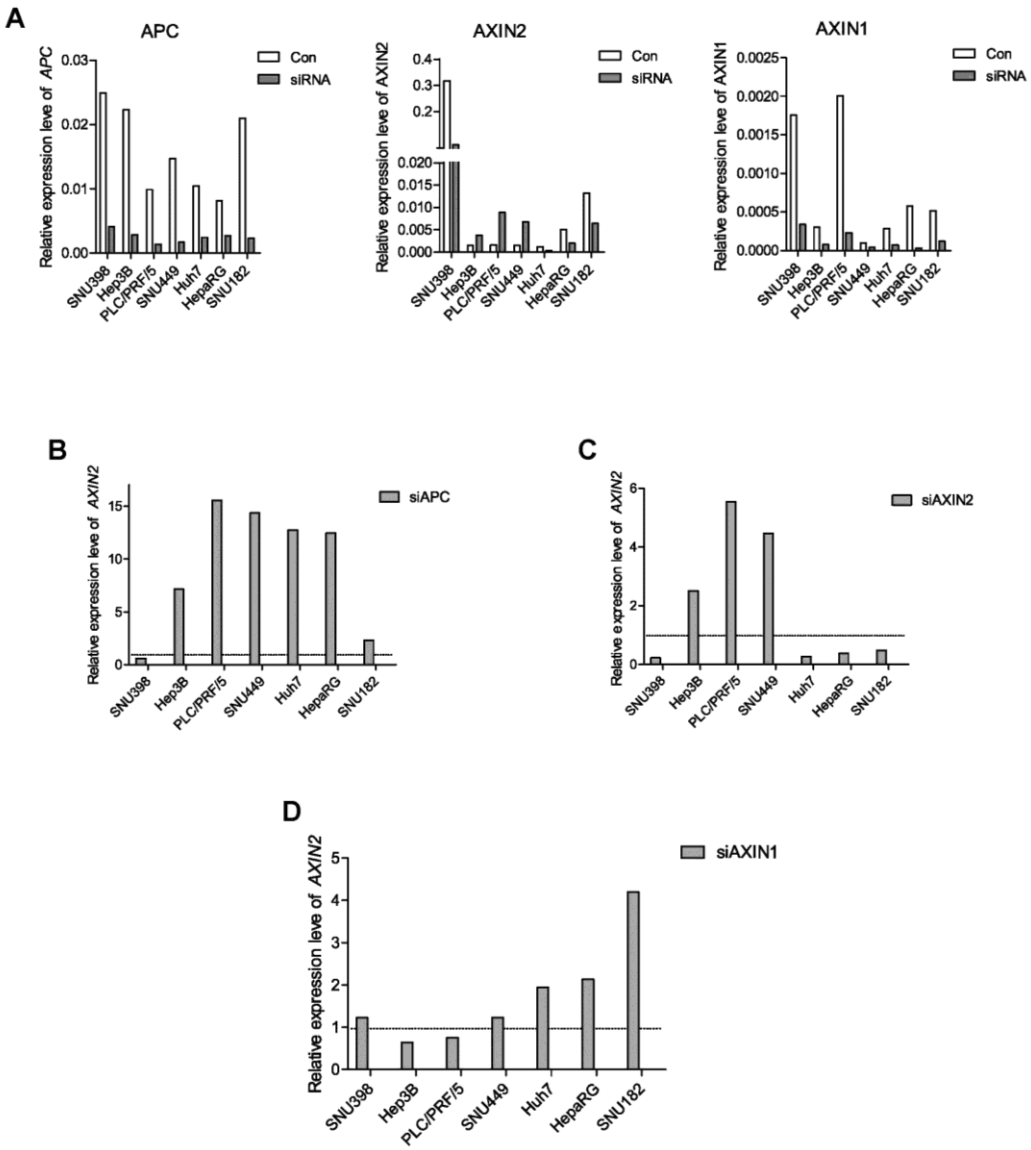

Figure S2. QRT-PCR results for *APC*, *AXIN1* and *AXIN2* in siRNA experiments. **(A)** SiRNA mediated knockdown of *APC*, *AXIN1* and *AXIN2* tested by qRT-PCR. Interpretation of *AXIN2* knock-down efficiency is complicated by the fact that total *AXIN2* RNA levels are simultaneously downregulated by siRNA as well as upregulated by the emerging enhanced β-catenin signaling. This is especially the case for the AXIN1-mutant lines, as they solely depend on AXIN2 in the breakdown complex. We envisage the following will happen. Directly following transfection, the siRNA mediated reduction in *AXIN2* RNA levels present at that time in these cells, will result in reduced AXIN2 protein levels and a strongly increased β-catenin signaling. As a result both the reporter activity (Figure 2B) as well as *AXIN2* RNA expression will be strongly increased. As the siRNA will not be 100% effective, this will temporarily lead to more AXIN2 protein contributing to enhanced β-catenin breakdown. Both reporter activity and *AXIN2* RNA production will diminish temporarily, after which this cycle will repeat itself. At the time of analysis, this may result in the apparent contradictory result that *AXIN2* RNA levels increase with *AXIN2* siRNA treatment. Also note that *AXIN2* RNA levels are about 60-80% lower in the *AXIN2* siRNA compared with *APC* siRNA treated AXIN1-mutant cells (S2B vs S2C), while β-catenin reporter levels are equally increased. **(B)** *AXIN2* RNA expression is increased in all AXIN1- and non-mutant lines following *APC* knockdown. No change is observed in the β-catenin mutant SNU398 line. Depicted values are normalized to *AXIN2* levels observed for the control siRNA, which are arbitrarily set to 1. **(C)** *AXIN2* RNA expression following *AXIN2* knockdown. The interpretation problem mentioned above also applies here. **(D)** *AXIN2* RNA expression is increased in all non-mutant lines following *AXIN1* knockdown, but not in the AXIN1- and β-catenin mutant lines.

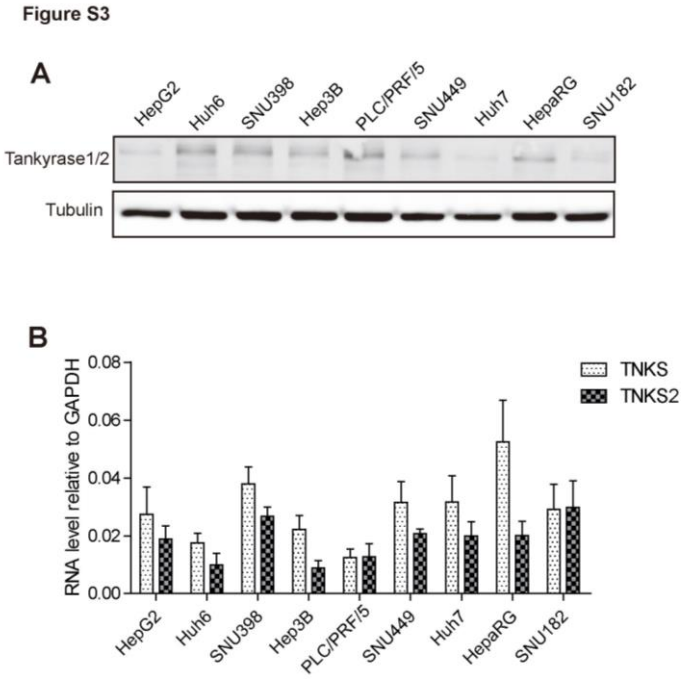

Figure S3. Baseline levels of tankyrase-1/2 in HCC cell lines. **(A)** Western blotting assay showing the basal protein levels of tankyrase1/2. **(B)** QRT-PCR assay showing expression of *TNKS* and *TNKS2* in HCC cell lines (mean ± SD, n=2, twice). Expression levels are depicted relative to the housekeeping gene *GAPDH*.

Figure S4

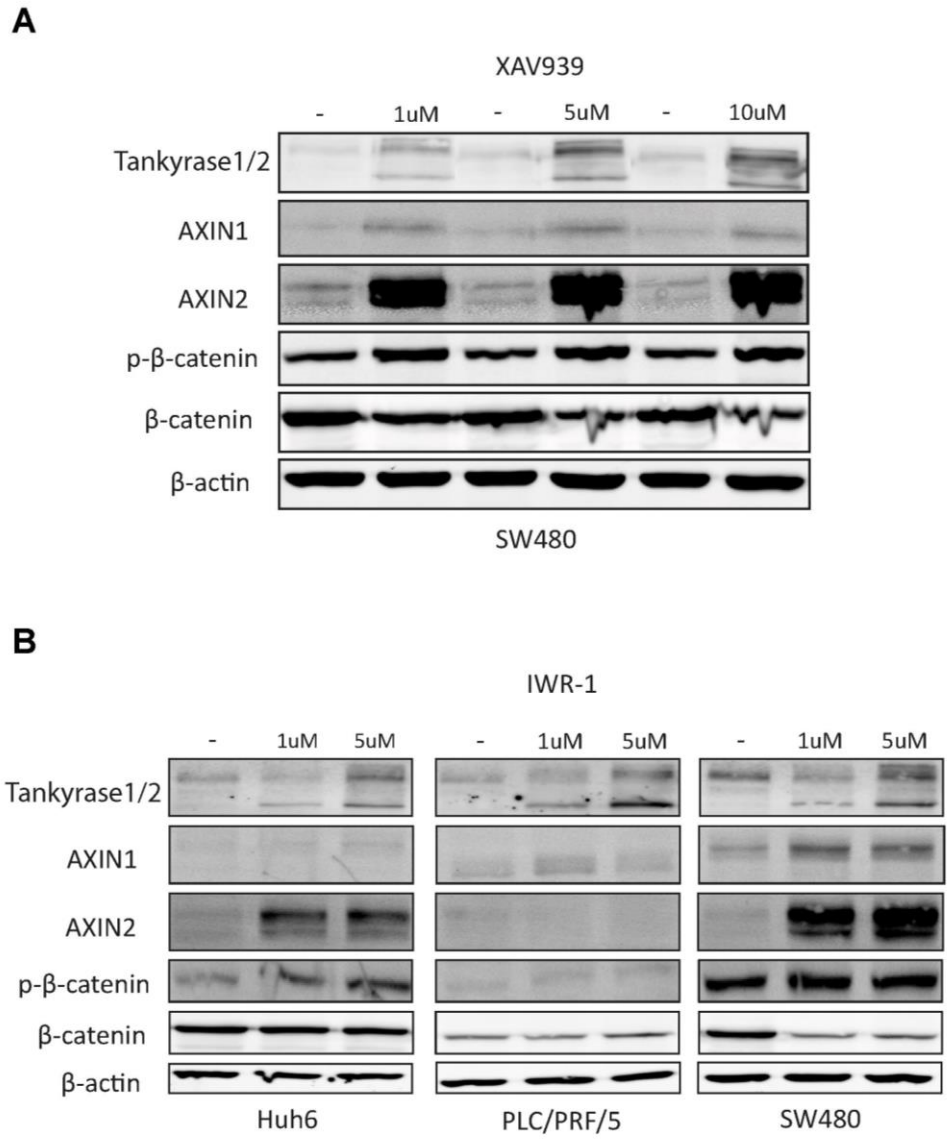

Figure S4. Effect of tankyrase inhibitors validated by western blotting. **(A)** In SW480 cells XAV939 stabilizes tankyrase-1/2 and AXIN1/2 protein levels, increases phospho-β-catenin (p-β-catenin) while simultaneously reducing total β-catenin. **(B)** Related proteins tested in SW480 and two HCC cell lines (Huh6 and PLC/PRF/5) using a second tankyrase inhibitor, i.e. IWR-1, showing basically identical results to XAV939. All these cells were treated with indicated tankyrase inhibitors for 16 h.

Figure S5

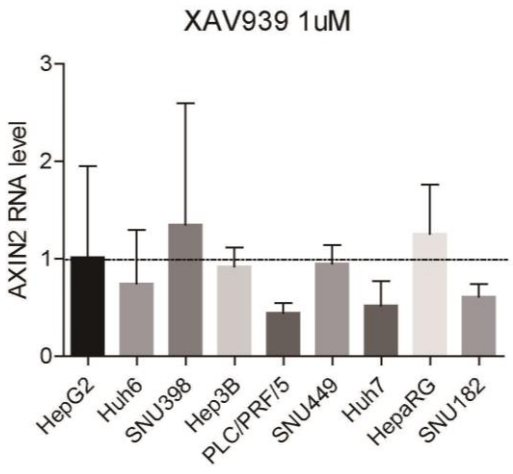

Figure S5. QRT-PCR of *AXIN2* in HCC cell lines treated with XAV939 (1µM, 24 h) (mean ± SD, n=2, twice). Depicted values are normalized to *AXIN2* levels observed for the control treated samples, which are arbitrarily set to 1.

Figure S6

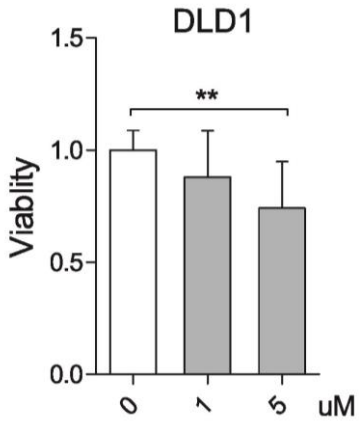

Figure S6. CRC DLD1 cells were treated with XAV939 at 1µM or 5µM for three days, showing a dose-dependent reduction in the MTT assay (mean ± SD, n=4).

Figure S7

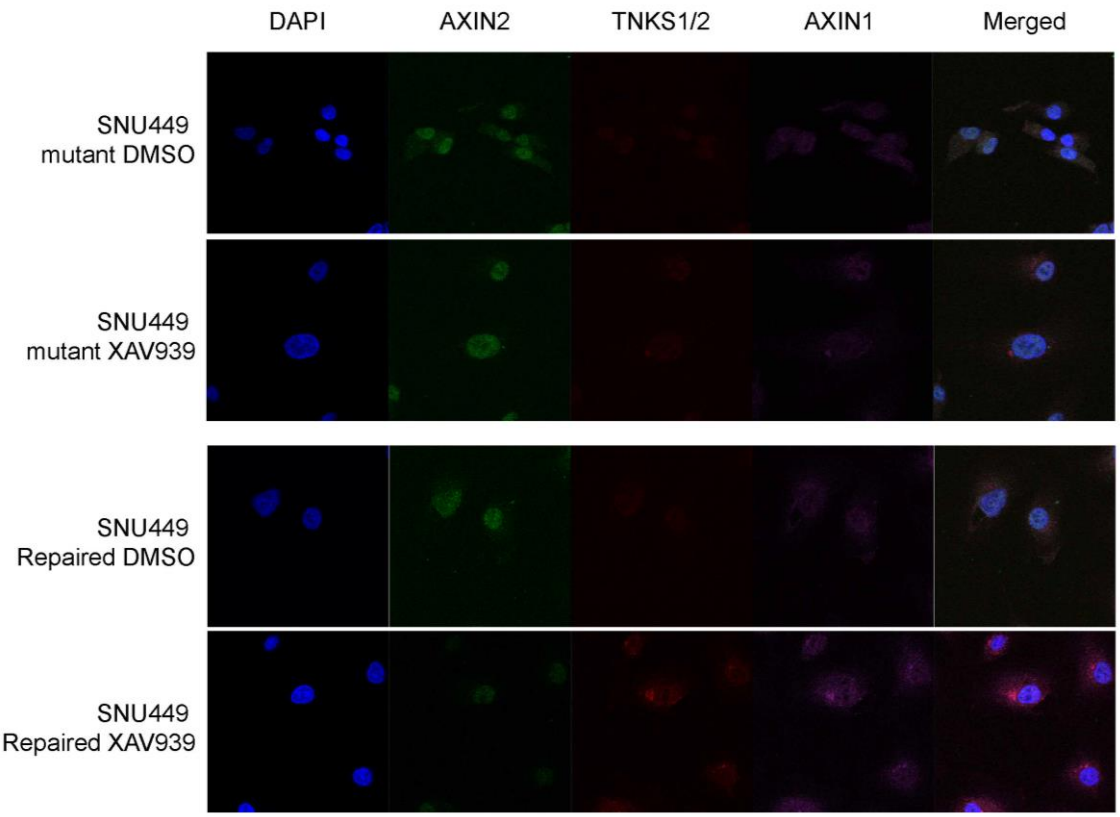

Figure S7. AXIN1- and tankyrase-positive puncta are exclusively observed in the AXIN1 repaired SNU449 cells following XAV939 treatment. In the mutant clone we do observe the formation of tankyrase-positive puncta. In general, the signals were difficult to capture, most likely because of low expression levels. The apparent AXIN2 signal is also observed in the negative control (not shown) and most likely represents unspecific signal. Original magnification is 63x. Cells were treated with 1μM XAV939 for 16h.

Supplemental Table S1. Gene mutations of Wnt/β-catenin signaling components in HCC cell lines

Cell line	Gene	AA alteration	Zygosity
HepG2	*CTNNB1*	p.W25_I140 del	Heterozygous
Huh6	*CTNNB1*	p.G34V	Heterozygous
SNU398	*CTNNB1*	p.S37C	Heterozygous
Hep3B	*AXIN1*	p.R146*	Homozygous
PLC/PRF/5	*AXIN1*	p.(R373_M418 del)	Homozygous
SNU449	*AXIN1*	p.R712*	Homozygous
Huh7			
HepaRG			
SNU182			

Supplemental Table S2. Primer sequences used for qRT-PCR

Gene	Forward Sequence(5'~3')	Reverse Sequence(5'~3')
AXIN1	AACGACAGCGAGCAGCAGAG	AGCTTGTGACACGGCCCTGG
AXIN1[a]	CAAGAGCAGGGTTTCCCCTT	GCCGTCGAAGTCTCACCTTT
AXIN1[b]	GAACTGGTGTCCACAGACCC	CCCATCTTGGTCATCCAGCA
AXIN2	TATCCAGTGATGCGCTGACG	TTACTGCCCACACGATAAGG
TNKS1	CCTGGCAGATCCTTCAGCAA	TTGTAGCCCGCTGCTAGATG
TNKS2	TGCCAGGAGTGGCAATGAAG	TTTCTGCCATCACTTGCGTG
APC	GCGCTTACTGTGAAACCTGT	GAACACACACAGCAGGACAG
GAPDH	TGTCCCCACCCCCAATGTATC	CTCCGATGCCTGCTTCACTACCTT

Supplemental Table S3. sgRNA and ssODN used for repair of *AXIN1* mutation in SNU449 cells. The lowercase "g" will mutate the PAM sequence while retaining Leucine coding. Underlined and bold **G** will repair the *AXIN1* nonsense mutation.

sgRNA	GGAGGAGGCGCGCTGACGTC
ssODN	GTAACCCCCAAGACCCACCCCACCCCACGACGCGGCCGTACCTCTGCTTGGAGGGTGCT CGGCTGGCTCTCTTTTCTTCCTCCTCgAGACGTC**G**GCGCGCCTCCTCCAGCTGGGTTAGG GGGTTGGG

References

1. Forner, A., *et al.* (2012) Hepatocellular carcinoma. *Lancet*, 379, 1245-55.

2. Sherman, M. (2010) Hepatocellular carcinoma: epidemiology, surveillance, and diagnosis. *Semin Liver Dis*, 30, 3-16.

3. Marquardt, J.U., *et al.* (2015) Functional and genetic deconstruction of the cellular origin in liver cancer. *Nat Rev Cancer*, 15, 653-67.

4. Dahmani, R., *et al.* (2011) The Wnt/beta-catenin pathway as a therapeutic target in human hepatocellular carcinoma. *Clin Res Hepatol Gastroenterol*, 35, 709-13.

5. Albuquerque, C., *et al.* (2011) Colorectal cancers choosing sides. *Biochim Biophys Acta Rev Cancer*, 1816, 219-231.

6. Zucman-Rossi, J., *et al.* (2015) Genetic Landscape and Biomarkers of Hepatocellular Carcinoma. *Gastroenterology*, 149, 1226-1239 e4.

7. Wang, W., *et al.* (2017) Action and function of Wnt/beta-catenin signaling in the progression from chronic hepatitis C to hepatocellular carcinoma. *J Gastroenterol*, 52, 419-431.

8. Network, C.G.A.R. (2017) Comprehensive and Integrative Genomic Characterization of Hepatocellular Carcinoma. *Cell*, 169, 1327-1341 e23.

9. Schulze, K., *et al.* (2015) Exome sequencing of hepatocellular carcinomas identifies new mutational signatures and potential therapeutic targets. *Nat Genet*, 47, 505-511.

10. Zucman-Rossi, J., *et al.* (2007) Differential effects of inactivated Axin1 and activated beta-catenin mutations in human hepatocellular carcinomas. *Oncogene*, 26, 774-80.

11. Feng, G.J., *et al.* (2012) Conditional disruption of Axin1 leads to development of liver tumors in mice. *Gastroenterology*, 143, 1650-9.

12. Abitbol, S., *et al.* (2018) AXIN deficiency in human and mouse hepatocytes induces hepatocellular carcinoma in the absence of beta-catenin activation. *J Hepatol*, 68, 1203-1213.

13. Arnold, H.K., *et al.* (2009) The Axin1 scaffold protein promotes formation of a degradation complex for c-Myc. *EMBO J*, 28, 500-12.

14. Rui, Y., *et al.* (2004) Axin stimulates p53 functions by activation of HIPK2 kinase through multimeric complex formation. *EMBO J*, 23, 4583-94.

15. Li, Q., *et al.* (2009) Axin determines cell fate by controlling the p53 activation threshold after DNA damage. *Nat Cell Biol*, 11, 1128-34.

16. Guo, X., *et al.* (2008) Axin and GSK3- control Smad3 protein stability and modulate TGF- signaling. *Genes Dev*, 22, 106-20.

17. Satoh, S., *et al.* (2000) AXIN1 mutations in hepatocellular carcinomas, and growth suppression in cancer cells by virus-mediated transfer of AXIN1. *Nat Genet*, 24, 245-50.

18. Wang, W., *et al.* (2016) Blocking Wnt Secretion Reduces Growth of Hepatocellular Carcinoma Cell Lines Mostly Independent of beta-Catenin Signaling. *Neoplasia*, 18, 711-723.

19. Zhang, Y., *et al.* (2011) RNF146 is a poly(ADP-ribose)-directed E3 ligase that regulates axin degradation and Wnt signalling. *Nat Cell Biol*, 13, 623-9.

20. Callow, M.G., *et al.* (2011) Ubiquitin ligase RNF146 regulates tankyrase and Axin to promote Wnt signaling. *PLoS One*, 6, e22595.

21. Thorvaldsen, T.E., *et al.* (2017) Differential Roles of AXIN1 and AXIN2 in Tankyrase Inhibitor-Induced Formation of Degradasomes and beta-Catenin Degradation. *PLoS One*, 12, e0170508.

22. Mariotti, L., *et al.* (2017) Regulation of Wnt/beta-catenin signalling by tankyrase-dependent poly(ADP-ribosyl)ation and scaffolding. *Br J Pharmacol*, 174, 4611-4636.

23. Bao, R., *et al.* (2012) Inhibition of tankyrases induces Axin stabilization and blocks Wnt signalling in breast cancer cells. *PLoS One*, 7, e48670.

24. Busch, A.M., *et al.* (2013) Evidence for tankyrases as antineoplastic targets in lung cancer. *BMC Cancer*, 13, 211.

25. Huang, S.M., *et al.* (2009) Tankyrase inhibition stabilizes axin and antagonizes Wnt signalling. *Nature*, 461, 614-20.

26. Tanaka, N., *et al.* (2017) APC mutations as a potential biomarker for sensitivity to tankyrase inhibitors in colorectal cancer. *Mol Cancer Ther*.

27. Lau, T., *et al.* (2013) A novel tankyrase small-molecule inhibitor suppresses APC mutation-driven colorectal tumor growth. *Cancer Res*, 73, 3132-44.

28. Waaler, J., *et al.* (2012) A novel tankyrase inhibitor decreases canonical Wnt signaling in colon carcinoma cells and reduces tumor growth in conditional APC mutant mice. *Cancer Res*, 72, 2822-32.

29. de la Roche, M., *et al.* (2014) LEF1 and B9L shield beta-catenin from inactivation by Axin, desensitizing colorectal cancer cells to tankyrase inhibitors. *Cancer Res*, 74, 1495-505.

30. Ma, L., *et al.* (2015) Tankyrase inhibitors attenuate WNT/beta-catenin signaling and inhibit growth of hepatocellular carcinoma cells. *Oncotarget*, 6, 25390-401.

31. Forbes, S.A., *et al.* (2015) COSMIC: exploring the world's knowledge of somatic mutations in human cancer. *Nucleic Acids Res*, 43, D805-11.

32. van Veelen, W., *et al.* (2011) beta-catenin tyrosine 654 phosphorylation increases Wnt signalling and intestinal tumorigenesis. *Gut*, 60, 1204-12.

33. Ran, F.A., *et al.* (2013) Genome engineering using the CRISPR-Cas9 system. *Nat Protoc*, 8, 2281-2308.

34. Richardson, C.D., *et al.* (2016) Enhancing homology-directed genome editing by catalytically active and inactive CRISPR-Cas9 using asymmetric donor DNA. *Nat Biotechnol*, 34, 339-44.

35. Song, J., *et al.* (2016) RS-1 enhances CRISPR/Cas9- and TALEN-mediated knock-in efficiency. *Nat Commun*, 7, 10548.

36. Schmieder, R., *et al.* (2011) Quality control and preprocessing of metagenomic datasets. *Bioinformatics*, 27, 863-4.

37. Bolger, A.M., *et al.* (2014) Trimmomatic: a flexible trimmer for Illumina sequence data. *Bioinformatics*, 30, 2114-20.

38. Dobin, A., *et al.* (2013) STAR: ultrafast universal RNA-seq aligner. *Bioinformatics*, 29, 15-21.

39. Tarasov, A., *et al.* (2015) Sambamba: fast processing of NGS alignment formats. *Bioinformatics*, 31, 2032-4.

40. Liao, Y., *et al.* (2014) featureCounts: an efficient general purpose program for assigning sequence reads to genomic features. *Bioinformatics*, 30, 923-30.

41. Love, M.I., *et al.* (2014) Moderated estimation of fold change and dispersion for RNA-seq data with DESeq2. *Genome Biol*, 15, 550.

42. Thorvaldsen, T.E. (2017) Targeting Tankyrase to Fight WNT-dependent Tumours. *Basic Clin Pharmacol Toxicol*, 121, 81-88.

43. Martino-Echarri, E., *et al.* (2016) Tankyrase Inhibitors Stimulate the Ability of Tankyrases to Bind Axin and Drive Assembly of beta-Catenin Degradation-Competent Axin Puncta. *PLoS One*, 11, e0150484.

44. Nagy, Z., *et al.* (2016) Tankyrases Promote Homologous Recombination and Check Point Activation in Response to DSBs. *PLoS Genet*, 12, e1005791.

45. Chang, P., *et al.* (2005) Tankyrase-1 polymerization of poly(ADP-ribose) is required for spindle structure and function. *Nat Cell Biol*, 7, 1133-9.

46. Smith, S., *et al.* (1998) Tankyrase, a poly(ADP-ribose) polymerase at human telomeres. *Science*, 282, 1484-7.

47. Bienz, M. (2014) Signalosome assembly by domains undergoing dynamic head-to-tail polymerization. *Trends Biochem Sci*, 39, 487-95.

48. Gammons, M., *et al.* (2018) Multiprotein complexes governing Wnt signal transduction. *Curr Opin Cell Biol*, 51, 42-49.

49. Mazzoni, S.M., *et al.* (2014) AXIN1 and AXIN2 variants in gastrointestinal cancers. *Cancer Lett*, 355, 1-8.

50. Chia, I.V., *et al.* (2005) Mouse axin and axin2/conductin proteins are functionally equivalent in vivo. *Mol Cell Biol*, 25, 4371-6.

51. Fodde, R., *et al.* (2010) Nuclear beta-catenin expression and Wnt signalling: in defence of the dogma. *J Pathol*, 221, 239-41.

52. Buchert, M., *et al.* (2010) Genetic dissection of differential signaling threshold requirements for the Wnt/beta-catenin pathway in vivo. *PLoS Genet*, 6, e1000816.

53. Bakker, E.R., *et al.* (2013) beta-Catenin signaling dosage dictates tissue-specific tumor predisposition in Apc-driven cancer. *Oncogene*, 32, 4579-85.

54. Lum, L., *et al.* (2015) Chemical Disruption of Wnt-dependent Cell Fate Decision-making Mechanisms in Cancer and Regenerative Medicine. *Curr Med Chem*, 22, 4091-103.

55. Guichard, C., *et al.* (2012) Integrated analysis of somatic mutations and focal copy-number changes identifies key genes and pathways in hepatocellular carcinoma. *Nat Genet*, 44, 694-8.

56. Kan, Z., *et al.* (2013) Whole-genome sequencing identifies recurrent mutations in hepatocellular carcinoma. *Genome Res*, 23, 1422-33.

Chapter 4

Blocking Wnt secretion reduces growth of hepatocellular carcinoma cell lines mostly independent of β-catenin signaling

Wenhui Wang, Lei Xu*, Pengyu Liu*, Kiran Jairam, Yuebang Yin, Kan Chen, Dave Sprengers, Maikel P. Peppelenbosch, Qiuwei Pan, Ron Smits*

Department of Gastroenterology and Hepatology, Erasmus MC-University Medical Center and Postgraduate School Molecular Medicine, Rotterdam, the Netherlands

Neoplasia. 2016;18(12):711-723

Abstract

Aberrant activation of Wnt/β-catenin signaling plays a key role in the onset and development of hepatocellular carcinomas (HCC), with about half of them acquiring mutations in either *CTNNB1* or *AXIN1*. However, it remains unclear whether these mutations impose sufficient β-catenin signaling or require upstream Wnt ligand activation for sustaining optimal growth, as previously suggested for colorectal cancers. Using a panel of nine HCC cell lines we show that siRNA mediated knock-down of β-catenin impairs growth of all these lines. Blocking Wnt secretion, either by treatment with the IWP12 porcupine inhibitor or knockdown of WLS, reduces growth of most of the lines. Unexpectedly, interfering with Wnt secretion does not clearly affect the level of β-catenin signaling in the majority of lines, suggesting that other mechanisms underlie the growth suppressive effect. However, IWP12 treatment did not induce autophagy or endoplasmic reticulum (ER) stress, which may have resulted from the accumulation of Wnt ligands within the ER. Similar results were observed for colorectal cancer cell lines used for comparison in various assays. These results suggest that most colorectal and liver cancers with mutations in components of the β-catenin degradation complex do not strongly rely on extracellular Wnt ligand exposure to support optimal growth. In addition, our results also suggest that blocking Wnt secretion may aid in tumor suppression through alternative routes currently unappreciated.

Keywords: Hepatocellular carcinoma; Wnt/β-catenin signaling

Introduction

Hepatocellular carcinoma (HCC) is considered as the fifth most common cancer and the third main reason for cancer related death with 748,000 cases and 695,000 deaths each year [1, 2]. The etiology of HCC includes Hepatitis B virus (HBV) or Hepatitis C virus (HCV) infection, alcohol liver disease, non-alcoholic steatohepatitis (NASH) and aflatoxin-B1 exposure [3]. More than 80% of all HCCs occur in Eastern and Southeastern Asia where the main cause is HBV combined with exposure to aflatoxin-B1 [4]. In Europe, Japan and the United States, HCV represents the dominant risk factor, together with alcohol abuse and nonalcoholic fatty liver diseases [5, 6].

Wnt/β-catenin signaling plays an important role in a wide range of biological processes, involving embryonic patterning, cell proliferation, differentiation, angiogenesis, carcinogenesis, metastasis and drug resistance [7-9]. Underscoring the relevance of this pathway, many tumor types including HCC, exhibit enhanced Wnt/β-catenin signaling that strongly contributes to tumor growth [10]. Activation of Wnt/β-catenin signaling starts with the secretion of Wnt ligands. Wnts produced within the endoplasmic reticulum (ER) are palmitoylated by the Wnt acyl-transferase porcupine (PORCN), which is essential for their secretion and signaling activity. Following this lipid modification, Wntless (WLS) is needed to shuttle the Wnt proteins from the Golgi to the plasma membrane where they can signal in an autocrine or paracrine manner [11]. In the absence of upstream Wnt signaling, β-catenin is phosphorylated at N-terminal Ser/Thr residues by a multiprotein complex consisting of the adenomatous polyposis coli (APC) tumor suppressor, scaffold proteins AXIN1, AXIN2 and AMER1, and the kinases GSK3 and CK1α. Phosphorylated β-catenin is then ubiquitinated, leading to its proteasomal degradation [12-14]. The overall effect is low β-catenin levels in the cytoplasm and nucleus of unstimulated cells.Upon binding of Wnt ligands to Frizzled and LRP5/6 co-receptors, Disheveled (DVL) becomes phosphorylated, subsequently resulting in the inhibition of the β-catenin destruction complex [15]. As a result, β-catenin is stabilized and is able to translocate to the nucleus and associate with members of the TCF/LEF family of transcription factors, thus regulating the expression of specific downstream Wnt/β-catenin target genes thereby affecting cellular decisions [4]. In addition to this classical (canonical) Wnt signaling pathway, Wnts can also signal in an alternative (non-canonical) fashion independent of β-catenin through associating

with Frizzled and ROR1/2 receptors instead of LRP5/6. Activation of non-canonical Wnt signaling mainly affects cellular processes involved in migration and cellular polarity [8].

Hepatocarcinogenesis is a multistep process, progressing from a normal hepatocyte to a transformed phenotype as a result of the accumulation of aberrant genetic and epigenetic modifications and activation of various signaling pathways [16-18]. Increasing evidence indicates that activation of Wnt/β-catenin signaling is critical in hepatic oncogenesis [19, 20]. About 40%-70% of HCCs are characterized by nuclear accumulation of β-catenin, the hallmark of active signaling. Various molecular and genetic alterations contribute to aberrant activation of Wnt/β-catenin signaling. Mutations within components of the canonical Wnt/β-catenin signaling enhance stabilization of β-catenin and transcriptional activity in the nucleus. Approximately one third of all HCCs carry oncogenic β-catenin mutations within exon 3 at the N-terminal phosphorylation residues, making the protein more resistant to proteolytic degradation [21]. In another subset of tumors, loss-of-function mutations of negative regulators are observed in the *APC* and *AXIN1* genes, respectively in 1-3% and 8-15% of tumors [19], both causing compromised ability to degrade β-catenin [8]. In addition to mutations, various other mechanisms have been suggested to promote β-catenin signaling, including overexpression of Wnt ligands and/or their corresponding receptors, and reduced expression of extracellular inhibitors [22]. Given the importance of β-catenin signaling for hepatic oncogenesis, various treatments targeting this route have been evaluated [23].

Cancers harboring mutations within intracellular components of the β-catenin signaling pathway, i.e., mutation of APC, AXIN or β-catenin itself, were often considered to become largely independent of upstream regulation by extracellular Wnt ligands. This belief has however been challenged during the last years. For example, Wnt antagonists SFRPs and DKKs are reported to attenuate Wnt signaling in colorectal cancer (CRC) [24, 25]. Recently, it was demonstrated that interfering with Wnt secretion or reducing the expression of specific Wnt ligands impaired the growth of APC and β-catenin mutant CRC cell lines [26]. These results also indicated that interfering with Wnt secretion, for example using the newly developed PORCN inhibitors [27, 28], could be useful as an additive treatment option for tumors characterized by enhanced β-catenin signaling.

Here, we have investigated whether this also holds truth for β-catenin or AXIN1 mutant liver cancer cells.

Materials and methods

Cell lines

Human HCC cell lines Hep3B, Huh6, Huh7, PLC/PRF/5, SNU182, SNU398, SNU449 and CRC cell lines CACO2, DLD1, HT29, SW480, HCT116, LS174T, SW48 and RKO were cultured in Dulbecco's modified Eagle medium (DMEM) (Invitrogen-Gibco, Breda, The Netherlands) complemented with 10% (v/v) fetal calf serum (Hyclone, Lonan, Utah), 100 IU/ml penicillin, 100 µg/ml streptomycin and 2 mM L-glutamine (Invitrogen-Gibco). The hepatoblastoma cell line HepG2 was cultured on fibronectin/collagen/albumin-coated plates (AthenaES) in Williams E medium (Invitrogen-Gibco, Breda, The Netherlands) complemented with 10% (v/v) fetal calf serum, 100 IU/ml penicillin, 100 µg/ml streptomycin and 2 mM L-glutamine. HepaRG was cultured in William's E medium supplemented with 10% (v/v) fetal calf serum, 100 IU/ml penicillin, 100 µg/ml streptomycin, 5 µg/ml insulin (Sigma-Aldrich, St Louis, MO), and 50 µM hydrocortisone hemisuccinate (Sigma-Aldrich, St Louis, MO). Identity of all cell lines was confirmed by STR genotyping. *CTNNB1* mutation status was confirmed in all the nine HCC cell lines by Sanger sequencing and was consistent with those reported at COSMIC, the Catalogue of Somatic Mutations in Cancer (http://cancer.sanger.ac.uk) [29].

For the preparation of conditioned medium, L-Control and L-Wnt3A cells were cultured in complete DMEM medium, followed by collection and filtration of medium according to standard procedures. HCC and CRC cell lines were stimulated with 25% L-Control or L-Wnt3A medium.

Reagents

IWP12 (Sigma-Aldrich, St Louis, MO) was dissolved in dimethyl sulfoxide (DMSO) (Sigma-Aldrich, St Louis, MO) with a final stock concentration of 10mM. Antibodies specific for β-catenin (Cat. #9561, Cell Signaling Technology), dishevelled adaptor protein (DVL2) (Cat. #3216, Cell Signaling Technology), WLS (Cat.#MABS87, clone YJ5 Millipore), LC3 Ⅰ/Ⅱ (Cat. #4108, Cell Signaling Technology), GPR177(Wls/Evi)

(Cat.#MABS87, Millipore) and β-actin (sc-47778, Santa Cruz), Tubulin (sc-8035, Santa Cruz) anti-rabbit or anti-mouse IRDye-conjugated secondary antibodies (Stressgen, Glandford Ave, Victoria, BC, Canada) were used for western blot analysis.

Table1. Gene mutations of Wnt/β-catenin signaling components in HCC and CRC cell lines

Cell line	Gene	AA alteration	Zygosity
HCC			
HepG2	*CTNNB1*	p.W25_I140 del	Heterozygous
Huh6	*CTNNB1*	p.G34V	Heterozygous
SNU398	*CTNNB1*	p.S37C	Heterozygous
Hep3B	*AXIN1*	p.R146*	Homozygous
PLC/PRF/5	*AXIN1*	p.(R373_M418 del)	Homozygous
SNU449	*AXIN1*	p.R712*	Homozygous
Huh7			
HepaRG			
SNU182			
CRC			
SW480	*APC*	p.Q1338*	Homozygous
HT29	*APC*	p.T1556fs*3	Heterozygous
		p.E853*	Heterozygous
Caco2	*APC*	p.Q1367*	Homozygous
DLD1	*APC*	p.R2166*	Heterozygous
		p.I1417fs*2	Heterozygous
	AXIN1	p.L396M	Heterozygous
	RNF43	p.G659fs*41	Heterozygous
SW48	*CTNNB1*	p.S33Y	Heterozygous
	RNF43	p.G659fs*41	Heterozygous
		p.V299fs*143	Heterozygous
HCT116	*CTNNB1*	p.S45del	Heterozygous
	RNF43	p.R117fs*41	Heterozygous
LS174T	*CTNNB1*	p.S45F	Homozygous
RKO	*RNF43*	p.G659fs*41	Heterozygous

Gene knockdown by small interfering RNA (siRNA)

Smartpool ON-TARGETplus siRNAs targeting *CTNNB1* and *WLS* were obtained from Dharmacon. The ON-TARGETplus Non-targeting siRNA #2 was used as negative control. Cells were reverse-transfected in a 96-well plate using a total of 0.2 ul DharmaFECT formulation 4 (Thermo Fischer Scientific) and 25nM of each siRNA per well. Following 72 hours incubation, the effect on knock-down was determined by western blotting.

Quantitative real-time polymerase chain reaction

RNA was isolated with a Machery-NucleoSpin RNA II kit (Bioke, Leiden, The Netherlands) and quantified using a Nanodrop ND-1000 (Wilmington, DE, USA). CDNA was prepared from total RNA using a cDNA Synthesis Kit (TAKARA BIO INC) and subjected to quantitative Real-Time PCR analyses. Analyses were performed using the StepOne Real-Time PCR System and the StepOnev2.0 software (Applied Biosystem, Darmstadt, Germany). Primer sequences are provided in supplementary Table1. All expression levels are depicted relative to the expression of *GAPDH*.

Western blot assay

Cells were lysed in Laemmli sample buffer with 0.1 M DTT and heated for 5-10 minutes at 95 ℃, followed by loading and separation on a 8-15% sodium dodecyl sulphate-polyacrylamide gels (SDS-PAGE). After 90 min running at 120 V, proteins were electrophoretically transferred onto a polyvinylidene difluoride (PVDF) membrane (Invitrogen) for 1.5 h with an electric current of 250 mA. Subsequently, the membrane was blocked with 2.5 ml Odyssey Blocking Buffer and 2.5 ml PBS containing 0.05% Tween 20 (PBS-T), followed by incubation with primary antibody (all 1:1000) overnight at 4 ℃. The membrane was washed 3 times with PBS-T followed by incubation for 1.5 h with anti-rabbit or anti-mouse IRDye-conjugated secondary antibodies (LI-COR Biosciences, Lincoln, USA) (1:5000) at room temperature. Blots were assayed for β-actin or Tubulin content as standardization of sample loading, scanned, and quantified by Odyssey infrared imaging (Li-COR Biosciences, Lincoln, NE, USA). Results were visualized and quantified with Odyssey 3.0 software.

β-catenin reporter assays

The β-catenin reporter assays were basically performed as previously described [30, 31]. In short, twenty hours before transfection, we plated 10^5 cells per well on 12-well

plates. Each well was transfected with 500 ng Wnt Responsive Element (WRE) or Mutant Responsive Element (MRE) vectors and 20 ng TK-Renilla using polyethylenimine (PEI) (Sigma-Aldrich, St Louis, MO) or Fugene HD (Promega). We measured luciferase activities in a LumiStar Optima luminescence counter (BMG LabTech, Offenburg, Germany) and normalized the data for the transfection efficiency by using the Dual Luciferase Reporter Assay system (Promega) according to the manufacturer's instruction. Transfections were performed in triplicate and the mean and standard error were calculated for each condition. The β-catenin reporter activities are shown as WRE/MRE ratios.

MTT assay

10 mM 3-(4,5-dimethylthiazol-2-yl)-2,5-diphenyltetrazolium bromide (MTT) (Sigma) was added to cells seeded in 96-well plates and incubated at 37°C with 5% CO2 for 3 h. The medium was removed and 100 µl DMSO was added to each well. The absorbance of each well was read on a microplate absorbance reader (BIO-RAD) at wavelength of 490 nm. For siRNA mediated knockdown of genes, 4 independent wells were assayed for each cell line at least two times, whereas for IWP12 treatment 6 independent wells were used. The mean and standard error were calculated for each condition.

Cell cycle analysis

Around 60%-80% confluency, cells were trypsinized and washed with PBS and then fixed in cold 70% ethanol overnight at 4℃. The cells were washed twice with PBS and incubated with 20ug/ml RNase at 37°C for 30 min followed by incubation with 50ug/ml Propidium Iodide (PI) at 4°C for 30min. Then samples were tested immediately by FACS. Cell cycle was analyzed by FlowJo_V10 software. For each treatment, two independent wells were tested for Huh6, SNU449 and Huh7 two times. The mean and standard error were calculated for each condition.

Statistical analysis

All results were presented as mean ± SD. Comparisons between groups were performed with one sample t test. Differences were considered significant at a p value less than 0.05.

Results

β-catenin signaling activity of HCC cell lines

To investigate the importance of β-catenin signaling and Wnt secretion for sustaining cell growth, we employed 9 HCC cell lines, listed in Table 1 in which gene mutations related to Wnt/β-catenin signaling are depicted. We also used 8 CRC cell lines for comparison in various assays, known to largely depend on β-catenin signaling for their growth. First, we determined the baseline β-catenin signaling activity for all these cell lines using a β-catenin reporter assay and qRT-PCR of *AXIN2*, a well-established β-catenin target gene. As indicated in Figure 1, in line with previous publications, all β-catenin mutant HCC lines (SNU398, HepG2 and Huh6) showed a robust induction of both reporter activity as well as high *AXIN2* expression. The AXIN1 mutant lines (PLC/PRF/5, Hep3B and SNU449) also displayed enhanced reporter activity, albeit generally more modest, whereas the expression of *AXIN2* was low. Interestingly, among the HCC lines without an obvious mutation, SNU182 presented with high β-catenin signaling activity, both on reporter level and *AXIN2* expression. Huh7 and HepaRG showed low reporter activity together with low *AXIN2* expression. All CRC lines, except RKO being wild type for *APC* and *CTNNB1*, showed the expected increase in reporter activity (Figure S1).

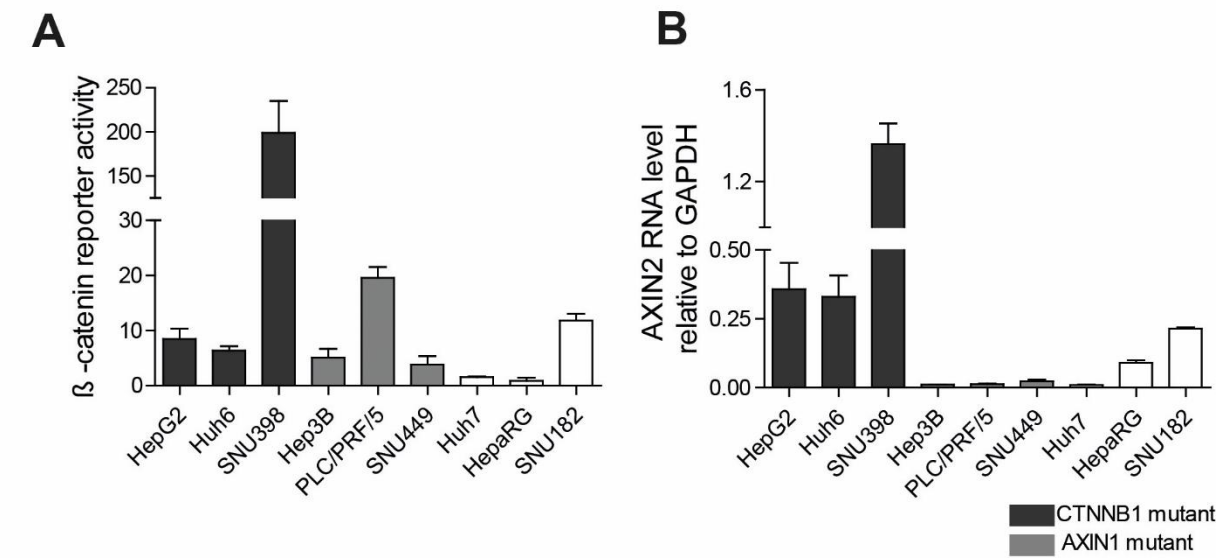

Fig.1. Baseline β-catenin signaling activity in HCC cell lines. (A) β-catenin luciferase reporter assay showing β-catenin signaling activity in HCC cell lines (mean ± SD, n = 3). The β-catenin reporter activities are depicted as WRE/MRE ratios. (B) QRT-PCR assay showing expression of the β-catenin target gene

AXIN2 in HCC cell lines (mean ± SD, n = 3). Expression levels are depicted relative to the housekeeping gene *GAPDH*.

Requirement for β-catenin signaling to sustain efficient cell growth

Next, we determined the dependence on β-catenin signaling for supporting efficient growth by transiently transfecting smartpool siRNAs targeting *CTNNB1* or a control siRNA, followed by a MTT assay to test cell numbers after 3 days of culture. For most cell lines we accomplished more than 80% knock-down of β-catenin at protein level as determined by quantitative western blot analysis, with the exception of HepaRG in which a 65% reduction was observed (see Figures 2A and S2). As indicated in Figure 2B, β-catenin signaling activity was clearly suppressed by siRNA mediated knockdown in the three lines tested for this purpose, i.e. Huh6, SNU449 and Huh7. All HCC cell lines were inhibited significantly in their growth (Figure 2C) suggesting that β-catenin signaling is important for the growth of these tumor cells, even in the ones that show only low to modest levels of signaling, such as Huh7 and HepaRG. Cell cycle analysis in three lines showed that β-catenin knockdown provoked a dramatic G0/G1 phase arrest in Huh6 (Fig 2D). Also in Huh7 a notable increase of cells in G0/G1 is observed with a significant reduction of cells in the G2/M phase, whereas for SNU449 a trend is observed towards more cells in G0/G1 and less cells in S-phase. As expected, all five tested CRC cell lines showed a significantly reduced growth upon β-catenin knockdown (Figure 2E).

Expression levels of WNT ligands in HCC cell lines

Taken together, the results above indicate that targeting the β-catenin signaling pathway represents an attractive route to suppress the growth of HCCs. This pathway has however been refractory to target in an efficient manner. More recently, inhibitors of Wnt secretion have been proposed as treatment options for malignancies dependent on Wnt-ligand secretion for their growth [26-28]. However, a prerequisite is that the tumor cells express sufficient levels of Wnt ligands capable of inducing β-catenin signaling. Hence, we investigated the expression profile of all 19 Wnt ligand genes in our HCC cell line panel by qRT-PCR. From the group of Wnt ligands more commonly associated with inducing β-catenin signaling (*WNT1, 2, 3, 3A, 8A, 8B, 10A* and *10B*), only *WNT3* was clearly expressed in all HCC cell lines, followed by high *WNT10A* expression restricted to the SNU182 and HepaRG cell lines, and high *WNT2* expression in SNU449

(Figure 3A). The remaining ligands of this group are barely detectable or expressed at least at 10-fold lower levels in all cell lines (Figure S3). When piling up the expression of all Wnt ligands from this group (Figure 3B), the SNU182 cell line clearly stands out as one with overall highest expression level, which may explain its high β-catenin signaling activity reported above. The β-catenin and AXIN1 mutant cell lines are among the low-to-intermediate ones.

Among the group of Wnt ligands more commonly associated with activating alternative pathways (*WNT4, 5A, 5B, 6, 7A, 7B* and *11*) depicted in Figure S4A, *WNT5A* was most prominently expressed, being very high in HepaRG and SNU182, and readily detectable in SNU398 and SNU449. The latter cell line also shows high expression of *WNT5B* and *WNT7B*. Other Wnt ligands of this group are detectable only at low levels or absent within

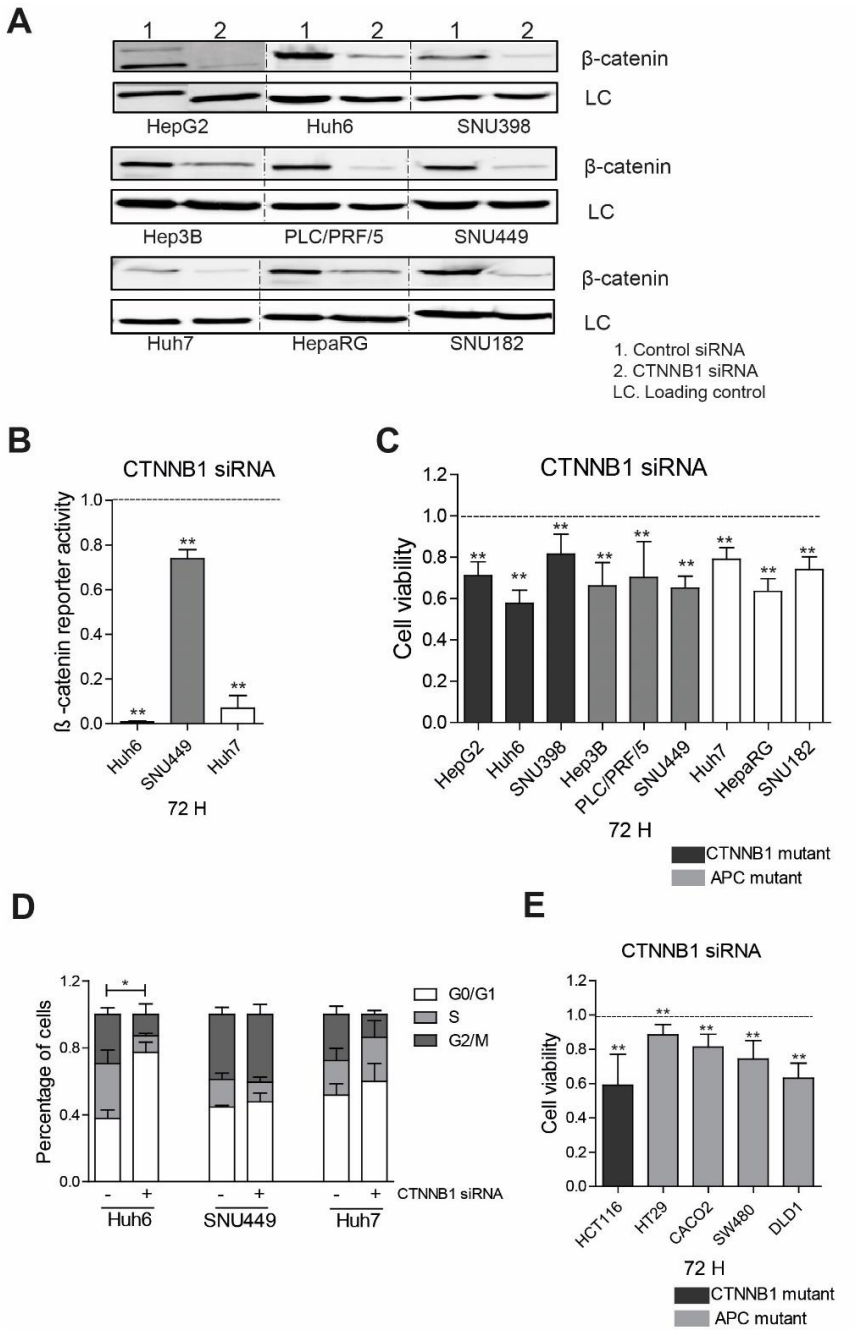

Fig.2. Requirement of β-catenin signaling for sustaining HCC cell growth. (A) HCC cell lines were transiently transfected with *CTNNB1* siRNAs for 72 hours. Cell lysates were collected for western blotting with indicated antibodies. Tubulin and β-actin served as loading control (LC). (B) Silencing of β-catenin caused the reduction of β-catenin signaling activity (mean ± SD, n=2, two times). (C) Silencing of β-catenin inhibited the growth of HCC cell lines as determined by MTT assay (mean ± SD, n=4, two times). (D) Silencing of β-catenin alters cell cycle progression in Huh6 (all phases significantly changed) and Huh7 cells (G2/M phase significantly reduced). SNU449 is less clearly altered, although the proportion of cells in S-phase is reduced (mean ± SD, n=2, two times). (E) β-catenin knockdown reduced cell growth in colorectal cancer cell lines. Values depicted are relative to the ones obtained with the non-targeting siRNA that are arbitrarily set to 1. *p<0.05; **p<0.01.

Most cell lines. Overall, SNU182 is again the most prominent expressing cell line, whereas the β-catenin and AXIN1 mutant cell lines are among the low-to-intermediate expressers (Figure 3B). Of the remaining Wnt ligands (*WNT2B, 9A, 9B* and *16*), *WNT2B* was highly expressed in PLC/PRF/5, SNU182, SNU398, and SNU449, while *WNT9B* was clearly expressed in Hep3B (Supplemental Figure S4B).

Combining the expression of all Wnt ligands shows that SNU182 has again the highest overall levels, followed by HepaRG and SNU449 (Figure 3B, right panel). As all Wnt ligands trigger the phosphorylation of DVL2 upon binding of either the FZD_LRP5/6 or FZD_ROR1/2 receptor complexes [32, 33], we determined baseline pDVL2 levels in all cell lines. As shown in Figure 3C, highest levels of phosphorylated DVL2 are observed in the three cell lines with highest Wnt levels, whereas for the remaining six lines no clear correlation can be observed.

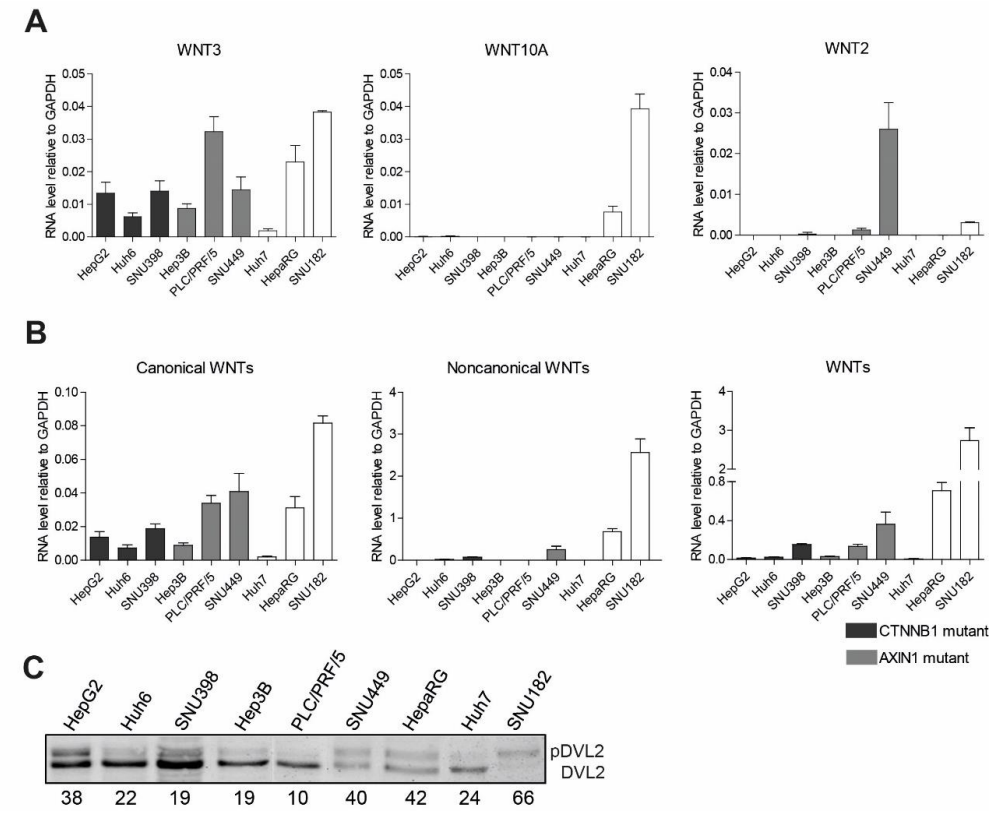

Fig.3. Expression levels of Wnt family members in HCC cell lines determined by qRT-PCR. (A) Expression levels of the top three expressed "canonical" Wnt ligands (mean ± SD, n=3). (B) Piled-up expression levels of canonical, non-canonical and overall Wnt ligands, respectively. All expression levels are depicted relative to the housekeeping gene *GAPDH*. (C) Baseline levels of phosphorylated DVL2 (pDVL2) in all HCC cell lines. Values below the image represent percentage of total DVL2 that is in the phosphorylated form (upper band).

In summary, although all HCC cell lines show a large variation in Wnt ligand expression, they all express Wnt ligands that can contribute to β-catenin signaling.

Wnt secretion blockage reduces growth of HCC cells

Given that most HCC cell lines show increased β-catenin signaling activity and expression of canonical Wnt ligands, we wished to investigate the consequences of suppressing the secretion of Wnt ligands. To this aim we used two methods, i.e., treatment with IWP12, an effective inhibitor of PORCN required for palmitoylation of Wnt proteins [34], and knockdown of *WLS*, which shuttles the palmitoylated Wnts from the Golgi to the plasma membrane. Both treatments are expected to reduce overall levels of secreted Wnt ligands. Following three days of IWP12 treatment, reduced cell numbers were observed for all β-catenin mutant cell lines (Figure 4A), ranging from 10% reduction (Huh6) to 35% (SNU398). Among the non-mutant lines, growth of HepaRG was strongly suppressed by IWP12, whereas Huh7 and SNU182 showed more modest reductions of their growth. The AXIN1 mutant lines were not clearly affected by IWP12 with the exception of PLC/PRF/5. Effects on growth following knockdown of *WLS* were largely in line with IWP12 treatment, with the exception of the AXIN1 mutant lines Hep3B and SNU449 that were significantly suppressed by *WLS* knockdown, and a less impressive growth reduction of HepaRG when compared with IWP12 (Figure 4B). Examples of efficient *WLS* knockdown are shown in supplemental Figure S5.

For comparison, the same assays were also performed on five CRC cell lines (Figure 4C, D). Both treatments showed the strongest growth suppression when applied to the β-catenin and RNF43 mutant HCT116 cell line. Intermediate effects were observed in DLD1, HT29, and SW480, whereas CACO2 was barely affected. In conclusion, most HCC and CRC cell lines are suppressed in their growth by both IWP12 treatment as well as *WLS* knockdown.

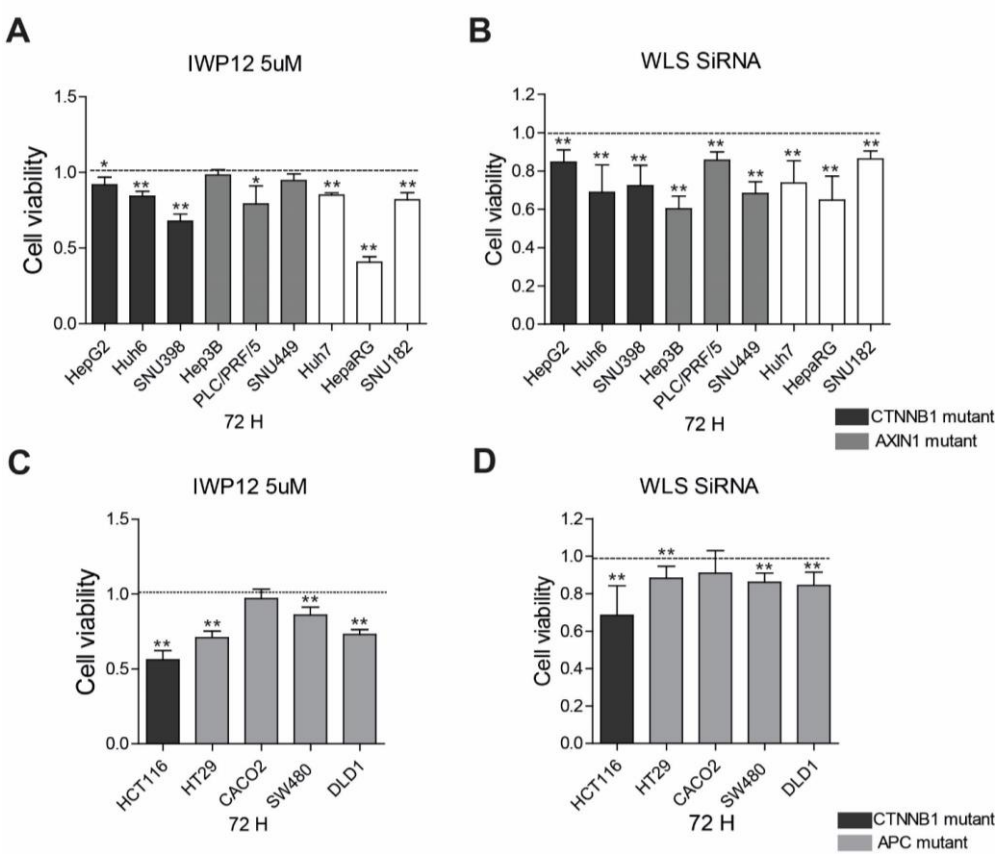

Fig.4. Inhibition of growth by Wnt secretion blockage. (A, C) IWP12 reduced cell growth of most HCC and CRC cell lines. Cell lines were incubated with 5 μM IWP12 for 72 hours and tested by MTT assay (mean ± SD, n=6, two times). Values depicted are relative to cell numbers obtained with the control DMSO treatment that are set to 1. (B, D) Cell lines were transiently transfected with *WLS* or non-targeting siRNAs for 72 hours, followed by MTT assay (mean ± SD, n = 4, two times). Values depicted are relative to cell numbers obtained with the non-targeting siRNA that are set to 1. *p<0.05; **p<0.01.

Altered exposure to extracellular Wnt ligands does not affect β-catenin signaling activity in most HCC cell lines

Previously, it was reported that Wnt secretion is required to maintain sufficiently high levels of canonical Wnt/β-catenin signaling activity in both APC and β-catenin mutant CRC cell lines [26]. Here, we asked whether the β-catenin and AXIN1 mutant HCC cell lines were also dependent on Wnt secretion to sustain this pathway activity. Exposure to extracellular Wnt ligands was again reduced by treating all cell lines with IWP12, after which we measured β-catenin signaling activity using the reporter assay and *AXIN2* qRT-PCR. After 48 hours, β-catenin reporter activity was clearly suppressed only in SNU182 (Figure 5A), whereas the remaining eight HCC lines were not or only modestly inhibited in their reporter activity. Reduction of *AXIN2* expression confirmed the strong

repressing effect of IWP12 in the SNU182 cell line, while no reduction was observed in the other cell lines (Figure 5B). Overall, this analysis shows that IWP12 treatment barely affects β-catenin signaling activity in most HCC cell lines, with the exception of SNU182.

In a true tumor setting, in addition to autocrine signaling, HCC cells are also exposed to Wnt ligands coming from the tumor microenvironment. Therefore, to determine the effects on β-catenin signaling of increased levels of extracellular Wnt ligands, we exposed them to L-Wnt3A conditioned medium. As shown in Figure 5C, β-catenin reporter activity was strongly enhanced in the Huh7 cell line and clearly activated in SNU182, both of which were confirmed by qRT-PCR for *AXIN2* (Figure 5D). Importantly, none of the β-catenin or AXIN1 mutant HCC lines showed enhanced β-catenin signaling following the addition of L-Wnt3A conditioned medium.

These results indicate that β-catenin and AXIN1 mutant HCC cell lines appear largely insensitive to the level of Wnt ligand exposure for sustaining intracellular β-catenin signaling, which could either mean that the expressed mutant β-catenin or AXIN1 protein determine overall signaling levels in a dominant fashion or, alternatively, that these cells have defects in their machinery to transduce Wnt signals. To test the latter option, we determined pDVL2 levels following treatment with IWP12 or L-Wnt3A conditioned medium (Figure 5E). Phosphorylation levels were not changed in Huh6, and only a modest reduction was observed in HepG2 following IWP12 treatment. In contrast, the SNU398 cell line showed a robust response in pDVL2 levels, decreasing from 21% to 7% by IWP12 treatment and upregulation to 59% following Wnt3A treatment. Thus, both options may hold true depending on the specific cell line under investigation. High variability in pDVL2 response was also observed in the remaining AXIN1-mutant and non-mutant HCC cell lines. The PLC/PRF/5 cell line showed a low baseline pDVL2 level, which was altered neither by IWP12 nor Wnt3A. The Huh7 and Hep3B cell lines also showed low baseline levels, which can however clearly be increased by the addition of Wnt3A. On the other hand, most DVL2 was phosphorylated at baseline in SNU182, which can be inhibited by IWP12, but can hardly be further stimulated by the addition of Wnt3A. Lastly, SNU449 and HepaRG showed intermediate pDVL2 levels at baseline that can both be reduced and activated by the respective treatments. Thus, all HCC cell lines show a large variation in both their baseline levels of pDVL2 as well as responsiveness to Wnt ligand exposure, irrespective of their mutation status.

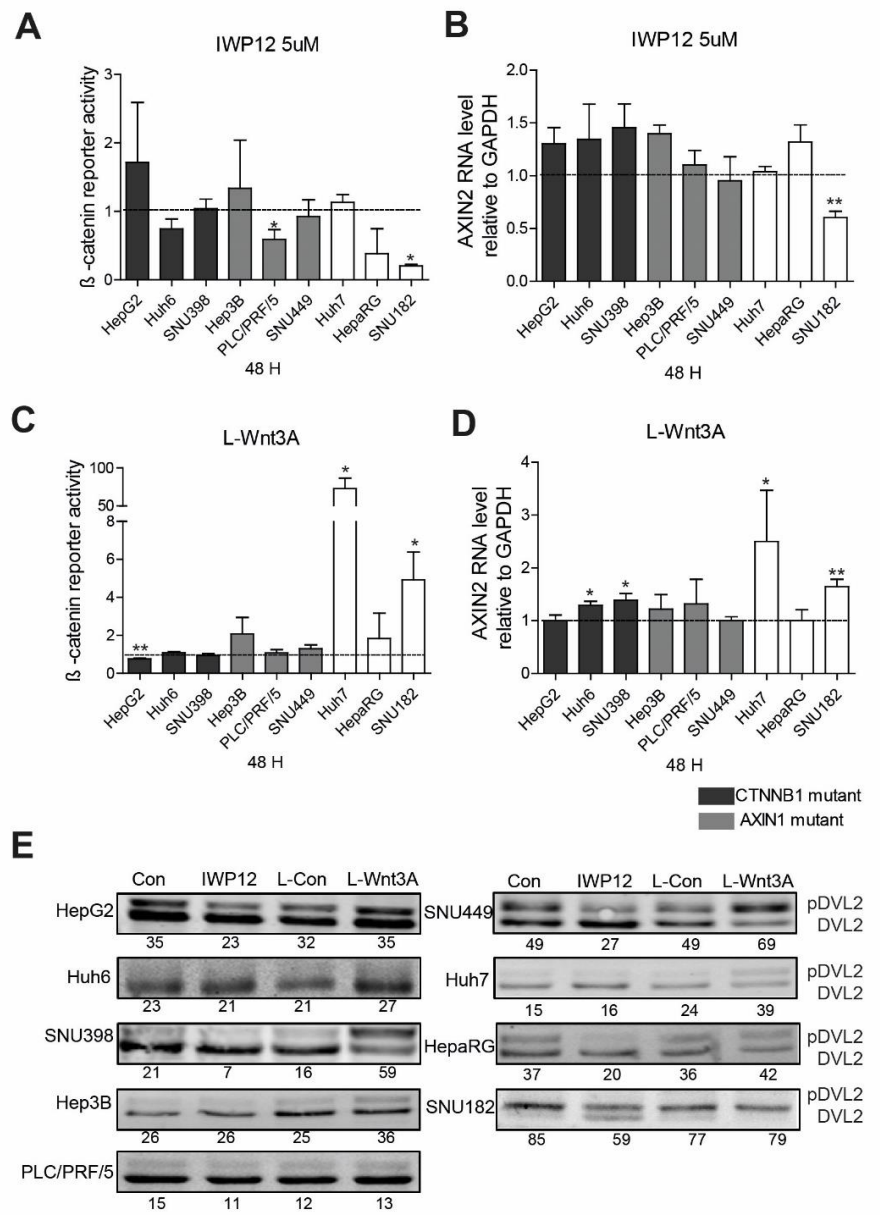

Fig.5. Growth reduction due to decreased Wnt secretion appears independent from β-catenin signaling. (A) β-catenin reporter activity was not clearly reduced by IWP12 in most HCC cell lines, except for SNU182 (mean ± SD, n=3). (B) QRT-PCR for *AXIN2* showed that its expression following IWP12 treatment was only reduced significantly in the SNU182 cell line (mean ± SD, n=3, two times). (C) L-Wnt3A conditioned medium significantly promoted β-catenin signaling activity in Huh7 and SNU182 cell lines. A significant albeit modest reduction of reporter activity was observed in HepG2. (mean ± SD, n=3). (D) Increased β-catenin signaling in SNU182 and Huh7 following L-Wnt3A treatment was confirmed by *AXIN2* qRT-PCR (mean ± SD, n=3, two times). All qRT-PCR and reporter values are depicted relative to the numbers obtained for the controls, which are arbitrarily set to 1. *p<0.05; **p<0.01. (E) Phosphorylation level of DVL2 protein following treatment with IWP12 or L-Wnt3A conditioned medium ("Con" is DMSO only, "L-Con" is L-Control conditioned medium). Values below the images represent percentage of total DVL2 that is in the phosphorylated form (upper band).

Response of CRC cell lines to alterations in Wnt ligand levels

Among the eight CRC cell lines treated with IWP12, only HCT116 showed a significant reduction in β-catenin reporter activity as well as *AXIN2* expression (Figure 6A,B). *AXIN2* expression was slightly reduced in HT29 and SW480, while CACO2 showed a reduced reporter activity only. Interestingly, HCT116 was also the only cell line in which both reporter activity and *AXIN2* expression could be significantly stimulated by the addition of extracellular Wnt3A (Figure 6C,D). Analysis of pDVL2 levels in a selection of 5 CRC lines showed that overall baseline levels were low with the exception of HCT116 in which 60% of DVL2 is phosphorylated (Figure 6E). IWP12 treatment shows the expected decrease in pDVL2 in HCT116, whereas none of the other cell lines showed clear alterations in pDVL2 levels following treatment with either IWP12 or Wnt3A.

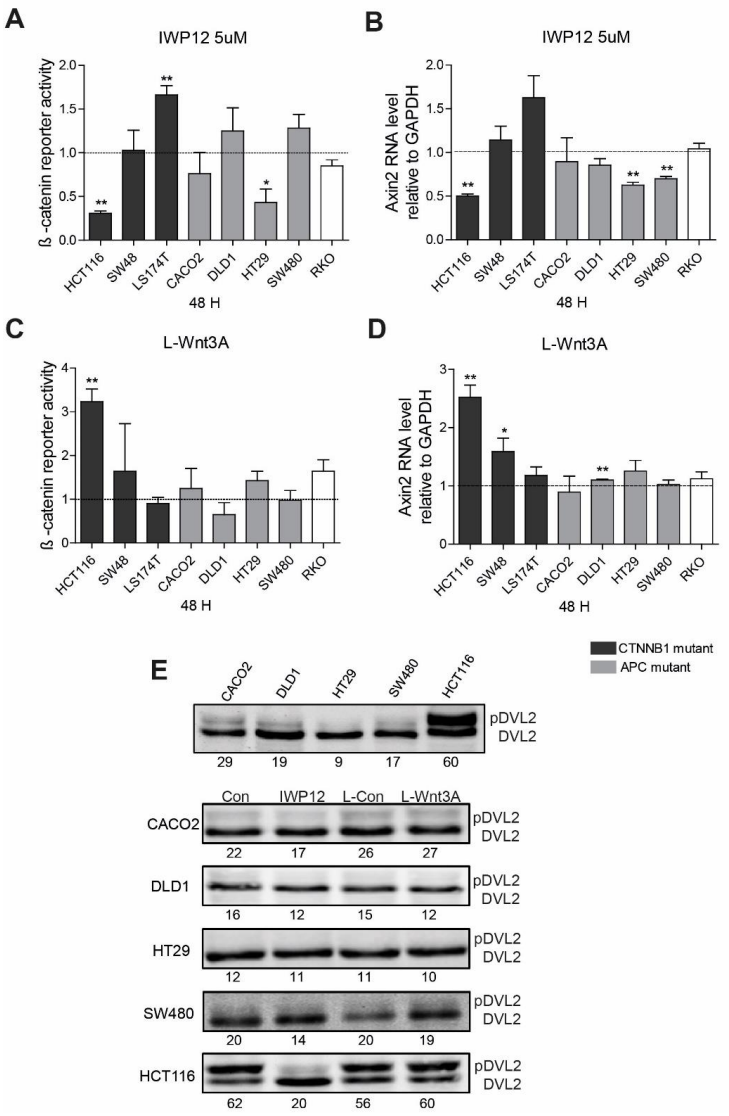

Fig.6. Responsiveness of CRC cell lines to alterations in Wnt ligand levels. (A) β-catenin reporter activity was significantly reduced by IWP12 in CACO2 and HCT116 cell lines (mean ± SD, n=3). (B) QRT-PCR for *AXIN2* showed that IWP12 treatment reduced its expression in HCT116. Modest but significant reductions were observed in HT29 and SW480 cell lines (mean ± SD, n=3, two times). (C) L-Wnt3A conditioned medium only increased β-catenin reporter activity significantly in HCT116 (mean ± SD, n=3).(D) *AXIN2* qRT-PCR confirmed upregulation of β-catenin signaling due to L-Wnta3A in HCT116. Significant but modest increases in *AXIN2* expression are seen in SW48 and DLD1 (mean ± SD, n=3). Reporter values are depicted relative to the numbers obtained for the controls, which are arbitrarily set to 1. *p<0.05; **p<0.01. (E) Top image shows comparison of baseline pDVL2 levels within a selection of five CRC cell lines. Bottom images show pDVL2 levels following treatment with IWP12 or L-Wnt3A conditioned medium ("Con" is DMSO only, "L-Con" is L-Control conditioned medium). Values below the images represent percentage of total DVL2 that is in the phosphorylated form (upper band).

Blocking Wnt secretion does not lead to increased ER stress

Blocking Wnt secretion using IWP12 or *WLS* knockdown reduces growth of HCC cell lines, apparently largely independent of β-catenin signaling. These treatments however also predict the accumulation of Wnt ligands in the ER, which may lead to activation of an ER stress response thereby reducing proliferation or inducing apoptosis. Therefore, ER stress was evaluated after IWP12 treatment in HCC cell lines using the expression of the ER-stress induced genes *CHOP* and *GRP94* as a read-out. As shown in Figure 7A and 7B, expression of *CHOP* was clearly increased in SNU398 (4.5-fold), whereas *GRP94* expression was elevated in SNU182 (2.8-fold). However, none of the other HCC cell lines displayed strong signs of induction. Overall, these results suggest that blocking Wnt secretion is not associated with the induction of a strong ER stress response.

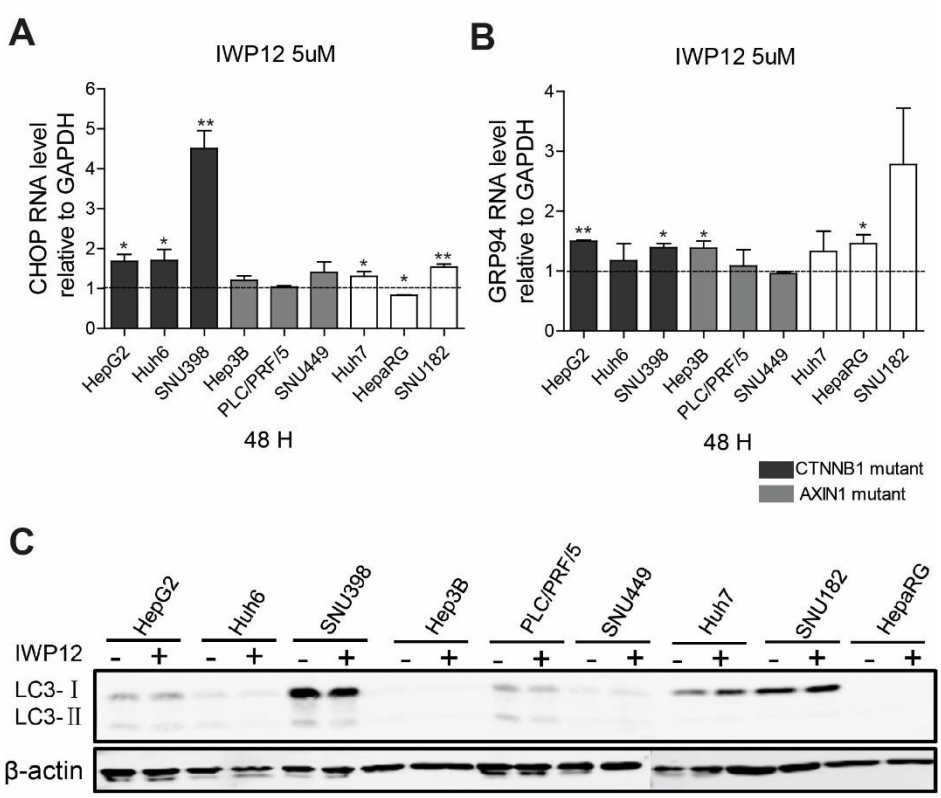

Fig.7. IWP12 treatment does not lead to the induction of a strong ER stress response or autophagy. Following 48 hours of IWP12 treatment, the expression of the ER stress induced response genes *CHOP* (A) and *GRP94* (B) was evaluated by qRT-PCR (mean ± SD, n=3). Except for a clear induction of *CHOP* in SNU398 and *GRP94* in SNU182, IWP12 caused slight or no induction of an ER stress response in other cell lines. Values depicted are relative to those obtained for the untreated control samples that are arbitrarily set to 1. *p<0.05; **p<0.01. (C) Wnt secretion inhibition does not enhance autophagy in HCC cell lines. After incubation with IWP12 for 48 hours, the expression of LC3-Ⅱ was tested by western blot.

Wnt secretion inhibition does not induce autophagy

Since knockdown of β-catenin or suppression of β-catenin signaling induced autophagy and even autophagic cell death in head and neck squamous cell carcinoma cells [35] and breast cancer stem-like cells [36], we further hypothesized that blocking Wnt secretion could exert similar effects on HCC cell lines. During autophagy the microtubule-associated protein 1A/1B-light chain 3 (LC3) is converted through lipidation into a lower migrating isoform (LC3-II) detectable by western blot, which is used as an indicator of autophagosome formation. As indicated in Figure 7C, IWP12 treatment does not change the LC3 pattern in any of the HCC cell lines, showing that it does not induce autophagy.

Discussion

In this article we have investigated the importance of β-catenin signaling and Wnt secretion for sustaining hepatocellular carcinoma growth. Using a panel of 9 HCC cell lines we show that β-catenin signaling is required to support optimal growth in all of them, in line with other reports using a limited number of cell lines [37, 38]. This is to be expected for cell lines carrying oncogenic β-catenin mutations in which the activating mutation will have provided a selective growth advantage during tumor formation, but it also holds true for the non-mutant ones that show only low levels of baseline signaling, such as Huh7 and HepaRG, as well as the AXIN1 mutant lines. The latter observation is of relevance as it has been debated whether AXIN1 mutations lead to a significant enhancement of β-catenin signaling within liver cancers. This subset of tumors apparently lacks a robust nuclear β-catenin accumulation and shows no clear upregulation of target genes such as *AXIN2* or *GLUL* [39, 40]. Also in our hands, the AXIN1 mutant lines are among the lowest expressors of *AXIN2*. Nevertheless, in these lines *AXIN2* was readily detectable by qRT-PCR (Ct values below 28), in addition to β-catenin reporter activities approaching those of the β-catenin mutant ones. Given that also these lines are suppressed in their growth following β-catenin knockdown, it shows that the majority of HCCs independent of their mutational profile, rely on β-catenin signaling for optimal growth.

Besides its role in signaling, β-catenin is also involved in cell-cell adhesion by directly binding to cadherins [41]. As such, the siRNA mediated knock-down that we apply here, will also likely reduce the amount of β-catenin sequestered at these adherens junctions. However, several investigations have shown that complete loss of β-catenin does not automatically lead to alterations in cell adhesion, including hepatocytes and hepatocellular cancer cells [42-45]. In all cases, it was shown that ɣ-catenin compensates for its loss, thereby retaining normal cell adhesion. Importantly, these studies show that it is mainly the signaling function of β-catenin that is affected following knock-down.

Next we addressed the question to what extent extracellular exposure to Wnt ligands contributes to the observed levels of β-catenin signaling. Using qRT-PCR we tested the expression of all 19 Wnt ligands in our cell line panel. The Wnt expression profile that

we observed largely corresponds with the semi-quantitative analyses performed by others [22, 46]. *WNT3* is the most abundantly expressed "canonical" Wnt ligand uniformly expressed in all cell lines, whereas all the others are expressed at low level or only in a subset of the cell lines. SNU182 clearly stands out as the overall highest expressor of Wnt ligands, likely explaining the high level of phosphorylated DVL2 that we observed in this cell line [33]. Among the non-mutant lines, SNU182 also showed the highest β-catenin reporter activity and level of *AXIN2* expression, comparable with the β-catenin mutant ones. As such, it is not unexpected that this cell line strongly relies on Wnt ligand secretion to retain increased β-catenin signaling. In fact, it is the only HCC cell line that shows a clear reduction following Wnt secretion blockage on both reporter activity as well as *AXIN2* expression level. On the other hand, the non-mutant Huh7 cell line expresses the lowest amount of Wnt ligands explaining its low baseline signaling levels, but it is highly responsive to Wnt ligand exposure for inducing strong β-catenin signaling. Within a true tumor setting it may represent a subtype of liver cancers that heavily depends on Wnt ligands expressed by cells within the tumor microenvironment, whose secretion would also be inhibited by the porcupine inhibitors employed here, whereas the SNU182 line is largely autonomous in this respect. Importantly, none of the β-catenin and AXIN1-mutant HCC cell lines are clearly affected in β-catenin signaling upon alterations in Wnt ligand exposure, irrespective of their source, suggesting that the expressed oncogenic β-catenin or mutant AXIN1 proteins determine overall signaling levels in a dominant fashion.

In our hands this also holds true for most of the APC and β-catenin mutant CRC lines that we investigated. Among 8 CRC lines tested, only HCT116 shows a strongly reduced reporter activity and *AXIN2* levels following IWP12 treatment, while it is also the only one in which both β-catenin signaling readouts are clearly increased after Wnt3A exposure. Analysis of pDVL2 levels is largely in accordance with this lack of response, i.e. most cell lines tested show only low baseline levels that are barely changed by either treatment (DLD1, HT29, SW480), suggesting that these lines are not actively signaling through Wnt ligand receptors. These results also challenge the universal validity of the conclusions drawn by Voloshanenko et al. who proposed that colorectal cancers still strongly depend on Wnt ligand exposure for maintaining optimal β-catenin signaling levels [26]. Their overall well-performed study depended on a thorough analysis of the HCT116 cell line and to a lesser extent on other lines such as DLD1. Importantly, the

β-catenin mutant HCT116 cell line is nowadays known to carry an inactivating mutation in the transmembrane E3 ubiquitin ligase RNF43, which strongly sensitizes these cells to exposure by Wnt ligands (see discussion below) [28, 47-49]. As such, their study may have unknowingly overstated the importance of Wnt ligand signaling for CRC growth in general, warranting a more extensive analysis in a larger cohort of CRC samples and cell lines.

In recent years, Wnt secretion inhibitors, such as the porcupine inhibitor used in our study, have emerged as candidate drugs for treating Wnt-driven cancers. Cancers that are considered to be especially responsive to these treatments are the ones carrying somatic mutations resulting in a persistent presence of Wnt receptors at the cell surface [28, 48]. In normal cells, the Wnt/Frizzled receptors are continuously endocytosed and degraded following ubiquitination by RNF43 or its close homolog ZNRF3. Both these ubiquitin ligases are inhibited in their action by one of four secreted R-spondin proteins [50]. Consequently, mutational inactivation of RNF43/ZNRF3 or a strongly increased production of R-spondins through the generation of aberrant fusion transcripts, both lead to tumor cells with high levels of Wnt/Frizzled receptor at their surface and hyper-responsiveness to Wnt ligands. These genetic aberrations have been identified in 10-20% of CRCs and in various other tumor types [28, 51, 52], but are to the best of our knowledge not present in HCCs, suggesting that these tumors are not prime candidates for treatment with Wnt secretion inhibitors. Nevertheless, our analysis shows that most of the HCC cell lines are reduced in their growth to varying extents, following both WLS knockdown as well as IWP12 treatment.

The mechanism of the growth suppression remains more elusive at present. Except for the SNU182 cell line, we do see little evidence of β-catenin signaling modulation, suggesting that other mechanisms are at play. One possibility is the induction of ER stress resulting from the aberrant accumulation of Wnt ligands in the ER. However, except from increased expression of the ER-induced genes *CHOP* and *GRP94*, in resp. SNU398 and SNU182, we do not see strong evidence that Wnt secretion blockage leads to high levels of ER stress. In addition, autophagy did not contribute to the growth suppression either as there was no visible change in the pattern of the autophagy marker LC3 following IWP12 treatment. An alternative explanation may reside in the reduced secretion of Wnt ligands more commonly signaling through β-catenin

independent pathways. Activation of these alternative pathways has however mainly been shown to affect cellular processes involved in migration and cellular polarity and actually to counteract cell proliferation [8]. This "non-canonical" pathway has not been extensively studied in liver cancer, but the available literature does indeed support a growth suppressive effect [46, 53]. Therefore, interfering with the secretion of this subset of Wnt ligands is expected to support cellular growth, which is in contrast to the growth suppression that we observe. In line with our results, Covey et al. have shown that knocking-down PORCN in various tumor cell lines reduced their growth through a Wnt-independent pathway [54]. Also in their case no obvious explanation could be uncovered, but both studies highlight the importance of considering alternative roles for proteins involved in Wnt secretion and their role in regulating cell growth.

In conclusion, our study shows that the majority of HCC cell lines depend on β-catenin signaling for maintaining optimal growth. Extracellular exposure to Wnt ligands has a minor contribution to overall β-catenin signaling strength in the β-catenin and AXIN1-mutant cell lines. Despite this observation, interfering with Wnt secretion through WLS knockdown or inhibition of porcupine function results in reduced growth, indicating that these proteins may have alternative roles currently unappreciated.

Supplementary Figures and Tables

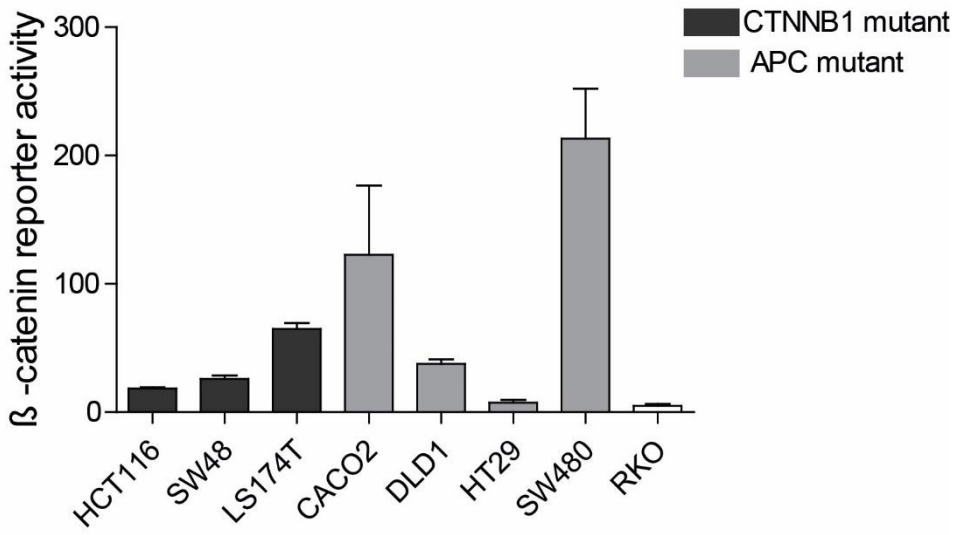

Fig.S1. Wnt/β-catenin signaling activity in CRC cell lines determined by a β-catenin luciferase reporter assay (mean ± SD, n=3).

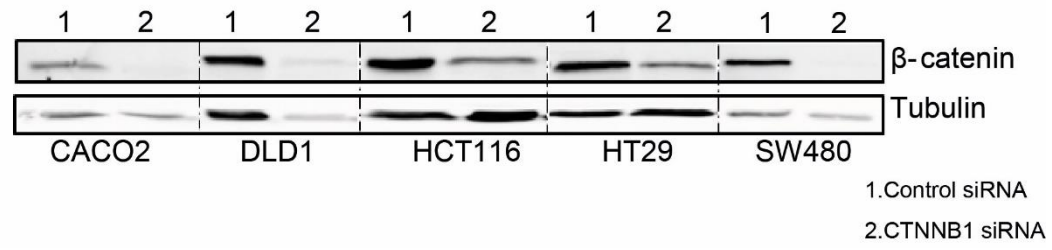

Fig.S2. SiRNA mediated silencing of β-catenin in CRC cell lines confirmed by western blotting.

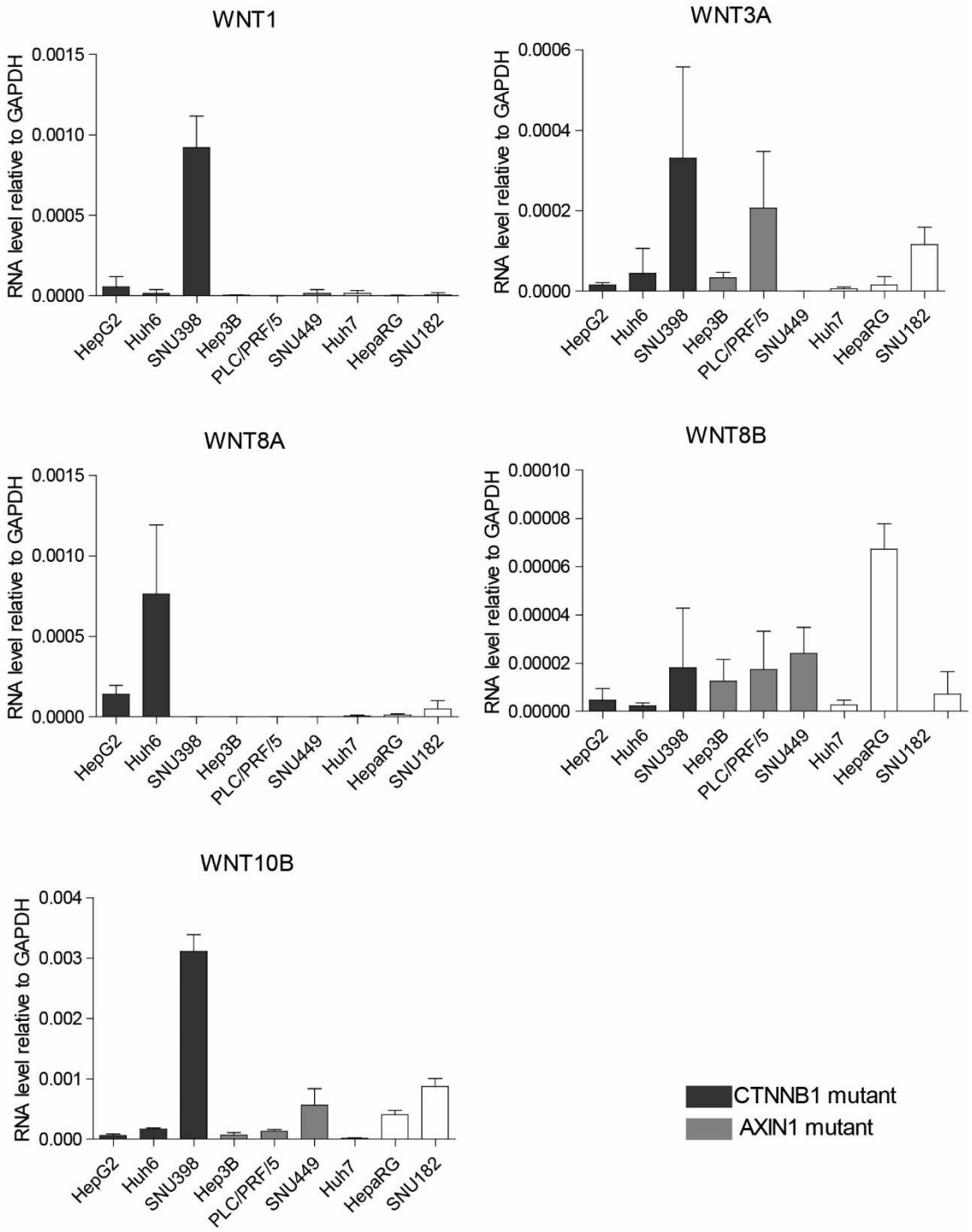

Fig.S3. Expression levels of remaining "canonical" Wnt ligands in HCC cell lines tested by qRT-PCR (mean ± SD, n =3).

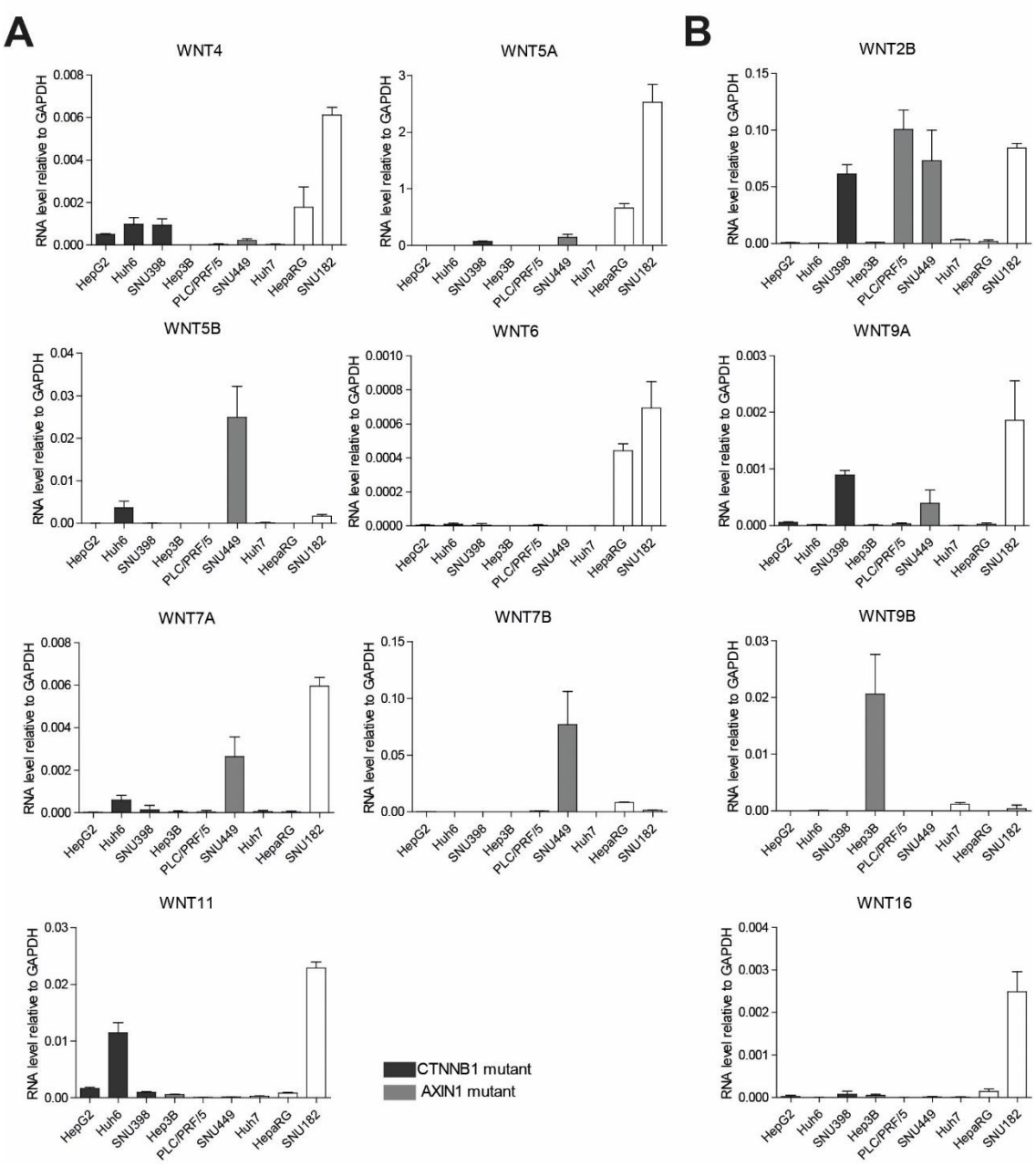

Fig.S4. Expression levels of "non-canonical" (A) and unclassified (B) Wnt ligands in HCC cell lines tested by qRT-PCR (mean ± SD, n =3).

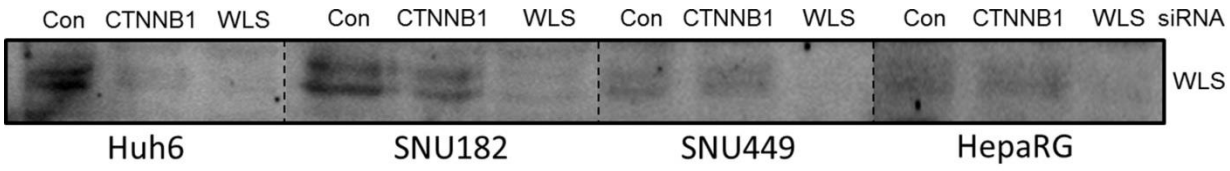

Fig.S5. SiRNA mediated silencing of *WLS* in HCC cell lines tested by western blotting.

References

[1] Forner A, Llovet JM, Bruix J (2012). Hepatocellular carcinoma *Lancet* 379, 1245-1255.

[2] Ferlay J, Shin HR, Bray F, Forman D, Mathers C, Parkin DM (2010). Estimates of worldwide burden of cancer in 2008: GLOBOCAN 2008 *International Journal of Cancer* 127, 2893-2917.

[3] Shi J, Keller JM, Zhang J, Evan TK (2014). A review on the diagnosis and treatment of hepatocellular carcinoma with a focus on the role of wnts and the dickkopf family of wnt inhibitors *Journal of Hepatocellular Carcinoma* 1, 7.

[4] Ma L, Wei W, Chua MS, So S (2014). WNT/β-catenin pathway activation in hepatocellular carcinoma: a clinical perspective *Gastrointest Cancer Targets Ther*, 49-63.

[5] Llovet JM, Bruix J (2008). Molecular targeted therapies in hepatocellular carcinoma *Hepatology* 48, 1312-1327.

[6] El-Serag HB (2012). Epidemiology of viral hepatitis and hepatocellular carcinoma *Gastroenterology* 142, 1264-1273. e1261.

[7] Klaus A, Birchmeier W (2008). Wnt signalling and its impact on development and cancer *Nature Reviews Cancer* 8, 387-398.

[8] Anastas JN, Moon RT (2012). WNT signalling pathways as therapeutic targets in cancer *Nature Reviews Cancer* 13, 11-26.

[9] Qu B, Liu BR, Du YJ, Chen J, Cheng YQ, Xu W, Wang XH (2014). Wnt/β‐catenin signaling pathway may regulate the expression of angiogenic growth factors in hepatocellular carcinoma *Oncology Letters* 7, 1175-1178.

[10] Reya T, Clevers H (2005). Wnt signalling in stem cells and cancer *Nature* 434, 843-850.

[11] Hausmann G, Banziger C, Basler K (2007). Helping Wingless take flight: how WNT proteins are secreted *Nat Rev Mol Cell Biol* 8, 331-336.

[12] Hart M, Concordet JP, Lassot I, Albert I, Del los Santos R, Durand H, Perret C, Rubinfeld B, Margottin F, Benarous R (1999). The F-box protein β-TrCP associates with phosphorylated β-catenin and regulates its activity in the cell *Current biology* 9, 207-211.

[13] Dahmani R, Just P-A, Perret C (2011). The Wnt/β-catenin pathway as a therapeutic target in human hepatocellular carcinoma *Clinics and research in hepatology and gastroenterology* 35, 709-713.

[14] Albuquerque C, Bakker ER, van Veelen W, Smits R (2011). Colorectal cancers choosing sides *Biochim Biophys Acta* 1816, 219-231.

[15] Fukumoto S, Hsieh C-M, Maemura K, Layne MD, Yet S-F, Lee K-H, Matsui T, Rosenzweig A, Taylor WG, Rubin JS (2001). Akt participation in the Wnt signaling pathway through Dishevelled *Journal of Biological Chemistry* 276, 17479-17483.

[16] Thorgeirsson SS, Grisham JW (2002). Molecular pathogenesis of human hepatocellular carcinoma *Nature genetics* 31, 339-346.

[17] Hoshida Y, Villanueva A, Kobayashi M, Peix J, Chiang DY, Camargo A, Gupta S, Moore J, Wrobel MJ, Lerner J (2008). Gene expression in fixed tissues and outcome in hepatocellular carcinoma *New England Journal of Medicine* 359, 1995-2004.

[18] Laurent-Puig P, Zucman-Rossi J (2006). Genetics of hepatocellular tumors *Oncogene* 25, 3778-3786.

[19] Pez F, Lopez A, Kim M, Wands JR, de Fromentel CC, Merle P (2013). Wnt signaling and hepatocarcinogenesis: molecular targets for the development of innovative anticancer drugs *Journal of hepatology* 59, 1107-1117.

[20] Monga SP (2015). beta-Catenin Signaling and Roles in Liver Homeostasis, Injury, and Tumorigenesis *Gastroenterology* 148, 1294-1310.

[21] de La Coste A RB, Billuart P, Renard CA, Buendia MA, Soubrane O, Fabre M, Chelly J, Beldjord C, Kahn A, Perret C. (1998). Somatic mutations of the beta-catenin gene are frequent in mouse and human hepatocellular carcinomas *Proc Natl Acad Sci USA* 95, 8847-8851.

[22] Bengochea A, De Souza MM, Lefrancois L, Le Roux E, Galy O, Chemin I, Kim M, Wands JR, Trepo C, Hainaut P (2008). Common dysregulation of Wnt/Frizzled receptor elements in human hepatocellular carcinoma *British journal of cancer* 99, 143-150.

[23] Vilchez V, Turcios L, Marti F, Gedaly R (2016). Targeting Wnt/beta-catenin pathway in hepatocellular carcinoma treatment *World J Gastroenterol* 22, 823-832.

[24] Baehs S, Herbst A, Thieme SE, Perschl C, Behrens A, Scheel S, Jung A, Brabletz T, Goke B, Blum H, et al. (2009). Dickkopf-4 is frequently down-regulated and inhibits growth of colorectal cancer cells *Cancer Lett* 276, 152-159.

[25] Suzuki H, Watkins DN, Jair KW, Schuebel KE, Markowitz SD, Chen WD, Pretlow TP, Yang B, Akiyama Y, Van Engeland M, et al. (2004). Epigenetic inactivation of SFRP genes allows constitutive WNT signaling in colorectal cancer *Nat Genet* 36, 417-422.

[26] Voloshanenko O, Erdmann G, Dubash TD, Augustin I, Metzig M, Moffa G, Hundsrucker C, Kerr G, Sandmann T, Anchang B, et al. (2013). Wnt secretion is required to maintain high levels of Wnt activity in colon cancer cells *Nat Commun* 4, 2610.

[27] Ho SY, Keller TH (2015). The use of porcupine inhibitors to target Wnt-driven cancers *Bioorg Med Chem Lett* 25, 5472-5476.

[28] Madan B, Virshup DM (2015). Targeting Wnts at the source--new mechanisms, new biomarkers, new drugs *Mol Cancer Ther* 14, 1087-1094.

[29] Forbes SA, Beare D, Gunasekaran P, Leung K, Bindal N, Boutselakis H, Ding M, Bamford S, Cole C, Ward S, et al. (2015). COSMIC: exploring the world's knowledge of somatic mutations in human cancer *Nucleic Acids Res* 43, D805-811.

[30] Bakker ER, Das AM, Helvensteijn W, Franken PF, Swagemakers S, van der Valk MA, ten Hagen TL, Kuipers EJ, van Veelen W, Smits R (2013). Wnt5a promotes human colon cancer cell migration and invasion but does not augment intestinal tumorigenesis in Apc1638N mice *Carcinogenesis* 34, 2629-2638.

[31] van Veelen W, Le NH, Helvensteijn W, Blonden L, Theeuwes M, Bakker ER, Franken PF, van Gurp L, Meijlink F, van der Valk MA, et al. (2011). beta-catenin tyrosine 654 phosphorylation increases Wnt signalling and intestinal tumorigenesis *Gut* 60, 1204-1212.

[32] Lee HJ, Shi DL, Zheng JJ (2015). Conformational change of Dishevelled plays a key regulatory role in the Wnt signaling pathways *Elife* 4, e08142.

[33] Grumolato L, Liu G, Mong P, Mudbhary R, Biswas R, Arroyave R, Vijayakumar S, Economides AN, Aaronson SA (2010). Canonical and noncanonical Wnts use a common mechanism to activate completely unrelated coreceptors *Genes Dev* 24, 2517-2530.

[34] Wang X, Moon J, Dodge ME, Pan X, Zhang L, Hanson JM, Tuladhar R, Ma Z, Shi H, Williams NS, et al. (2013). The development of highly potent inhibitors for porcupine *J Med Chem* 56, 2700-2704.

[35] Chang HW, Lee YS, Nam HY, Han MW, Kim HJ, Moon SY, Jeon H, Park JJ, Carey TE, Chang SE, et al. (2013). Knockdown of beta-catenin controls both apoptotic and autophagic cell death through LKB1/AMPK signaling in head and neck squamous cell carcinoma cell lines *Cell Signal* 25, 839-847.

[36] Fu Y, Chang H, Peng X, Bai Q, Yi L, Zhou Y, Zhu J, Mi M (2014). Resveratrol inhibits breast cancer stem-like cells and induces autophagy via suppressing Wnt/beta-catenin signaling pathway *PLoS One* 9, e102535.

[37] Zeng G, Apte U, Cieply B, Singh S, Monga SP (2007). siRNA-mediated beta-catenin knockdown in human hepatoma cells results in decreased growth and survival *Neoplasia* 9, 951-959.

[38] Wang XH, Sun X, Meng XW, Lv ZW, Du YJ, Zhu Y, Chen J, Kong DX, Jin SZ (2010). beta-catenin siRNA regulation of apoptosis- and angiogenesis-related gene expression in hepatocellular carcinoma cells: potential uses for gene therapy *Oncol Rep* 24, 1093-1099.

[39] Zucman-Rossi J, Benhamouche S, Godard C, Boyault S, Grimber G, Balabaud C, Cunha A, Bioulac-Sage P, Perret C (2007). Differential effects of inactivated Axin1 and activated β-catenin mutations in human hepatocellular carcinomas *Oncogene* 26, 774-780.

[40] Feng GJ, Cotta W, Wei XQ, Poetz O, Evans R, Jarde T, Reed K, Meniel V, Williams GT, Clarke AR, et al. (2012). Conditional disruption of Axin1 leads to development of liver tumors in mice *Gastroenterology* 143, 1650-1659.

[41] Brembeck FH, Rosario M, Birchmeier W (2006). Balancing cell adhesion and Wnt signaling, the key role of beta-catenin *Curr Opin Genet Dev* 16, 51-59.

[42] Fukunaga Y, Liu H, Shimizu M, Komiya S, Kawasuji M, Nagafuchi A (2005). Defining the roles of beta-catenin and plakoglobin in cell-cell adhesion: isolation of beta-catenin/plakoglobin-deficient F9 cells *Cell Struct Funct* 30, 25-34.

[43] Zhou J, Qu J, Yi XP, Graber K, Huber L, Wang X, Gerdes AM, Li F (2007). Upregulation of gamma-catenin compensates for the loss of beta-catenin in adult cardiomyocytes *Am J Physiol Heart Circ Physiol* 292, H270-276.

[44] Wickline ED, Awuah PK, Behari J, Ross M, Stolz DB, Monga SP (2011). Hepatocyte gamma-catenin compensates for conditionally deleted beta-catenin at adherens junctions *J Hepatol* 55, 1256-1262.

[45] Wickline ED, Du Y, Stolz DB, Kahn M, Monga SP (2013). gamma-Catenin at adherens junctions: mechanism and biologic implications in hepatocellular cancer after beta-catenin knockdown *Neoplasia* 15, 421-434.

[46] Yuzugullu H, Benhaj K, Ozturk N, Senturk S, Celik E, Toylu A, Tasdemir N, Yilmaz M, Erdal E, Akcali KC (2009). Canonical Wnt signaling is antagonized by noncanonical Wnt5a in hepatocellular carcinoma cells *Molecular cancer* 8, 1.

[47] Ivanov I, Lo KC, Hawthorn L, Cowell JK, Ionov Y (2007). Identifying candidate colon cancer tumor suppressor genes using inhibition of nonsense-mediated mRNA decay in colon cancer cells *Oncogene* 26, 2873-2884.

[48] Boone JD, Arend RC, Johnston BE, Cooper SJ, Gilchrist SA, Oelschlager DK, Grizzle WE, McGwin G, Jr., Gangrade A, Straughn JM, Jr., et al. (2016). Targeting the Wnt/beta-catenin pathway in primary ovarian cancer with the porcupine inhibitor WNT974 *Lab Invest* 96, 249-259.

[49] van de Wetering M, Francies HE, Francis JM, Bounova G, Iorio F, Pronk A, van Houdt W, van Gorp J, Taylor-Weiner A, Kester L, et al. (2015). Prospective derivation of a living organoid biobank of colorectal cancer patients *Cell* 161, 933-945.

[50] de Lau W, Peng WC, Gros P, Clevers H (2014). The R-spondin/Lgr5/Rnf43 module: regulator of Wnt signal strength *Genes Dev* 28, 305-316.

[51] Seshagiri S, Stawiski EW, Durinck S, Modrusan Z, Storm EE, Conboy CB, Chaudhuri S, Guan Y, Janakiraman V, Jaiswal BS, et al. (2012). Recurrent R-spondin fusions in colon cancer *Nature* 488, 660-664.

[52] Giannakis M, Hodis E, Jasmine Mu X, Yamauchi M, Rosenbluh J, Cibulskis K, Saksena G, Lawrence MS, Qian ZR, Nishihara R, et al. (2014). RNF43 is frequently mutated in colorectal and endometrial cancers *Nat Genet* 46, 1264-1266.

[53] Bi L, Liu X, Wang C, Cao Y, Mao R, Li P, Geng M (2014). Wnt5a involved in regulation of the biological behavior of hepatocellular carcinoma *Int J Clin Exp Pathol* 7, 987-995.

[54] Covey TM, Kaur S, Tan Ong T, Proffitt KD, Wu Y, Tan P, Virshup DM (2012). PORCN moonlights in a Wnt-independent pathway that regulates cancer cell proliferation *PLoS One* 7, e34532.

Chapter 5

Oncogenic STRAP Supports Hepatocellular Carcinoma Growth by Enhancing Wnt/β-catenin Signaling

Wenhui Wang[1], Shan Li[1*], Pengyu Liu[1*], Kostandinos Sideras[1], Harmen J. G. van de Werken[2,3], Marieke van der Heide[1], Wanlu Cao[1], Marla Lavrijsen[1], Maikel P. Peppelenbosch[1], Marco Bruno[1], Qiuwei Pan[1] and Ron Smits[1]

1 Department of Gastroenterology and Hepatology, Erasmus MC, University Medical Center Rotterdam, The Netherlands.

2 Department of Urology, Erasmus MC, University Medical Center Rotterdam, The Netherlands.

3 Department of Cancer Computational Biology Center, Erasmus MC, University Medical Center Rotterdam, The Netherlands.

* Equal contribution

Mol Cancer Res. 2019 17(2):521-531.

Abstract

Aberrant activation of Wnt/β-catenin signaling plays a key role in the onset and development of hepatocellular carcinomas (HCC), with about half of them acquiring mutations in either CTNNB1 or AXIN1. The serine/threonine kinase receptor-associated protein (STRAP), a scaffold protein, was recently shown to facilitate the aberrant activation of Wnt/β-catenin signaling in colorectal cancers. However, the function of STRAP in HCC remains completely unknown. Here, increased levels of STRAP were observed in human and mouse HCCs. RNA sequencing of STRAP knockout clones generated by gene editing of Huh6 and Huh7 HCC cells revealed a significant reduction in expression of various metabolic and cell-cycle–related transcripts, in line with their general slower growth observed during culture. Importantly, Wnt/β-catenin signaling was impaired in all STRAP knockout/down cell lines tested, regardless of the underlying CTNNB1 or AXIN1 mutation. In accordance with β-catenin's role in (cancer) stem cell maintenance, the expressions of various stem cell markers, such as AXIN2 and LGR5, were reduced and concomitantly differentiation associated genes were increased. Together, these results show that the increased STRAP protein levels observed in HCC provide growth advantage among others by enhancing Wnt/β-catenin signaling. These observations also identify STRAP as a new player in regulating β-catenin signaling in hepatocellular cancers.

Keywords: Hepatocellular carcinoma, STRAP, Wnt/β-catenin signaling, tissue microarray, RNA sequencing

Introduction

Hepatocellular carcinoma (HCC) is the sixth most prevalent cancer and the third leading cause for cancer related deaths worldwide with around 500,000 new cases diagnosed each year (1, 2). Hepatocarcinogenesis initiates with the accumulation of aberrant genetic and epigenetic modifications leading to the dysregulation of signaling pathways, which transform the normal hepatocytes towards malignant phenotypes (3).

Inappropriate activation of Wnt/β-catenin signaling has been frequently reported in HCC (4). As the central component of Wnt/β-catenin signaling, the transcription factor β-catenin is tightly regulated by a multiprotein complex composed of the adenomatous polyposis coli (APC) tumor suppressor, scaffold proteins AXIN1, AXIN2 and the kinases GSK3 and CK1α (4, 5). In the absence of Wnt ligands, β-catenin is constitutively phosphorylated and degraded to maintain a minimal level in the cytoplasm. On Wnt stimulation, the multiprotein complex dissociates causing the accumulation of cytosolic and nuclear β-catenin. The latter triggers the transcription of specific target genes. Aberrant activation of Wnt/β-catenin signaling in HCC has been attributed to activating mutations in *CTNNB1* (20-25%) or loss of function mutations in *AXIN1* (10%), AXIN2 (3-4%) and *APC* (1%~2%) (4, 6, 7).

The serine-threonine kinase receptor-associated protein (STRAP) encoded by the *STRAP* gene, harbors seven WD40-repeat domains (8). It is considered to be a scaffolding protein without enzymatic function that exerts regulatory functions on a variety of cellular processes ranging from signal transduction, transcriptional regulation, RNA processing, vesicular trafficking to cell cycle progression (9). STRAP was shown to be overexpressed and exert oncogenic properties in breast cancer, colorectal cancer (CRC) and lung carcinomas (10-12). Originally, STRAP was shown to inhibit canonical transforming growth factor-beta (TGF-β) signaling (13). Later, it became apparent that STRAP modulates various other cellular processes and signaling pathways such as signaling through ASK1, P53, PI3K/PDK1, and $P21^{Cip1}$ (9, 14, 15). More recently, Wnt/β-catenin signaling was demonstrated to be stimulated by increased STRAP in CRC through binding with GSK-3β around the catalytic domain, which diminished subsequent ubiquitin-dependent degradation of β-catenin (16). However, the function of STRAP in HCC progression remains elusive.

In this study, we investigated the expression level of STRAP in HCC tumor tissues and used clustered regularly interspaced short palindromic repeat (CRISPR)/Cas9-mediated gene editing to knockout *STRAP* in HCC cell lines. Our results suggest that upregulation of STRAP protein provides growth advantage to HCC cells via enhancing Wnt/β-catenin signaling. These observations identify STRAP as a new player in regulating Wnt/β-catenin signaling in HCC.

Materials and methods

Cell lines

Human HCC cell lines Hep3B, HepG2, HepaRG, Huh6, Huh7, PLC/PRF/5, SNU398, SNU182 and SNU449 were cultured as reported previously (7). Identity of all cell lines was confirmed by STR genotyping. *CTNNB1* and *AXIN1* mutations reported in Supplemental Table S1, were confirmed in these HCC cell lines by Sanger sequencing and were in accordance with those reported at COSMIC, the Catalogue Of Somatic Mutations In Cancer (http://cancer.sanger.ac.uk) (17). For the preparation of Huh7 conditioned medium, cells were cultured in complete DMEM medium for 3 days, followed by collection and filtration of medium according to standard procedures.

Tissue microarray (TMA)

TMA construction was described previously (18). Briefly, archived formalin fixed paraffin-embedded tissue samples from 141 patients who underwent hepatic resection for HCC at the Erasmus MC-University Medical Center Rotterdam, between 2004 and 2013 were collected. Three or four 0.6mm cores from the tumor area as well as two 0.6mm cores from the corresponding tumor free liver (TFL) area of these patients were taken. The TMAs were made using an automated tissue-arrayer ATA-27 (Beecher Instruments, Silver Spring MD, USA) or a manual tissue arrayer MTA-1 (Beecher Instruments). Clinicopathologic characteristics are presented in Supplemental Table S2.

Database analysis

The TCGA LIHC illuminahiseq_rnaseqv2_RSEM_genes_normalized (MD5) data were obtained from the Broad Institute's Firehose GDAC website

(http://firebrowse.org/?cohort=LIHC&download_dialog=true). In this dataset 373 hepatocellular carcinoma samples are available for which gene expression analysis was performed (19). In addition, 50 paired adjacent tumor-free tissues are also available for gene expression analysis. RNAseq levels of *STRAP* were obtained and matched to the available survival data.

DEN induction of liver tumors in mice

Mice of C57BL/6J background or mixed with C3H/HeOuJ or CD1 (all 3-4 weeks of age) were administrated weekly with Diethylnitrosamine (DEN) (intraperitoneal injection; 100 mg/kg) for 6-17 weeks to induce liver tumor formation. Mice were sacrificed 3-16 months after the last DEN injection, after which livers were fixed in PBS-buffered formalin and embedded in paraffin according to routine procedures. All animal experiments were approved by the Committee on the Ethics of Animal Experiments of the Erasmus Medical Center.

Reagents

The following antibodies were used for western blot analysis or immunohistochemistry staining. STRAP (611346, BD Transduction Laboratories™ and HPA027320, Atlas antibodies), β-catenin (610154, BD Transduction Laboratories™), Non-phospho (Active) β-catenin (Ser33/37/Thr41) (#8814, Cell Signaling Technology), Tubulin (sc-8035, Santa Cruz), β-actin (sc-47778, Santa Cruz) and anti-rabbit or anti-mouse IRDye-conjugated secondary antibodies (LI-COR Biosciences, Lincoln, USA), HRP-conjugated anti-mouse polymer secondary antibody (Envision™, DAKO, Glostrup, Denmark). Propidium iodide solution, diaminobenzidine (DAB) and crystal violet solution were purchased from Sigma (St. Louis, MO).

Immunohistochemistry

Paraffin embedded tumor slides were deparaffinized in xylene, rehydrated in graded alcohols and then rinsed in PBS with 0.025%Trition. Antigen retrieval was performed in a microwave in Tris/EDTA (pH 8) for 10 min. Endogenous peroxidase activity was blocked by incubation in 1.5% H2O2 at room temperature for 15 min. After blocking by 5% nonfat dry milk in PBS, the sections were incubated with STRAP antibody (611346, BD Transduction Laboratories™) (1:100) at 4°C overnight. HRP-conjugated anti-mouse

polymer secondary antibody was then applied for 1 h. Then reaction products were visualized using DAB and counterstained with hematoxylin. STRAP staining was scored by two independent observers. The intensity of STRAP staining was classified in three categories: 0, 1, 2, respectively correlating with weak, moderate or strong staining, and scored by two independent investigators resulting in a Kappa test of 0.609 (for STRAP in HCC tumors), which was deemed acceptable. In our study, we generated STRAP knockout HCC cell lines that were used to test the specificity of the antibody (Supplemental Figure S1).

β-catenin reporter assays

The β-catenin reporter assays were basically performed as previously described (20, 21). In short, twenty hours before transfection, we plated 0.5×10^5 cells per well on 24-well plates. Each well was transfected with 250 ng Wnt Responsive Element (WRE) or Mutant Responsive Element (MRE) vectors and 10 ng CMV-Renilla using FuGENE® HD Transfection Reagent (E2311, Promega). We measured luciferase activities in a LumiStar Optima luminescence counter (BMG LabTech, Offenburg, Germany) and normalized the data for the transfection efficiency by using the Dual Luciferase Reporter Assay system (E1980, Promega) according to the manufacturer's instruction. Transfections were performed twice in duplicate and the mean and standard error were calculated for each condition. The β-catenin reporter activities are shown as WRE/MRE ratios.

Western blotting

Cells were lysed in Laemmli sample buffer with 0.1 M DTT and heated for 10 minutes at 95°C, followed by loading and separation on a 10% sodium dodecyl sulphate-polyacrylamide gels (SDS-PAGE). After 90 min running at 120 V, proteins were electrophoretically transferred onto a polyvinylidene difluoride (PVDF) membrane (Invitrogen) for 1.5 h with an electric current of 250 mA. The membrane was blocked with Odyssey Blocking Buffer followed by incubation with primary antibody (1:1000) overnight at 4°C. Anti-rabbit or anti-mouse IRDye-conjugated secondary antibodies (1:5000) were applied for 1 hour at room temperature. Blots were assayed for Tubulin or β-actin content as standardization of sample loading, scanned, and quantified by

Odyssey infrared imaging (Li-COR Biosciences, Lincoln, NE, USA). Results were visualized and quantified with Odyssey 3.0 software.

Gene knockdown by small interfering RNA (siRNA)

Smartpool ON-TARGETplus siRNAs targeting *STRAP* were purchased from Dharmacon. The ON-TARGETplus Non-targeting siRNA #2 was used as negative control. Cells were reverse-transfected in a 24-well plate using a total of 0.8 µl DharmaFECT formulation 4 (Thermo Fischer Scientific) and 25nM of each siRNA per well. Following 72 h incubation, the effect of knockdown was tested by western blotting. Alternatively, 48h after reverse transfection, the cells were transfected with WRE or MRE vectors and CMV-Renilla for β-catenin reporter assay.

Construction of CRISPR/Cas9 *STRAP*-targeting vectors

Single guide RNAs (sgRNAs) targeting exon 1 or 2 of human *STRAP* were designed using the following CRISPR design tool (http://crispr.mit.edu/). Supplemental table S3 depicts the three selected sgRNAs, chosen because of lowest predicted potential exonic off-target sites. Oligos were dissolved at 100 pmol/µl and annealed by combining 10 µl of each with 2 µl of NEB buffer 3, heated in a PCR machine to 94°C for 4 minutes, removed and allowed to cool down to room temperature. Annealed oligos were diluted 1000x in water of which 1 µl was combined with 100 ng of BbsI-digested and purified pX330 in a total ligation volume of 20 µl using 1.5 units T4 DNA ligase. Next, ligated plasmids were electroporated into DH10B E. coli. After plating, correct plasmids were identified and sequence-verified using standard procedures.

Generation of STRAP knockout HCC cell lines

Huh6 and Huh7 cell lines were transfected in 6-well plates using 7.5 µl FuGENE® HD Transfection Reagent (E2311, Promega) and 2 µg of each pX330 plasmid per well together with 0.2 µg GFP expression construct. GFP expression was used to select the cells that received high levels of the pX330 CRISPR/Cas9 constructs. After incubation at 37°C for 24 h, single cells were prepared for fluorescence activated cell sorting (FACS) to a 96-well plate. After single cell sorting, Huh7 cells were maintained in DMEM supplemented with either 20% FCS or 25% Huh7-conditioned medium. Huh6 was cultured in complete DMEM medium.

Clones grown successfully from single cells were first subjected to western blotting with anti-STRAP antibody (611346, BD Transduction Laboratories). For each cell line, apparently successful STRAP knockout and control clones were selected for DNA sequence verification using oligos shown in Supplemental Table S4. For clones with complicated chromatograms, we also employed next-generation sequencing (NGS) on an Ion-Torrent device using the fusion method for amplicon library preparation. This method uses oligos designed to directly include barcodes and adaptors required for processing on the Ion-Torrent device (see Supplemental Table S5). PCR products were generated using Q5 proofreading polymerase (NEB) according to manufacturer's instructions, followed by purification and NGS according to routine protocols. All selected clones were re-tested for STRAP-loss using an additional STRAP antibody (HPA027320, Atlas antibodies). Western blot result and observed sequence alterations are depicted in Supplemental Figure S2.

Colony formation assays

We performed two types of clonogenic assays, i.e. plating of single cells directly on cell culture surface or plating in soft-agar. For the former, 1000 cells for each clone were seeded in 6-well plates and were cultured in 2ml complete DMEM medium per well. Two weeks later, the cells were washed with PBS, fixed in 4% PBS-buffered paraformaldehyde for 10 min and stained with crystal violet solution. Number of colonies were counted under a microscope.

For the soft-agar assay, a base layer of 0.3 ml of complete DMEM/F12 medium (2% B27, 1% N-2, 20 ng/ml FGF, 20 ng/ml EGF, 100 µg/ml Primocin) containing 0.6% soft-agar was allowed to settle in 24-well plates. Next, 0.6 ml of complete 0.6% soft-agar DMEM/F12 medium was added containing 1000 (Huh6) or 2000 (Huh7) single cells. After settling of the agar, 0.5 ml of liquid medium was added, which was replaced every other day. After 2 weeks of culturing, colonies were fixed and stained with 0.005% Crystal violet in 10% PBS-buffered Formalin. Pictures were taken of the complete 24-well and colonies were automatically counted with ImageJ. All colony formation assays were performed in triplicates. The mean and standard error were calculated for each condition.

Periodic Acid Schiff (PAS) staining of cultured cells

Cells were cultured in 6-well plates until they reached 60-70% confluency, Next, they were washed with PBS twice followed by fixation in 10% PBS-buffered formalin for 10 min. After two ddH_2O washes, cells were incubated with 0.5% Periodic Acid solution for 10 min, followed by two ddH_2O washes and incubation in Schiff's reagent (Sigma Aldrich) for 15 min. Cells were washed in tap water and visualized under an inverted microscope.

Quantitative real-time polymerase chain reaction (qRT-PCR)

RNA was isolated with the Machery-NucleoSpin RNA II kit (BIOKE, Leiden, The Netherlands) and quantified using a Nanodrop ND-1000 (Wilmington, DE, USA). CDNA was prepared from total RNA using a random-primed cDNA Synthesis Kit (TAKARA BIO INC) and subjected to quantitative Real-Time PCR analyses. Analyses were performed using the StepOne Real-Time PCR System and the StepOnev2.0 software (Applied Biosystem, Darmstadt, Germany). All expression levels are depicted relative to the expression of *GAPDH*. Primer sequences are provided in Supplemental Table S6.

RNA extraction, Ilumina library preparation and sequencing

Total RNA was isolated with the Machery-NucleoSpin RNA II kit (BIOKE, Leiden, The Netherlands) and quantified using a Nanodrop ND-1000 (Wilmington, DE, USA). RNA quality was checked using a RNA Pico chip on the Agilent Bioanalyzer. Library was constructed and sequenced with an Illumina HiSeqTM2000 (GATC Biotech, Konstanz, Germany). Briefly, the mRNA was enriched using oligo-dT magnetic beads, followed by fragmentation (about 200 bp). Then the first strand of cDNA was synthesized using random hexamer-primer and the second strand was further synthesized in a reaction buffer including dNTPs, RNase H and DNA polymerase I. Double stranded cDNA was purified with magnetic beads. Then, the 3'-end single nucleotide A (adenine) was added and adapters were ligated to the fragments which were enriched by PCR amplification.

RNA-sequencing analysis

The Illumina single-end reads were trimmed to remove the TrueSeq adapter sequences using Trimmomatic (v.0.33). Subsequently, the reads were mapped to the human reference genome build hg38 with the RNA-seq aligner STAR (v2.4.2a) and the

Homo sapiens GENCODE v23 annotation. Raw counts were measured with summarizeOverlaps function from the Bioconductor GenomicAlignments package (v1.12.1) using the setting mode union. The differentially expressed genes were called with a generalized linear model using a negative binomial distribution and accounting for the different cell lines (Huh6 and Huh7). The calculations were performed by the DESeq2 package (v1.16.1). We applied a Wald-test to identify statistical significant differently expressed genes with a False Discover Rate (FDR) that was calculated using Benjamini Hochberg correction and set a threshold value of 0.01. After blind variance stabilizing $\log_2$ transformation of the counts, the differentially expressed genes were used to calculate scaled gene-wise values (Z-score). The scaled values were, clustered hierarchically with complete linkage using Euclidean distances and subsequently plotted in a heat map with pheatmap package(v1.0.8). Gene Ontology (GO) and Kyoto Encyclopedia of Genes and Genomes (KEGG) gene enrichment analyses were carried out as described previously (22). We used R(v 3.4.0) for statistics and visualization of the data.

Statistical analysis

All results were presented as mean ± SD or mean ± SEM as described in the figure legends. Comparison of STRAP protein staining between HCC tumor group and adjacent normal groups were performed with test of proportion. The t-test was used for statistical evaluation of number of colonies formed in the soft-agar colony assay. Differences were considered significant at a *P* value less than 0.05.

Data accessibility

The RNA-sequencing data from this study have been submitted to the Gene Expression Omnibus (GEO)(23) database under the accession number GSE101061.

Results

STRAP protein is up-regulated in HCC tumor tissues

In order to assess the expression level of STRAP protein in HCC lesions, we stained a tissue microarray (TMA) containing HCC tumors and patient matched adjacent normal tissues. For 109 tumor samples a STRAP intensity score could be obtained. In most normal samples STRAP protein was expressed at low to moderate levels, while it was significantly elevated in the majority of HCC tumors (Figure 1). Within the tumor cells, STRAP showed a predominant cytoplasmic location (Figure 1D). Similar results were observed in Diethylnitrosamine (DEN) induced liver tumors in mice, in which 22 out of 28 tumor nodules showed increased STRAP expression relative to flanking normal liver tissue (Supplemental Figure S3).

In our cohort, IHC-evaluated STRAP expression was not significantly associated with any of the available clinicopathologic characteristics presented in supplemental Table S2 (data not shown), including tumor recurrence (HR 1.10; 95% CI 0.57-2.10, p=.785) or HCC specific mortality (HR 0.79; 95% CI 0.37-1.71, p=.557). Given that our semi-quantitative IHC analysis may miss subtle differences in expression levels, we explored an independent dataset, that is the TCGA liver cancer cohort, which includes 373 HCC cases that were analyzed by RNA expression profiling (19). No significant difference in STRAP RNA expression was observed between tumors and 50 normal adjacent liver tissues. Survival analysis of the top and bottom 30% STRAP expressors revealed a significant trend (p=0.011) of reduced survival in the high expressing group, suggesting that higher STRAP levels may contribute to tumor progression (Supplemental Figure S4).

Overall, these analyses show that STRAP protein levels are increased in most liver tumors of man and mouse, but that its expression level is only modestly associated with patient characteristics.

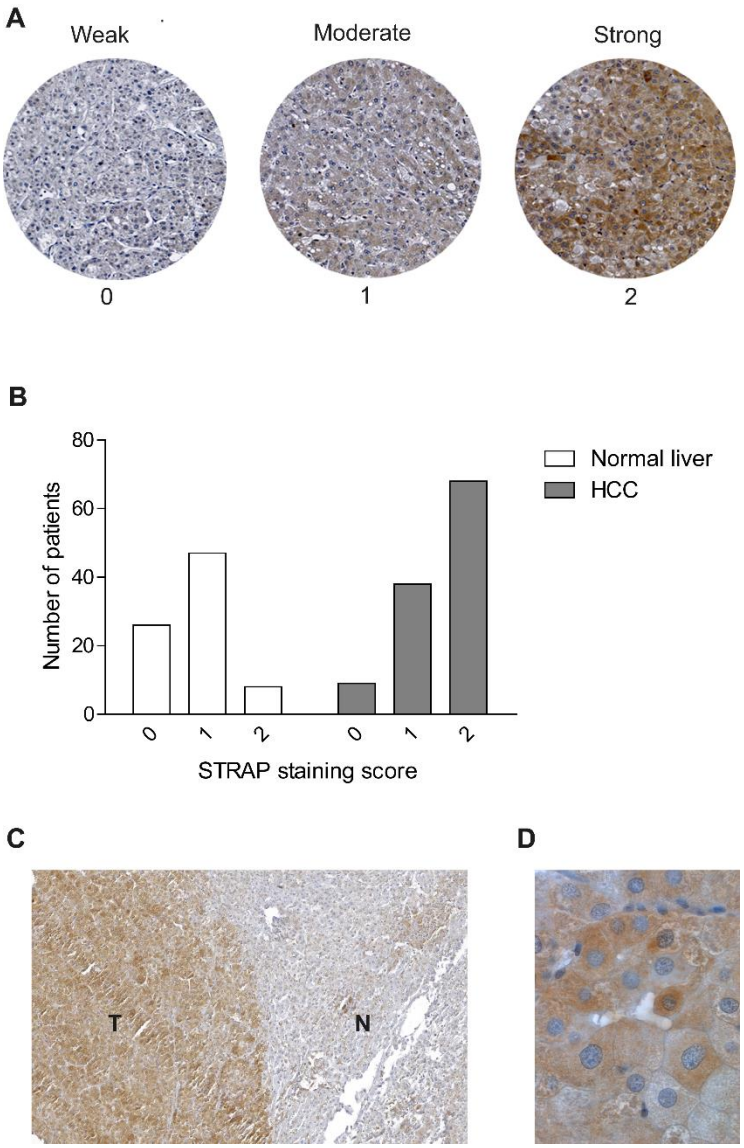

Figure 1. Elevated expression of STRAP in patient HCC tumor tissues. (A) The levels of STRAP protein positivity were scored from weak (0), moderate (1) to strong (2), both in the adjacent normal liver and HCC tumor tissue. (B) Distribution of normal liver and HCC tissues classified by above categories. Differences in the number of patients between normal liver and HCC tumors are highly significant ($P<0.001$, test of proportion). (C) Representative STRAP staining of a HCC tumor (T) with adjacent normal liver tissue (N); original magnification 100x. (D) STRAP shows a predominant cytoplasmic location in hepatocellular carcinoma cells; original magnification 630x.

Transcriptome analysis of STRAP knock-out clones by RNA sequencing

We tested the baseline expression of STRAP in our panel of nine liver cancer cell lines. All showed readily detectable STRAP protein and RNA, with little variation between cell lines (Supplemental Figure S5). In order to determine the function of STRAP protein for supporting cell growth, we used the CRISPR/Cas9 technology to disrupt STRAP expression in Huh6 and Huh7 cell lines. As shown in Supplemental Figure S2, the STRAP protein was completely lost in the selected knockout clones of both cell lines.

To investigate the genome-wide effects of STRAP in regulating gene expression in HCC cell lines, total RNA of selected STRAP knockout and control clones (n=3 each) was subjected to RNA sequencing. The hierarchical clustering results successfully distinguished the Huh6 from the Huh7 cell line. Importantly, the STRAP KO Huh6 clones preferentially clustered with Huh7 KO ones. Likewise, control Huh6 and Huh7 clones were clustered. According to STRAP genotype, 5605 differentially expressed genes (threshold FDR<0.01) were clustered in both Huh6 and Huh7 (Figure 2A).

For validation of the differentially expressed genes identified from RNA sequencing, a total of eight genes were selected for qRT-PCR in Huh6 and Huh7 cell lines, which were among the top genes either up- or down-regulated. As shown in Figure 2B, $\log_2$ fold change of these genes tested by qRT-PCR significantly correlated with those from RNA sequencing (R=0.998 in Huh6 and R=0.913 in Huh7). Taken together, these data indicate that STRAP plays an important role, directly or indirectly, in the transcriptional regulation of many genes in HCC cell lines.

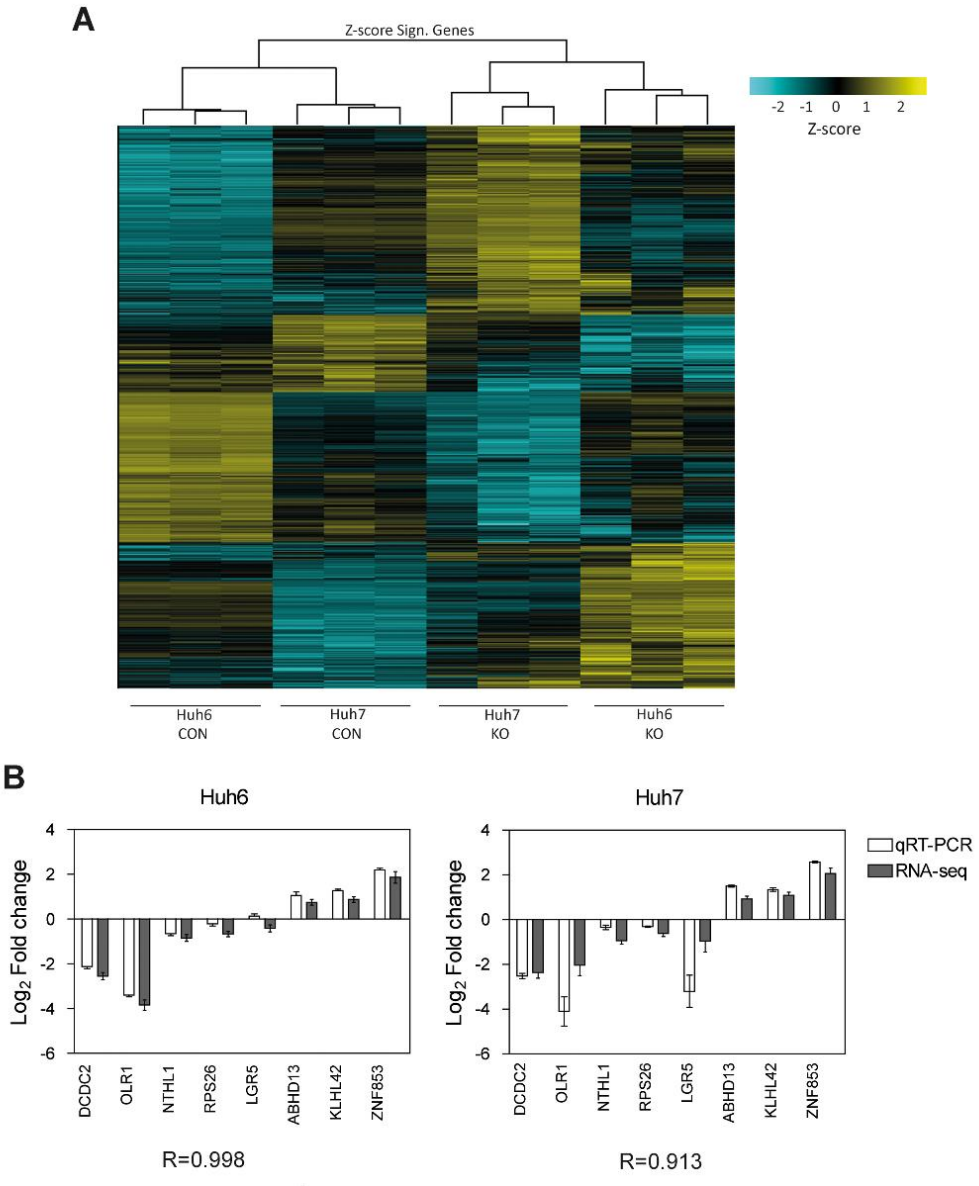

Figure 2. Differential expression profiles in STRAP knockout Huh6 and Huh7 clones. (A) Hierarchically clustered heat map using complete linkage showing scaled Z-score color key of normalized counts of 5605 differentially expressed genes in 3 control (CON) and 3 STRAP knockout (KO) clones of Huh6 and Huh7. Columns represent clones and rows show the differentially expressed genes. (B) Comparison of relative log2 fold changes of selected genes tested by RNA-seq and qRT-PCR. The results are presented as log2 fold change ± Standard Error, n=3..

Loss of STRAP reduces expression of many metabolic and cell cycle related genes

Both Kyoto Encyclopedia of Genes and Genomes (KEGG) pathway enrichment and Gene Ontology (GO) enrichment analysis revealed that many metabolic processes were

reduced in activity in the STRAP knockout clones. In addition, this analysis showed that cell cycle progression was significantly affected, as a result of STRAP loss in both Huh6 as well as Huh7 (Figure 3A and B). Both the reduced expression of metabolic and cell cycle related genes are in line with the general slower growth of all knockout clones observed during routine culture (data not shown). To assess the role of STRAP on the reproductive viability of HCC cells, a colony formation assay on regular culture plates was employed with the STRAP knockout-clones and controls thereof. We observed that loss of STRAP dramatically decreased not only the number but also the size of Huh6 and Huh7 colonies (Figure 4). These results indicate that STRAP is important for an efficient outgrowth of single HCC cells.

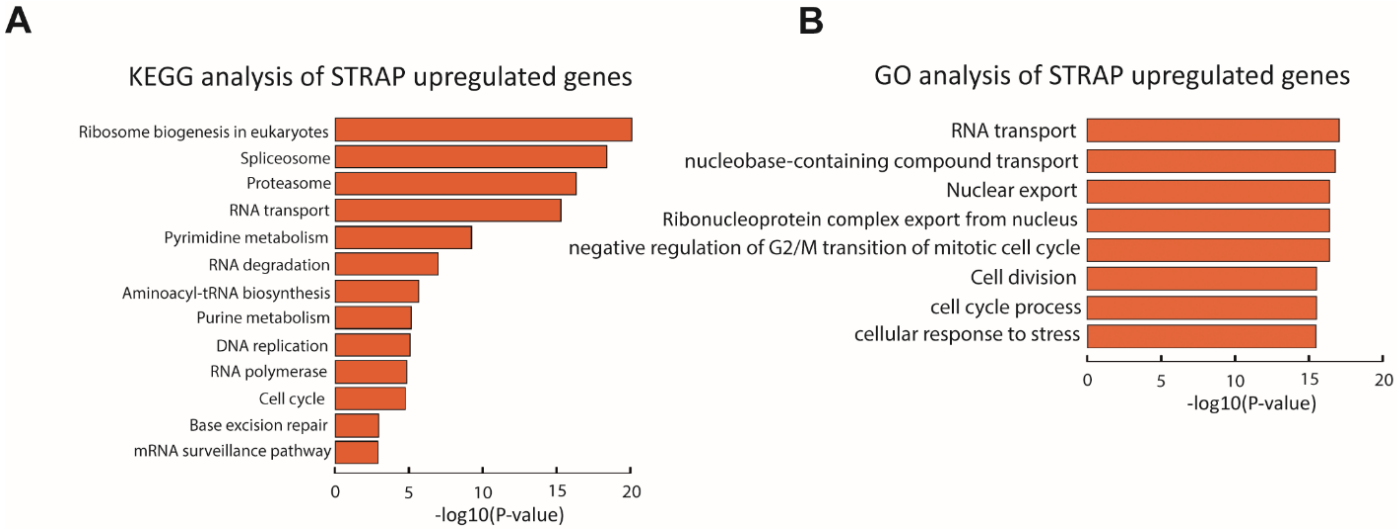

Figure 3. Loss of STRAP reduces expression of metabolic and cell cycle related genes. (A) KEGG Pathway Gene Set Enrichment and (B) Gene Ontology analysis of genes significantly higher expressed in the control clones. X-axis indicates P-value in the –log10 scale.

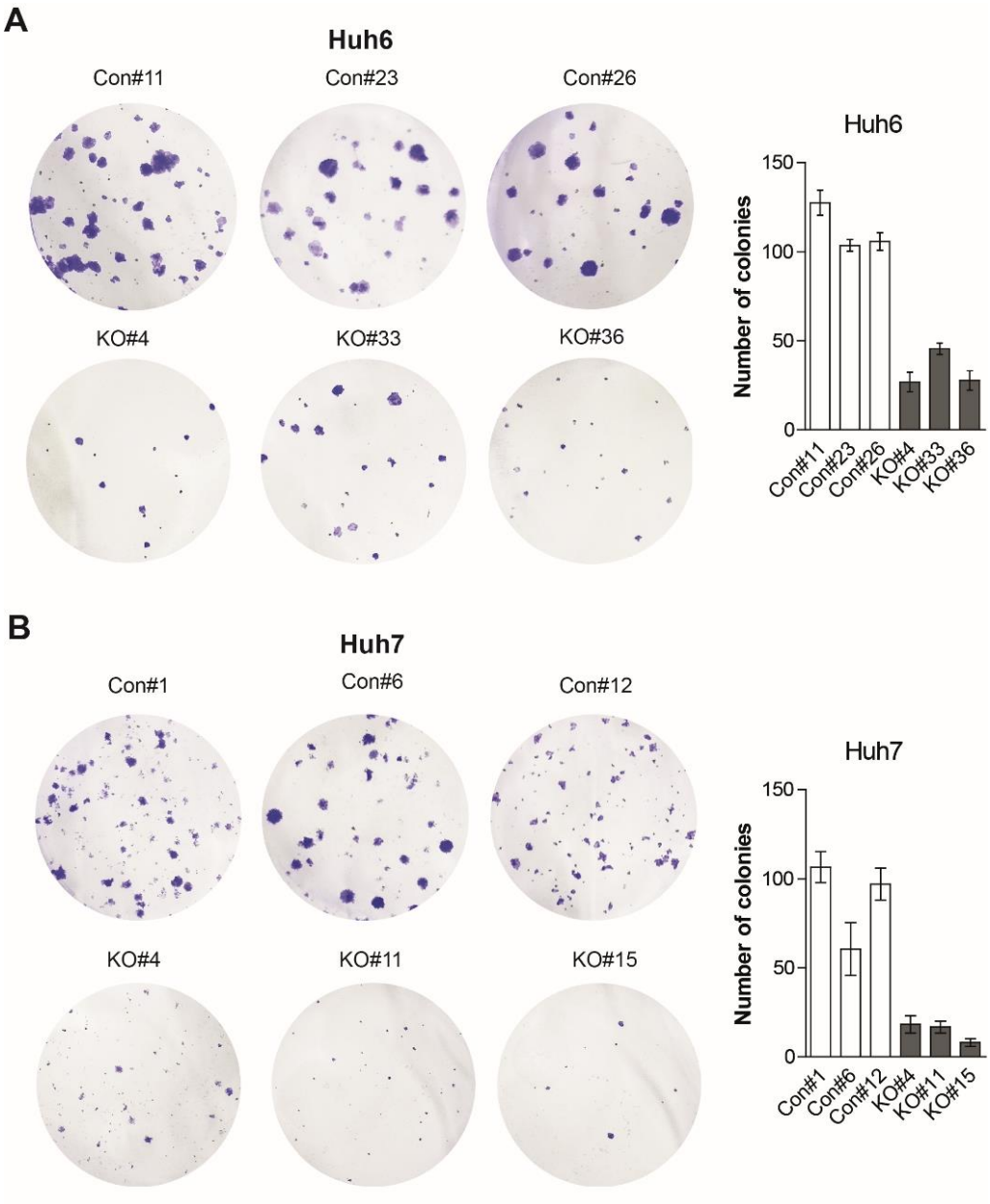

Figure 4. Loss of STRAP perturbs the capacity of colony formation in HCC cell lines. (A,B) Deletion of STRAP dramatically inhibits the colony formation of Huh6 and Huh7 cell lines. The number of colonies in each well was counted (mean ± SD, n=4 for each clone)

Loss of STRAP attenuates Wnt/β-catenin signaling activity

It has been reported that upregulation of STRAP correlates with increased Wnt/β-catenin signaling activity in colorectal cancer (16). We wondered whether this also holds true for HCC cells, most of which are known to also depend on β-catenin signaling for sustaining optimal growth (24). To this aim, we evaluated the expression change within the RNA-seq data of several (liver specific) β-catenin signaling target

genes reported previously, i.e. *AXIN2*, *LGR5*, *MYC*, *CCND1*, *GLUL*, *RGN* and *BIRC5* (also known as Survivin) (25). In Huh7 all these genes were downregulated in the STRAP knockout clones with the exception of *RGN* and *GLUL*. In the *CTNNB1* mutant Huh6 cells the differences were less obvious but most genes showed a trend towards lower expression (Figure 5A). The effect of STRAP on Wnt/β-catenin signaling activity was confirmed using a more sensitive β-catenin reporter assay (Figure 5B).

Using siRNA mediated knockdown of *STRAP*, similar reductions in β-catenin reporter activity were observed in the parental Huh6 and Huh7 lines as well as in four additional HCC lines, indicating that STRAP is required to maintain optimal β-catenin signaling in most, if not all, HCC lines (Figure 5C). This even is the case in the cell lines endogenously expressing a dominant acting β-catenin variant (Huh6, SNU398 and HepG2).

STRAP has been shown to bind to GSK3β around the catalytic domain, thereby reducing the N-terminal phosphorylation of β-catenin (16, 26) and subsequently increasing the active signaling pool of β-catenin, i.e. unphosphorylated at S33/ S37/T41. Hence, we investigated the amount of the active β-catenin signaling pool present in the HCC clones. As shown in Figure 5D, Huh6 showed reduced levels of active β-catenin in the STRAP knockout clones, whereas no change was observed in Huh7.

Besides N-terminal phosphorylation, the signaling strength of β-catenin is also regulated by phosphorylation at its C-terminus. For example, S675 phosphorylation by protein kinase A (PKA) has been shown to increase Wnt signaling by recruiting transcriptional co-activators (21, 27-29). To investigate whether STRAP promotes Wnt/β-catenin signaling through indirectly affecting the phosphorylation of S675, we tested its levels. As indicated in Figure 5E, reduced levels of phosphorylated β-catenin at S675 were observed in the STRAP knockout clones of Huh6 while no clear change was seen in the Huh7 cell line. Thus, in Huh6 loss of STRAP is accompanied by lower levels of unphosphorylated N-terminal β-catenin and reduced phosphorylation at its C-terminus, both features that are associated with reduced signaling, whereas no alteration is observed in Huh7.

Together, these findings suggest that STRAP enhances Wnt/β-catenin signaling in all tested HCC cells. The exact molecular mechanism appears however to differ between cell lines.

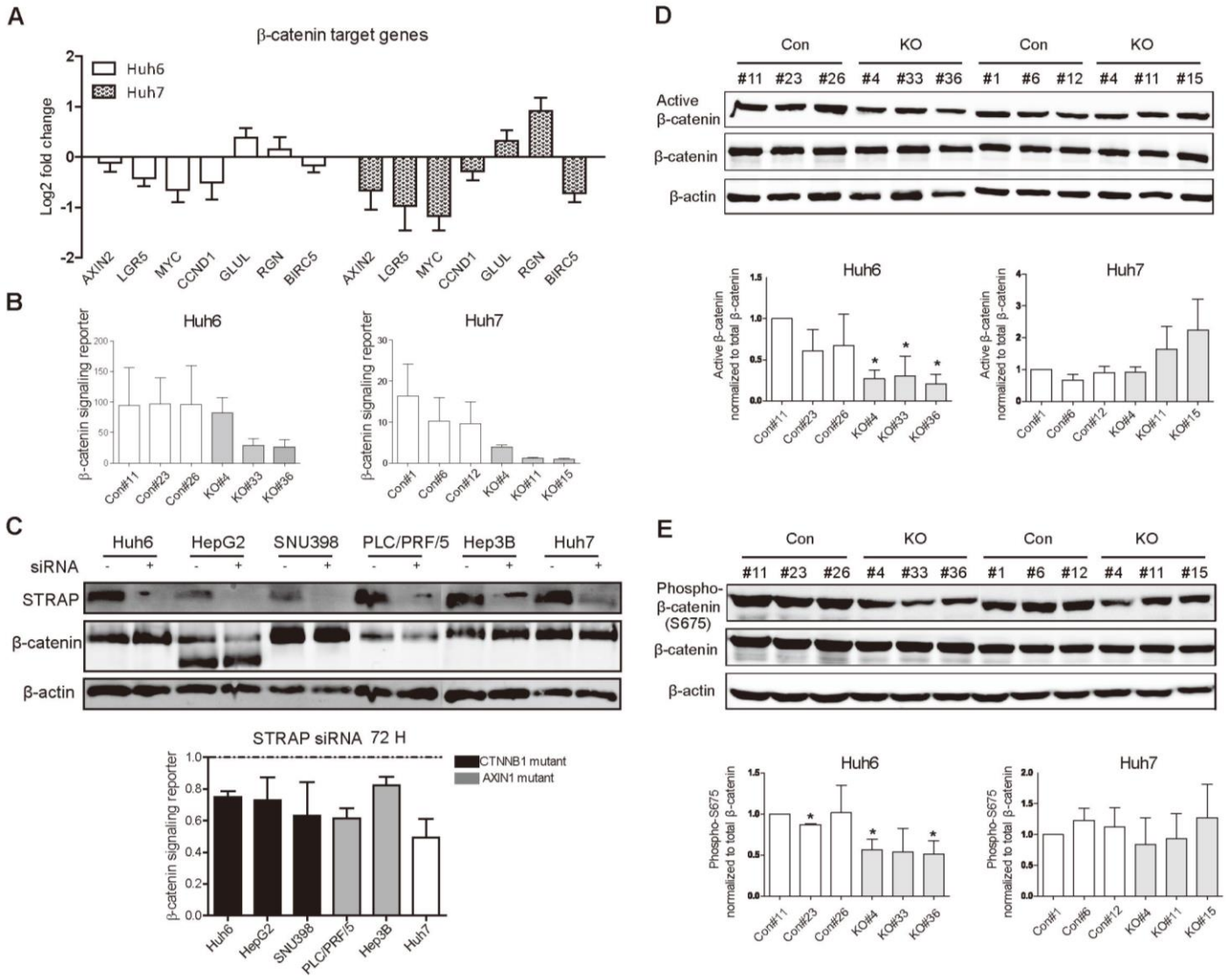

Figure 5. Loss of STRAP reduces Wnt/β-catenin signaling activity in HCC cell lines. (A) Log2 fold change of (liver specific) target genes of Wnt/β-catenin signaling in STRAP knockout clones derived from the RNA-seq data. (B) β-catenin luciferase reporter assay showing reduced β-catenin signaling activity in STRAP knockout clones of Huh6 and Huh7 cell lines compared to controls (mean ± SD, n=2, two times). The β-catenin reporter activities are depicted as WRE/MRE ratios. (C) SiRNA mediated knockdown of STRAP suppresses β-catenin signaling activity in HCC cell lines (mean ± SD, n=2, two times). Values are depicted relative to the WRE/MRE ratios obtained for the controls, which are arbitrarily set to 1. (D) Deletion of STRAP decreases the abundance of active β-catenin (unphospho-Ser33/Ser37/Thr41) in Huh6 cells. (E) The level of phosphorylated β-catenin at S675 is diminished in STRAP knockout Huh6 cell clones. Values for active and pS675 β-catenin are depicted relative to signal intensities obtained for total β-catenin. Cells were grown and blotted 3 independent times. Mean ± SD is shown; values were analyzed using GraphPad column t-test; * $p<0.05$.

Loss of STRAP associates with reduced stemness and increased differentiation markers

Wnt/β-catenin signaling is essential for the homeostatic self-renewal and proliferation of the hepatic stem/progenitor cells (30). In particular, Wnt/β-catenin driven AXIN2+ (31) and LGR5+ (32) cells have been identified as stem cells that self-renew and give rise to mature hepatocytes. STRAP itself has also been linked to stemness in colorectal cancer (33). Therefore, loss of STRAP and the resulting reduction in β-catenin signaling may lead to reduced expression of stem/progenitor cell markers. We observed a clear reduction at the transcription level of *AXIN2* and *LGR5* and other liver progenitor markers (*SOX9*, *CD44* and *PROM1/CD133*) (34) in STRAP knockout Huh6 cells. In Huh7, expression of *AXIN2*, *LGR5* and *PROM1* but not *SOX9* and *CD44* were decreased (supplemental Figure S6A).

The colony formation assay shown in Figure 4 partially supports the stem cell assumption, but may be biased by differences in plating efficiency associated with STRAP-loss. Therefore, we performed a similar assay by plating the cells in soft agar. As shown in Figure 6 a significant reduction in colonies is formed in the STRAP knockout clones of Huh6 ($p=0.001$), while no clear difference is seen for Huh7.

Conversely, STRAP loss increased most liver differentiation related genes, such as *ALB*, *AFP* and *HNF4A* (35, 36) in Huh6 and more obviously in Huh7 cells (Supplemental Figure S6B). To corroborate this observation, we explored glycogen storage as a marker of differentiation in liver cancer cells using PAS staining (Figure 7). All knockout clones of Huh6 showed multiple cells with a prominent PAS staining, while this was rarely visible in the control clones. In Huh7 the difference was less obvious, although also here a trend towards more positivity was observed in the knock-out clones.

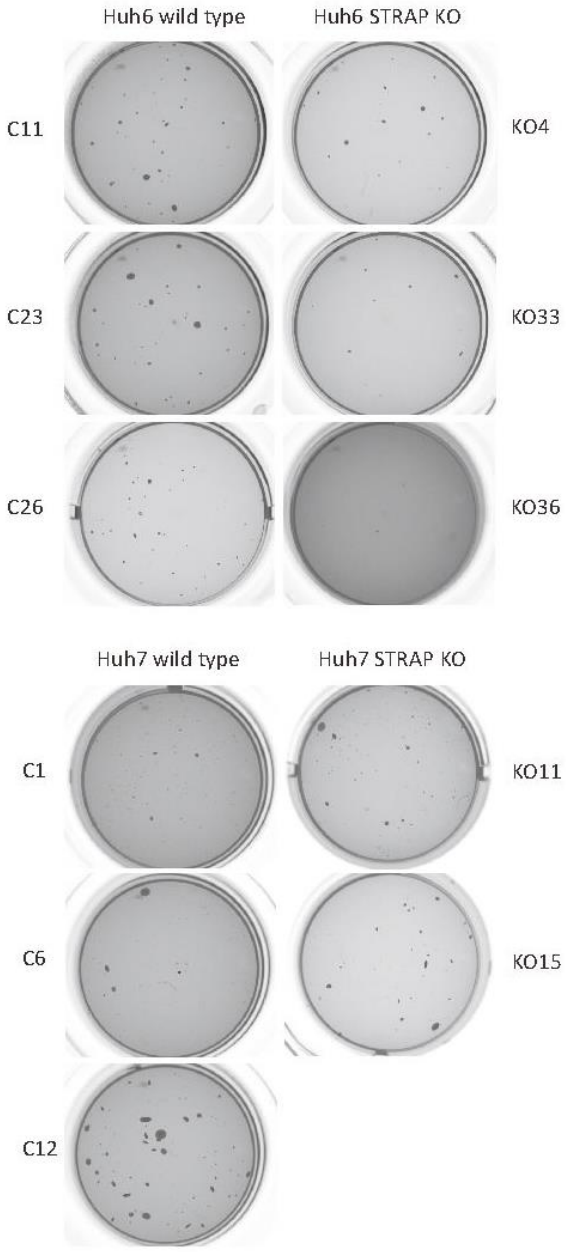

Huh6	C11	C23	C26	KO4	KO33	KO36
Count 1	24	23	27	17	7	2
Count 2	33	12	25	18	12	3
Count 3	16	12	22	14	6	1
Mean	24	16	25	16	8	2
SD	6.9	5.1	2.0	1.6	2.6	0.8

Huh7	C1	C6	C12	KO11	KO15
Count 1	12	6	51	11	20
Count 2	14	15	55	28	32
Count 3	14	26	95	36	44
Mean	13.3	15.7	67.0	25.0	32.0
SD	1.2	10.0	24.3	12.8	12.0

Figure 6. Soft-agar colony formation assay. STRAP knockout significantly (P¼0.001) reduces the number of colonies formed from single Huh6 cells. No significant difference is observed for Huh7

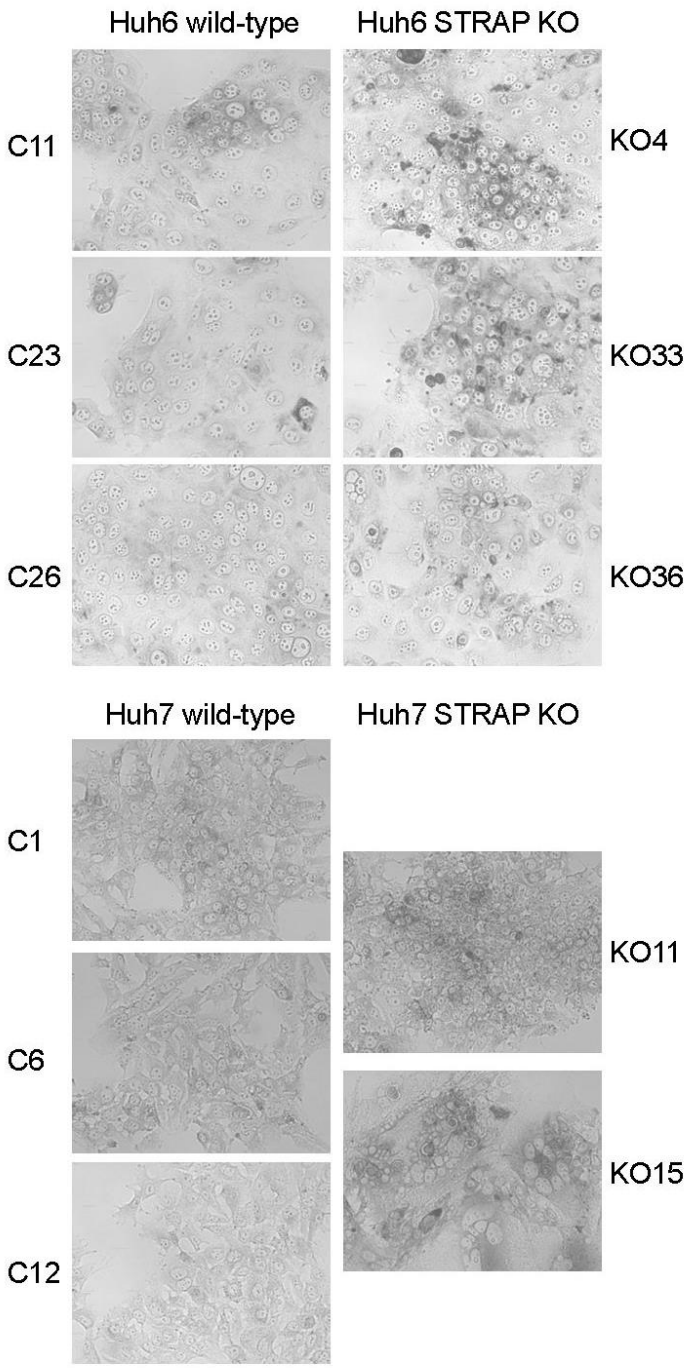

Figure 7. Glycogen storage is increased in STRAP knockout clones. PAS staining ofclones grown to 60% to 70% confluency shows increased glycogen storage in all Huh6 knockout clones, whereas a trend in the same direction is visible for Huh7.

Discussion

STRAP has been identified as a scaffolding protein that is upregulated in breast, lung and colorectal cancers, and was shown to promote their growth (10-12). Here we show that also in most hepatocellular cancers increased levels of STRAP protein can be observed. Furthermore, knockout experiments in two different HCC cell lines showed that its expression is required to support optimal growth. Mechanistically we provide evidence that many signaling pathways and metabolic processes are affected following STRAP loss, including the Wnt/β-catenin signaling pathway.

Given the well-known importance of β-catenin signaling to sustain HCC growth, we have investigated this pathway in more detail (24, 25). Knockout/down of *STRAP* resulted in reduced β-catenin signaling in all six HCC lines investigated, regardless of the underlying *CTNNB1* or *AXIN1* mutation being present in these lines. This is largely in line with the observation of Yuan et al for colorectal cancer cells (16). Mechanistically, STRAP has been shown to bind to the catalytic site of GSK3β, effectively resulting in reduced N-terminal phosphorylation and reduced breakdown of β-catenin (16, 26). Hence, loss of STRAP is expected to result in more GSK3-mediated phosphorylation of β-catenin, which is in accordance with the notable decrease in non-phosphorylated (active) β-catenin observed in Huh6. In Huh6 a second mechanism appears active by which STRAP increases overall β-catenin signaling. PKA-mediated phosphorylation of β-catenin at S675, previously shown to result in increased signaling (21, 27-29), is about 2-fold higher in the clones that have retained STRAP expression. This result suggests that STRAP may be involved in modulating PKA activity through yet unknown mechanisms. Nevertheless, Huh7 cells apparently share neither mechanism for STRAP to support Wnt/β-catenin signaling, despite being one of the more sensitive cell lines (see Figures 5B and 5C), suggesting alternative routes involved. As Wnt/β-catenin signaling can be fine-tuned at multiple levels (37), uncovering the exact mechanism specifically for Huh7 is outside the scope of this current manuscript. Whichever the exact mechanism, our results show that the increased STRAP expression observed in most HCCs will support their growth by increasing overall β-catenin signaling.

The Wnt/β-catenin signaling pathway is well-known for its role in (cancer) stem cell maintenance (30-32, 38, 39). Accordingly, the reduced β-catenin signaling following

knockout of STRAP, is associated with lower expression of the β-catenin regulated stem cell markers *AXIN2* and *LGR5*. In addition, several other liver progenitor markers (*SOX9*, *CD44* and *PROM1/CD133)* are reduced in expression, whereas differentiation markers are elevated. These results suggest that one mechanism by which elevated STRAP expression supports HCC growth is to shift the balance towards the induction of stem cell features. This observation is in line with the work of Jin et al. who showed that STRAP promotes stem cell features in several colorectal cancer cell lines (33).

Besides its role in fine-tuning β-catenin signaling, STRAP has also been linked to various other cellular processes likely contributing to HCC cell viability (9, 14). One of the first functions attributed to STRAP was its role in inhibiting TGF-β signaling (13). In the normal liver this signaling pathway has a crucial role in limiting hepatocyte proliferation and inducing differentiation (40). Likewise, TGF-β signaling is considered to act as a tumor suppressor during the early stages of liver tumor formation by inducing cell-cycle arrest and apoptosis. As such, the elevated STRAP levels that we observe in HCC may contribute to tumor growth by restraining the tumor-suppressive effects of TGF-β, which is supported by the re-activation of several TGF-β anti-proliferative (CDKN1A, CDKN2B, CDKN1C and EIF4EBP1) and pro-apoptotic (BIK, BCL2L11, DAPK1, FAS and GADD45B) target genes (41, 42) derived from RNA-seq data following STRAP loss in Huh6 and Huh7 cells (Supplemental Figure S6C). However, the role of TGF-β signaling in liver cancer is complicated by the observation that a subset of tumors become resistant to the cytostatic and apoptotic effects of TGF-β, and in fact exploit TGF-β to support their growth, migration and invasion during later stages (40, 43). This indicates that the specific contribution of STRAP to TGF-β-mediated tumor suppression has to be evaluated on a case-by-case basis.

In summary, we show that most HCCs show upregulation of STRAP expression. Our *in vitro* analyses suggest that its elevated expression is important to support optimal growth by affecting a variety of metabolic processes and signaling pathways of known importance for liver cancer. Especially, its contribution to increase Wnt/β-catenin signaling is likely to be a major effector of its tumor-promoting role.

Supplementary Figures and Tables

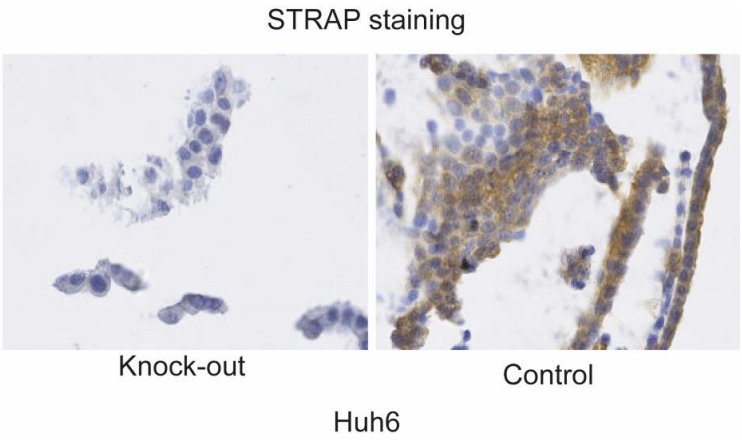

Figure S1. Specificity of STRAP antibody tested on a STRAP knock-out Huh6 clone and control thereof. For this purpose, both cell lines were formalin-fixed and embedded in paraffin.

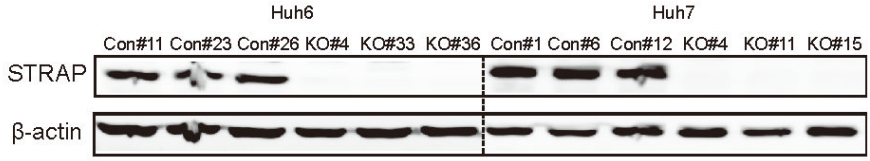

Exons	Clones	AA alteration	Size	Sequences
1	Wild type	-	-	CACGCGACCCGTGGTTGATTTGGCCTTCAGTGGCATCACGCCTTATGGGTATTTCT TAATCAGCTGGCCACACGCGACCCGTGGTTGAATT
1	Huh6 KO#33	Insertion	+81	CACGCGACCCGTGGTTGA**CCCCGTCTCCCTGGCTTTAGCCACCTCTCCATCCTCTT GCTTTCTTTGCCTGGACACCCCGTTCTCCTGTGGATTCGGGTA**TT
2	Wild type	-	-	TGCAACACTGAATAAGGATGCCACCAAAGCAGCTACAG
2	Huh6 KO#4	Deletion	-1	TGCAACACTGA:TAAGGATGCCACCAAAGCAGCTACAG
		Insertion	+1	TGCAACACTGAA**A**TAAGGATGCCACCAAAGCAGCTACAG
		Deletion	-22	TGCAACAC::::::::::::::::::::::AGCTACAG
2	Huh6 KO#36	Insertion	+2	TGCAACACTGAA**AA**TAAGGATGCCACCAAAGCAGCTACAG
		Insertion	+1	TGCAACACTGAA**A**TAAGGATGCCACCAAAGCAGCTACAG
2	Huh7 KO#4	Insertion	+1	TGCAACACTGAA**A**TAAGGATGCCACCAAAGCAGCTACAG
2	Huh7 KO#11	Insertion	+1	TGCAACACTGAA**A**TAAGGATGCCACCAAAGCAGCTACAG
		Deletion	-1	TGCAACACTGA:TAAGGATGCCACCAAAGCAGCTACAG
		Insertion	+~300	from Ecoli and other unknown sources
2	Huh7 KO#15	Insertion	+1	TGCAACACTGAA**A**TAAGGATGCCACCAAAGCAGCTACAG
		Deletion	-1	TGCAACACTGA:TAAGGATGCCACCAAAGCAGCTACAG

Figure S2. Knockout of the STRAP gene by CRISPR/Cas9 technology in HCC cell lines.Huh6 and Huh7 were transfected with STRAP-targeting vectors and single-cell sorted by FACS. The surviving clones were subjected to western blot. Depicted are STRAP protein levels of independent control and knock-out clones selected for further analysis. The lower panel shows the sequence alterations of each STRAP knock-out clone. All control clones showed only the wild-type sequence. The insertion of 81 nucleotides in Huh6 KO#33 results in additional 27 amino acids within the WD40 region, which apparently makes the protein highly unstable as demonstrated by no detectable protein using two antibodies

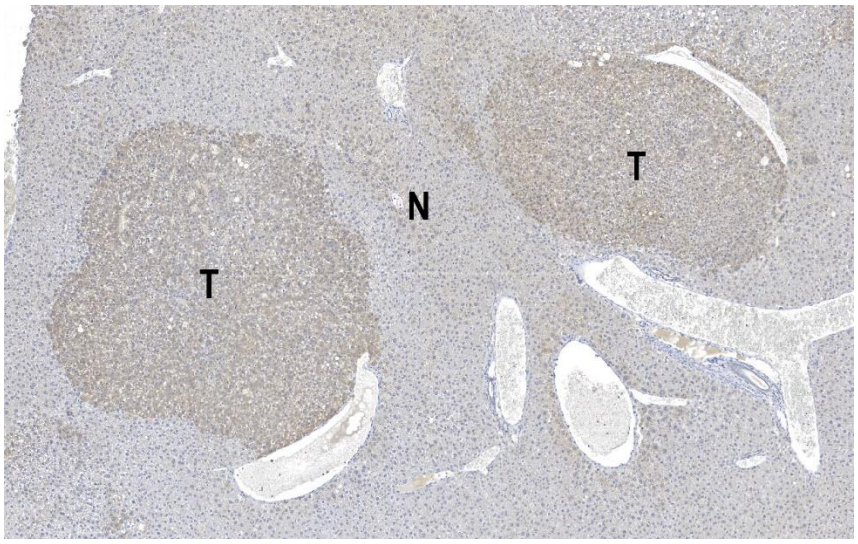

Figure S3. Elevated expression of STRAP in DEN-induced mouse liver tumors (T) compared with flanking normal liver tissue (N).

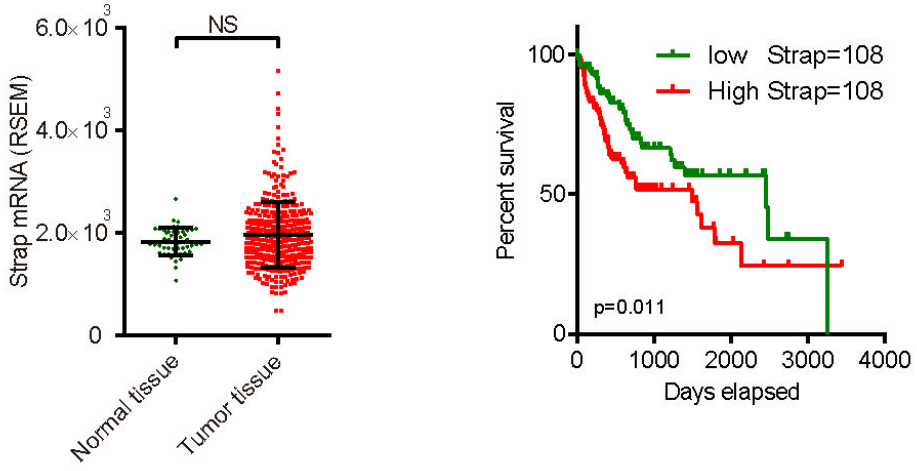

Figure S4. Analysis of the TCGA liver cancer cohort reveals that no significant difference in average *STRAP* RNA levels is observed between normal and tumor samples. Kaplan-Meier survival analysis and a log-rank test of the top and bottom 30% *STRAP* expressors revealed a significant trend (p=0.011) of reduced survival in the high expressing group.

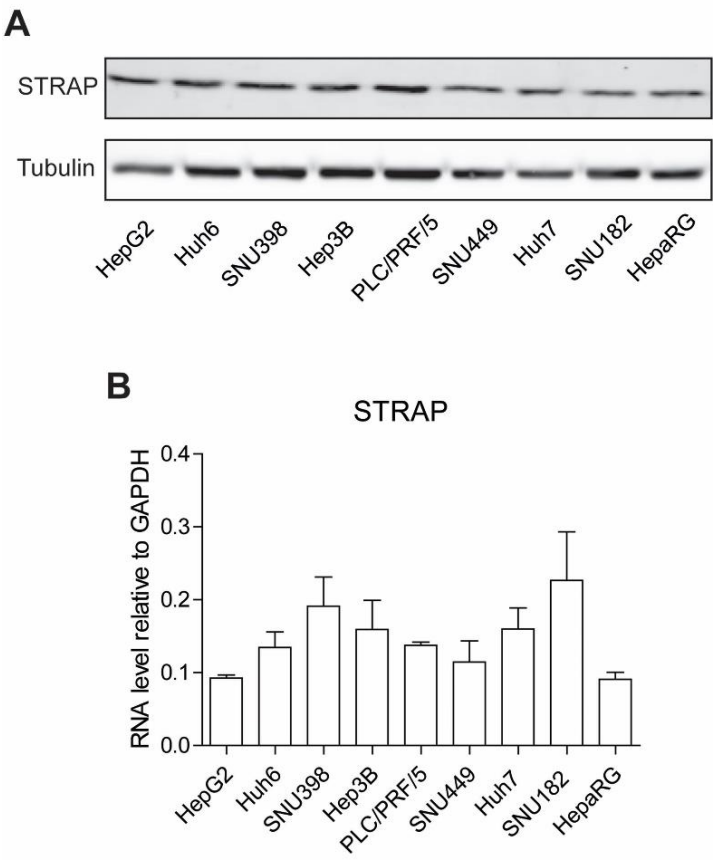

Figure S5. Baseline levels of STRAP protein and RNA in a panel of 9 HCC cell lines.

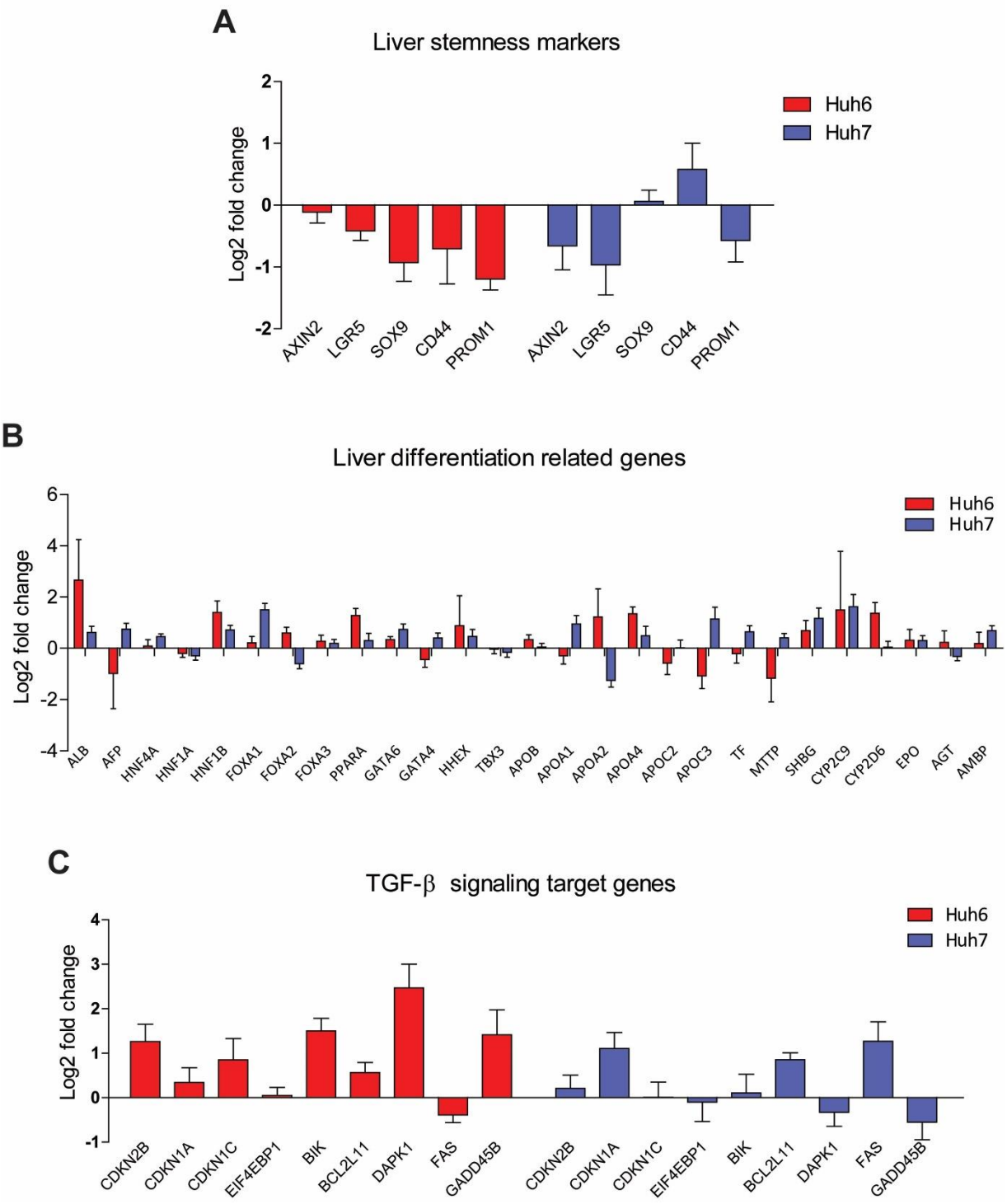

Figure S6. Log2 fold change of liver stemness markers (A), liver differentiation related genes (B) and TGF-β signaling target genes (C) in STRAP knock-out clones compared to controls. The results are presented as log2 fold change ± Standard Error, n=3.

Supplemental Table S1. Selected *STRAP* sgRNAs

Species	Gene target	gRNA	Sequence
Human	STRAP exon2	sgRNA1	TTGGGGTGCAACACTGAATA
	STRAP exon1	sgRNA2	AATCAACCACGGGTCGCGTG
	STRAP exon1	sgRNA3	CACGCGACCCGTGGTTGATT

Supplemental Table S2. Primer sequences of *STRAP* used for Sanger sequencing

Exons	Forward Sequence (5'~3')	Reverse Sequence (5'~3')
Exon1	CCCTTCTTTTCCTGTTGCC	GTGTTGGCTCTCATCTCAG
Exon2	GGTGGTAGTTAAATAGCTG	TGGGATCAAACATGCGTTC

Supplemental Table S3. Primer sequence used for Ion Torrent sequencing

Gene	Forward Sequence (5'~3')	Reverse Sequence (5'~3')
STRAP	Adapter A-Barcode-CCCTTCTTTTCCTGTTGCC	Adapter PI-Barcode-GTGTTGGCTCTCATCTCAG

Supplemental Table S4. Primer sequences used for qRT-PCR

Gene	Forward Sequence (5'~3')	Reverse Sequence (5'~3')
DCDC2	ACTTGGACATAGGAGAAATCAAGA	CGAGCTGACACGTTGATCCT
NTHL1	TATGAGGGCTCGGACAGTGA	TTTGGTTTGGCTGGAGAGCA
RPS26	AAACATAGTGGAGGCCGCAG	CACATACAGCTTGGGAAGCAC
OLR1	CCTTGCTCGGAAGCTGAATG	TCTCCATGCCAGATCCAGTC
ABHD13	CCGGCGACACCCGAG	ACAAAGTTCCACAGCATCCAG
KLHL42	GGCCTCCATGAACCAGAAGA	GTTCCGGTCTCTGGTAGTGTAT
ZNF853	AGCAGGAAATGCTCCACCAG	GTGGACTGCTGTTCCTCTCC
LGR5	ACACGTACCCACAGAAGCTC	CTAAAAGCCTGGACGGGGAT

Supplemental Table S5. Symmetric Measures

	Value	Asymp.Std. Error[a]	Approx. T[b]	Approx. Sig.
Measure of Agreement Kappa	,609	,064	8,453	,000
N of Valid Cases	115			

a. Not assuming the null hypothesis.

b. Using the asymptotic standard error assuming the null hypothesis.

Supplemental Table S6 Genes information

Gene	Protein	
STRAP	STRAP	A scaffolding protein without enzymatic function exerting regulatory functions on a variety of cellular processes
CTNNB1	β-catenin	A dual function protein involved in regulation and coordination of cell–cell adhesion and gene transcription
AXIN1	AXIN1	To form a destruction complex with APC, GSK3 and CK1α leading to the degradation of β-catenin
AXIN2	AXIN2	To form a destruction complex with APC, GSK3 and CK1α leading to the degradation of β-catenin
APC	APC	A tumor suppressor, negatively regulating β-catenin by forming a destruction complex with AXIN1/2, GSK3 and CK1α
GSK3	GSK3	A Ser/Thr kinase
CSNK1A1	CK1a	Kinase with preferential acidic protein targets
LGR5	LGR5	The receptor of R-spondin family of stem cell factors to potentiate Wnt/β-catenin signaling
ASK1	MAP3K5	Mitogen-activated protein kinase
PI3K	PIK3CA	Phosphatidylinositol 3-kinase
PDK1	PDK1	Pyruvate dehydrogenase kinase
DCDC2	DCDC2	A protein with two doublecortin peptide domains binding to tubulin and enhancing microtubule polymerization
NTHL1	NTHL1	A bifunctional DNA glycosylase that has an associated beta-elimination activity
RPS26	40S ribosomal protein S26	A ribosomal protein as a component of the 40S subunit
OLR1	OLR1	The protein binds, internalizes and degrades oxidized low-density lipoprotein
ABHD13	ABHD13	Unknown
KLHL42	KLHL42	Unknown
ZNF853	Zinc finger protein 853	A protein contains the zinc finger, a structural motif, for the coordination of one or more zinc ions in order to stabilize the fold.
MYC	MYC	A multifunctional, nuclear phosphoprotein that plays a role in cell cycle progression, apoptosis and cellular transformation
CCND1	Cyclin D1	A member of highly conserved cyclin family, whose members are characterized by a dramatic periodicity in protein abundance throughout the cell cycle
GLUL	glutamate-ammonia ligase	It catalyzes the synthesis of glutamine from glutamate and ammonia in an ATP-dependent reaction
RGN	Regucalcin	It may have an important role in calcium homeostasis
BIRC5	BIRC5/ Survivin	This protein functions to inhibit caspase activation, thereby leading to negative regulation of apoptosis or programmed cell death

SOX9	SOX-9	A transcription factor
CD44	CD44	*CD44 participates in a wide variety of cellular functions including lymphocyte activation, recirculation and homing, hematopoiesis, and tumor metastasis.*
PROM1	Prominin-1/CD133	The precise function of CD133 remains unknown, it has been proposed to act as an organizer of cell membrane topology
ALB	Albumin	Its main function is to regulate the Oncotic pressure of blood
AFP	alpha fetoprotein	Alpha-fetoprotein expression in adults is often associated with hepatoma or teratoma
HNF4A	HNF4A/ NR2A1	HNF4A is a nuclear transcription factor
HNF1A	HNF1A	A transcription factor expressed in organs of endoderm origin
HNF1B	HNF1B	HNF1B *is a nuclear transcription factor*
FOXA1	FOXA1/ HNF-3A	A transcriptional activator for liver-specific transcripts such as albumin and transthyretin
FOXA2	FOXA2/ HNF-3B/ TCF-3B	A transcriptional activator for liver-specific transcripts such as albumin and transthyretin
FOXA3	FOXA3/ HNF-3G/ TCF-3G	A transcriptional activator for liver-specific transcripts such as albumin and transthyretin
PPARA	PPARα/NR1C1	A transcription factor and a major regulator of lipid metabolism in the liver
GATA6	GATA6	This protein preferentially binds (A/T/C)GAT(A/T)(A) of the consensus binding sequence.
GATA4	GATA4	A member of the GATA family of zinc finger transcription factors
HHEX	HHEX	A member of the homeobox family of transcription factors, many of which are involved in the development of liver, thyroid, forebrain etc.
TBX3	TBX3	A member of T-box family which are the transcription factors involved in the regulation of developmental processes
APOB	Apolipoprotein B	Apolipoprotein B is the primary apolipoprotein of chylomicrons, VLDL, IDL, and LDL particles
APOA1	Apolipoprotein A1	Apolipoprotein A1 is the major protein component of high density lipoprotein particles in plasma.
APOA2	Apolipoprotein A2	The second most abundant protein of the high density lipoprotein particles
APOA4	Apolipoprotein A4	Apolipoprotein A4 is secreted into circulation on the surface of newly synthesized chylomicron particles
APOC2	Apolipoprotein C2	A component of very low density lipoproteins and chylomicrons
APOC3	Apolipoprotein C3	A component of very low density lipoprotein
TF	Transferrin	Transferrins are iron-binding blood plasma glycoproteins that control the level of free iron (Fe) in biological fluids
MTTP	MTTP	This protein plays a central role in lipoprotein assembly
SHBG	SHBG/SSBG	A glycoprotein that binds to the two sex hormones: androgen and estrogen

CYP2C9	CYP2C9	An important cytochrome P450 enzyme with a major role in the oxidation of both xenobiotic and endogenous compounds
CYP2D6	CYP2D6	A member of the cytochrome P450 mixed-function oxidase system, is one of the most important enzymes involved in the metabolism of xenobiotics in the body
EPO	Erythropoietin/ hematopoietin	A hormone that induces red blood cell production
AGT	Angiotensinogen	Angiotensin is a peptide hormone that causes vasoconstriction and a subsequent increase in blood pressure
AMBP	AMBP	AMBP interacts with CD79A
CDKN1A	$p21^{Cip1}$	A cyclin-dependent kinase inhibitor (CKI) that is capable of inhibiting all cyclin/CDK complexes
CDKN2B	CDKN2B	A cyclin-dependent kinase inhibitor
CDKN1C	CDKN1C	A tight-binding inhibitor of several G1 cyclin/Cdk complexes and a negative regulator of cell proliferation
EIF4EBP1	4E-BP1	Interaction of this protein with eIF4E inhibits complex assembly and represses translation
BIK	Bcl-2-interacting killer	Interaction of this protein with cellular and viral survival-promoting proteins, such as BCL2 and the Epstein-Barr virus enhances programmed cell death
BCL2L11	BCL2L11	Interaction of this protein with other members of the BCL-2 protein family, including BCL2, BCL2L1/BCL-X(L), and MCL1, activates apoptosis
DAPK1	DAPK1	A positive mediator of gamma-interferon induced programmed cell death
FAS	Fas cell surface death receptor	The Fas receptor is a death receptor on the surface of cells that leads to programmed cell death (apoptosis)
GADD45B	GADD45B	GADD45B responds to environmental stresses by mediating activation of the p38/JNK pathway and is involved in the regulation of growth and apoptosis

Abbreviations

STRAP, serine-threonine kinase receptor-associated protein; HCC, hepatocellular carcinoma; CRC, colorectal cancer; TMA, tissue microarray; siRNA, gene knockdown by small interfering RNA; CRISPR, Clustered Regularly Interspaced Short Palindromic Repeats; qRT-PCR, quantitative real-time polymerase chain reaction; FDR, false discover rate; KEGG, Kyoto Encyclopedia of Genes and Genomes; GO, Gene Ontology; WRE, Wnt Responsive Element; MRE, Mutant Responsive Element; SDS-PAGE, Sodium dodecyl sulphate-polyacrylamide gel; PVDF, Polyvinylidene difluoride; sgRNA, Single guide RNA; NGS, Next-generation sequencing; PI, Propidium Iodide; FACS, Fluorescence activated Cell Sorting; GEO, Gene Expression Omnibus. Supplemental Table S6 depicts all used gene names and their functions.

Author contributions

WW performed the majority of experimental work as well as data analysis and authored the manuscript. SL, PL, WC and ML assisted with part of experiments. KS provided TMA slides and helped with scoring STRAP staining. HW analyzed the raw data generated by RNA sequencing. MH assisted with the single cell sorting. MP, MB and QP reviewed and improved the manuscript. RS coordinated the project and participated in authoring of the manuscript. All authors reviewed the results and approved the final version of the manuscript.

Acknowledgements

We thank Manzhi Zhao for helping to score the TMA and Katya Mauff for help with statistical analyses.

References

1. Forner A, Llovet JM, Bruix J. Hepatocellular carcinoma. Lancet 2012;379:1245-55.

2. Sherman M. Epidemiology of hepatocellular carcinoma. Oncology 2010;78 Suppl 1:7-10.

3. Marquardt JU, Andersen JB, Thorgeirsson SS. Functional and genetic deconstruction of the cellular origin in liver cancer. Nat Rev Cancer 2015;15:653-67.

4. Dahmani R, Just PA, Perret C. The Wnt/beta-catenin pathway as a therapeutic target in human hepatocellular carcinoma. Clin Res Hepatol Gastroenterol 2011;35:709-13.

5. Albuquerque C, Bakker ER, van Veelen W, Smits R. Colorectal cancers choosing sides. Biochim Biophys Acta 2011;1816:219-31.

6. Zucman-Rossi J, Villanueva A, Nault JC, Llovet JM. Genetic Landscape and Biomarkers of Hepatocellular Carcinoma. Gastroenterology 2015;149:1226-39 e4.

7. Wang W, Pan Q, Fuhler GM, Smits R, Peppelenbosch MP. Action and function of Wnt/beta-catenin signaling in the progression from chronic hepatitis C to hepatocellular carcinoma. J Gastroenterol 2017;52:419-31.

8. Datta PK, Chytil A, Gorska AE, Moses HL. Identification of STRAP, a novel WD domain protein in transforming growth factor-beta signaling. J Biol Chem 1998;273:34671-4.

9. Reiner JE, Datta PK. TGF-beta-dependent and -independent roles of STRAP in cancer. Front Biosci (Landmark Ed) 2011;16:105-15.

10. Matsuda S, Katsumata R, Okuda T, Yamamoto T, Miyazaki K, Senga T, et al. Molecular cloning and characterization of human MAWD, a novel protein containing WD-40 repeats frequently overexpressed in breast cancer. Cancer Res 2000;60:13-7.

11. Buess M, Terracciano L, Reuter J, Ballabeni P, Boulay JL, Laffer U, et al. STRAP is a strong predictive marker of adjuvant chemotherapy benefit in colorectal cancer. Neoplasia 2004;6:813-20.

12. Halder SK, Anumanthan G, Maddula R, Mann J, Chytil A, Gonzalez AL, et al. Oncogenic function of a novel WD-domain protein, STRAP, in human carcinogenesis. Cancer Res 2006;66:6156-66.

13. Datta PK, Moses HL. STRAP and Smad7 synergize in the inhibition of transforming growth factor beta signaling. Mol Cell Biol 2000;20:3157-67.

14. Seong HA, Manoharan R, Ha H. A crucial role for the phosphorylation of STRAP at Ser(188) by MPK38 in STRAP-dependent cell death through ASK1, TGF-beta, p53, and PI3K/PDK1 signaling pathways. Cell Cycle 2014;13:3357-74.

15. Jin L, Datta PK. Oncogenic STRAP functions as a novel negative regulator of E-cadherin and p21(Cip1) by modulating the transcription factor Sp1. Cell Cycle 2014;13:3909-20.

16. Yuan G, Zhang B, Yang S, Jin L, Datta A, Bae S, et al. Novel role of STRAP in progression and metastasis of colorectal cancer through Wnt/beta-catenin signaling. Oncotarget 2016;7:16023-37.

17. Forbes SA, Beare D, Gunasekaran P, Leung K, Bindal N, Boutselakis H, et al. COSMIC: exploring the world's knowledge of somatic mutations in human cancer. Nucleic Acids Res 2015;43:D805-11.

18. Sideras K, Biermann K, Verheij J, Takkenberg BR, Mancham S, Hansen BE, et al. PD-L1, Galectin-9 and CD8(+) tumor-infiltrating lymphocytes are associated with survival in hepatocellular carcinoma. Oncoimmunology 2017;6:e1273309.

19. Cancer Genome Atlas Research Network. Electronic address wbe, Cancer Genome Atlas Research N. Comprehensive and Integrative Genomic Characterization of Hepatocellular Carcinoma. Cell 2017;169:1327-41 e23.

20. Bakker ER, Das AM, Helvensteijn W, Franken PF, Swagemakers S, van der Valk MA, et al. Wnt5a promotes human colon cancer cell migration and invasion but does not augment intestinal tumorigenesis in Apc1638N mice. Carcinogenesis 2013;34:2629-38.

21. van Veelen W, Le NH, Helvensteijn W, Blonden L, Theeuwes M, Bakker ER, et al. beta-catenin tyrosine 654 phosphorylation increases Wnt signalling and intestinal tumorigenesis. Gut 2011;60:1204-12.

22. Meinders M, Kulu DI, van de Werken HJ, Hoogenboezem M, Janssen H, Brouwer RW, et al. Sp1/Sp3 transcription factors regulate hallmarks of megakaryocyte maturation and platelet formation and function. Blood 2015;125:1957-67.

23. Edgar R, Domrachev M, Lash AE. Gene Expression Omnibus: NCBI gene expression and hybridization array data repository. Nucleic Acids Res 2002;30:207-10.

24. Wang W, Xu L, Liu P, Jairam K, Yin Y, Chen K, et al. Blocking Wnt Secretion Reduces Growth of Hepatocellular Carcinoma Cell Lines Mostly Independent of beta-Catenin Signaling. Neoplasia 2016;18:711-23.

25. Monga SP. beta-Catenin Signaling and Roles in Liver Homeostasis, Injury, and Tumorigenesis. Gastroenterology 2015;148:1294-310.

26. Kashikar ND, Zhang W, Massion PP, Gonzalez AL, Datta PK. Role of STRAP in regulating GSK3beta function and Notch3 stabilization. Cell Cycle 2011;10:1639-54.

27. Hino S, Tanji C, Nakayama KI, Kikuchi A. Phosphorylation of beta-catenin by cyclic AMP-dependent protein kinase stabilizes beta-catenin through inhibition of its ubiquitination. Mol Cell Biol 2005;25:9063-72.

28. Taurin S, Sandbo N, Qin Y, Browning D, Dulin NO. Phosphorylation of beta-catenin by cyclic AMP-dependent protein kinase. J Biol Chem 2006;281:9971-6.

29. Taurin S, Sandbo N, Yau DM, Sethakorn N, Dulin NO. Phosphorylation of beta-catenin by PKA promotes ATP-induced proliferation of vascular smooth muscle cells. Am J Physiol Cell Physiol 2008;294:C1169-74.

30. Mokkapati S, Niopek K, Huang L, Cunniff KJ, Ruteshouser EC, deCaestecker M, et al. beta-catenin activation in a novel liver progenitor cell type is sufficient to cause hepatocellular carcinoma and hepatoblastoma. Cancer Res 2014;74:4515-25.

31. Wang B, Zhao L, Fish M, Logan CY, Nusse R. Self-renewing diploid Axin2(+) cells fuel homeostatic renewal of the liver. Nature 2015;524:180-5.

32. Huch M, Dorrell C, Boj SF, van Es JH, Li VS, van de Wetering M, et al. In vitro expansion of single Lgr5+ liver stem cells induced by Wnt-driven regeneration. Nature 2013;494:247-50.

33. Jin L, Vu T, Yuan G, Datta PK. STRAP Promotes Stemness of Human Colorectal Cancer via Epigenetic Regulation of the NOTCH Pathway. Cancer Res 2017;77:5464-78.

34. Dorrell C, Erker L, Schug J, Kopp JL, Canaday PS, Fox AJ, et al. Prospective isolation of a bipotential clonogenic liver progenitor cell in adult mice. Genes Dev 2011;25:1193-203.

35. Kang SJ, Park YI, Hwang SR, Yi H, Tham N, Ku HO, et al. Hepatic population derived from human pluripotent stem cells is effectively increased by selective removal of undifferentiated stem cells using YM155. Stem Cell Res Ther 2017;8:78.

36. DeLaForest A, Nagaoka M, Si-Tayeb K, Noto FK, Konopka G, Battle MA, et al. HNF4A is essential for specification of hepatic progenitors from human pluripotent stem cells. Development 2011;138:4143-53.

37. Fodde R, Brabletz T. Wnt/beta-catenin signaling in cancer stemness and malignant behavior. Curr Opin Cell Biol 2007;19:150-8.

38. Oishi N, Yamashita T, Kaneko S. Molecular biology of liver cancer stem cells. Liver Cancer 2014;3:71-84.

39. Nusse R, Clevers H. Wnt/beta-Catenin Signaling, Disease, and Emerging Therapeutic Modalities. Cell 2017;169:985-99.

40. Fabregat I, Moreno-Caceres J, Sanchez A, Dooley S, Dewidar B, Giannelli G, et al. TGF-beta signalling and liver disease. FEBS J 2016;283:2219-32.

41. Datto MB, Li Y, Panus JF, Howe DJ, Xiong Y, Wang XF. Transforming growth factor beta induces the cyclin-dependent kinase inhibitor p21 through a p53-independent mechanism. Proc Natl Acad Sci U S A 1995;92:5545-9.

42. Yoo J, Ghiassi M, Jirmanova L, Balliet AG, Hoffman B, Fornace AJ, Jr., et al. Transforming growth factor-beta-induced apoptosis is mediated by Smad-dependent expression of GADD45b through p38 activation. J Biol Chem 2003;278:43001-7.

43. Caja L, Sancho P, Bertran E, Fabregat I. Dissecting the effect of targeting the epidermal growth factor receptor on TGF-beta-induced-apoptosis in human hepatocellular carcinoma cells. J Hepatol 2011;55:351-8.

Chapter 6

Action and clinical significance of CCAAT/Enhancer Binding Protein Delta in Hepatocellular Carcinoma

Pengyu Liu[1], Wanlu Cao[1*], Buyun Ma[1*], Meng Li[1], Kan Chen[1,2], Kostandinos Sideras[1], Jan-Willem Duitman[3], Dave Sprengers[1], T.C. Khe Tran[5], Jan N.M. Ijzermans[5] Katharina Biermann[1]， Joanne Verheij[4], C.Arnold Spek[3], Jaap Kwekkeboom[1], Qiuwei Pan[1], Maikel P. Peppelenbosch[1]

[1.] Department of Gastroenterology and Hepatology, Erasmus MC Cancer Institute, Erasmus MC-University Medical Center, Rotterdam, The Netherlands

[2]. College of Life Science, Zhejiang Sci-Tech University, Hangzhou, China

[3]. Center for Experimental and Molecular Medicine (CEMM), Academic Medical Center, Amsterdam, The Netherlands,

[4]. Department of Pathology, Academic Medical Center, Amsterdam, The Netherlands

[5.] Department of Surgery, Erasmus MC Cancer Institute, Erasmus MC-University Medical Center, Rotterdam, The Netherlands

[*] These authors contributed equally to this article

Carcinogenesis 2019 40(1):155–163

Abstract

CCAAT/Enhancer Binding Protein Delta (CEBPD) is associated with the regulation of apoptosis and cell proliferation and is a candidate tumor suppressor gene. Here we investigated its role in hepatocellular carcinoma (HCC). We observe that CEBPD mRNA expression is significantly down-regulated in HCC tumors as compared to adjacent tissues. Protein levels of CEBPD are also lower in tumors relative to adjacent tissues. Reduced expression of CEBPD in the tumor correlates with worse clinical outcome. In both Huh7 and HepG2 cells, shRNA-mediated CEBPD knockdown significantly reduces cell proliferation, single cell colony formation and arrests cells in the G0/G1 phase. Subcutaneous xenografting of Huh7 in nude mice show that CEBPD knockdown results in smaller tumors. Gene expression analysis shows that CEBPD modulates interleukin-1 (IL-1) signaling. We conclude that CEBPD expression uncouples cancer compartment expansion and clinical outcome in HCC, potentially by modulating interleukin-1 signaling. Thus although our results support the notion that CEBPD acts as a tumor suppressor in HCC, its action does not involve impairing compartment expansion *per se* but more likely acts through improving anti-cancer immunity.

Short summary

We demonstrate that candidate tumor suppressor gene CCAAT/Enhancer Binding Protein Delta (CEBPD) downregulation provokes poor prognosis of clinical hepatocellular carcinoma (HCC). Remarkably, CEBPD drives HCC compartment expansion in experimental HCC. Interaction of CEBP with interleukin signaling may explain this discrepancy.

Introduction

Cancerous disease is characterized by abnormal cell growth with the potential to invade or spread to other parts of the body [1]. As it ultimately involves the withdrawal of physiological anti-expansionary control from the cancer cells, suppression of expansion of the cancer cell compartment size is the mainstay of current pre-clinical research. To this end, novel anti-cancer strategies are explored by measuring cell proliferation and death in cell cultures and by visualizing tumor expansion in experimental rodents, most-often in xenograft models. Although this approach has been proven successful in forming the conceptual basis for novel therapy in many forms of cancers, it is fair to say that this approach has proven disappointing for a range of therapy-resistant oncological manifestations, suggesting that these cancer models only partially capture disease dynamics in humans [2]. Nevertheless, the notion that cancer compartment expansion constitutes the most relevant parameter in therapy-directed oncological research remains largely unchallenged. This is especially the case for those tumor types that are refractory to current therapies and thus are clinically only subject to palliative therapy [3].

An important cancer type in this regard is hepatocellular carcinoma (HCC). HCC is the second cause of cancer-related death world-wide [4,5]. The disease is unusually resistant to therapies other as surgery, and thus is associated with very high fatality [6], especially in metastatic disease. The latter is depressingly common as early symptoms are inconspicuous and disease only becomes manifest at advanced stages. With more than 0.5 million new cases arising every year, the quest for devising a novel therapy for the treatment of HCC is one of utmost urgency [7]. Numerous studies have been directed at understanding the molecular processes driving HCC cell proliferation and to develop strategies aimed at inhibiting this proliferation. These studies, however, have yet largely failed to establish strategies that counteract clinical HCC, raising questions as to the extent to which the experimental models used reflect human disease faithfully.

An important consideration to take into account in this respect is the influence and to a certain extent also the species-specific actions of the tumor stroma [8]. Although HCC xenografts in mice are supported by murine-derived stromal structures, we observed earlier that co-grafting human HCC with human mesenchymal cells substantially

promotes HCC progression [9]. It is thus possible that the incomplete HCC-stromal interaction in preclinical models, as a consequence of defective species compatibility, results in the loss of important aspects of the regulation of the HCC tumor expansion process. In vitro modeling often does not involve stromal-cancer cell interactions at all. Thus if it could be shown that biological effects in HCC have alternative consequences in often-used preclinical models of disease and in clinical practice.

This consideration prompted us to explore both the clinical and preclinical importance of CCAAT/Enhancer Binding Protein Delta (CEBPD), which appears involved in oncological processes in general through modulating stroma-cancer cell interaction. CEBPD is recognized as an inflammatory response factor and plays a critical role in activating the innate immune response [10]. CEBPD is a bZIP transcription factor that belongs to the CEBPD family, which members exert their action through forming homo- and hetero-dimers and subsequent binding to specific DNA regulatory sequences, especially in the control of target gene expression [11,12] and regulation of proliferation [13], cell cycle, apoptosis, metastasis and inflammation cytokine signalling [14] following appropriate extracellular cues. On one hand, CEBPD expression is closely linked to the cancer tumorigenesis, whereas, on the other hand, its action appears highly context dependent. CEBPD seems, therefore, a candidate gene for testing whether preclinical compartment expansion and clinical effects can be uncoupled in relation to HCC.

Our results demonstrate that CEBPD has a dualistic role in HCC. Its expression appears protective in HCC patients, but in preclinical models, it supports the HCC process. Our results thus show that CEBPD uncouples preclinical models of HCC with clinical disease. The apparent lack of correlation suggests that current preclinical models do not fully capture HCC and this may explain the failure of such models to identify novel treatment approaches.

Materials and methods

Cell culture

Monthly short tandem repeat identity-verified (verification commercially performed by the molecular pathology department of the Erasmus MC) and American Type Culture Collection (ATCC, Manassas, VA)-obtained mycoplasma-free (monthly commercially checked by GATC Biotech, Konstanz, Germany) human HCC cell lines were maintained as described previously [15]. In brief, HEK29, Hep3B, Huh6, Huh7, PLC/ PRF/5, SNU182, SNU398 and SNU449 were cultured in DMEM medium (Lonza, Breda, The Netherlands) supplemented with 10% fetal bovine serum (Sigma–Aldrich) and 1% penicillin/streptomycin (Gibco, Bleiswijk, The Netherlands). HepG2 cells were cultured on fibronectin/collagen/albumin-coated plates (AthenaES) in Williams E medium (Invitrogen-Gibco, Breda, the Netherlands) complemented with 10% (v/v) fetal calf serum, 100 IU/ml penicillin, 100 µg/ml streptomycin, and 2 mM L-glutamine. The human liver organoids were cultured as described previously [16]. Cell lines were routinely confirmed to be mycoplasma free using the LookOut Mycoplasma PCR Detection Kit (Sigma-Aldrich). Cell counting process was performed by using Countess™ II Automated Cell Counter (Termo Fisher Scientifc).

Tissue Microarray and TCGA dataset

Archived formalin fixed paraffin-embedded tissue samples from 154 patients who underwent hepatic resection for HCC at Erasmus MC-University Medical Center (EMC, n = 94) or Amsterdam Medical Center (AMC, n = 60) between June 2001 and July 2014, were used for this study. Clinical data of this HCC cohort have been published previously [17]. For TMA slides, three or four 0.6 mm cores had been obtained from the tumorous area of 141 HCC patients and two 0.6 mm cores had been obtained from the paired tumor-free liver (TFL) area of 133 of these patients. Vital tumor areas and tumor-free liver tissue were identified by experienced gastrointestinal pathologists using earlier-archived hematoxylin-stained slides. The TMAs were constructed employing an automated tissue-arrayer (ATA-27). The use of patient materials was approved by the medical ethical committee of Erasmus MC (Medisch Ethische Toetsings Commissie Erasmus MC). Immunohistochemical scoring was conducted by two independent investigators (PL and KC) blinded to clinical outcome and differences resolved by

mutual agreement. In tumor tissues stained nuclei of tumor cells were scored, and in TFL stained hepatocyte nuclei. Percentages of stained nuclei were scored as 1 (<25%), 2 (25%- 70%), or 3 (>70%). In addition, the intensity of staining was defined from zero to three. Expression level was calculated by multiplication of intensity score and percentage score, resulting in levels ranging from 0 – 9.

TCGA LIHC RNA-Seq (level 3) and corresponding clinical data were downloaded from (https://tcgadata.nci.nih.gov/tcga/). There are 371 patient's tumor samples and corresponding 50 paired adjacent tumor-free tissues in this publically available dataset.

Lentiviral-shRNA packaging and infection

Hek293 cells were transfected with packaging plasmids and pLKO.1 based shRNA lentiviral vectors (Biomics Center in Erasmus Medical Center) targeting CEBPD, a scrambled control vector (shCTR) was also used. After 3 days infection, HepG2 and Huh7 cells were subjected to selection by puromycin (3 μg/mL); shRNA sequences are listed in the Supplementary Table S1. The knockdown efficiency is further confirmed by qRT-PCR (Supplementary Figure1) and Western Blot.

Western blot analysis

Western blot analysis has been extensively described elsewhere [18]. In short, protein samples were collected in a Laemmli sample buffer with 0.1 M DTT, and subsequently heated for 5 minutes at 95°C. Protein lysates were then subjected to polyacrylamide gel electrophoresis on a 8%-15% SDS gel for protein size-based separation by electrophoresis. All the Primary antibodies against CEBPD (sc-636), β-actin (sc-47778) (at a final dilution of 1:1000, Supplementary Table S2) were incubated with the membranes at 4°C for an overnight period. Next, 1 hour with an IRDye-conjugated secondary antibody (1:5000 anti-rabbit or 1:10000 anti-mouse dilution) at room temperature. Protein intensity was detected with the Odyssey 3.0 Infrared Imaging System.

Quantitative Real-time PCR(qRT-PCR)

A Machery-NucleoSpin RNA II kit (Bioke, Leiden, the Netherlands) was used for RNA isolation. The reverse transcription to produce cDNA was performed using a Takara

cDNA Synthesis Kit with random primers (Takara Bio, Inc., Shiga, Japan). Quantification of gene expression in HCC cell lines was quantified using SYBR-Green-based (Applied Biosystems® SYBR® Green PCR Master Mix) real-time PCR on the StepOnePlus™ System (Thermo Fisher Scientific Life Sciences). GAPDH was used as a housekeeping gene and expression level of target genes was normalized to GAPDH by the $2^{-\Delta\Delta CT}$ method. Primers sequences involved in this study were listed in Supplementary Table S3.

Cell proliferation and Colony formation assay

Cell proliferation was measured essentially similar as described earlier [19]. In short, CEBPD stable knockdown cells and scrambled sequence control cells were seeded in a 96-well microtiter plate with 6 replicate wells. Measurements were taken from day 1 to 7, with an interval of two days. For measurements 10 mM 3-(4,5-dimethylthiazol-2-yl)-2,5-diphenyltetrazolium bromide (MTT) (Sigma) was added to each well. After 3 hours of incubation at 37°C under a 5% CO2 atmosphere, the medium was completely removed and replaced by 100 µl DMSO which dissolves reaction products that indicate cell viability. The absorbance of each well will be measured at absorbance 490 nm by a microplate absorbance reader (BIO-RAD).

For colony formation, cells were harvested and resuspended in culture medium. A total of 1000 cells were seeded in 6-well tissue culture plates, with 3 independent wells for each experimental condition. After 14 days, the medium was thoroughly removed followed by two times of washing with PBS and the addition of a 0.5% crystal violet solution was then used for 15 min to stain cells. The number of colonies that contained >20 cells was analyzed and counted by Image J.

Cell cycle analysis by propidium iodide

5 x 10^5 cells were seeded in 6-well plates and harvested when a confluence of about 80% was reached. Cells were washed two times with PBS and fixed in ice-cold 70% ethanol. Cells were pelleted by centrifugation at 2000 rpm for 5mins, followed by 2 washes in PBS. The resulting pellets were subsequently stained employing 50 mg/ml propidium iodide and 0.1 mg/ml RNase for 30mins at room temperature and then

subjected to flow cytometric analysis. Cell cycle status was analyzed by FlowJo_V10 software.

In vivo HCC xenograft study in nude mice

HCC xenograft models were established by subcutaneous transplantation of Huh7 cells into nude mice (2.5×10^6 cells per mouse; n = 11 mice per group). CEBPD knockdown cells and corresponding control cells were injected into the lower left or right flank of the same mice, respectively. After four weeks, mice were sacrificed and tumors were immediately removed and analyzed. All animal experiments were approved by the Committee on the Ethics of Animal Experiments of the Erasmus Medical Center.

Statistical analysis

Protein and mRNA expression of CEBPD between the HCC tumor tissues and normal adjacent tissues were compared using the paired Student's *t*-test and the Mann–Whitney test. For all the functional studies, potential differences between the experimental groups were analyzed using a paired Student's *t*-test. $P < 0.05$ (indicated in the figures as single asterisk) was considered statistically significant. $P < 0.01$ (indicated in the double asterisks) and $P < 0.001$ (triple asterisks) were regarded as highly significant. All statistical analyses were performed in GraphPad Prism 5.

Results

Down-regulation of CEBPD mRNA in HCC tumors and its clinical significance

As a first analysis of the potential clinical significance of CEBPD in HCC, we exploited the TGCA resource that allows analysis of transcript levels in cancers and adjacent tissues. We identified data on CEBPD transcript levels in primary HCC of 371 patients and for 50 of those also data on adjacent tumor-free liver tissue is available. An overall analysis of transcript levels in all HCC and adjacent tissues showed that CEBPD mRNA levels are significantly lower in tumor as compared to adjacent tumor-free liver tissue ($P < 0.0001$, **Figure 1A**) and a paired analysis of the 50 cases in which data from both tumor-free liver tissue as well as HCC is present of the same patients made this point even more clear ($P<0.0001$, **Figure 1B**). We aimed to correlate the CEBPD expression data to clinical descriptors such as gender, age, a history of viral hepatitis, and pathology grade, but no relationships emerged.

However, we observe the link between CEBPD expression and tumor progression as assessed by American Joint Committee on Cancer (AJCC) staging [20]. We found that higher staging is associated with significantly lower CEBPD mRNA expression in tumors (**Figure 1C**). Thus clinical progression of HCC is strongly associated with lower CEBPD mRNA levels. Next, we investigated the relationship between CEBPD mRNA expression and patients' overall survival in the TCGA LIHC cohort by Kaplan–Meier test. When comparing the 20% patients with the highest CEBPD mRNA tumor expression with the 20% patients with the lowest tumor expression, we found that low CEBPD mRNA expression was associated with poorer survival ($P = 0.043$, log- rank test; **Figure 1D**).

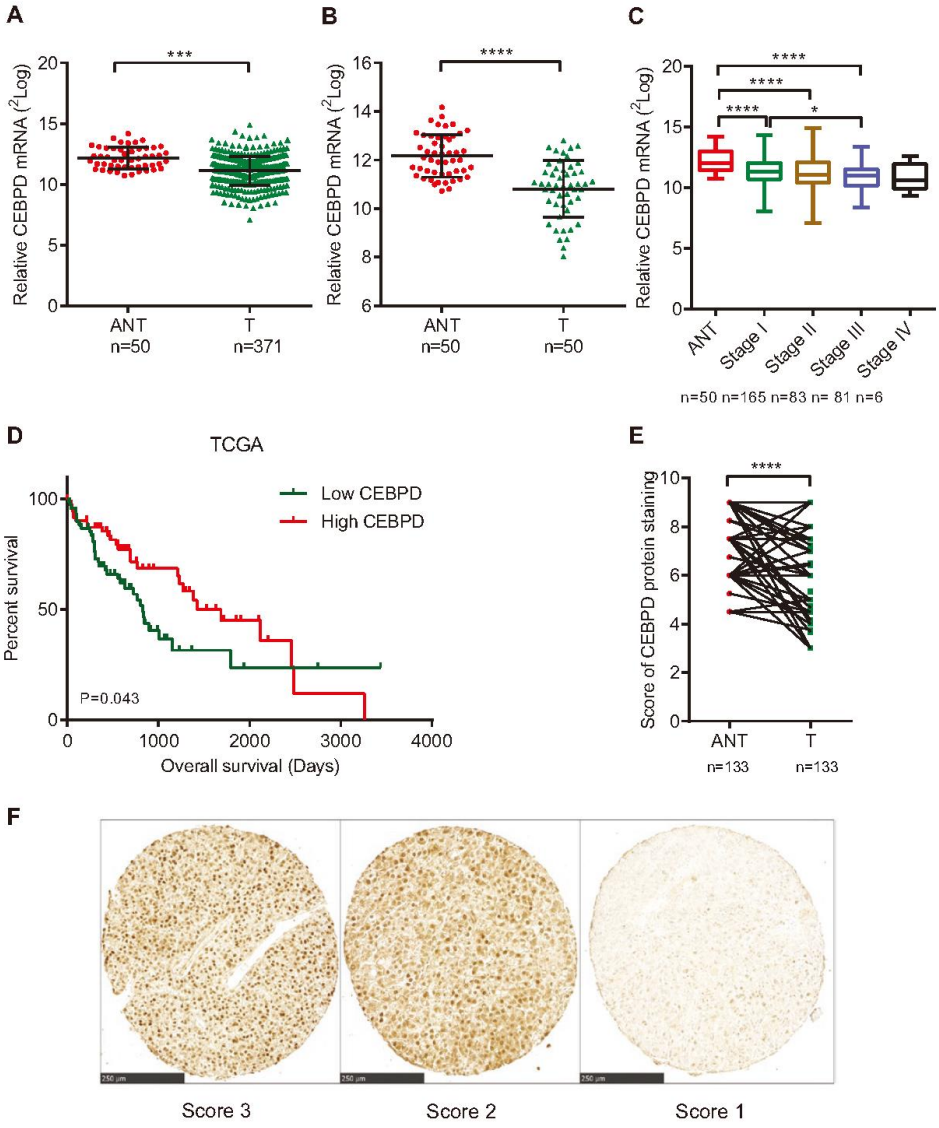

Figure 1. CEBPD downregulation in HCC Analysis of the TCGA dataset. (A) The results show that CEBPD mRNA expression is significantly decreased in HCC (unpaired tissue comparison). (B) Analysis of the TCGA dataset. Substantial downregulation of CEBPD mRNA is observed in the comparison of paired HCC tumor tissue (T) and adjacent tumor-free liver (ANT). (C) Analysis of the TCGA dataset. CEBPD mRNA expression is related to HCC clinical staging. More advanced cancer stages are related to lower CEBPD mRNA levels. (D) Low CEBPD mRNA expression was associated with poorer survival in TCGA dataset. (E) CEBPD protein expression was determined by immunohistochemistry on tissue microarrays of HCC patients of the Erasmus MC (Rotterdam) and the Academic Medical Center (Amsterdam), and semiquantified according to the staining intensity. CEBPD protein is significantly lower in HCC tumor tissues compared with paired adjacent liver tissues. (F) Slides were scored on a three grade scale: weak (1), moderate (2) or strong (3); and for percentages of positive nuclei (<25%=1, 25%-70%=2, >70%=3). *P < 0.05; ***P <0 .001; ****P <0 .001.

Downregulation of CEBPD protein expression in HCC tumors and tumor cell lines

To confirm that the observed downregulation of CEBPD transcripts in HCC as detected in our analysis of the TGCA resource corresponds to lower protein levels of CEBPD in HCC tumor cells (and does not derive from *e.g.* stromal cells), we analyzed TMAs of tumors of 154 HCC patients resected at Erasmus MC or AMC, and paired tumor-free liver tissues from 133 of these patients. We observed that lower levels of tumor cell-specific CEBPD protein expression in HCC tissues as compared with adjacent paired tumor-free liver tissues (P <0.0001, **Figure 1E**). In apparent agreement, when we used qRT-PCR and Western blot to examine the CEBPD mRNA levels and protein levels in 9 often used HCC cell lines and compared results to healthy human liver organoids, we observed that compared with healthy liver tissue, the expression of CEBPD is markedly reduced in all the HCC cell lines (**Figure 2A** and **2B**). We concluded that CEBPD downregulation is an intrinsic property of the HCC process and initiated investigations as to test whether preclinical models of HCC capture this aspect of liver cancer.

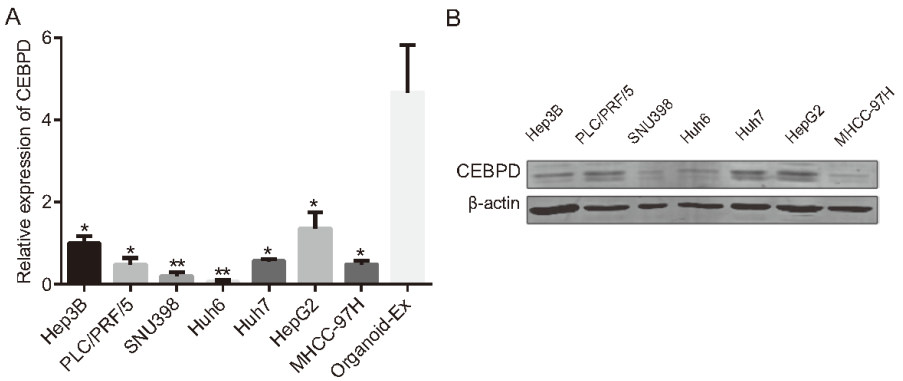

Figure 2. CEBPD in HCC cell lines is low when compared to normal healthy liver organoids. (A) CEBPD mRNA expression in HCC cell lines compared to normal healthy liver organoids. Organoids were grown in organoid expansion medium (Data represent mean ± SEM, n=3) (B) Western blot showing CEBPD protein expression in HCC cell lines. *P < 0.05; **P <0 .01

Paradoxal reduction of cell proliferation and colony formation following knockdown of CEBPD in HCC cell lines

To investigate whether the clinical relevance of CEBPD downregulation in HCC is mirrored by increased aggressiveness in in vitro models of HCC, we constructed CEBPD

knock down derivatives of both Huh7 and HepG2 employing an RNAi-mediated approach. This approach was successful in that various clones with reduced levels of CEBPD were created (henceforth referred to as CEBP-KD cells), especially when compared to cells transfected with a scrambled control vector (shCTR cells; **Figure 3**). Subsequently, the resulting clones were interrogated for overall proliferation, their capacity for single cell-derived colony formation as well as the effects of loss of CEBPD on cell cycling. We observed that CEBPD–KD cells are substantially hampered with respect to proliferative and colony forming potential (**Figure 4A** and **4B**). We also investigated the effects of loss-of-CEBPD expression on cell cycling in these preclinical models of HCC, employing PI staining and FACS analysis. We found that CEBPD-KD cells display G0/G1 cell cycle arrest **(Figure 4C)**. In conjunction, these results reveal a paradoxical inhibition of apparent pro-oncogenic behavior in CEBPD-KD cells, which contrasts the loss of CEBPD expression in clinical HCC and suggests that these in vitro models fail to capture important aspects of the HCC process.

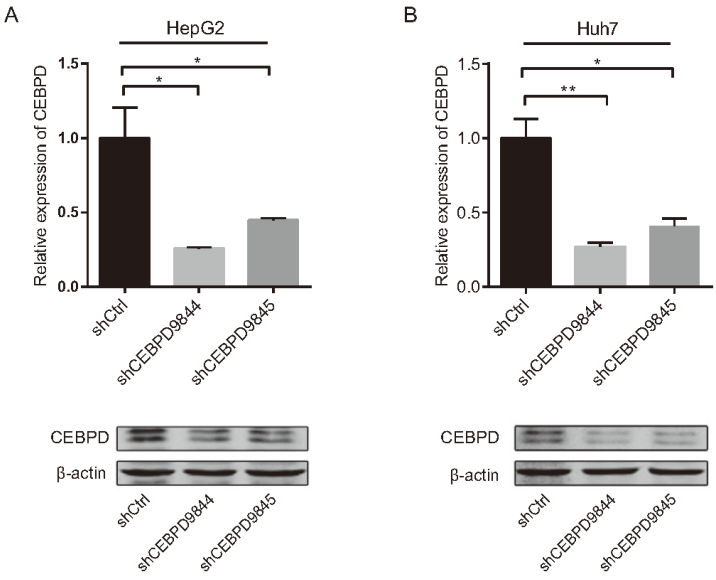

Figure 3. CEBPD knockdown efficiency. Knockdown was performed in (A) HepG2 cell line and (B) Huh7 cell line and efficacy was quantified by both qRT-PCR (upper graphs, mean ± SEM, n=3) and Western Blot (lower figures). *P < 0.05; **P <0 .01.

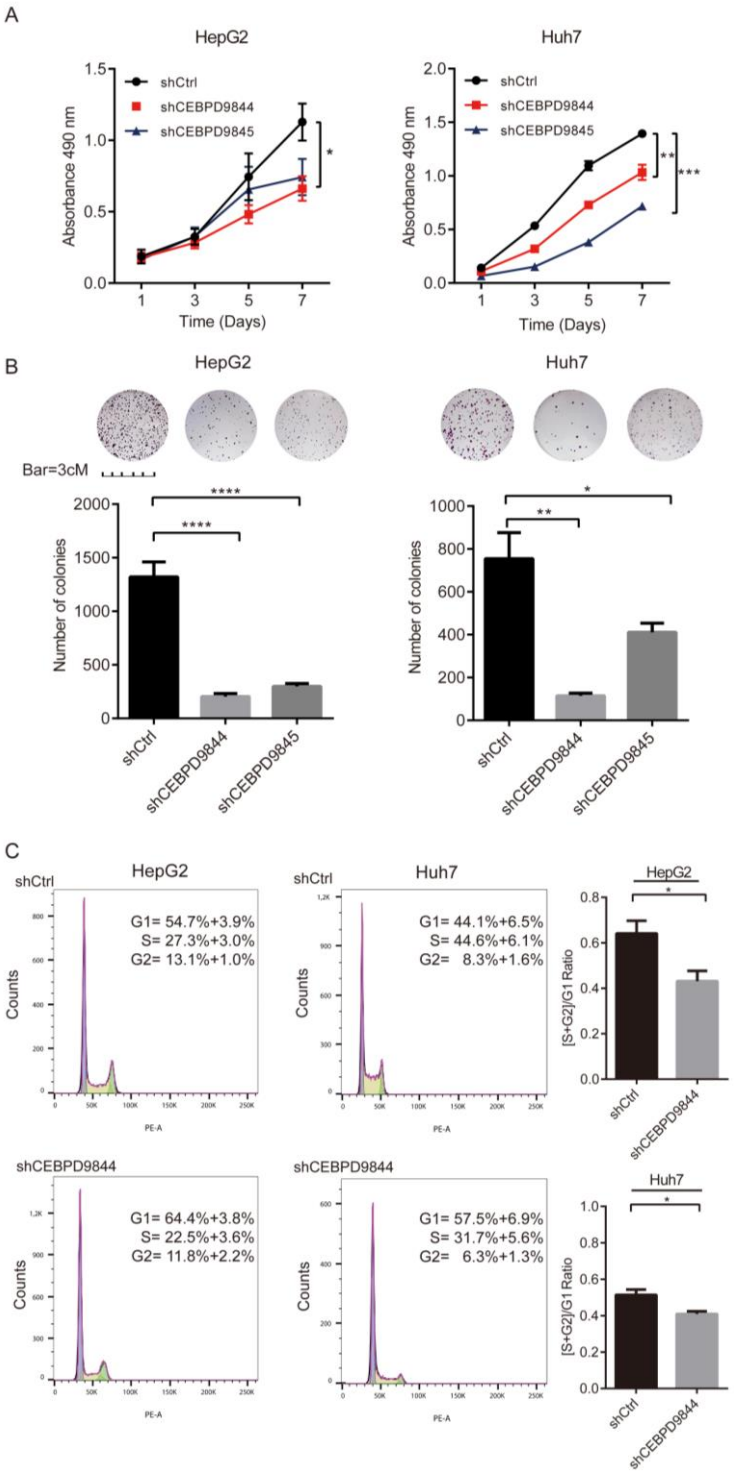

Figure 4 CEBPD expression drives HCC compartment expansion. Depletion of CEBPD expression strongly inhibits cell growth and the capacity for single cell colony formation in HCC cell lines. (A) Effects od CEBPD KD on cell proliferation as measured by MTT assay following 7 days of culture (mean ± SEM, n=3) (B) CEBPD KD effects the number of single cell-derived colonies as assayed 2 weeks following seeding (mean ± SEM, n=6 for each clone) (C) CEBPD knockdown induces G0/G1 cell cycle arrest. Propidium Iodide staining is used to distinguish the different stages of the cell cycle. The faction of cells in G0/G1 is increased in CEBPD-depleted cells (mean ± SEM, n=5 for each clone). *P < 0.05; **P <0 .01; ***P <0 .001; ****P <0 .0001.

Stable lentiviral-mediated knockdown of CEBPD in HCC cell lines impairs tumorigenesis *in vivo*

The notion that the clinical effects of downregulation of CEBPD expression in clinical HCC are not reflected in current pre-clinical models of disease is substantiated in experiments in which we used nude mouse xenografting to examine the tumorigenicity of shRNA-mediated CEBPD-KD cell lines. At bay with the observed negative relationship between CEBPD downregulation and the clinical outcome of HCC, we observed that CEBPD-KD cells form much smaller tumors in mice as compared to control cells (P<0.05, **Figure 5**). Subsequently, we initiated experiments as to dissect the potential mechanistic basis of the observed discrepancy.

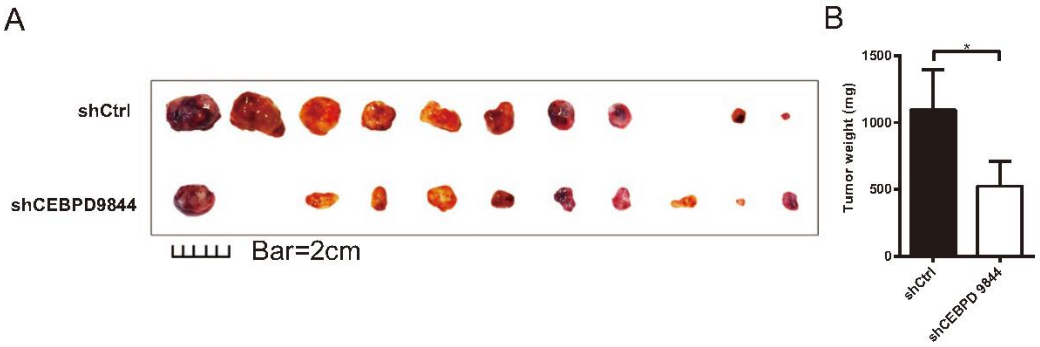

Figure 5. Downregulation of CEBPD inhibits HCC tumor growth in vivo. (A) A xenograft model of HCC by subcutaneous transplantation of Huh7 cells into nude mice was used CEBPD knockdown cells and corresponding control cells (2.5×106 cells per injection) were injected into the lower left or right flank of the same mice (n = 11), respectively. Tumor size after 4 weeks is shown. shCTR = upside; shCEBPD = downside) (B) Summary of tumor weights, indicating that CEBPD knockdown significantly decreases the tumor volume in the nude mice xenograft model (*:P=0.03)

RNA-seq analysis of the effects of CEBPD target genes

To provide mechanistic clues as to the effect of CEBPD downregulation, we exploited the GEO RNA-seq resource. Under accession number GSE69604 [21] this resource catalogues the effect of CEBPD-KD in MCF-7 cancer cells. A list of genes differentially expressed in the presence or absence of CEBPD was created based on a p-value cutoff of <0.05 and fold-change of >1.5 or < -1.5, and we used IPA software to establish the signaling pathways affected by CEBPD-KD. Also as a consequence of a cutoff Z-score ≥ 2 only a single signal transduction category was considered relevant by IPA, in case "acute phase response signalling" is mapped by IPA software, and includes 11 genes (**Figure**

6A). Although the background of the cell line in this IPA analysis is non-hepatic, the results may indicate that difference between the clinical and pre-clinical behavior of CEBPD expression maybe due to a role of CEBPD in supporting acute phase response signaling.

Confirmation of differential gene expression by qRT-PCR

A potential role for acute phase response signaling in explaining the differential effects between clinical HCC and preclinical models was supported by experiments in which the effects of CEBP-KD in Huh7 and HepG2 cell lines on the expression of the gene products involved in acute phase response signaling was determined using qRT-PCR. The results demonstrate that, with the possible exception of RRAS, the effects of CEBPD-KD mirror those seen in the GEO resource for MCF-7 cells (**Figure 6B**). Especially expression of IL1RN (interleukin 1 receptor antagonist), ITIH2 (inter-alpha-trypsin inhibitor heavy chain 2) and SERPINA3 (serpin peptidase inhibitor, clade A [alpha-1 antiproteinase, antitrypsin], member 3) are significantly reduced, up to 50% following CEBPD-KD. Conversely, the expression level of CRABP2 (cellular retinoic acid binding protein 2) was doubled. We also verified that the link between CEBPD and interleukin 1 receptor antagonist existed in the TCGA resource liver cancer dataset (Spearman Score were 0.31 and 0.39; **Figure 6C**). Acute phase response signaling involves multiple cell types and its importance may only emerge in the context of interaction of different types of cell that may not exist in in vitro cultures are may require species-specific signaling. Thus the observation that acute phase response genes are a target of CEBPD provide a rational explanation for the difference between preclinical models and clinical HCC.

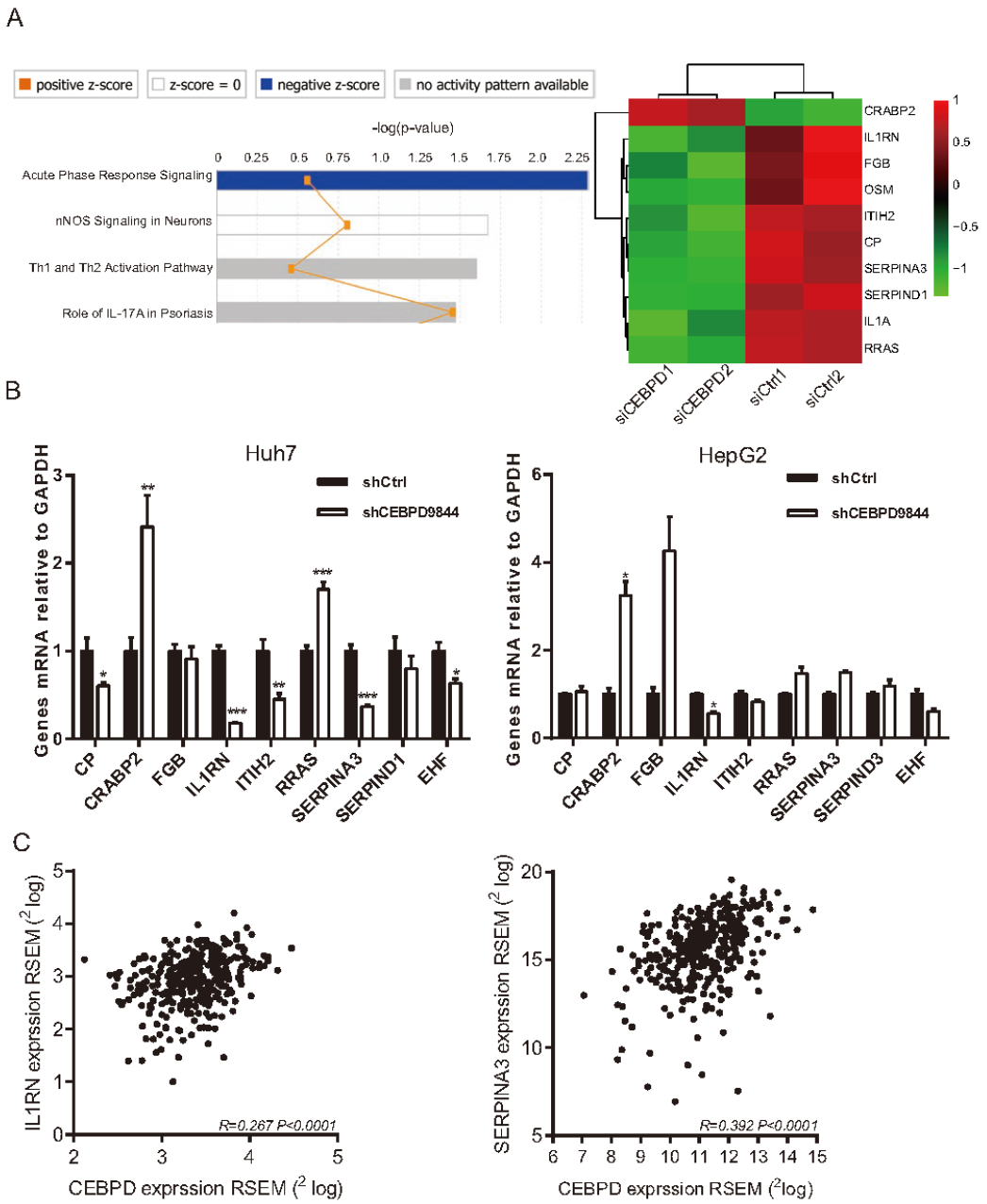

Figure 6. Effects of CEBPD knockdown on gene expression. Gene set enrichment analysis was performed on a differentially expressed genes identified in RNA-seq data sets (A) Pathway analysis on RNA-seq data (GSE69604). In this data set MCF7 cells were transfected with siRNAs against CEBPD or control siRNA). The blue color represents the signal pathways that are inhibited at this condition. The heat map depicts the differentially expressed genes and highlights the effects on the Phase Response signaling category (B) Differential gene expression HCC cell lines with or without CEBPD knockdown (mean ± SEM, n=4-5) (C) Co-expression between CEBPD and IL1RN and SERPINA3 in the TCGA dataset. *P < 0.05; **P <0 .01; ***P <0.001.

Discussion

In line with their recognized status as a relevant family of transcription factors, all five C/EBP family members have been associated with altered cellular fate, including cell cycle arrest, differentiation [22], and apoptosis [23]. In this study, we observed that outcome of clinical HCC associates with reduced CEBPD expression. This fits with observations that in genetic murine models prone to develop mammary cancer CEBPD appears to act as a tumor suppressor [24] and the observations from the present study suggest a similar functionality of CEBPD with respect to clinical HCC as well. The failure of preclinical models to capture this effect appears to relate either the absence of interaction between different cell types for in vitro models or possibly hampered intracellular communication due to species differences in xenograft models. In support of this latter notion is also the apparent role of CEBPD in acute phase response signaling but this line of thinking is fostered by literature data as well, that show in glioblastoma CEBPD mRNA overexpression in mesenchymal cells in a manner related to adverse prognosis [25]. Nevertheless, a role of CEBPD as a tumor suppressor gene appears certainly not universal: for urothelial carcinoma, CEBPD copy number amplification and overexpression can be related to poor prognosis and promote tumor metastasis [26]. However, CEBPD mRNA expression downregulation had been found in many different tumor types, such as hepatocellular carcinoma [27], leukemia [28], breast cancer [29], cervical cancer [30], and it also can be a biomarker for predicting better survival in breast cancer patients [31]. Thus the status of CEBPD as a candidate tumor suppressor gene is strong and the present work adds to the current momentum in the field in this respect.

The discrepancy between preclinical models and clinical HCC with regard to CEBPD probably relates to its function in inflammation [32], which although relevant for clinical disease course is poorly captured in current models of disease. CEBPD is well established to become transcriptionally active in ongoing inflammatory reactions and the current work shows that its downregulation is associated with loss of immune-related signaling. It has become clear that the immune system is an important disease-constraining factor in HCC [33] and one can envision that loss of CEBPB provokes an immune tolerant environment that enables cancer to thrive even in the presence of functional immunity. In support of this notion is our finding that CEBPD-KD

leads to upregulation of CRABP, which is well known to stimulate regulatory lymphocytes and may thus foster immune escape of cancers. Preclinical models that involve overall proliferation or colony formation obviously do not measure immune system involvement. Likewise, xenografting cancer cells in immunodeficient mice also only minorly involves the immune system. Nevertheless, the effects on compartment expansion of CEBPD in HCC in the absence of immune interaction are quite strong and the observation that CEBPD behaves in clinical HCC as tumor suppressor shows that the importance of immunological pressure in clinical HCC development is even larger as contemplated hitherto and emerges from the current studies the major force driving the HCC process.

Disregarding the exact details as to the discrepancy in the effects of loss of CEBPD expression in clinical HCC versus the effect of CEBPD-KD in preclinical models, the present study has established that translation of findings obtained in often used models of this disease like cell proliferation, single cell colony formation and xenografting is not straightforward and may actually be counterproductive. As these models continue to form the mainstay of current HCC research, this lack of translational capacity may be a reason why efforts to combat this disease have been so notably unsuccessful. Thus we interpret the current study as a call reevaluate current models and concentrate on those which do involve functional interaction with the immune system.

Funding

This research was financially supported by a China Scholarship Council PhD fellowship (File NO. 2014 0822 0029) to Pengyu Liu.

References

1. Hanahan, D. et al. (2000) The hallmarks of cancer. Cell, 100, 57.
2. Becher O.J. et al. (2006) Genetically engineered models have advantages over xenografts for preclinical studies. Cancer Res.,. 66, 3355.
3. Hammad, A.Y. et al. (2017) Palliative interventions for hepatocellular carcinoma patients: analysis of the National Cancer Database. Ann. Palliat. Med. 6, 26.
4. GLOBOCAN. International Agency for Research on Cancer (IARC). 2002 Available at: http://www-dep.iarc.fr
5. World Health Organization. Mortality Database. WHO Statistical Information System. 2008 Available at: http://www.who.int/whosis
6. Jemal, A. et al. (2011) Global cancer statistics. CA Cancer J. Clin. 61,69.
7. El-Serag, H.B. (2011) Hepatocellular carcinoma. N. Engl. J. Med. 365, 1118.
8. Leonardi, G.C. et al. (2012) The tumor microenvironment in hepatocellular carcinoma. Int. J. Oncol. 2012;40: 1733.
9. Hernanda, P.Y. et al. (2013) Tumor promotion through the mesenchymal stem cell compartment in human hepatocellular carcinoma. Carcinogenesis 34, 2330.
10. Ramji, D.P. et al. (2002) CCAAT/enhancer-binding proteins: structure, function and regulation. Biochem. J. 365, 561.
11. Lekstrom-Himes, J. et al. (1998) Biological role of the CCAAT/enhancer-binding protein family of transcription factors. .J Biol. Chem. 273, 28545.
12. Grigoryan, G. et al. (2009) Design of protein-interaction specificity gives selective bZIP-binding peptides. Nature. 2009;458: 859-864.
13. Pawar, S.A. et al. (2010) C/EBP{delta} targets cyclin D1 for proteasome-mediated degradation via induction of CDC27/APC3 expression. Proc. Natl. Acad. Sci. U. S. A. 107, 9210.
14. Balamurugan, K. et al. (2013). The many faces of C/EBPdelta and their relevance for inflammation and cancer. Int. J. Biol Sci. 9, 917.
15. Wang, W. et al. (2016) Blocking Wnt Secretion Reduces Growth of Hepatocellular Carcinoma Cell Lines Mostly Independent of beta-Catenin Signaling. Neoplasia18. 711.
16. Cao, W. et al.(2017) Dynamics of Proliferative and Quiescent Stem Cells in Liver Homeostasis and Injury. Gastroenterology 153, 1133.
17. Sideras, K. et al. (2017) PD-L1, Galectin-9 and CD8(+) tumor-infiltrating lymphocytes are associated with survival in hepatocellular carcinoma. Oncoimmunology. 6, e1273309.
18. de Sousa, R.R. et al. (2007) Phosphoprotein levels, MAPK activities and NFkappaB expression are affected by fisetin. J. Enzyme. Inhib. Med. Chem. 22, 439.
19. Wang, Y. et al. (2014) Calcineurin inhibitors stimulate and mycophenolic acid inhibits replication of hepatitis E virus. Gastroenterology 146, 1775.
20. Edge SB. American Joint Committee on Cancer, American Cancer Society. AJCC cancer staging manual. 7th ed. New York: Springer. 2009.

21. Mendoza-Villanueva, D. et al. (2016) The C/EBPdelta protein is stabilized by estrogen receptor alpha activity, inhibits SNAI2 expression and associates with good prognosis in breast cancer. Oncogene. 35, 6166-6176.

22. Johnson, P.F. (2005) Molecular stop signs: regulation of cell-cycle arrest by C/EBP transcription factors. J. Cell. Sci. 118, 2545.

23. Gade, P. et al. (2008) Critical role for transcription factor C/EBP-beta in regulating the expression of death-associated protein kinase 1. Mol. Cell. Biol. 28, 2528.

24. Balamurugan, K. et al. (2010) The tumour suppressor C/EBPdelta inhibits FBXW7 expression and promotes mammary tumour metastasis. EMBO J. 29, 4106.

25. Cooper, L.A. et al. (2012) The tumor microenvironment strongly impacts master transcriptional regulators and gene expression class of glioblastoma. Am J Pathol. 2012;180: 2108-2119.

26. Wang, Y.H. et al. (2015) CEBPD amplification and overexpression in urothelial carcinoma: a driver of tumor metastasis indicating adverse prognosis. Oncotarget 6, 31069.

27. Ko, C.Y. et al. (2008) Epigenetic silencing of CCAAT/enhancer-binding protein delta activity by YY1/polycomb group/DNA methyltransferase complex. J. Biol. Chem. 283, 30919.

28. Agrawal, S. et al. (2007) The C/EBPdelta tumor suppressor is silenced by hypermethylation in acute myeloid leukemia. Blood. 109, 3895.

29. Sivko, G.S. et al. (2004) CCAAT/Enhancer binding protein delta (c/EBPdelta) regulation and expression in human mammary epithelial cells: I. "Loss of function" alterations in the c/EBPdelta growth inhibitory pathway in breast cancer cell lines. J. Cell. Biochem. 93, 830.

30. Pan, Y.C. et al. (2010) CEBPD reverses RB/E2F1-mediated gene repression and participates in HMDB-induced apoptosis of cancer cells. Clin. Cancer Res. 16, 5770.

31. Naderi, A. et al. (2007) A gene-expression signature to predict survival in breast cancer across independent data sets. Oncogene. 26, 1507.

32. Hsiao, Y.W. et al. (2013) CCAAT/enhancer binding protein delta in macrophages contributes to immunosuppression and inhibits phagocytosis in nasopharyngeal carcinoma. Sci. Signal. 6: ra59.

Chapter 7

Summary and Discussion

Summary

The critical components of Wnt signaling in HCC

Hepatocellular carcinoma (HCC) is a serious malignancy associated with high morbidity and mortality. Aberrant activation of Wnt/β-catenin signaling has been shown to significantly contribute to the initiation and progression of HCC [1]. In this tumor type this is mainly accomplished by acquiring activating somatic mutations in the *CTNNB1* gene coding for β-catenin (20-25%), or less frequently inactivating mutations within *AXIN1* (10%). In this thesis, I investigated how novel hotspot β-catenin variants lead to enhanced β-catenin signaling. In addition, I explored to what extent *AXIN1* mutation leads to enhanced signaling in liver cancer cell lines, as this has been debated in several papers in the last decade. Liver cancer cell lines were also tested for their dependency on extracellular Wnt ligand activation to sustain their growth. Furthermore, we also identified STRAP as a novel protein that modulates β-catenin signaling in HCC. Lastly, I identified CEBPD whose expression levels appear to be associated with HCC prognosis.

During the last decades, great progress has been made in our understanding of Wnt/β-catenin signaling. Especially the process of N-terminal phosphorylation in exon3 encoded S/T residues of β-catenin and its subsequent proteolytic degradation, are well-understood. Mutations in this domain lead to aberrant activation of Wnt/β-catenin signaling activation by making the protein more resistant to proteolytic degradation [2-4]. More recently amino acid alterations within armadillo repeats 5 and 6 of β-catenin (residues K335, W383 and K387) are also being recognized as novel hotspots for mutation, especially in liver cancers [5]. In **Chapter 2**, we show that these mutants behave comparably to the wild-type protein with respect to half-life, N-terminal S/T phosphorylation and β-TrCP binding. In contrast, using immunoprecipitation we observe that these mutants associate less strongly with APC, one of the core proteins of the destruction complex, while simultaneously retaining the interaction with their nuclear TCF/LEF transcriptional co-factors. The latter is important to allow sufficient enhancement of β-catenin target genes driving tumor formation. Available structural and mutational data further support the observed change in relative binding affinities. In contrast to the exon3 mutations that occur in a mutually exclusive fashion with inactivating *APC* mutations in colorectal cancer [6], the armadillo repeat mutants often

co-occur with other "weak" mutations of the *APC* or *AXIN* genes. In liver cancers however, these armadillo repeat mutations appear to be sufficient to support tumor growth as they are not clearly associated with defects in other Wnt/β-catenin signaling related components. Overall, our analyses uncover a novel mode of β-catenin signaling activation, that is by acquiring β-catenin mutations that selectively reduce the binding to APC.

Besides oncogenic β-catenin mutations, aberrant signaling in liver cancers can also be accomplished through *AXIN1* mutation. These mutations are observed in about 10% of HCCs and originally were considered to support tumor growth by aberrantly enhancing β-catenin signaling. This view has however been challenged in the last decade by several reports showing neither a clear nuclear β-catenin accumulation nor clearly enhanced expression of β-catenin target genes [7]. **In Chapter 3**, using nine HCC lines, we show that AXIN1 mutation or siRNA mediated knockdown contributes to enhanced β-catenin signaling in all AXIN1-mutant and non-mutant lines, also confirmed by reduced signaling in AXIN1 repaired SNU449 cells. Both AXIN1 and AXIN2 work synergistically to control β-catenin signaling. While in the AXIN1-mutant lines AXIN2 is solely responsible for keeping signaling in check, in the non-mutant lines both AXIN variants contribute to β-catenin regulation to varying levels. In addition, our results also showed that their activity in the β-catenin destruction complex can be increased by tankyrase inhibitors, which thus may serve as a therapeutic option to reduce the growth of β-catenin-dependent cancers. Application of the tankyrase inhibitor XAV939 does however not clearly stabilize AXIN1 or AXIN2 protein in our HCC cell lines, with the exception of AXIN2 in the *CTNNB1*-mutant ones. Nevertheless, tankyrase inhibition diminished β-catenin signaling in most non-*CTNNB1*-mutant lines, which was however not sufficient to suppress their growth. Overall, our analyses show that AXIN1 mutation leads to enhanced β-catenin signaling in HCC, questioning the strong statements that have been made in this regard. Enhancing AXIN activity by tankyrase monotherapy provides however no effective treatment to affect their growth.

Except for β-catenin and AXIN1 mutation, Wnt ligands themselves are also recognized as factors which may promote tumor growth in a subset of tumors. Therefore, therapies that reduce Wnt ligand exposure to the tumor cells could be a promising option for HCC treatment [8]. **In Chapter 4** we investigate to what extent the growth of HCC cell lines

(n=9) can be affected by reducing Wnt ligand exposure, taking colorectal cancer cell lines along as controls. First, we show that siRNA mediated knock-down of β-catenin impairs the growth of all HCC cell lines. Blocking Wnt secretion, either by treatment with the IWP12 porcupine inhibitor or knockdown of WLS, also reduces the growth of most lines. Unexpectedly, inhibition of Wnt secretion does not show clear changes on Wnt/β-catenin signaling activities, which is reflected by minor changes in neither β-catenin reporter activity nor the expression of a well-known β-catenin target gene *AXIN2*. Similar results were observed for colorectal cancer cell lines used for comparison in various assays.

Our results suggest that most colorectal and liver cancers with mutations in components of the β-catenin degradation complex do not strongly rely on extracellular Wnt ligand exposure to support optimal growth. Blocking Wnt secretion may however aid in tumor suppression through alternative routes currently unappreciated.

In addition to somatic mutations of Wnt signaling components, there are many other regulators which may affect the activation of the Wnt/β-catenin signaling pathway. **In Chapter 5**, we revealed the importance of the oncogenic serine-threonine kinase receptor-associated protein (STRAP) to maintain optimal levels of β-catenin signaling and provide growth advantage in HCC cell lines. Increased expression of STRAP was observed in HCC patient's tissues, in accordance with previous studies for other tumor types [9-11]. For functional analysis, siRNA and CRISPR/Cas9 mediated loss-of-function studies of STRAP were performed on HCC cell lines, leading to inhibition of cell growth, cell cycle arrest and the impaired ability to form colonies. In accordance with a colorectal cancer study as described in the previous [12], STRAP downregulation or knockout significantly inhibited β-catenin target gene expression and induction of a β-catenin reporter system.

In conclusion, the increased STRAP protein levels observed in HCC, provide growth advantage among others by affecting Wnt/β-catenin signaling. These observations also identify STRAP as a new player in regulating β-catenin signaling in hepatocellular cancers.

Previous studies have shown that the function of CEBPD is highly linked to carcinogenesis and innate immune responses [13, 14], however, due to its multifunctional characteristics its exact role remains controversial [15]. **In Chapter 6** we

investigate its role in HCC. Our results showed that CEBPD mRNA expression is significantly downregulated in HCC tumor tissues as compared to adjacent liver tissues, further confirmed by protein expression analysis on TMA slides. In both Huh7 and HepG2 cells shRNA-mediated CEBPD knockdown significantly reduces cell proliferation, single cell colony formation and arrests cell cycling in the G0/G1 phase. Next, by analyzing RNA-sequencing data of CEBPD-KD experiments in MCF-7 cancer cells, we performed Gene Set Enrichment analysis, which indicated that CEBPD knockdown indirectly enhanced interleukin-1 (IL-1) signaling by affecting *IL1RN* expression, which is a natural inhibitor of IL-1 signaling. The reduction in *IL1RN* levels was confirmed by q-PCR in our CEBPD-KD Huh7 and HepG2 cells. Subcutaneous xenografting of Huh7 in nude mice showed that CEBPD knockdown results in smaller tumors. We conclude that CEBPD expression uncouples cancer compartment expansion and clinical outcome in HCC, potentially by modulating interleukin-1 signaling. Thus, although our results support the notion that CEBPD acts as a tumor suppressor in HCC, its action does not involve impairing compartment expansion per se but more likely acts through improving anticancer immunity.

Discussion

1 mutational mechanisms of increased Wnt/β-catenin signaling in HCC

Although the pathogenesis of HCC is multifactorial and heterogeneous, it is widely accepted that the Wnt/β-catenin signaling pathway is in a state of aberrant activation in the majority of liver cancers. In the first section of the thesis we focused on the role of key mutational components in the Wnt/β-catenin signaling pathway with regard to aberrant activation.

The best understood mechanism for aberrant Wnt signaling is the β-catenin mutations that are located at exon3, which account for 20-25% of all HCC cases. They lead to a defect in N-terminal S/T phosphorylation or β-TrCP binding, resulting in a β-catenin protein more resistant to proteolytic degradation and enhanced nuclear signaling. More recently, amino acid alterations within armadillo repeats 5 and 6 of β-catenin are being recognized as novel hotspots for mutation. We have shown that they reduce the binding to APC while simultaneously maintaining the ability to bind to TCF/LEF. Two clusters of β-catenin seem critical for binding with APC. The first cluster is centered around K335, mutation of which apparently interferes with binding to the phosphorylated 20AA repeats of APC. Previous studies have shown that the phosphorylation level of these 20AA repeats strongly increases the binding affinity with β-catenin up to 300-500 fold, and prevents the interaction of β-catenin with TCF/LEF [16]. For the second critical cluster around residues W383 and N387, the protein models do not provide a clear rationale for the selective loss of APC-binding, as their mutation is expected to affect binding of various partners. Nevertheless, our IP experiments clearly show that binding is selectively lost for the APC protein.

In our study we focused on four main binding partners of β-catenin, that is APC, AXIN, E-cadherin and TCF. However, many additional proteins have been identified to associate with β-catenin, especially in the armadillo repeat domain (https://web.stanford.edu/group/nusselab/cgi-bin/wnt/protein_interactions) [17]. Several of these interacting proteins have been reported in a limited number of papers with little follow-up, questioning their relevance. Nevertheless, we cannot formerly exclude at present that some of them may also be affected in functionality by the armadillo repeat mutations. For example, the intracellular tyrosine kinase PTK6 was

shown to interact with β-catenin and reduce its signaling activity [18]. PTK6 phosphorylates various β-catenin residues including Y333, meaning that mutations in this region could theoretically affect the ability of PTK6 to inhibit β-catenin's activity. Likewise, the glycolytic enzyme PKM2 was shown to bind Y333 phosphorylated β-catenin in the nucleus and activate its transcriptional activity [19]. Thus in theory mutations in this region can increase the binding of PKM2, thereby leading to enhanced signaling. However, both these interacting proteins are unlikely to be affected by W383 and N387 mutations, the second involved cluster. Therefore, we do not consider them to be main players in activating signaling of the armadillo repeat mutants.

Ideally, a thorough analysis should be performed for all identified binding partners to determine whether their association is altered by the armadillo repeat mutations, followed by functional assays to investigate possible transcriptional responses, but this is a daunting task. Despite this potential shortcoming of our analysis, the reduced binding to APC, one of the main players in the β-catenin breakdown complex, provides in our opinion the most likely rationale for the increased signaling of these novel mutants.

A second potential shortcoming of our work is that we had to rely on overexpression to investigate the interactions to other proteins. This likely alters the stoichiometry of proteins relevant for β-catenin regulation, thereby limiting the ability to uncover more subtle effects of such mutations on the assembly of various β-catenin protein complexes. Unfortunately, no cell lines exist expressing these mutant proteins at endogenous levels. For that reason, we are in the process of generating knock-in cell lines using Crispr-Cas technology. If successful, these cell lines will allow a more correct analysis of our finding at physiological levels.

The armadillo mutations represent about 40% of all *CTNNB1* mutations observed in hepatocellular adenomas, but only about 5% in carcinomas where the exon3 mutations predominate [20]. This suggests that they require more or stronger additional oncogenic hits to efficiently contribute to tumor progression than the classical exon3 mutants. The underlying reason is most likely the modest activation of β-catenin signaling, which does not mean they cannot significantly contribute to tumor formation. In support, several examples have been presented in the literature showing that minor alterations in the level of β-catenin signaling can have profound biological effects. In case of hepatocellular cancer, Buchert et al. have shown that late-onset hepatocellular tumors were present in

all mice carrying a hypomorphic APC mutation associated with just a modest increase in β-catenin signaling, while tumor formation was absent or largely prevented with slightly increased or decreased signaling [21]. This narrow window of signaling effective in liver cancer formation highlights the importance of low level signaling for some cancer types, and shows that it is difficult to fully exclude a role for β-catenin signaling when only modest effects on signaling are observed.

The same argument applies to *AXIN1* mutations as well, which are observed in about 8-10% of HCCs. The last decade several papers emerged suggesting that *AXIN1* mutation does not contribute to tumor formation by aberrantly activating β-catenin signaling. These statements were largely based on observing only a weak or seemingly negligible activation of β-catenin target genes in liver cancers, and no obvious nuclear accumulation of β-catenin. Apparently, many researchers still believe that only a strong induction of signaling efficiently contributes to tumor growth, but as explained above a weak activation can already provide a growth advantage depending on tissue type and context. In our cell line analysis we observe that in all cases with *AXIN1* mutation, or when we knockdown its expression, we can observe a significant albeit sometimes modest activation of β-catenin signaling. This observation was further supported by repairing the *AXIN1* mutation in SNU449 cells, which resulted in reduced expression of the well-established β-catenin target gene *AXIN2*. Although our results make clear that signaling is clearly higher in AXIN1-impaired liver cancer cells, it does not formerly proof that β-catenin signaling is required to sustain their growth. In that respect, we show in chapter 4 that *CTNNB1* knock-down reduces the growth of all three AXIN1-mutant lines tested [22]. Recently, stronger evidence was provided by Qiao et al [23]. By simultaneously knocking-out *Axin1* and *Ctnnb1* in mouse livers, the tumors formed by *Axin1* deletion alone could be completely prevented, showing that β-catenin signaling is absolutely required.

Overall, our work highlights two mutational mechanisms leading to only a modest increase in β-catenin signaling that nevertheless appears to be very relevant for liver tumorigenesis.

2 Therapies targeting Wnt signaling in HCC

Due to the lack of sensitive and valid biomarkers for early diagnosis of HCC, the

majority of HCC patients are diagnosed at a late stage, leaving a limited number of treatment options. At present, for patients detected at an early stage of tumor formation, tumor resection and liver transplantation are the main suitable treatment options, resulting in a 5-year overall survival rate of only 30%-40%. For HCC patients with advanced disease, Sorafenib is the only treatment option, which can extend the median overall survival with a modest 2-3 months.

Given the strong involvement of Wnt/β-catenin signaling in the pathogenesis of HCC, we have evaluated two inhibitors targeting components of Wnt signaling for their effectiveness in reducing the growth of HCC cell lines. The first one is IWP12 belonging to the class of Porcupine-inhibitors, which inhibits the secretion of Wnt ligands. The underlying rationale for this approach was that HCC cells may still partially depend on extracellular Wnt ligand exposure to sustain sufficient β-catenin signaling, especially in cell lines with weaker activation of the pathway, i.e. *AXIN1*- and non-mutant lines. Using this inhibitor we observe a modest but significant reduction in growth in most lines. Surprisingly, this was not accompanied by a clear reduction in nuclear β-catenin signaling, indicating that the growth inhibition was induced through other mechanisms. Our analysis of ER-stress and autophagy did however not provide indications that these mechanisms are involved. Following our publication it was shown by others that IWP-molecules also possess an inhibitory capacity towards Casein Kinase 1δ/ε [24]. These kinases are involved in regulating a large number of cellular processes, and as such their inhibition may have contributed to the growth inhibition that we observed. If true, it may also indicate an alternative method of reducing HCC growth by testing more specific Casein kinase inhibitors.

The second Wnt signaling related compounds tested by us were the so-called tankyrase-inhibitors. Blocking tankyrase activity is expected to stabilize AXIN-proteins, thereby theoretically leading to a more efficient breakdown of β-catenin. Although we do see some inhibition of β-catenin signaling in the AXIN1- and non-mutant lines, the reduction is not sufficient to very effectively reduce their growth. These lines have a relatively low baseline expression of the AXIN proteins, which likely explains why it was technically difficult to show a clear accumulation of AXIN following tankyrase inhibition and the modest overall effect on β-catenin signaling. All three tested *CTNNB1* mutant lines were largely resistant to tankyrase inhibition, in line with their dominant effect on

signaling. Overall, this analysis suggests that tankyrase inhibition is not likely to become an effective therapy for HCC, at least not as a monotherapy.

References

1 Liu, L.J., *et al.* (2016) Aberrant regulation of Wnt signaling in hepatocellular carcinoma. *World journal of gastroenterology* 22, 7486-7499

2 Dajani, R., *et al.* (2003) Structural basis for recruitment of glycogen synthase kinase 3beta to the axin-APC scaffold complex. *The EMBO journal* 22, 494-501

3 Wang, Z., *et al.* (2003) Phosphorylation of beta-catenin at S33, S37, or T41 can occur in the absence of phosphorylation at T45 in colon cancer cells. *Cancer research* 63, 5234-5235

4 Xia, J., *et al.* (2006) beta-Catenin mutation and its nuclear localization are confirmed to be frequent causes of Wnt signaling pathway activation in pilomatricomas. *Journal of dermatological science* 41, 67-75

5 Pilati, C., *et al.* (2014) Genomic profiling of hepatocellular adenomas reveals recurrent FRK-activating mutations and the mechanisms of malignant transformation. *Cancer cell* 25, 428-441

6 Sparks, A.B., *et al.* (1998) Mutational analysis of the APC/beta-catenin/Tcf pathway in colorectal cancer. *Cancer research* 58, 1130-1134

7 Zucman-Rossi, J., *et al.* (2007) Differential effects of inactivated Axin1 and activated beta-catenin mutations in human hepatocellular carcinomas. *Oncogene* 26, 774-780

8 Blagodatski, A., *et al.* (2014) Targeting the Wnt pathways for therapies. *Molecular and cellular therapies* 2, 28

9 Buess, M., *et al.* (2004) STRAP is a strong predictive marker of adjuvant chemotherapy benefit in colorectal cancer. *Neoplasia* 6, 813-820

10 Halder, S.K., *et al.* (2006) Oncogenic function of a novel WD-domain protein, STRAP, in human carcinogenesis. *Cancer research* 66, 6156-6166

11 Matsuda, S., *et al.* (2000) Molecular cloning and characterization of human MAWD, a novel protein containing WD-40 repeats frequently overexpressed in breast cancer. *Cancer research* 60, 13-17

12 Yuan, G., *et al.* (2016) Novel role of STRAP in progression and metastasis of colorectal cancer through Wnt/beta-catenin signaling. *Oncotarget* 7, 16023-16037

13 Ramji, D.P. and Foka, P. (2002) CCAAT/enhancer-binding proteins: structure, function and regulation. *The Biochemical journal* 365, 561-575

14 Roos, A.B. and Nord, M. (2012) The emerging role of C/EBPs in glucocorticoid signaling: lessons from the lung. *The Journal of endocrinology* 212, 291-305

15 Balamurugan, K. and Sterneck, E. (2013) The many faces of C/EBPdelta and their relevance for inflammation and cancer. *International journal of biological sciences* 9, 917-933

16 Xing, Y., *et al.* (2004) Crystal structure of a beta-catenin/APC complex reveals a critical role for APC phosphorylation in APC function. *Molecular cell* 15, 523-533

17 Valenta, T., *et al.* (2012) The many faces and functions of beta-catenin. *The EMBO journal* 31, 2714-2736

18 Palka-Hamblin, H.L., *et al.* (2010) Identification of beta-catenin as a target of the intracellular tyrosine kinase PTK6. *Journal of cell science* 123, 236-245

19 Yang, W., *et al.* (2011) Nuclear PKM2 regulates beta-catenin transactivation upon EGFR activation. *Nature* 480, 118-122

20 Rebouissou, S., *et al.* (2016) Genotype-phenotype correlation of CTNNB1 mutations reveals different ss-catenin activity associated with liver tumor progression. *Hepatology* 64, 2047-2061

21 Buchert, M., *et al.* (2010) Genetic dissection of differential signaling threshold requirements for the Wnt/beta-catenin pathway in vivo. *PLoS genetics* 6, e1000816

22 Wang, W., *et al.* (2016) Blocking Wnt Secretion Reduces Growth of Hepatocellular Carcinoma Cell Lines Mostly Independent of beta-Catenin Signaling. *Neoplasia* 18, 711-723

23 Qiao, Y., *et al.* (2019) Axin1 deletion induced hepatocarcinogenesis requires intact beta-Catenin but not Notch cascade in mice. *Hepatology*

24 Garcia-Reyes, B., *et al.* (2018) Discovery of Inhibitor of Wnt Production 2 (IWP-2) and Related Compounds As Selective ATP-Competitive Inhibitors of Casein Kinase 1 (CK1) delta/epsilon. *Journal of medicinal chemistry* 61, 4087-4102

Appendices

Nederlandse samenvatting

De belangrijkste componenten van Wnt signalering in HCC

Het hepatocellulair carcinoom (HCC) is een ernstige maligniteit die geassocieerd is met een hoge morbiditeit en mortaliteit. Een afwijkende toename van Wnt/β-catenine signalering levert een belangrijke bijdrage aan de initiatie en progressie van HCC. In dit tumortype wordt dit voornamelijk veroorzaakt door het verkrijgen van activerende somatische mutaties in het *CTNNB1* gen (20-25%), coderend voor β-catenine, of minder vaak door inactiverende mutaties in *AXIN1* (10%). In dit proefschrift heb ik onderzocht hoe nieuw ontdekte β-catenine varianten leiden tot verhoogde β-catenine signalering. Daarnaast onderzocht ik in welke mate *AXIN1* mutaties leiden tot verhoogde signalering in leverkankercellijnen, omdat hierover de laatste jaren een controverse is ontstaan. Leverkankercellijnen werden ook getest op hun afhankelijkheid van extracellulaire Wnt ligand activatie om een optimale groei te kunnen behouden. We ontdekten ook dat het STRAP-eiwit de sterkte van het β-catenine signaal beïnvloed in HCC. Als laatste identificeerden we CEBPD, waarvan de expressie-niveaus associëren met HCC prognose.

De afgelopen decennia is er grote vooruitgang geboekt in ons begrip van Wnt/β-catenine signalering. Vooral het mechanisme van N-terminale fosforylatie van exon3 gecodeerde S/T residuen en de daaropvolgende eiwitafbraak, wordt goed begrepen. Mutaties in dit domein leiden tot verhoogde β-catenine signalering doordat ze het eiwit meer resistent maken tegen afbraak. Recent worden mutaties in armadillo repeats 5 en 6 van het β-catenine eiwit (residuen K335, W383 en N387) echter ook erkend als een nieuwe hotspot van mutatie, vooral in leverkankers. **In hoofdstuk 2** laten we zien dat deze mutanten een vergelijkbaar gedrag vertonen als het wild-type eiwit wat betreft halfwaardetijd, N-terminale S/T fosforylatie en β-TrCP binding. Met behulp van immunoprecipitatie zien we echter dat deze mutanten veel minder sterk binden aan het APC eiwit, één van de belangrijkste componenten van het β-catenine afbraakcomplex, terwijl ze tegelijkertijd even sterk blijven binden aan hun nucleaire TCF/LEF transcriptionele cofactoren. Het laatste is belangrijk om voldoende versterking van β-catenine doelgenen te kunnen bewerkstelligen en daarmee tumorvorming te ondersteunen. Onze bevinding van verlaagde bindingsaffiniteit wordt verder ondersteund door de analyse van beschikbare eiwitstructuren. In tegenstelling tot de

exon3 mutaties die nooit tegelijkertijd gevonden worden met inactiverende *APC* mutaties, worden de armadillo repeat mutaties vaak gezien in darmtumoren die ook al "zwakke" *APC* of *AXIN* mutaties hebben. In leverkanker lijken deze mutaties op zich zelf echter voldoende te zijn om tumorgroei te ondersteunen. Samenvattend ontdekken we in dit onderzoek een nieuw mechanisme van activatie van β-catenine signalering in tumoren, namelijk door het verkrijgen van β-catenine mutaties die selectief de binding aan APC verminderen.

Naast de activerende β-catenine mutaties, kan een verhoogde signalering ook verkregen worden door middel van AXIN1 mutaties. Deze mutaties worden waargenomen in ongeveer 10% van de HCC tumoren. Oorspronkelijk werd verondersteld dat ze tumorgroei ondersteunen door het onnatuurlijk verhogen van β-catenine signalering. Deze aanname is echter minder zeker geworden door enkele artikelen die laten zien dat deze AXIN1-mutante tumoren geen duidelijke nucleaire stapeling van β-catenine vertonen, noch een duidelijke verhoogde expressie van β-catenine doelgenen. **In hoofdstuk 3**, gebruikmakend van 9 leverkankercellijnen, laten we zien dat AXIN1 mutatie of siRNA gemedieerde knockdown, leidt tot verhoogde β-catenine signalering in alle AXIN1 mutante en niet-gemuteerde lijnen; een observatie die we ook bevestigen in SNU449 cellen met een gerepareerde *AXIN1* mutatie. AXIN1 en AXIN2 werken synergistisch in hun controle van β-catenine signalering. Terwijl in de AXIN1-mutante cellijnen AXIN2 als enige verantwoordelijk is voor het onder controle houden van signalering, dragen in de niet-mutante lijnen beide AXIN-varianten bij aan de β-catenine regulatie.

Er is een tweede reden waarom de AXIN eiwitten veel aandacht krijgen in het kankeronderzoek. Hun activiteit in het β-catenine afbraakcomplex kan namelijk verhoogd worden door zogenaamde tankyrase-remmers, die dus kunnen dienen als een therapeutische optie om de groei van β-catenine-afhankelijke kankers te verminderen. Toepassing van de tankyrase-remmer XAV939 stabiliseert het AXIN1- en AXIN2-eiwit echter niet duidelijk in onze HCC-cellijnen, met uitzondering van AXIN2 in de *CTNNB1*-mutante lijnen. Desondanks verlaagde tankyrase-remming de β-catenine signalering in de meeste niet-*CTNNB1*-mutante lijnen, wat echter niet voldoende was om hun groei te onderdrukken. Samengevat laten onze analyses zien dat AXIN1-mutatie leidt tot een verhoogde β-catenine signalering in HCC cellijnen, daarmee vraagtekens

plaatsent bij enkele sterke uitspraken in de literatuur die suggereren dat dit niet het geval is. Het verbeteren van de AXIN-activiteit door monotherapie met tankyrase-remmers biedt echter geen effectieve behandeling om hun groei te beïnvloeden.

Naast mutaties in β-catenine en AXIN1, zijn er aanwijzingen dat de Wnt-liganden zelf ook tumorgroei kunnen bevorderen in een deel van de tumoren. Therapieën die de blootstelling van tumorcellen aan Wnt liganden kunnen verminderen, zouden daarom mogelijk ook bruikbaar zijn voor de behandeling van HCC. **In hoofdstuk 4** onderzoeken we in welke mate de groei van HCC cellijnen (n=9) beïnvloed kan worden door verminderde blootstelling aan Wnt-liganden, waarbij we darmkanker cellijnen meenemen ter controle. Allereerst laten we zien dat knockdown van β-catenine door middel van siRNA, leidt tot een verminderde groei van alle HCC cellijnen. Het blokkeren van Wnt-secretie d.m.v. een behandeling met de IWP12 Porcupine-remmer of knockdown van WLS, resulteert ook tot in een verminderde groei van de meeste lijnen. Deze remming van Wnt-secretie is onverwacht echter niet geassocieerd met een veranderde β-catenine signalering. Vergelijkbare resultaten zagen we bij darmkankercellijnen die we als controle hadden meegenomen.

Onze resultaten suggereren dat de meeste darm- en leverkankers met mutaties in componenten van het β-catenine afbraakcomplex of β-catenine zelf, niet duidelijk afhankelijk zijn van extracellulaire blootstelling aan Wnt-liganden voor een optimale groei. Het remmen van Wnt-secretie kan echter bijdragen aan tumoronderdrukking via een mechanisme dat we nog niet begrijpen.

Naast somatische mutaties in Wnt signaleringscomponenten, bestaan er diverse regulerende eiwitten die de activatie van Wnt/β-catenine signalering kunnen beïnvloeden. **In hoofdstuk 5** ontdekken we het belang van het STRAP-eiwit om in leverkanker cellijnen een optimaal β-catenine signaal in stand te houden en hun groei te bevorderen. We zagen een verhoogde expressie van STRAP in levertumoren van patiënten, in overeenstemming met eerdere studies in ander tumortypes. Voor een functionele analyse gebruikten we siRNA en CRISPR/Cas9 technologieën om de hoeveelheid STRAP in cellijnen te verminderen of volledig uit te schakelen. Dit leidde tot een vermindering in celgroei, een verslechterde celcyclus en een afgenomen vermogen om kolonies te vormen. In overeenstemming met een darmkankerstudie, leidde verlies

van STRAP ook tot minder expressie van β-catenine doelgenen en inductie van een β-catenine reportersysteem. Samenvattend ondersteunt de verhoogde expressie van STRAP de groei van levertumoren onder andere door het positief beïnvloeden van β-catenine signalering.

Eerdere studies hebben laten zien dat de functie van CEBPD sterk gekoppeld is aan carcinogenese en aangeboren immuunresponsen. Door het multifunctionele karakter van CEBPD blijft zijn exacte functie echter controversieel. In hoofdstuk 6 onderzoeken we de rol in leverkanker. We laten zien dat *CEBPD* mRNA expressie significant lager is in leverkankers in vergelijking met normaal leverweefsel. Dit wordt verder bevestigd door verminderde eiwitexpressie zichtbaar op TMA-coupes. Zowel in de Huh7 als ook de HepG2 leverkankercellijnen leidt CEBPD knockdown tot minder celproliferatie, vorming van kolonies vanuit losse cellen en een blokkade in de G0/G1-fase van celcyclus. Een analyse van beschikbare RNA-sequentie data van MCF-7 kankercellen met CEBPD knockdown, liet zien dat interleukin-1 (IL-1) signalering indirect versterkt werd door het verlagen van *IL1RN* expressie, een natuurlijke remmer van IL-1 signalering. Hetzelfde werd waargenomen in onze Huh7 en HepG2 cellen met CEBPD knockdown. De Huh7 cellen met verminderde CEBPD-expressie resulteren ook in kleinere tumoren na subcutane injectie in muizen. We concluderen dat CEBPD-expressie een loskoppeling geeft van de expansie van de kankercomponent en de klinische HCC prognose, mogelijk door het beïnvloeden van IL-1 signalering. Ondanks dat onze resultaten de rol van CEBPD als tumoronderdrukker in HCC bevestigen, lijkt dit niet door middel van het remmen van de expansie van de kankercomponent maar waarschijnlijker door het bevorderen van de antikanker-immuniteit.

Acknowledgements

Thanks to all the MDL members. I wish to express my sincerest thanks to all those who have given me support and help.

First of all, I would like to express my appreciation to Dr. Ron Smits for his careful guidance. In the past four years, you not only teach me how to do scientific research, but also let me know how to behave. You are knowledgeable, generous, humble, and scrupulous. These good personality qualities deeply affect me for my future work. Just like an old saying in china. "Ancient scholars certainly had teachers. A teacher is one who passes on the truth, imparts knowledge and solves puzzles". Your behavior perfectly fits this sentence.

I would like to express my sincere appreciation to my Promoter Prof. Dr. Maikel P. Peppelenbosch. Thanks for giving me the great opportunity to join this big family. You are not only a rigorous scientist, but also a very patient, responsible master. You are smart, open-minded and sharp-witted. You are talented!!!

My heartfelt gratitude goes to the members of the reading committee, Prof. Winand Dinjens, Prof. Marco Bruno, Dr. Peter Hohenstein. Thank you for taking your valuable time to evaluate my thesis.

Dear Jaap, thanks for your suggestions and corrections on my paper. I also need to appreciate your precious resource-TMA. It was a big support and gift for my article.

Dear Kostas and Patrick, thank you for your great help for providing TMA slices and analyzing the results again and again. Wish you every success in your future work.

To Dr. Stefan J. Erkeland, thanks for your plasmids and teach me how to perform the knock-in strategy.

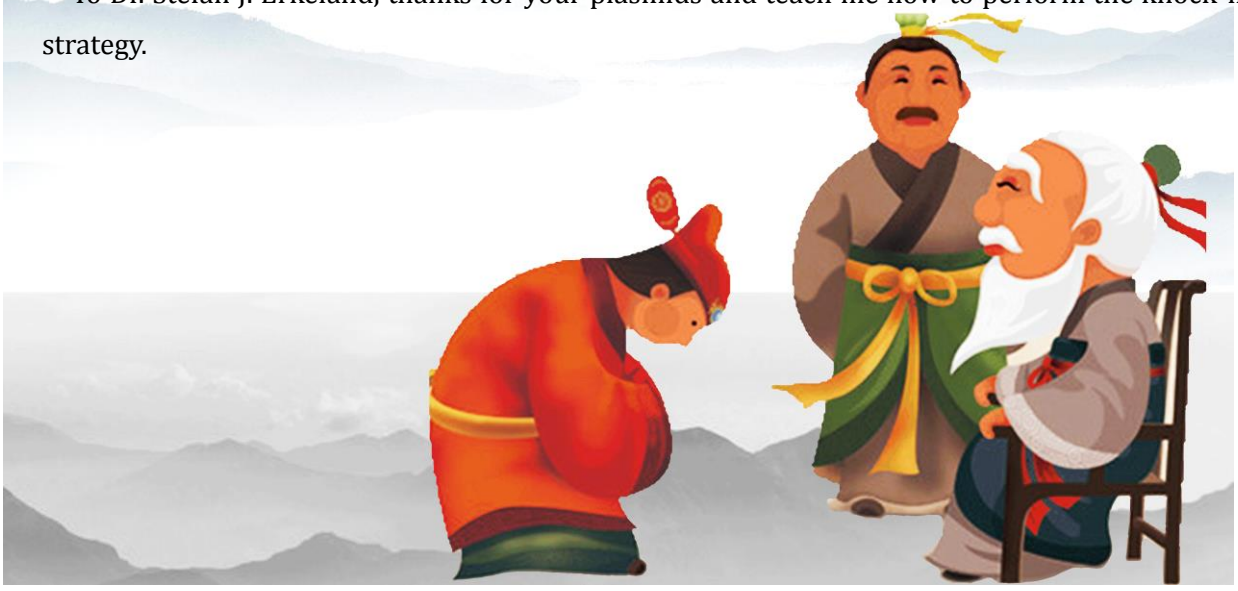

感谢恩师，中山大学肿瘤防治中心黄文林教授，陈帅教授。感谢你们一直以来的鼓励和支持。

感谢南开大学生科院孔德领教授，化学院陈军院士，刘君老师，王艳铭教授的无私帮助和悉心指导。

感谢上海交大陈丹师姐对我找工作的关心和帮助，祝工作顺利。

感谢温州医科大学刘勇教授提出的宝贵建议。

感谢苏州大学李桢教授对我工作的支持和帮助。

感谢大姑，大姑父。你们在科研上的成就是我永远无法企及的。谢谢你们给我树立了追赶目标，谢谢你们让我一次又一次在失败中学会成长。

感谢二姑，二姑夫对我从小到大一直的无私帮助。我的每一步都有你们作为坚实的后盾。每次我遇到抉择的时候，你们都会给我非常多宝贵的意见。祝你们身体健康。

感谢岳父，岳母对我的支持和理解。祝你们身体健康，工作顺利。

感谢父亲，母亲。每当我遇到困难，你们都在背后默默的支持我，鼓励我，让我有勇气一步一步的走下去。你们的支持才是我最大的动力。

感谢妻子闫睿一路的支持和陪伴。四年前我们一起来到荷兰这个陌生的地方。时光飞逝，非常怀念在这里的时光。感谢你给我带来了小廷廷，让我们有一个温馨快乐的家。

PhD Portfolio

Name PhD Student	Pengyu Liu
Erasmus MC Department	Gastroenterology and Hepatology
PhD Period	October 2014 - June 2019
Promotor	Prof. Dr. Maikel P. Peppelenbosch
Copromotor	Dr. Ron Smits

Seminars

- Weekly MDL seminar program in experimental gastroentrology and hepatology (attending) (42 weeks/year; @1,5 h) 2014-2019
- Weekly MDL seminar program in experimental gastroentrology and hepatology (presenting) (preparation time 16 h; 2 times/year) 2014-2019
- Biweekly research group education (attending) (20 times/year; @1,5 h) 2014-2019
- Biweekly research group education (presenting) (preparation time 8 h; 4 times/year) 2014-2019

General Courses

- 2015 Basic and translational oncology
- 2016 Microscope Image Analysis: From Theory to Practice
- 2016 Galaxy for NGS
- 2016 The workshop on NCBI&other open source software
- 2016 Ensembl Workshop
- 2016 Next generation sequencing training: CLC Workbench/Ingenuit Variant Analysis Workshop

National and International Conferences

- International Liver Congress™ 2017, Amsterdam, Netherlands
- 2018, EASL HCC Summit, Geneva, Switzerland (ePoster and Poster presentation)

Reviewing for Scientific Journals

- One paper for OncoTarget
- One paper for Scientific report
- One paper for Canadian Journal of Gastroenterology and Hepatology

Academic Awards

- 2014, China Scholarship Council (CSC) Scholarship (File NO. 2014 0822 0029)
- 2017,Young Investigator Bursary, Amsterdam, Netherlands
- 2018, Young Investigator Travel Awards (EASL HCC Summit 2018)

About the author

Pengyu Liu was born on May 4, 1983, in Jilin, Jilin Province, China. He attended primary, middle and high school in Jilin. In 2002, he moved to Dalian in the Liaoning Province and started his undergraduate study. He majored in Bioengineering in the Dalian National University where he obtained his Bachelor degree of Engineering in 2006. After graduation, he worked at Jilin Connell Pharmaceutical Co, Ltd for two years. In 2009, he started his master research at Nankai University, TianJin Province, China. He studied in the college of Life science under the supervision of Prof. Wenlin Huang. In 2012, he defended his master thesis titled "Delivery of Mminicircle-DNA by using G5-PAMAM-D" and obtained a master degree in Science. From 2012 to 2014, he started to work as a Research Assistant at the Chinese Academy of Sciences Institute of Microbiology.

In 2014, with the support of the China Scholarship Council, he got an opportunity to start his PhD research at the department of Gastroenterology and Hepatology, Erasmus Medical Center Rotterdam, the Netherlands. Under the supervision of Prof. Maikel P. Peppelenbosch and Dr. Ron Smits, he mainly focused on the function of high frequency mutations of Wnt signaling components in HCC.

.

List of Publications

1. **Pengyu Liu**, Auke Verhaar, Maikel P. Peppelenbosch. Signaling size: Ankyrin and SOCS box containing ASB E3 ligases in action. ***Trends in Biochemical Sciences 2019 Jan;44(1):64-74***

2. **Pengyu Liu**, Wanlu Cao, Buyun Ma, Meng Li, Kan Chen, Kostandinos Sideras, JanWillem Duitman, Dave Sprengers, T.C. Khe Tran, Jan N.M. Ijzermans, Katharina Biermann，Joanne Verheij, C.Arnold Spek, Jaap Kwekkeboom, Qiuwei Pan, Maikel P. Peppelenbosch. Action and clinical significance of CCAAT/Enhancer Binding Protein Delta in Hepatocellular Carcinoma. ***Carcinogenesis. 2019 Mar 12;40(1):155-163***

3. Wenhui Wang, Lei Xu*, **Pengyu Liu***, Kiran Jairam, Yuebang Yin, Kan Chen, Dave Sprengers, Maikel P. Peppelenbosch, Qiuwei Pan, Ron Smits. Blocking Wnt Secretion Reduces Growth of Hepatocellular Carcinoma Cell Lines Mostly Independent of β-Catenin Signaling. ***Neoplasia.*** 2016;18(12):711-723.

4. Wenhui Wang, Shan Li*, **Pengyu Liu***, Kostandinos Sideras, Harmen J. G. van de Werken, Marieke van der Heide, Wanlu Cao, Marla Lavrijsen, Maikel P. Peppelenbosch, Marco Bruno, Qiuwei Pan and Ron Smits. Oncogenic STRAP Supports Hepatocellular Carcinoma Growth by Enhancing Wnt/β-Catenin Signaling. ***Mol Cancer Res. 2019 Feb;17(2):521-531.***

5. Hendrikus J. Dubbink, Iris H.I.M. Hollink*, Carolina Avenca Valente*, Wenhui Wang*, **Pengyu Liu***, Michail Doukas, Max M. van Noesel, Winand N.M. Dinjens, Anja Wagner, Ron Smits. A novel tissue-based β-catenin gene and immunohistochemical analysis to exclude Familial Adenomatous Polyposis among children with hepatoblastoma tumors. ***Pediatr Blood Cancer. 2018 Jun;65(6):e26991. (* equal contribution)***

6. Dichotomal functions of phosphorylated and unphosphorylated STAT1 in hepatocellular carcinoma. Ma B, Chen K, **Liu P**, Li M, Liu J, Sideras K, Sprengers D, Biermann K, Wang W, IJzermans JNM, Cao W, Kwekkeboom J, Peppelenbosch MP, Pan Q. ***J Mol Med (Berl). 2019 Jan;97(1):77-88***

7. **Pengyu Liu**, Menggang Liu, Joyce H.G. Lebbink, Shan Li, Marla Lavrijsen, Maikel P. Peppelenbosch, Ron Smits. A new mechanism for β-catenin stabilization in cancer through reduced APC binding. ***(In revision for resubmission to Gastroenterology)***

8. Wenhui Wang*, **Pengyu Liu***, Shan Li, Marla Lavrijsen, Maikel P. Peppelenbosch, Ron Smits. Evaluation of AXIN1 and AXIN2 as targets of tankyrase inhibition in hepatocellular carcinoma cells. (***Submitted***)

9 Wenshi Wang, Yuebang Yin, Lei Xu, Junhong Su, Fen Huang, Yijin Wang, Patrick P. C. Boor, Kan Chen, Wenhui Wang, Wanlu Cao, Xinying Zhou, **Pengyu Liu**, Luc J. W. van der Laan, Jaap Kwekkeboom, Maikel P. Peppelenbosch and Qiuwei Pan. Unphosphorylated ISGF3 drives constitutive expression of interferon-stimulated genes to protect against viral infections. ***Sci Signal. 2017;25;10(476)***

10 Wang Q, Jiang W, Chen Y, **Liu P**, Sheng C, Chen S, Zhang H, Pan C, Gao S, Huang W In vivo electroporation of minicircle DNA as a novel method of vaccine delivery to enhance HIV-1-specific immune responses.. ***J Virol. 2014 Feb;88(4):1924-34***

11 Jiang W, Wang Q, Chen S, Gao S, Song L, **Liu P**, Huang W. Influenza A virus NS1 induces G0/G1 cell cycle arrest by inhibiting the expression and activity of RhoA protein. J Virol. 2013 Mar;87(6):3039-52